FLAC (Fast Lagrangian Analysis of Continua) Version 2.20

Verification, Example and Benchmark Problems

Prepared by Mark Board

Itasca Consulting Group, Inc.

Prepared for
U.S. Nuclear Regulatory Commission

FLAC (Fast Lagrangian Analysis of Continua) Version 2.20

Verification, Example and Benchmark Problems

Prepared by
Mark Board

Itasca Consulting Group, Inc.
1313 5th Street SE, Suite 210
Minneapolis, MN 55414

ABSTRACT

FLAC (Fast Lagrangian Analysis of Continua), Version 2.20, is a
two-dimensional, large-strain, explicit finite difference code
written for analysis of problems in geotechnical engineering.
FLAC has the ability to perform static mechanical analyses as
well as transient heat transfer and fluid flow simulations.
Various constitutive models are available to describe linear and
non-linear response of the solid. Coupling can be performed be-
tween the thermal and mechanical, as well as the fluid and me-
chanical, models. The following report presents the documenta-
tion specified in NUREG-0856, Documentation of Computer Codes for
High Level Waste Management. The documentation is presented in
three volumes. Volume 1 contains the mathematical basis for the
various aspects of the code; Volume 2 is the code User's Manual,
and Volume 3 presents FLAC verification, example and benchmark
problems.

VOLUME 3

VERIFICATION, EXAMPLE AND BENCHMARK PROBLEMS

TABLE OF CONTENTS

TABLE OF CONTENTS
(continued)

TABLE OF CONTENTS
(continued)

LIST OF FIGURES

LIST OF FIGURES
(continued)

LIST OF FIGURES
(continued)

LIST OF FIGURES
(continued)

LIST OF FIGURES
(continued)

LIST OF FIGURES
(continued)

LIST OF FIGURES
(continued)

LIST OF FIGURES
(continued)

LIST OF FIGURES
(continued)

LIST OF FIGURES
(continued)

LIST OF FIGURES
(continued)

LIST OF FIGURES
(continued)

LIST OF TABLES

LIST OF TABLES
(continued)

3.1 INTRODUCTION

This document is the third in a series of three volumes which
provide documentation on the code FLAC, Version 2.20, as pres-
cribed in NUREG-0856, Final Technical Position on Documentation
of Computer Codes for High-Level Waste Management (Silling,
1983). Volume 3 provides documentation on the assessment and
support of FLAC for mechanical, thermal and fluid flow analyses
of geotechnical materials. Section 3.2 of this volume presents
verification problems in which FLAC is compared to analytical
solutions for problems in mechanical, thermal and fluid flow an-
alysis. These problems are given to provide assurance of the
correct operation of the various component parts of the FLAC pro-
gram. Section 3.3 provides example problems. These problems are
necessarily more complex than those presented in Section 3.2 and,
therefore, have no analytical solutions. The problems chosen ex-
ercise the features which are commonly employed in geotechnical
analysis. Section 3.4 presents a benchmark study in which FLAC
was compared to a variety of existing numerical models for the
thermomechanical analysis of the steady-state creep of salt to
nuclear waste disposal. This benchmark is commonly referred to
as the "Second Problem". Finally, the procedures used by Itasca
Consulting Group in the development and testing of FLAC are pre-
sented.

Reference

Silling, S. A. Final Technical Position on Documentation of Com-
puter Codes for High-Level Waste Management. U.S. Nuclear Regu-
latory Commission, NUREG-0856, June 1983.

3.2 VERIFICATION PROBLEMS

The following verification analyses compare FLAC to analytically-derived solutions for a variety of mechanical, thermal and fluid flow problems.

3.2.1 Mechanical Problems

The following verification analyses compare FLAC to analytically-derived solutions for a variety of mechanical problems.

3.2.1.1 Cylindrical Hole in an Infinite Body for Elastic and Mohr-Coulomb Materials

Problem Statement

This problem concerns the determination of stresses and displacements for the case of a cylindrical hole in an infinite elastic, elasto-plastic or transversely-isotropic media subject to in-situ stresses.

Purpose

The purpose of this problem is to compare the performance of FLAC on an elastic, elasto-plastic and transversely-isotropic problem with an analytical solution.

Problem Specifications

A cylindrical hole exists in an infinite body under a uniform in-situ compressive stress of 30 MPa. For the elastic solution, the following properties were used.

shear modulus (G)	2.9 GPa
bulk modulus (K)	3.9 GPa
density (ρ)*	2500 kg/m^3

For the elasto-plastic solution, the elastic properties remained the same and the strength parameters listed below were also included.

friction (ϕ)	30°
cohesion (S)	3.45 MPa

---

*not necessary for solution

For the transversely-isotropic solution, the following initial conditions and properties are used:

$$E_x = 0.976e6 \text{ Pa}$$

$$E_y = 0.953e6 \text{ Pa}$$

$$G_{xy} = 0.1103e6 \text{ Pa}$$

$$v_{yx} = 0.167$$

$$v_{zx} = 0.165$$

$$\sigma_{xx} = 0.5e6 \text{ Pa}$$

$$\sigma_{yy} = 1.0e6 \text{ Pa}$$

Assumptions

The cylindrical hole is assumed to exist in a homogeneous, continuous, infinite media subject to plane strain conditions. The material is either linearly elastic, transversely-isotropic or, in the elasto-plastic case, perfectly plastic after undergoing Mohr-Coulomb failure. It is assumed that the problem is symmetric about both the horizontal and vertical axes. Further, it is assumed that the radius of the hole is small compared to the length of the cylinder. This assumption permits the 3-D problem to be reduced to a 2-D plane strain problem.

Analytic Solution

For a cylindrical hole in an infinite elastic media under plane strain conditions (Fig. 3.2.1.1-1), the radial and tangential stress distributions are given by the Kirsch Solution (Kirsch, 1898).

$$\sigma_r = \frac{P_1+P_2}{2} \left[1-a^2/r^2 \right] + \frac{P_1-P_2}{2} \left[1 - \frac{4a^2}{r^2} + \frac{3a^3}{r^4} \right] \cos2\theta$$

$$\sigma_\theta = \frac{P_1+P_2}{2} \left[1+a^2/r^2 \right] - \frac{P_1-P_2}{2} \left[1 + 3a^4/r^4 \right] \cos2\theta$$

$$u_r = \frac{P_1+P_2}{4G} \cdot a^2/r + \frac{P_1-P_2}{4G} \cdot a^2/r \left[4(1-v) - a^2/r^2 \right] \cos2\theta$$
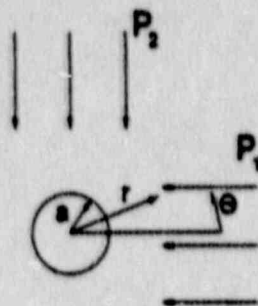
Fig. 3.2.1.1-1 Cylindrical Hole in an Infinite Medium

Since the tunnel is assumed to be under a uniform stress field (i.e., $p_1 = p_2$), the stress field can be normalized by in-situ stress and the radial displacement normalized by the radius of the hole:

$$\sigma_r/p = 1 - 1/r^2$$

$$\sigma_\theta/p = 1 + 1/r^2$$

$$u_r/a = \frac{pa}{2Gr}$$

where p is the in-situ stress,

a is the hole radius, and

G is the shear modulus.

In the elasto-plastic case, the thickness of the plastic zone is $(R - a)$, where R is the radial distance to the elasto-plastic interface. The analytically-determined yield zone radius, R, is given by a theoretical model proposed by John Bray (Goodman, 1980):

$$R = a\left[\frac{2p - q_u + (1 + \tan^2(45 + \phi/2))\, S \cot \phi}{(1 + \tan^2(45 + \phi/2))\,(p_i + S \cot \phi)}\right]^{1/Q}$$

where $Q = \dfrac{\tan\ (45 + \phi/2)}{\tan\ (45 - \phi/2)} - 1$,

q_u = the unconfined compressive strength, or $2S \tan(45 + \phi/2)$,

S = cohesion,

ϕ = friction angle, and

p_i = internal hole pressure, which is zero.

Material at a radial distance less than R is plastic; greater than R is elastic.

The stresses in the elastic and plastic regions can be determined as given by Bray's solution (Goodman, 1980). The stresses in the elastic region are given by

$$\sigma_r/p = 1 - b/pr^2$$

$$\sigma_\theta/p = 1 + b/pr^2$$

where
$$b = \left[\frac{(\tan^2(45 + \phi/2) - 1)\ p + q_u}{\tan^2(45 + \phi/2) + 1}\right] R^2$$

In the plastic region, the stresses are given by

$$\sigma_r/p = \left[\frac{pi + S \cot \phi}{p}\right]\left[\frac{r}{a}\right]^Q - \frac{S \cot \phi}{p}$$

$$\sigma_\theta/p = \left[\frac{pi + S \cot \phi}{p}\right]\left[Q + 1\right]\left[\frac{r}{a}\right]^Q - \frac{S \cot \phi}{p}$$

Since it is assumed that there is no internal pressure (i.e.,
$p_i = 0$), and dimensions are normalized to the size of the hole
i.e., $a = 1$),

$$\sigma_r/p = \frac{s}{p} \cot\phi \ (r^2 - 1)$$

$$\sigma_\theta/p = \frac{s}{p} \cot\phi \ [(Q + 1) \ r^2 - 1]$$

Finally, the analytical results for the displacements around the
periphery of a circular hole in a biaxial stress field for a
transversely-isotropic media are given by Eissa (1980). The re-
sults are given in tabular form in the comparison to the FLAC so-
lution presented later.

Computer Model

Only a quarter of the problem needs to be modeled in the FLAC an-
alysis because of symmetry. The boundary conditions applied to
the model are shown in Fig. 3.2.1.1-2. The area representing a
quarter of the problem was divided into finite difference zones,
as shown in Figs. 3.2.1.1-3 and -4. A total of 900 quadrilateral
zones are used in this grid. The location of the boundary was
varied to illustrate its effect on solution accuracy. Pressure
equal to the in-situ stress was applied to both free faces of the
model, and the zones were allowed to come to stress equilibrium
throughout the mesh prior to excavation of the hole. The problem
was stepped 1000 times, using only the elastic material model, to
ensure equilibrium conditions were achieved. The procedure was
repeated for the Mohr-Coulomb yield model. For the transversely-
isotropic model, 3000 timesteps were used.
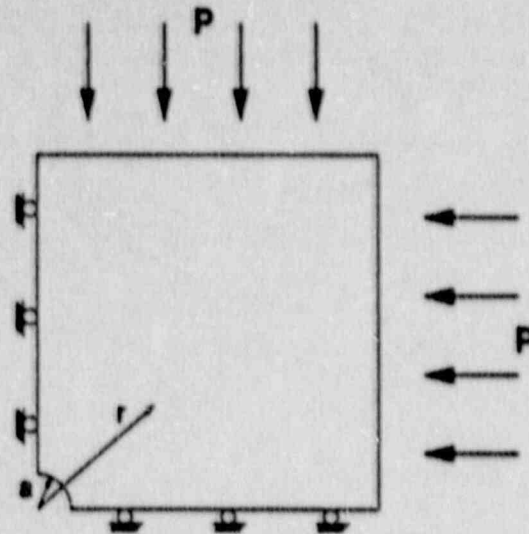
Fig. 3.2.1.1-2   Model for FLAC Analysis of Cyclical Hole in an
Infinite Medium
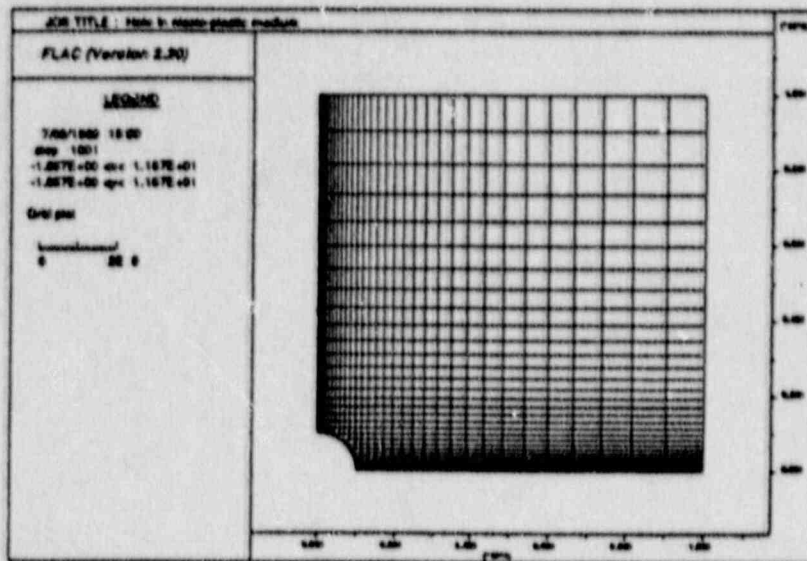
Fig. 3.2.1.1-3   FLAC Zone Geometry
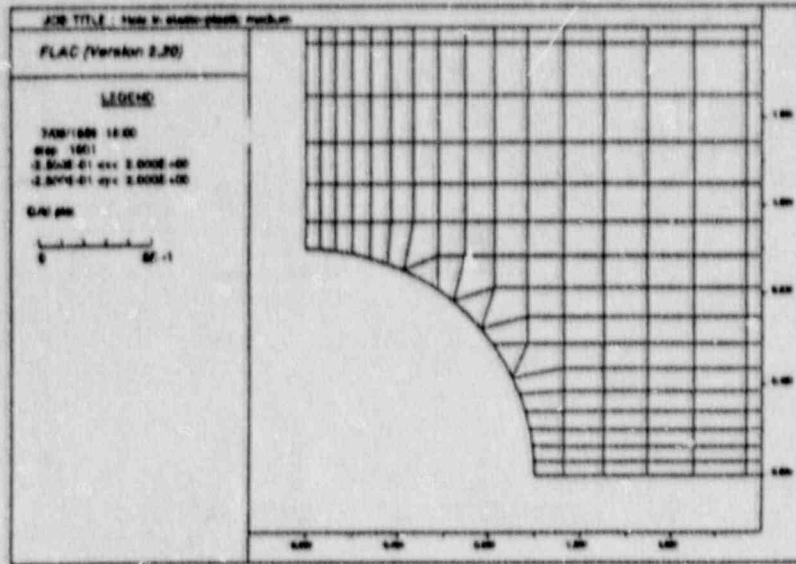
Fig. 3.2.1.1-4   Zone Geometry in Region Around Hole

The problem was re-analyzed using the axisymmetric logic in FLAC, for both the elastic and the elasto-plastic cases. The location of the boundary and conditions at the boundary were the same. Figures 3.2.1.1-5 and -6 show the axisymmetric geometry and boundary conditions used. The number of zones was greatly reduced and calculation timesteps were correspondingly decreased.
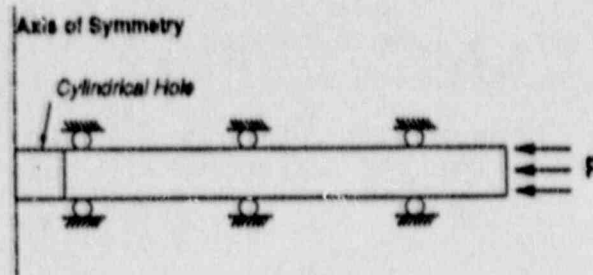
Fig. 3.2.1.1-5   Axisymmetry Model
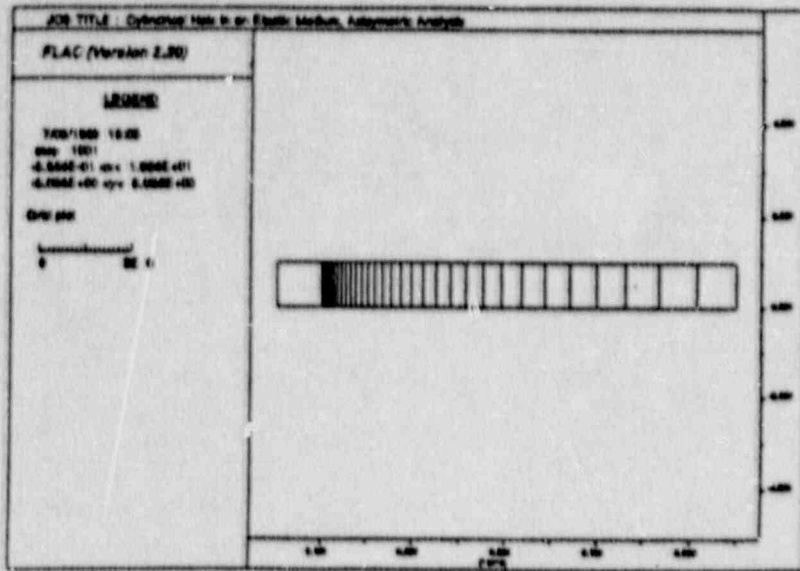
Fig. 3.2.1.1-6   FLAC Axisymmetric Zone Geometry

Results

Figure 3.2.1.1-7 shows the elastic radial and tangential stresses as a function of radial distance as compared to the analytic solution, while Fig. 3.2.1.1-8 shows the same for displacements. Figure 3.2.1.1-9 shows the stresses for the elasto-plastic solutions. Figure 3.2.1.1-10 shows the plastic zones generated in the elasto-plastic case. Table 3.2.1.1-1 shows agreement at four locations along a radial line outward from the hole. The results are discussed in the following section.

Figures 3.2.1.1-11 through 3.2.1.1-13 and Table 3.2.1.1-2 show equivalent information for the axisymmetric solution.
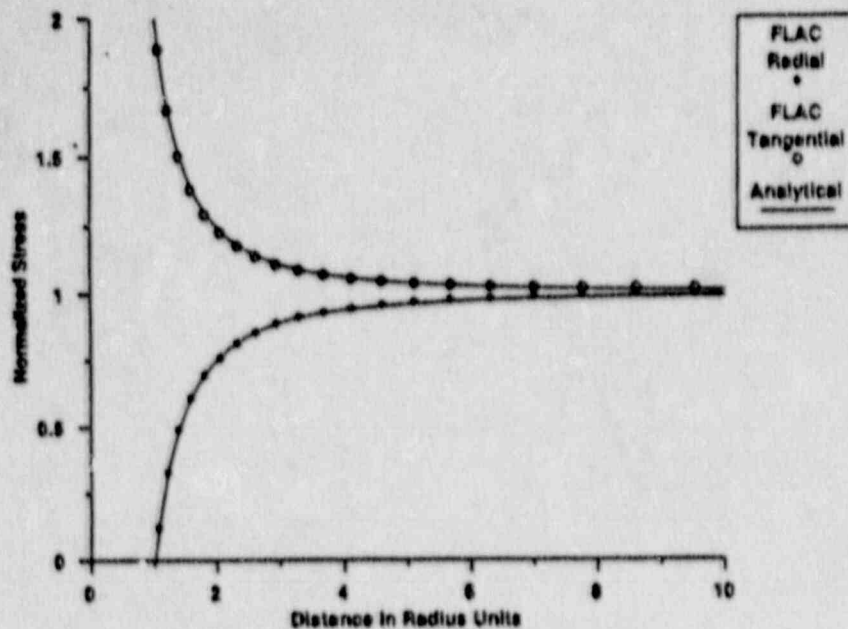
Fig. 3.2.1.1-7   Comparison of Radial (σ_r/p) and Tangential (σ_θ/p) Stresses in the Elastic Case for FLAC and Analytic Solutions
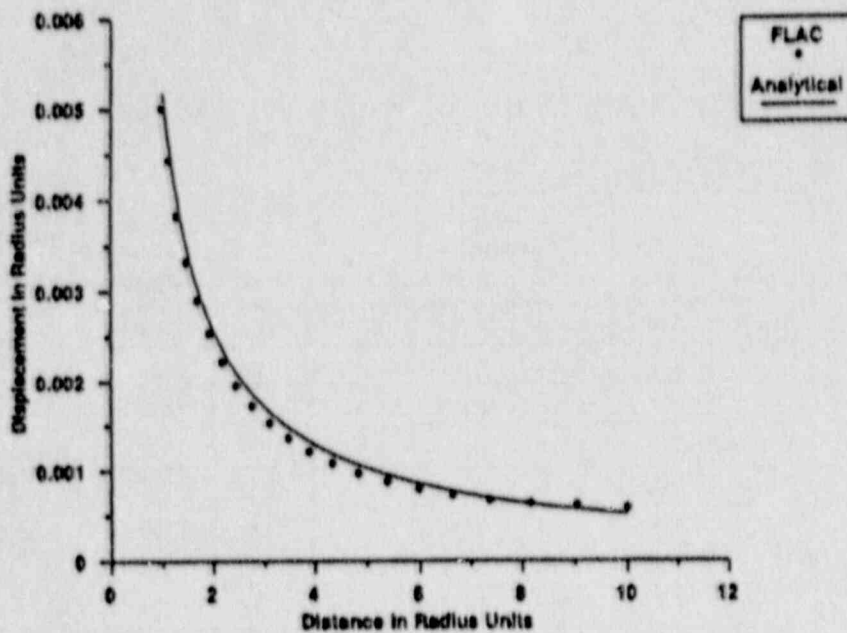
Fig. 3.2.1.1-8   Comparison of Elastic Displacements (u_r/a) vs Radial Distance
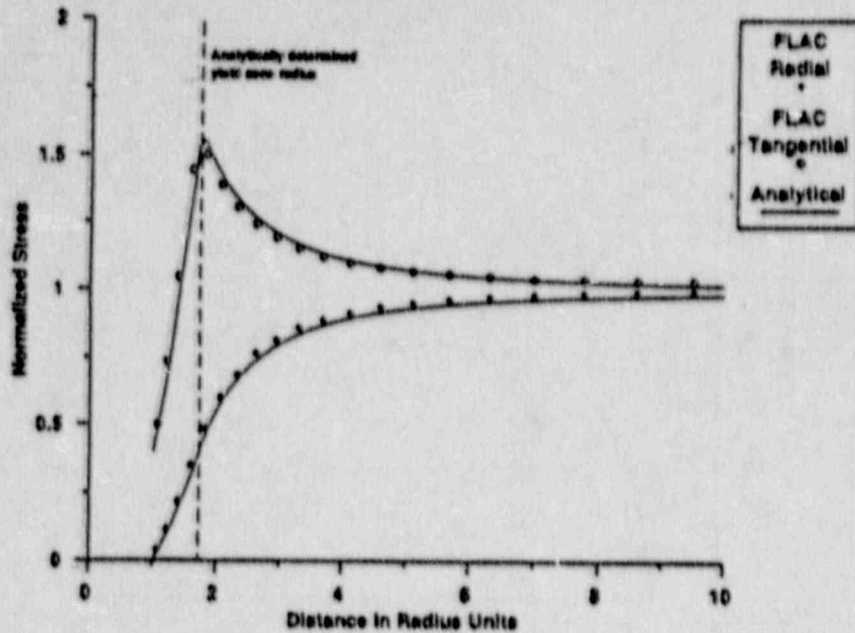
Fig. 3.2.1.1-9 Comparison of Radial (σ_r/p) and Tangential (σ_θ/p) Stresses for the Elasto-Plastic Case. Plane Strain Geometry

Table 3.2.1.1-1

COMPARISON OF FLAC RESULTS TO ANALYTICAL SOLUTION

Model	r/a	Normalized Radial Stress			Normalized Tangential Stress		
		FLAC	Analytical	% Error	FLAC	Analytical	% Error
Elastic	2.06	0.759	0.764	-0.65	1.228	1.236	-0.65
	4.12	0.944	0.941	0.32	1.058	1.059	-0.09
	6.31	0.981	0.975	0.62	1.027	1.025	0.20
	7.76	0.994	0.983	1.12	1.021	1.016	0.49
Plastic	2.06	0.600	0.576	4.17	1.388	1.424	-2.53
	4.12	0.914	0.894	2.24	1.099	1.106	-0.63
	6.31	0.972	0.955	1.78	1.048	1.045	-0.29
	7.76	0.987	0.970	1.75	1.036	1.030	0.58

Model	r/a	Normalized Radial Displacement		
Elastic	1.00	0.00501	0.00517	-5.22
	1.93	0.00121	0.00133	-9.02
	3.89	0.000803	0.000865	-7.17
	5.98	0.000639	0.000634	0.79
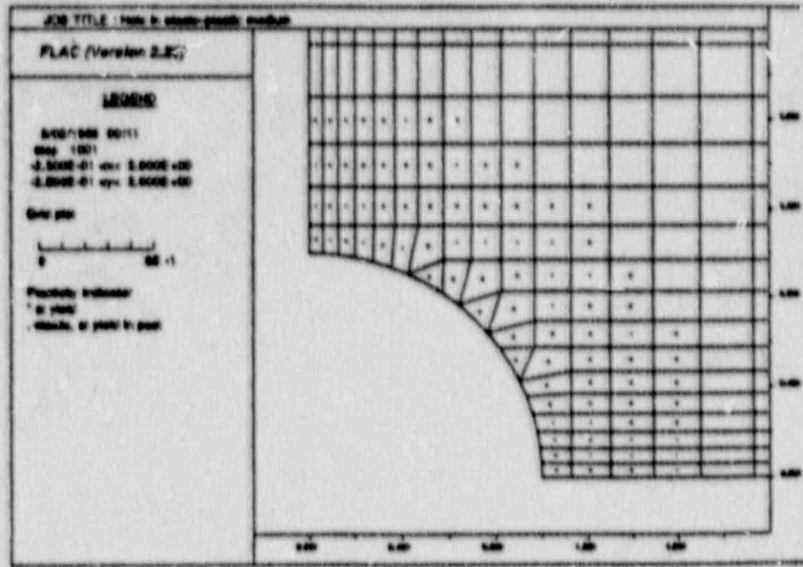
Fig. 3.2.1.1-10   Yielded Zones from FLAC Elasto-Plastic Solution
(Figure 3.2.1.1-9 shows comparison of yield zone
radius, FLAC vs analytic solution.)
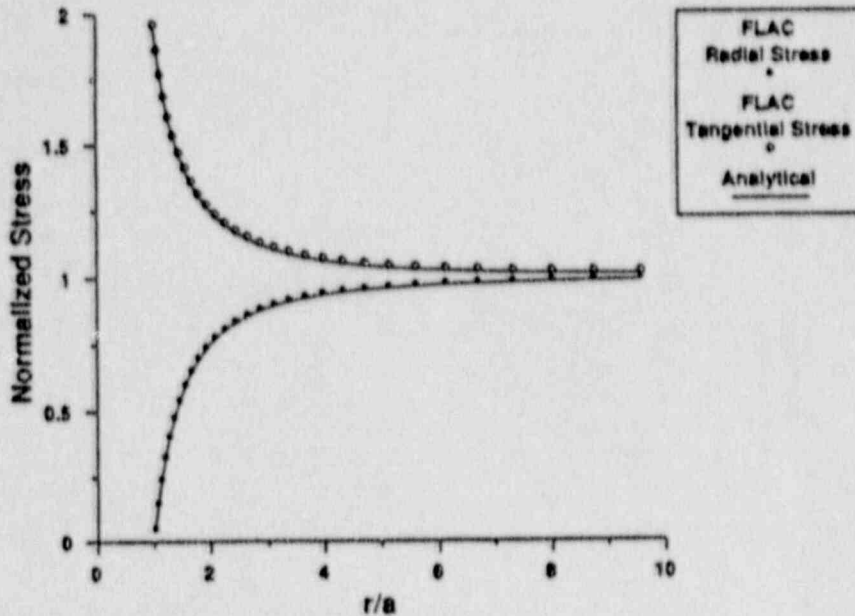
Fig. 3.2.1.1-11   Elastic Radial (σ_r/p) and Tangential (σ_θ/p)
Stresses from FLAC Axisymmetric and Analytical
Solutions
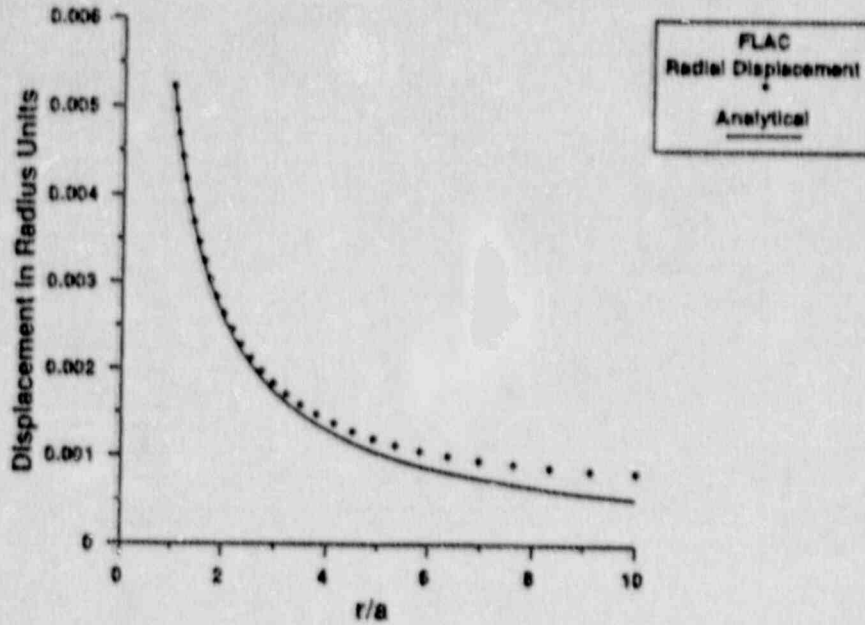
Fig. 3.2.1.1-12   Axisymmetric Elastic Radial Displacements (u_r/a)
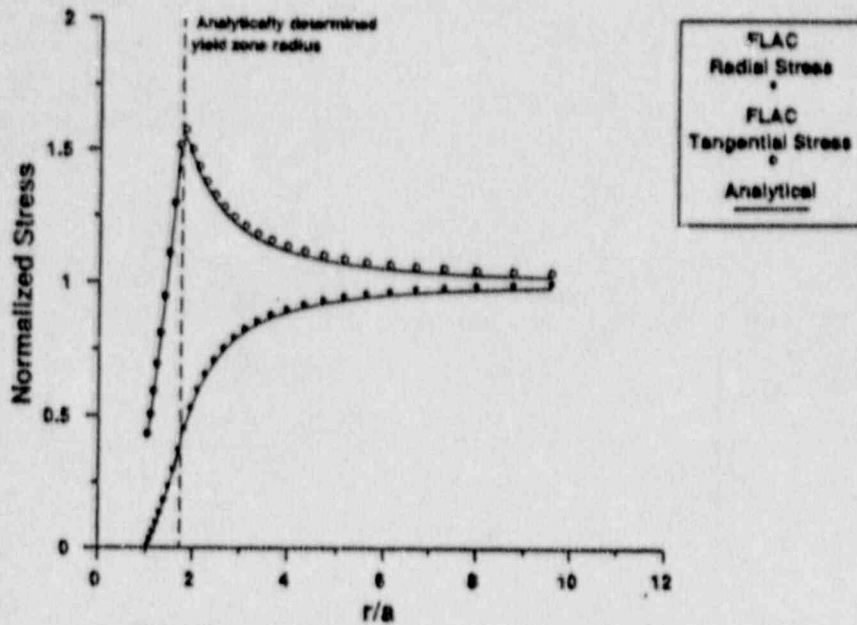
Fig. 3.2.1.1-13   Elasto-Plastic Radial and Tangential Stresses
from FLAC Axisymmetric and Analytical Solutions

Table 3.2.1.1-2

COMPARISON OF AXISYMMETRIC FLAC RESULTS TO ANALYTIC SOLUTION[*]

Model	r/a	Normalized Radial Stress			Normalized Tangential Stress		
		FLAC	Analytical	% Error	FLAC	Analytical	% Error
Elastic	2.09	0.779	0.771	1.04	1.239	1.229	0.81
	3.97	0.946	0.937	0.96	1.073	1.063	0.94
	6.12	0.983	0.973	1.03	1.037	1.027	0.97
	7.99	0.994	0.984	1.02	1.026	1.016	0.99
Plastic	2.09	0.597	0.589	1.36	1.434	1.411	1.63
	3.97	0.901	0.886	1.69	1.133	1.114	1.71
	6.12	0.969	0.952	1.79	1.066	1.048	1.72
	7.99	0.989	0.972	1.75	1.046	1.028	1.75

Model	r/a	Normalized Radial Displacement		
Elastic	1.00	0.00523	0.00517	1.16
	2.01	0.00264	0.00257	2.72
	4.13	0.00138	0.00125	10.4
	5.84	0.00106	0.000885	19.77

---

[*]Note that large error in displacement at large r/a is a result of the use of a pressure boundary condition. Improved results can be obtained using fixed displacement far-field boundary conditions.

Comparison to x- and y-displacements at various locations around the hole for the transversely-isotropic problem is shown in Fig. 3.3.2.1-14. The angle, θ, refers to the angle counterclockwise from the horizontal. The maximum error occurs in vertical (y) displacement at $\theta = 90°$, and is less than 3%.
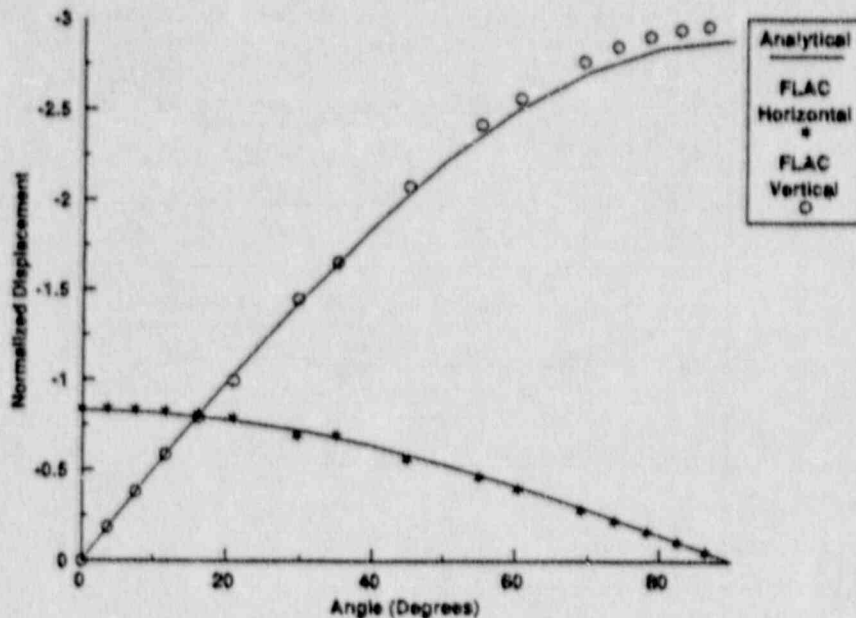
Fig. 3.2.1.1-14 Displacements at the Hole Wall for Various
                 Angles Taken Counterclockwise from the
                 Horizontal for the Transversely-Isotropic Case

Discussion

The stresses from the FLAC analysis show close agreement (<2% elastic, <5% elasto-plastic error) to those given by the analytical solution. For the purposes of this problem, the same geometry was used for both the elastic and the elasto-plastic solution. Error in the elasto-plastic case could be reduced by increasing the number of zones in the expected yield zone and by extending the boundaries to 15 or 20 hole radii. However, if a rough stress analysis is all that is required, both problems (especially the elastic case) probably could be scaled down considerably.

Some displacement results show a larger disagreement (<10% error) with the analytic solutions. Due to the finite size of the model (10 radii), the pressure boundary used to simulate the in-situ stress of an infinite media would be expected to cause a discrepancy in displacement, and this is the result seen from FLAC. If more accurate displacements are desired, the boundaries of the problem could be extended to reduce their effects. A radial grid configuration could also increase agreement, as the rectangular grid used is not particularly well suited to the geometry (Radial grid results should be comparable to axisymmetric results; see below.). The transversely-isotropic displacements show excellent agreement with less than a maximum 3% error on displacements at the hole wall.

This problem also provides an example for the use of FLAC's axisymmetry logic. For the axisymmetric case, all stresses were within 2% of the analytic solution. The results show that comparable results are obtained with a considerably smaller number of zones, and thus a much shorter calculation time. The displacements near the hole radius are more accurate using axisymmetry (< 3% error up to 2 tunnel radii) than the normal 2-D case, though displacements deviate closer to the far-field boundary, as is expected from the pressure condition. Using axisymmetry and the same number of zones as in the normal 2-D case, the boundaries could be extended considerably with the result of much more accurate displacements over a greater range.

Reference

Eissa, Esa. "Stress Analysis of Underground Excavations in Isotropic and Stratified Rock Using the Boundary Element Method," Ph.D. Thesis, Imperial College of Science and Technology, London, 1980.

Goodman, Richard E. Introduction to Rock Mechanics. New York: John Wiley and Sons, 1980.

Kirsch, G. "Die Theorie der Elastizitat und die Bedürfnisse der Festigkeitslehre," Veit. Ver. Deut. Ing., 42, 797-807 (1898).

Data Input File

Elastic Model

```
***********************************************************************
* FLAC Verification Problem - Circular Hole in an Elastic Body
***********************************************************************
tit
Hole in elastic medium
*
* 900 Zones in grid
*
gr 30,30
*
* Elastic material
*
m e
*
* Put boundaries at 10 Radii, concentrate zones near hole
*
gen 0,0 0,10 10,10 10,0 rat 1.1 1.1
*
* Create hole boundary
*
gen arc 0,0 1,0 90
*
* Material properties
*
prop s=2.9e9 b=3.9e9 dens=2500
*
* Initial hydrostatic stresses
*
ini sxx=-30e6 syy=-30e6
*
* Boundary conditions for quarter-symmetry
*
fix x    i=1
fix y    j=1
*
* Pressure conditions for infinite boundaries
*
apply press 30e6 i=1,31 j=31
apply press 30e6 i=31 j=1,31
*
```

```
* Histories
*
his nste=1
his syy i=1 j=11
his sxx i=1 j=11
his ydis i=1 j=11
*
* Let system come to initial equilibrium state
*
solve
*
* Excavate hole
*
mod null region=1,1
*
* Step to equilibrium
*
step 1000
*
* Save state
*
save ehole210.sav
* end of problem
```

Plastic Model

```
*****************************************************************
* FLAC Verification Problem - Circular Hole in an Elasto-Plastic
* (Mohr-Coulomb) Material, Hydrostatic Initial Stress
*****************************************************************
tit
Hole in elasto-plastic medium
*
* 900 Zones in grid
*
gr 30,30
*
* Elasto-plastic material
*
m m
*
* Put boundaries at 10 Radii, concentrate zones near hole
*
gen 0,0 0,10 10,10 10,0 rat 1.1 1.1
*
* Create hole boundary
*
gen arc 0,0 1,0 90
*
* Material properties
*
prop s=2.8e9 b=3.9e9 dens=2500 fric=30 coh=3.45e6
*
* Initial Stress
*
ini sxx=-30e6 syy=-30e6
*
* Boundary conditions for quarter-symmetry
*
fix x    i=1
fix y    j=1
*
* Pressure conditions at infinite boundaries
*
apply press 30e6 i=1,31 j=31
apply press 30e6 i=31 j=1,31
*
```

```
* Histories
*
his nste=1
his syy i=1 j=11
his sxx i=1 j=11
his ydis i=1 j=11
*
* Let system come to equilibrium prior to hole excavation
*
solve
*
* Excavate hole
*
mod null region=1,1
*
* Solve for elastic equilibrium
*
step 1000
*
* Save state
*
save phole210.sav
* end of problem
```

Elastic Model — Axisymmetric

```
************************************************************
* FLAC Verification Problem - Circular Hole in an Elastic Material
* Axisymmetric Model
************************************************************
tit
Cylindrical Hole in an Elastic Medium, Axisymmetric Analysis
*
*   Set FLAC to axisymmetric model
*
config ax
*
*   Create grid
*
gr 31,1
*
*   Material model
*
m e
*
*   Contract grid to fit geometry
*
gen 0,0 0,1 1,1 1,0 i=1,2 j=1,2
gen 1,0 1,1 10,1 10,0 rat 1.1 1 i=2,32 j=1,2
*
*   Material properties
*
prop d=2500 sh=2.9e9 b=3.9e9
*
*   Fix boundaries and set initial hydrostatic stresses in 3-D
*
fix y j=1,2
ini sxx=-30e6
ini syy=-30e6
ini szz=-30e6
*
*   Apply pressure to outer boundary
*
apply press 30e6 i=32
*
*   Let system equilibrate before excavation
*
solve
*
*   Excavate tunnel and step to elastic equilibrium
*
mod null i=1,j=1
```

```
step 1000
*
*save state
*
save ehax2.sav
* end of problem
```

Plastic Model — Axisymmetric

```
*******************************************************************
* FLAC Verification Problem - Cylindrical Hole in an Elasto-
* Plastic (Mohr-Coulomb) Medium, Axisymmetric Analysis
*******************************************************************
tit
Cylindrical Hole in an Elastic Medium, Axisymmetric Analysis
*
*    Set FLAC to axisymmetric logic
*
config ax
*
*  Create grid
*
gr 31,1
*
*   Mohr-Coulomb material model
*
m m
*
*   Contract grid to fit geometry
*
gen 0,0 0,1 1,1 1,0 i=1,2 j=1,2
gen 1,0 1,1 10,1 10,0 rat 1.1 1 i=2,32 j=1,2
*
*   Material properties
*
prop d=2500 sh=2.9e9 b=3.9e9 fric=30 coh=3.45e6
*
*   Fix boundaries and set initial stresses in 3-D
*
fix y j=1,2
ini sxx=-30e6
ini syy=-30e6
ini szz=-30e6
*
*   Apply pressure to infinite boundary
*
apply press 30e6 i=32
*
*   Let system equilibrate under initial stresses
*
solve
*
```

```
*   Excavate tunnel in pre-stressed body and step to equilibrium
*
mod null i=1,j=1
step 1000
*
* Save state
*
save phax2.sav
* end of problem
```

Transversely-Isotropic Model

```
*********************************************************************
* FLAC Verification Problem - Circular Hole in a Transversely
* Isotropic, Elastic Medium
*********************************************************************
tit
Hole in transversely-isotropic elastic medium
*
* Grid
*
gr 30,30
*
* Anisotropic model
*
m anis
*
* Stretch grid and form tunnel
*
gen 0,0 0,10 10,10 10,0 rat 1.1 1.1
gen arc 0,0 1,0 90
*
* Properties
*
prop s=.1103e6 xm=.976e6 ym=.953e6
prop nuy=.167 nuz=.165 dens=2000
*
* Initial and boundary conditions
*
ini sxx=-0.5e6
ini syy=-1e6
fix x    i=1
fix y    j=1
apply press 1e6 i=1,31 j=31
apply press 0.5e6 i=31 j=1,31
*
* Histories
*
his nste=10
his syy i=1 j=11
his sxx i=1 j=11
his ydis i=1 j=11
*
* Set up initial stress state
*
solve
*
```

```
* Excavate hole in pre-stressed body
*
mod null region=1,1
* Step to equilibrium
step 3000
*
* Save
*
save ehan.sav
* end of problem
```

3.2.1.2 Bearing Capacity of a Rough Footing on a Cohesive Frictionless Soil

Problem Statement

The prediction of collapse loads under steady plastic flow conditions is one that can be difficult for a numerical model to simulate accurately (Sloan and Randolph, 1982). A simple example of a problem involving steady flow is the determination of the bearing capacity of a strip footing on a cohesive frictionless soil. The bearing capacity found is dependent on the steady plastic flow beneath the footing, and so provides a measure of the ability of the code to model this condition.

Objective

The objective of this problem is to test the plasticity model under steady plastic flow conditions.

Problem Specifications

The strip footing has a half width of 3.1125 m and is located on the surface of the soil, represented by an elasto-plastic medium with the following properties:

density (ρ)	1000	kg/m^3
shear modulus (G)	30	MPa
bulk modulus (k)	100	MPa
cohesion (S)	100	MPa
friction angle (ϕ)	0	

Assumptions

The footing material is assumed to be homogeneous, isotropic, weightless and continuous. The soil is assumed to behave as a frictionless, linearly-elastic and perfectly-plastic solid. The soil medium is semi-infinite, and its behavior is assumed to be symmetric about the footing centerline. The analytic solution which follows assumes that all displacements and strains are small.

Analytical Solution

The bearing capacity from the solution to "Prandtl's Wedge" is given by (Terzaghi and Peck, 1967):

$$q = (2+\pi)S$$

or

$$q = 5.14S$$

where q is the bearing capacity stress at failure, and

S is the cohesion of the material.

The solution is based on the mode of failure as shown in Fig. 3.2.1.2-1.
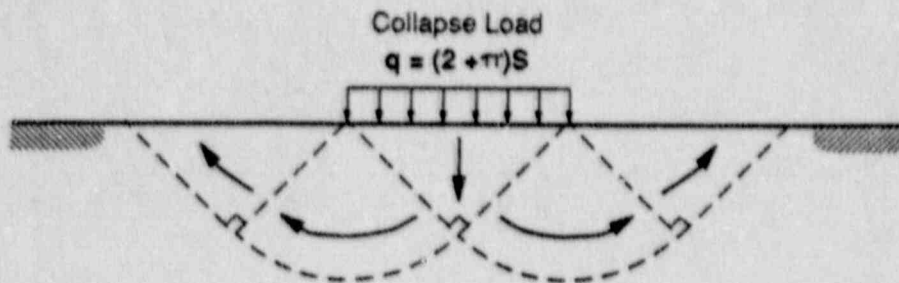
Fig. 3.2.1.2-1 Prandtl's Wedge Problem of a Strip Footing on a Frictionless Soil

Computer Model

For the FLAC analysis, the material was discretized into quadri-lateral, finite difference zones as shown in Fig. 3.2.1.2-2. These zones were concentrated in the area beneath the footing. A symmetry (roller displacement) boundary condition was placed on the left side, and the right side and bottom were sufficiently far away to simulate infinite (pinned displacement) boundaries. A constant downward velocity was applied to the area representing the footing. Figure 3.2.1.2-3 shows the FLAC problem geometry and boundary conditions.
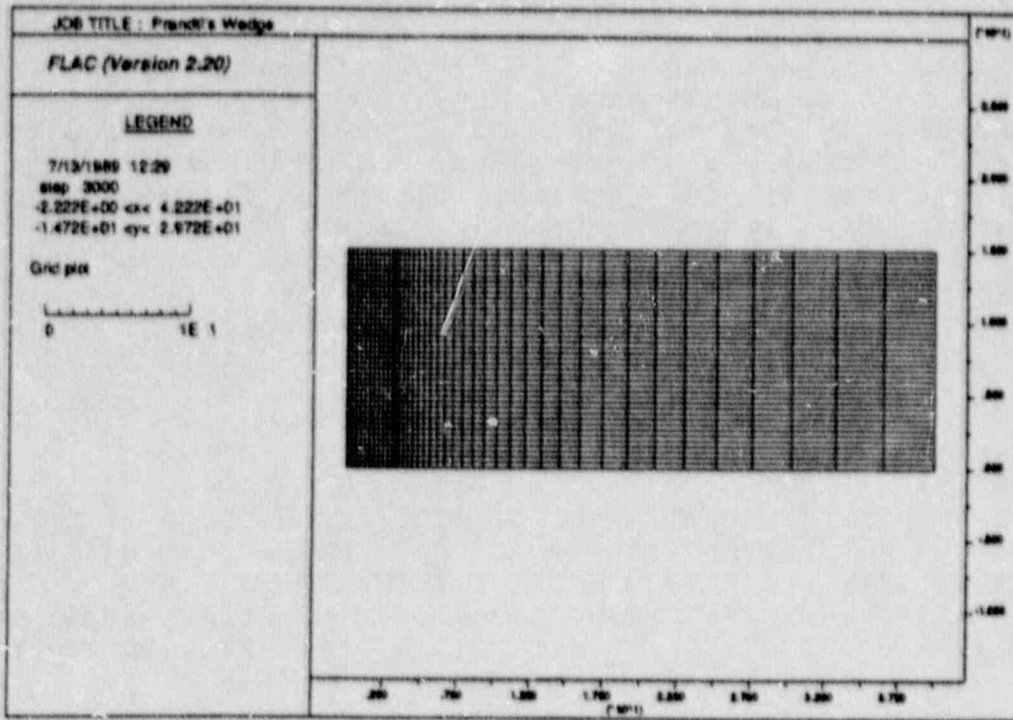
Fig. 3.2.1.2-2 FLAC Zone Geometry
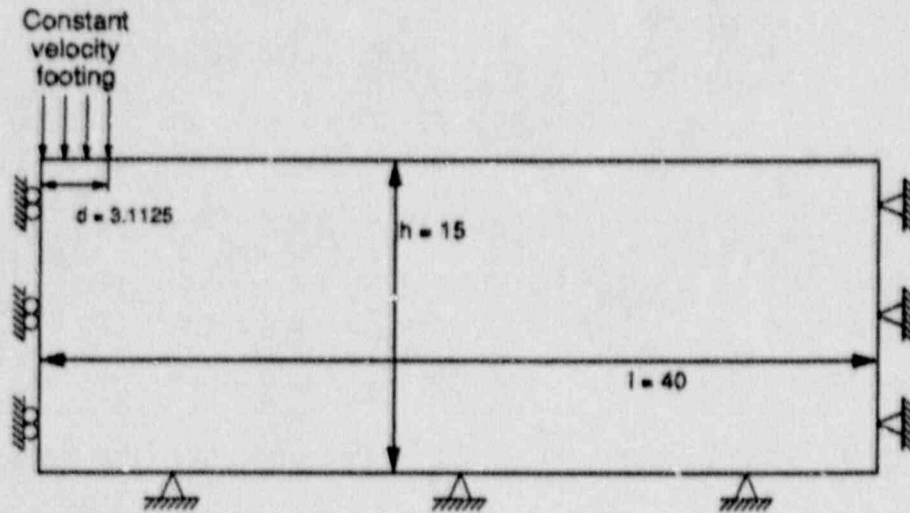
Fig. 3.2.1.2-3 FLAC Model Conditions

Small strain analysis was used to be consistent with the analytic
solution and to allow the problem to come to equilibrium without
being affected by grid deformation. The reaction forces of the
gridpoints underneath the footing were taken at intervals and di-
vided by the area of the footing to determine the bearing capa-
city. The footing width was taken to be the width over which the
constant velocity was applied plus one-half of the horizontal
width of the zone immediately adjacent to the loaded area. The
reason for this is that there is an indeterminacy in the "loaded"
area because velocity can only be applied to grid points.

Results

Figures. 3.2.1.2-4 and -5 show the model conditions at the end of
the analysis. The behavior shown is very close to that expected
from Fig. 3.2.1.2-1. Figure 3.2.1.2-6 shows a history of norm-
alized bearing capacity versus normalized vertical displacement.
The final value was 5.25, an error of 2.14% when compared to the
expected value of 5.14.
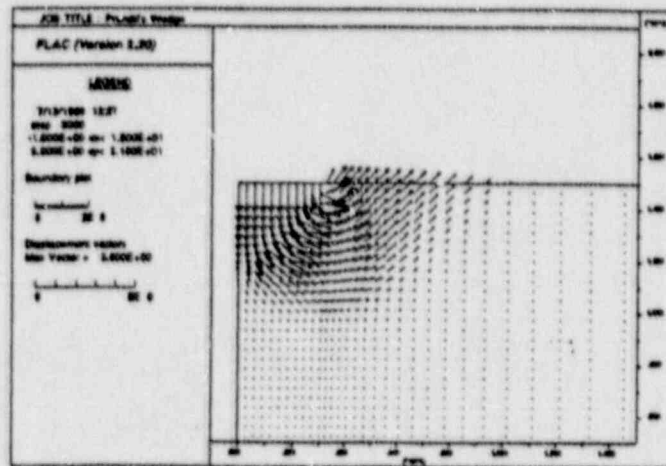
Fig. 3.2.1.2-4   Displacement Pattern Beneath Footing After 3000
                 Steps
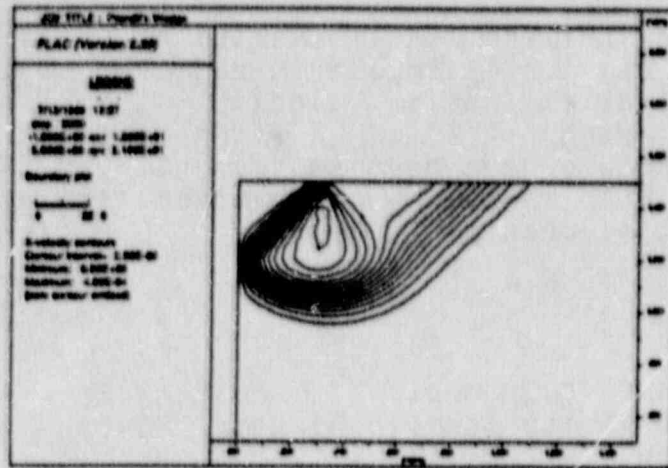
Fig. 3.2.1.2-5   Steady-State x-Velocity Contours at Collapse Load
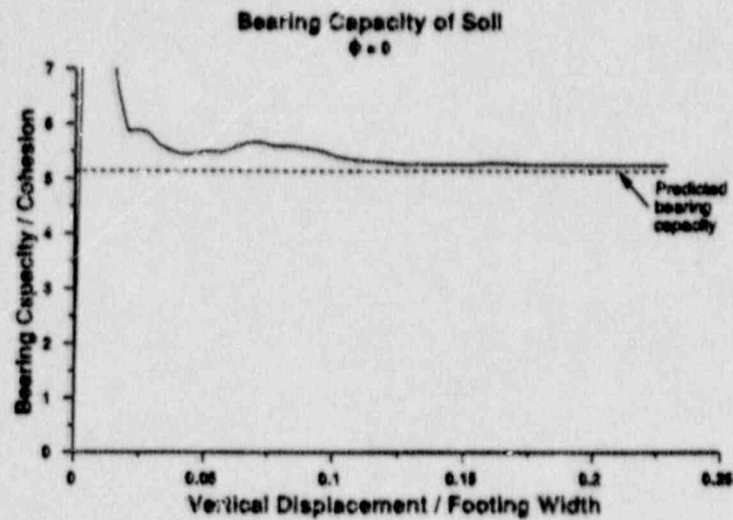
Fig. 3.2.1.2-6   History of Bearing Capacity Results

Discussion

The results shown indicate FLAC's ability to model steady plastic
flow. The model was not optimized in terms of problem size, dis-
cretization, or applied footing velocity. The size of the model
was excessive; a height of 10 and a width of 15 at the same zone
density would probably have been sufficient. In fact, the exam-
ple shown in the FLAC manual, which used considerably less zones,
had an error of less than 1%.

Reference

Sloan, S. W., and M. F. Randolf. "Numerical Prediction of Col-
lapse Loads Using Finite Element Methods," Int. J. Num. & Analy.
Methods in Geomech., 6, 47-76 (1982).

Terzaghi, K., and R. B. Peck. Soil Mechanics in Engineering
Practice, 2nd ed. New York: John Wiley and Sons, 1967.

Input Data File

```
************************************************************
* FLAC Verification Problem - Bearing Capacity of A Sand,
* Prandtl's Wedge
************************************************************
tit
Prandtl's Wedge
*
* Create grid
*
gr 30,30
*
* Model Mohr-Coulomb
m m
*
* Properties
*
prop s=.3e8 b=1e8 d=1000 fri=0 coh=1e5
*
* Stretch out grid boundaries
*
gen 0,0 0,15 3,15 3,0 i=1,11
gen 3,0 3,15 40,15 40,0 i=11,31 rat 1.1 1
*
* Boundary conditions
*
fix x i=1
fix x y j=1
fix x y i=41
fix x y i=1,11 j=31
*
* Velocity boundary condition to represent footing
*
ini yv=-5e-4 i=1,11 j=31
*
* Histories
*
his nste = 1
his ydis i=13
*
* Timestep
*
step 3000
*
* Save state
*
save bcap.dat
* end of problem
```

3.2.1.3 <u>Circular Tunnel in Dilatant and Non-Dilatant Mohr-Coulomb Continuum for a Non-Hydrostatic Stress Field</u>

Problem Statement

Crushing failure is identified as an important mechanism by which unlined tunnels may fail. Crushing is treated as a static phenomenon and involves massive failure around the excavation due to large-scale plastic flow. This verification example demonstrates the ability of FLAC to model large-scale plastic flow. The verification was accomplished by comparing FLAC results to those from a closed-form solution which accounts for plastic flow behavior.

The problem involves a circular tunnel subjected to a non-hydrostatic static load. The rock mass medium surrounding the tunnel is treated as an elasto-plastic material with failure defined by a Mohr-Coulomb yield function. The dilatency of the material at failure is defined by the flow rule, which is characterized by the angle of dilation. Here, the non-associated flow rule in FLAC is used to model both fully-dilatant and non-dilatant material behaviors.

Purpose

The purpose of this problem is to test the elasto-plastic material model used to describe the non-linear deformational behavior of large strain regions in FLAC. This example specifically addresses the ability of the code to simulate plastic flow accurately. In particular, the non-associated flow rule is examined.

Problem Specifications

A tunnel is excavated in a rock mass which is isotropic and elasto-plastic. The following parameters and values are used to describe the elastic and plastic behaviors:

Young's modulus (E)	11.72 GPa
Poisson's ratio (v)	0.25
cohesion (C)	9.9 MPa
angle of internal friction (ϕ)	30°

The strength parameters, C and ϕ, correspond to an unconfined compressive strength, q, of 34.5 MPa. Two tests are performed to verify the representation of dilatency in FLAC. In the first test, no dilatency is permitted (i.e., the angle of dilation is set equal to zero). In the second test, dilatant behavior is allowed, with

$$\psi = \phi = 30°$$

where ψ is the angle of dilation.

A 51 mm diameter circular hole is used for this example. A non-hydrostatic loading path is applied as an external load starting with no initial stress. The major principal stress, σ_1, applied in the vertical direction, and the minor principal stress, σ_3, applied in the horizontal direction, are both increased simultaneously in steps to peak values of $\sigma_1 = 86$ MPa and $\sigma_3 = 52$ MPa. The loading is in steps, keeping the ratio of σ_1/σ_3 constant at 1.667. The load steps shown in Table 3.2.1.3-1 (expressed in normalized form) were used. Tunnel closures (expressed as a percentage of the tunnel radius, a) are analyzed at the springline and the crown.

Table 3.2.1.3-1

LOADING STEPS USED IN ANALYSIS OF CIRCULAR TUNNEL
IN A NON-HYDROSTATIC STRESS FIELD

Step	$\dfrac{\sigma_1 + \sigma_3}{q}$	$\dfrac{\sigma_1 - \sigma_3}{q}$
0	1.0	0.25
1	1.5	0.375
2	2.0	0.5
3	2.5	0.625
4	3.0	0.75
5	3.5	0.875
6	4.0	1.0

Assumptions

Assumptions which are implicit in the theoretical solutions include the following.

1. Plane strain conditions apply, with one of the principal stresses aligned along the cylinder axis.

2. The material is homogeneous, isotropic and weightless.

3. The excavation is made instantaneously.

4. The strain field is small compared to the area of the tunnel.

5. The material is elastic, perfectly plastic.

6. The stress field is non-hydrostatic, with σ_1/σ_3 constant at 1.667.

7. The loading is static, and the load path is independent.

Analytical Solutions

Two conventional closed-form techniques used for preliminary analyses of circular tunnels subjected to far-field mechanical loading are the solutions presented by Newmark et al. (1970) and Hendron and Aiyer (1971). These solutions idealize the problem as a static, two-dimensional analysis of a circular tunnel in a hydrostatic stress field. The surrounding medium is treated as an elasto-plastic material with failure defined by a Mohr-Coulomb yield function. The dilatency of the material at failure is defined by the plasticity flow rule, which is characterized by the angle of dilation. The Newmark solution assumes a fully non-associated flow rule (i.e., no dilatancy occurs at failure). The Hendron and Aiyer solution assumes an associated flow rule (i.e., the angle of dilation equals the friction angle).

Detournay (1983) provided an extension to the solution for non-hydrostatic loading by the development of a semi-analytical technique. This approach applies for arbitrary dilatancy of the material and, therefore, makes the solutions of Newmark and Hendron

and Aiyer special cases of the Detournay solution. For this reason, the Detournay solution was selected as a more rigorous verification test of FLAC.

It is important to note that all three solutions are based on infinitesimal (small) strain theory, which assumes that the initial geometry of a deforming body is not appreciably altered during the deformation process. The consequence of this assumption is discussed later.

Detournay developed a set of design charts which consist of contours of springline and crown displacement. Figure 3.2.1.3-1 presents two charts, one for dilation angle equal to 30°, and one for dilation angle equal to zero. The normalized displacements for any particular free field stresses can be read from the charts by interpolating between the plotted contours. Radial displacements (U_r) can be calculated from the normalized displacements (U^*_r) from :

$$U_r = \frac{aq}{2G} U_r^*$$

where G is the elastic shear modulus of the material.

Alternatively, the percentage closure (u_r) can be expressed:

$$u_r = \frac{50q}{G} U_r^* \quad (\%)$$
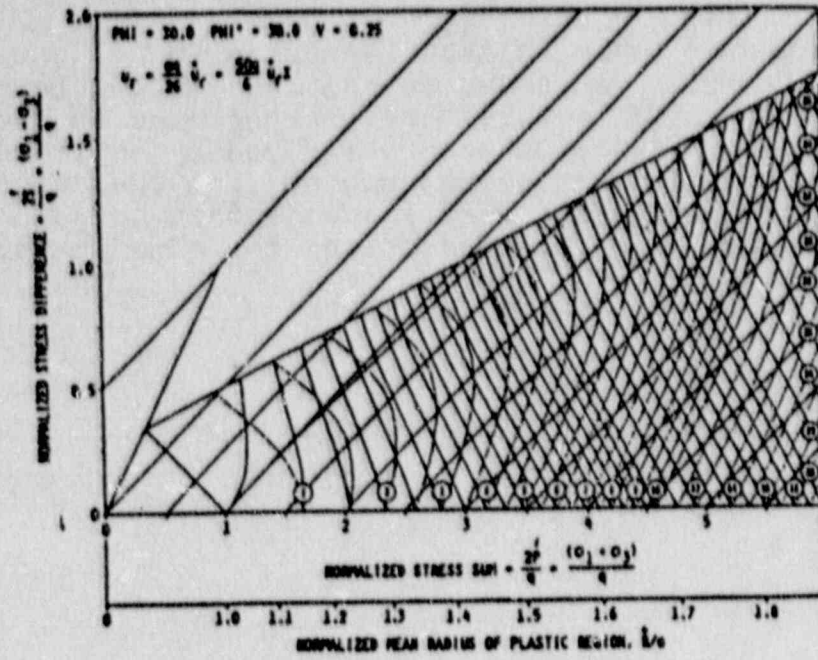
(a) fully-dilatant ($\phi = \psi = 30°$)
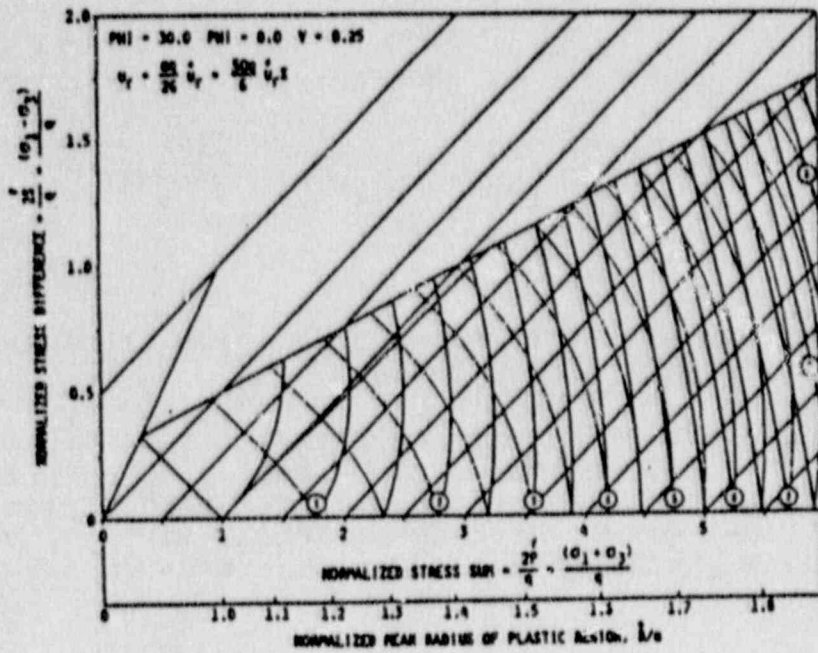
(b) no dilatancy ($\phi = 30°$; $\psi = 0$)

Fig. 3.2.1.3-i   Normalized Radial Displacements (U_r^*) of the Springline (Solid) and Crown (Dashed) Results of Closed-Form Solution [after St. John et al., 1984]

These displacements apply for the case of a tunnel excavation in a rock mass previously stressed to the far-field stress state. The charts therefore calculate displacements due to the initial state of stress. The displacements induced by additional external loading differ from those calculated from the charts by an amount equal to the elastic displacements that would occur in the absence of the tunnel. The corrections for added external loading are:

at the crown

$$(\Delta U_r^*)_c = (1-2v) \ \frac{\sigma_1 + \sigma_3}{2q} + \frac{\sigma_1 - \sigma_3}{2q}$$

at the springline

$$(\Delta U_r^*)_s = (1-2v) \ \frac{\sigma_1 + \sigma_3}{2q} - \frac{\sigma_1 - \sigma_3}{2q}$$

The percentage closure for added external loading is then

$$u_r = \frac{50q}{G} \ (U_r^* + \Delta U_r^*)$$

The calculated closures for the physical problem described above are summarized in Table 3.2.1.3-2.

These analytic results demonstrate the significant influence of dilatancy on the deformation of the tunnel at the springline. For these problem conditions, the closure at the springline is nearly three times greater for the dilatant material versus non-dilatant material, while the closure at the crown is virtually not affected.

Table 3.2.1.3-2

CALCULATED CLOSURE FROM DETOURNAY SOLUTION

$\dfrac{\sigma_1 - \sigma_3}{q}$	$\dfrac{\sigma_1 + \sigma_3}{q}$	Springline			Crown		
		$U_r{}^*$	$\Delta U_r{}^*$	$u_r\%$	$U_r{}^*$	$\Delta U^*{}_r$	$u_r\%$
$\psi = 0$							
0.375	1.5	0.55	0.19	0.27	1.25	0.56	0.67
0.50	2.0	0.9	0.25	0.42	1.75	0.75	0.92
0.625	2.5	1.5	0.31	0.66	2.4	0.94	1.23
0.75	3.0	2.25	0.38	0.97	3.15	1.12	1.57
0.875	3.5	3.1	0.44	1.30	3.8	1.31	1.88
1.0	4.0	4.0	0.5	1.65	4.7	1.5	2.28
$\psi = 30°$							
0.375	1.5	0.95	0.19	0.42	1.25	0.56	0.66
0.50	2.0	2.0	0.25	0.83	1.75	0.75	0.92
0.625	2.5	3.75	0.31	1.49	2.35	0.94	1.21
0.75	3.0	6.0	0.38	2.35	3.05	1.12	1.53
0.875	3.5	9.0	0.44	3.47	3.8	1.31	1.88
1.0	4.0	12.8	0.50	4.89	4.75	1.5	2.30

Computer Model

The FLAC model used for this analysis is shown in Fig. 3.2.1.3-2.
The grid consists of 900 elements, and extends 17.5 hole radii in
the vertical direction and 15.5 radii in the horizontal direc-
tion. A somewhat finer mesh is used in the area immediately sur-
rounding the hole. The rock mass is considered isotropic with
biaxial loading and, hence, is symmetric horizontally and verti-
cally. The geometry may be reduced to the quarter-symmetric sec-
tion shown in the figure. Plane strain conditions are assumed.
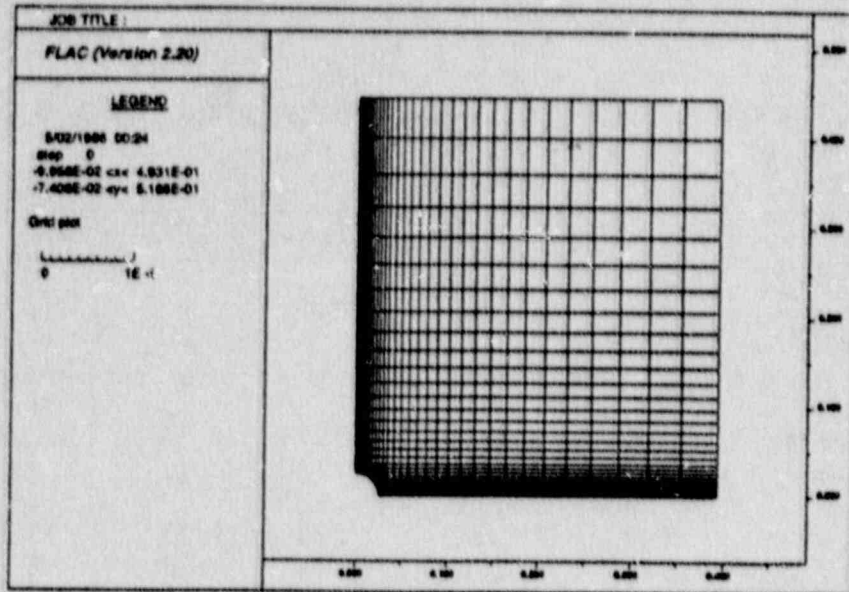
(a)   whole grid
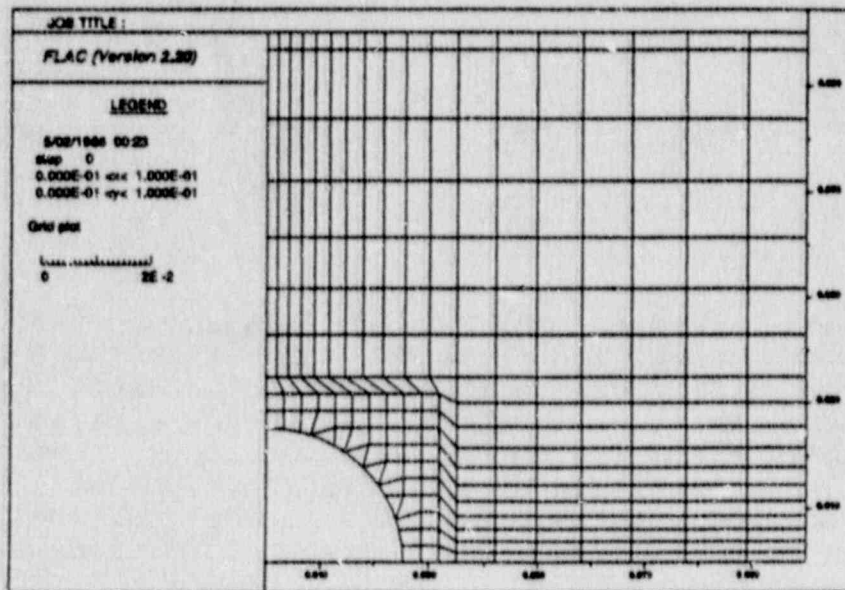
(b)   close-up of hole

Fig. 3.2.1.3-2   FLAC Grid Used in Elasto-Plastic Simulation

Results

The comparison of the FLAC results, for non-dilatant and fully-dilatant material behavior, to the Detournay solution is given in Table 3.2.1.3-3 and graphically in Fig. 3.2.1.3-3.

Table 3.2.1.3-3

COMPARISON OF FLAC RESULTS TO DETOURNAY SOLUTION

	Crown Closure			Springline Closure		
	Analytic (%)	FLAC (%)	Error (%)	Analytic (%)	FLAC (%)	Error (%)
Elastic	0.62	0.61	1.6	0.207	0.208	0.5
Elasto-plastic ($\psi = 0°$)						
Step 1	0.67	0.65	-3.0	0.27	0.25	-7.4
2	0.92	0.91	-1.1	0.42	0.41	-2.4
3	1.23	1.20	-2.4	0.66	0.63	-4.5
4	1.57	1.52	-3.2	0.97	0.89	-8.2
5	1.88	1.87	-0.5	1.30	1.22	-6.2
6	2.28	2.23	-2.2	1.65	1.59	-3.6
Elasto-plastic ($\psi = 30°$)						
Step 1	0.66	0.64	-3.0	0.42	0.37	-11.9
2	0.92	0.91	-1.1	0.83	0.78	-6.0
3	1.21	1.20	-0.1	1.49	1.38	-7.4
4	1.53	1.51	-1.3	2.35	2.19	-6.8
5	1.88	1.88	0.0	3.47	3.30	-4.9
6	2.30	2.29	-0.4	4.89	4.60	-5.0
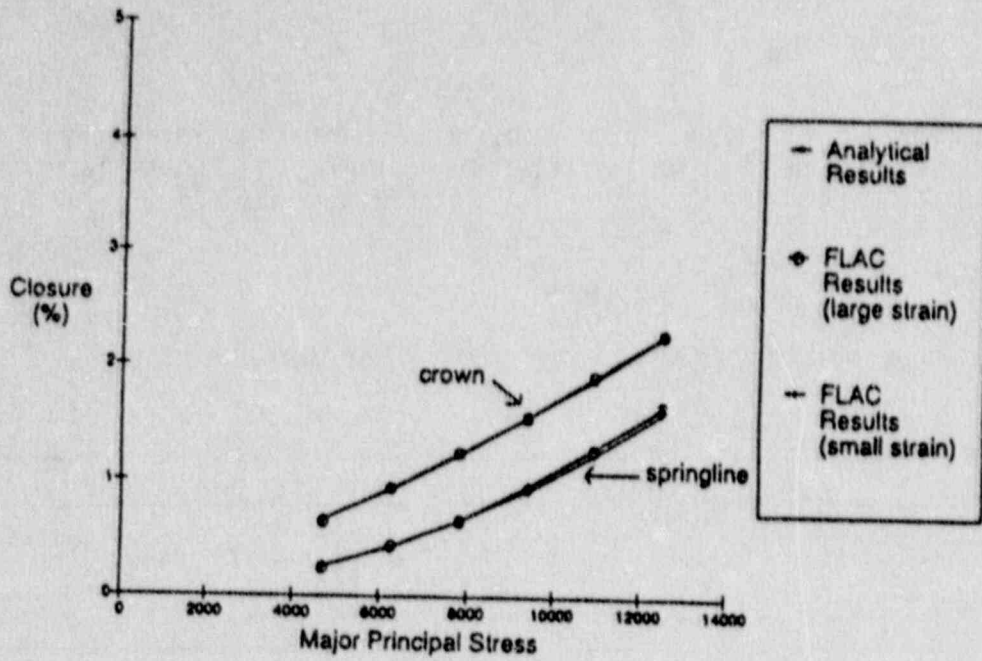
(a) $\psi = 0$
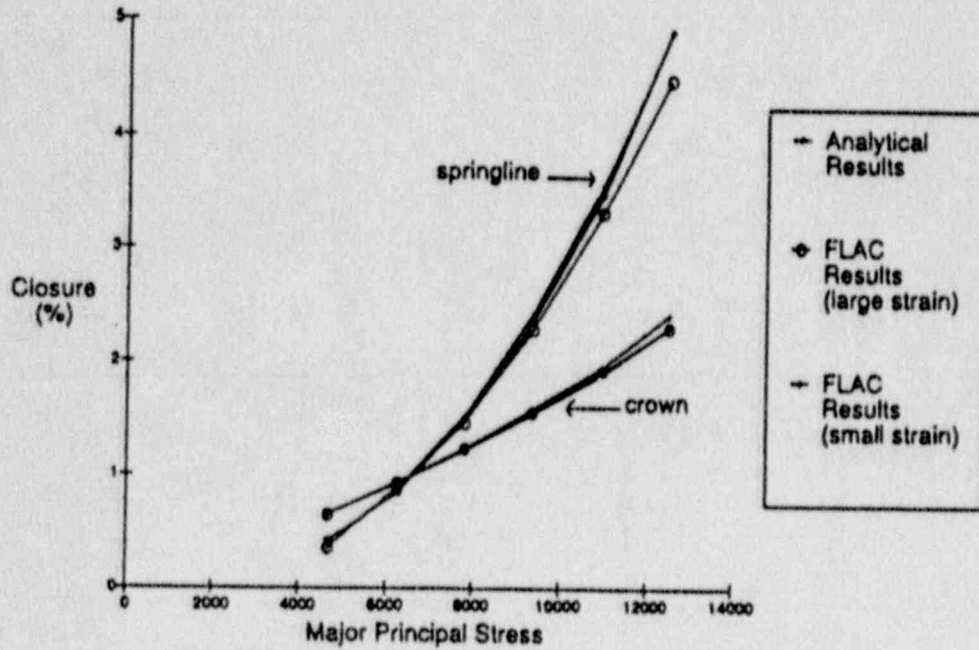
(b) $\psi = 30°$

Fig. 3.2.1.3-3 Tunnel Closure Comparison for FLAC

Discussion

In general, the agreement between the analytical results and FLAC
are reasonable. Errors are 3% of less for crown closure and gen-
erally 7% or less for springline closure. The errors here are
attributable to two sources: the number of zones in the yielding
material, and the boundary location. The error could be reduced
by increasing the number of elements in the yielding zone, and by
improving the distribution of zones around the hole. As seen,
the simplest possible mesh was used in which rectangular elements
were "pulled" out in the x- and y-directions to represent infi-
nite boundaries. This results in a fine discretization only at
the crown and springline. A more uniform radially symmetric mesh
with constant element area would improve accuracy. Additionally,
moving boundaries further from the hole would also improve
results.

The material deformation model used in FLAC is based upon finite
strain theory. Comparisons between small- and large-strain cal-
culations made by others (e.g., Carter et al., 1977) demonstrate
that at a given strain level, compressive stresses will be higher
for a large strain calculation than for a small strain calcula-
tion. This difference is attributed to the change in stress rate
vector as well as the change in strain rate vector, which is ac-
counted for in the large strain formulation and leads to in-
creased stress concentration with increased deformation. The
small strain formulation used in the closed-form solutions thus
will give higher tunnel closure than that calculated with the
large strain formulation.

The large closure produced for the given problem conditions, par-
ticularly at the associated flow state, poses a rigorous test for
the failure model used in FLAC. Problems which involve large
strain and collapse require a numerical scheme which allows lo-
cally incompressible plastic flow.

Constant-strain triangular elements such as those used in FLAC
tend to inhibit incompressible plastic flow and may produce an
excessively stiff and incorrect calculation for plastic flow.
Nagtegaal et al. (1974) discuss procedures to improve the repre-
sentation of plastic flow for triangular elements. The mixed-
discretization procedure (Marti and Cundall, 1982), used in FLAC
(see Vol. 1, Section 3) reduces the constraints on plastic flow
by using different numerical discretization for the isotropic and
deviatoric parts of the strain tensor. This scheme works well
for uniform grids composed of equal pairs of triangular elements.
Since FLAC internally subdivides the quadrilaterals into pairs of
triangular elements, this condition is met.

References

Carter, J. P., J. R. Booker and E. H. Davis. "Finite Deformation of an Elasto-Plastic Soil," Int. J. Num. & Analy. Meth. Geomech., 1, 25-43 (1977).

Detournay, E. "Two-Dimensional Elasto-Plastic Analysis of a Deep Cylindrical Tunnel Under Non-Hydrostatic Loading," Ph.D. Thesis, University of Minnesota, 1983.

Itasca Consulting Group, Inc. FLAC (Fast Lagrangian Analysis of Continua) User's Manual. Minneapolis, Minnesota: Itasca Consulting Group, Inc., 1988.

Goodman, R. E. Introduction to Rock Mechanics. New York: John Wiley & Sons, 1980.

Hendron, A. J., Jr., and A. K. Aiyer. "Stresses and Strains Around a Cylindrical Tunnel in an Elasto-Plastic Material with Dilatancy," U.S. Army Corps of Engineers, Omaha District, January 1971.

Marti, J., and P. A. Cundall. "Mixed Discretization Procedure for Accurate Solution of Plasticity Problems," Int. J. Num. Meth. Eng., 6, 129-139 (1982).

Nagtegaal, J. C., D. M. Parks and J. R. Rice. "On Numerically Accurate Finite Element Solutions in the Fully Plastic Range," Comp. Meth. Appl. Mech., 4, 153-177 (1974).

Newmark, N. M., et al. "Ground Motion Technology Review," SAMSO, TR-70-114, Nathan M. Newmark Consulting Engineering Services (Urbana, Illinois), April 1970.

St. John, C. M., E. Detournay and C. Fairhurst. "Design Charts for a Deep Circular Tunnel Under Non-Hydrostatic Loading," in Rock Mechanics in Productivity and Protection (Proceedings of the 25th Symposium on Rock Mechanics, Northwestern University, June 1984), pp. 849-856. New York: American Institute of Mining, Metallurgical and Petroleum Engineers, Inc., 1984.

Input Data File

```
************************************************************************
* FLAC Verification Problem - Elasto-plastic response of a circular
* hole for non-dilatant material and for associated flow.
* circular 51 mm. hole in non-hydrostatic stress field
* fric = 30 deg. dil = 0  or 30 deg.
* small strain
* Compare to Detournay solution
************************************************************************
*
tit
 Dilation = 0 degrees, small strain
*
* define grid
*
gr 30 30
*
* Mohr-Coulomb model
*
m m
*
* stretch grid for outer boundaries, leaving finer mesh around hole
*
gen 0,0 0,0.035 0.035,0.035 0.035,0 i=1,12 j=1,12
gen .035,.035 .035,.4445 .3935,.4445 .3935,.035 rat 1.1 1.1 i=12,31
j=12,31
gen 0,.035 0,.4445 .035,.4445 .035,.035 rat 1.1 1.1 i=1,12 j=12,31
gen .035,0 .035,.035 .3935,.035 .3935,0 rat 1.1 1.1 i=12,31 j=1,12
*
* generate quarter circle for hole
*
gen arc 0,0 0.0254,0 90
*
* material properties, put cohesion high initially for
* elastic solution
*
prop den=1850 bulk=7.814e9 she=4.69e9
prop coh=9.95e20 fri=30.0 dil=30.0
*
* boundary conditions
*
fix y j=1
fix x i=1
apply press = 32.32e6 i=1,31 j=31
apply press = 19.39e6 i=31 j=31,1
*
```

```
* time histories
*
his nste=50
his unbal
his syy i=16 j=30
his sxx i=30 j=16
his xdis i=9 j=1
his ydis i=1 j=9
*
*excavate hole in unstressed plate
*solve for elastic solution
model null reg 1 1
*
*timestep to equilibrium
*
step 4000
save elastic.sav
*
*reset plasticity properties, continue stepping to equilibrium after
*each load increment
*
prop  dil = 0.0 coh=9.95e6
*
*step to equilibrium
*
step 4000
*new load increment
apply press = 43.09e6 i=1,31 j=31
apply press = 25.86e6 i=31 j=31,1
step 4000
apply press = 53.86e6 i=1,31 j=31
apply press = 32.32e6 i=31 j=31,1
step 4000
apply press = 64.64e6 i=1,31 j=31
apply press = 38.78e6 i=31 j=31,1
step 4000
apply press = 75.42e6 i=1,31 j=31
apply press = 45.24e6 i=31 j=31,1
step 4000
apply press = 86.19e6 i=1,31 j=31
apply press = 51.71e6 i=31 j=31,1
step 4000
return
*end of problem
```

3.2.1.4 Lined Circular Tunnel In an Elastic Continuum Subjected to Non-Hydrostatic Stress

Problem Statement

This problem concerns the analysis of a circular tunnel in an elastic continuum which is lined with a concrete liner that is in intimate contact with the surrounding mass. The medium is subjected to an anisotropic biaxial stress field at infinity.

Purpose

The purpose of this problem is to check the complex interactions which occur between the rock mass and the liner. The problem will check for proper operation of the structural element formulation as well as the coupling between the rock mass and liner. A previous problem (Section 3.2.1.1) examined the two-dimensional continuum solution for an elastic hole in a plate.

Problem Specifications

A tunnel of radius r is excavated in a pre-stressed body subjected to a biaxial stress field, σ_{xx}, σ_{yy}, applied at infinity. The following parameters and values are used to describe the problem.

Geometry

excavated tunnel radius (m)	a = 2.5

Material Properties

modulus of elasticity (GPa)	E = 6
Poisson's ratio	v = 0.2
density (kg/m³)	ρ = 3000

<u>In-Situ Stresses</u>

horizontal stress (MPa)	$\sigma_{xx} = 30$
vertical stress (MPa)	$\sigma_{yy} = 15$

<u>Tunnel Lining Properties</u>

thickness (m)	$t = 0.5$
modulus of elasticity (GPa)	$E = 20$
Poisson's ratio	$v = 0.20$
density (kg/m³)	$\rho = 3000$

Note that the density is not required by the analytical solution, but some value must be provided in FLAC. The solution is independent of the choice of density.

<u>Assumptions</u>

Assumptions which are implicit in the theoretical solutions include the following.

1. Plane strain conditions apply, with one of the principal stresses aligned with the tunnel axis.

2. The material is homogeneous, isotropic and weightless.

3. The liner and medium are both linear-elastic materials.

4. The lining is installed coincidentally with tunnel excavation.

5. The lining is bonded to the surrounding material so no slip or separation of material occurs.

Analytic Solution

The analytic solution for an elastic liner embedded in an elastic solid with non-slipping interface is given by Einstein and Schwartz (1979). The thrust or axial force in the liner, N, and bending moment, M, are given by the following expressions.

$$\frac{N}{P\,r} = \frac{1}{2}\,(1 + K)\,(1 - a_0^*) + \frac{1}{2}\,(1 - K)\,(1 + 2a_2^*)\,\cos 2\theta$$

$$\frac{M}{P\,r^2} = \frac{1}{4}\,(1 - K)\,(1 - 2a_2^* + 2b_2^*)\,\cos 2\theta$$

where P = vertical stress component,

   K = ratio of horizontal to vertical stress,

   E = Young's modulus of the rock,

   ν = Poisson's ratio of the rock,

   E_s = Young's modulus of the liner,

   ν_s = Poisson's ratio of the liner,

   A = cross-sectional area of the liner for a 1 m long section,

   θ = angular location from the horizontal,

   r = radius of the tunnel,

$$a_0^* = \frac{C^* F^* (1 - \nu)}{C^* + F^* + C^* F^* (1 - \nu)}\,,$$

$$a_2^* = \frac{(F^* + 6)(1 - \nu)}{2F^*(1 - \nu) + 6(5 - 6\nu)}\,,$$

$$\beta = \frac{(6 + F^*) \, C^* \, (1 - \nu) + 2F^*\nu}{3F^* + 3C^* + 2C^* \, F^* \, (1 - \nu)},$$

$$b_2^* = \frac{C^* \, (1 - \nu)}{2 \, (C^* \, (1 - \nu) + 4\nu - 6\beta - 3\beta \, C^* \, (1 - \nu)},$$

$$C^* = \frac{E \, r \, (1 - \nu_s^2)}{E_s \, A \, (1 - \nu^2)}, \text{ and}$$

$$F^* = \frac{E \, r^3 \, (1 - \nu_s^*)}{E_s \, I \, (1 - \nu^2)}.$$

Computer Model

The problem is symmetrical about the vertical axis, allowing a
1/2-symmetry geometry, as illustrated in Fig. 3.2.1.4-1. A total
of 1440 elements are used, with the boundaries placed at 20 radii
from the hole center. Pressure boundaries are used to apply the
in-situ stress state. A total of 18 elements (19 nodes) define
the boundary of the half circle. Structural elements are con-
nected between successive nodes on the boundary periphery. The
nodes of the grid along the vertical boundary are fixed in the
horizontal direction to represent a symmetry line. The struc-
tural element nodes which lie on the symmetry line are given
fixed rotations, also to fulfill the symmetry condition.

Stresses are applied to the grid and allowed to equilibrate prior
to excavation of the hole. The hole is excavated, and the struc-
tural elements placed simultaneously. The body is then time-
stepped to equilibrium.
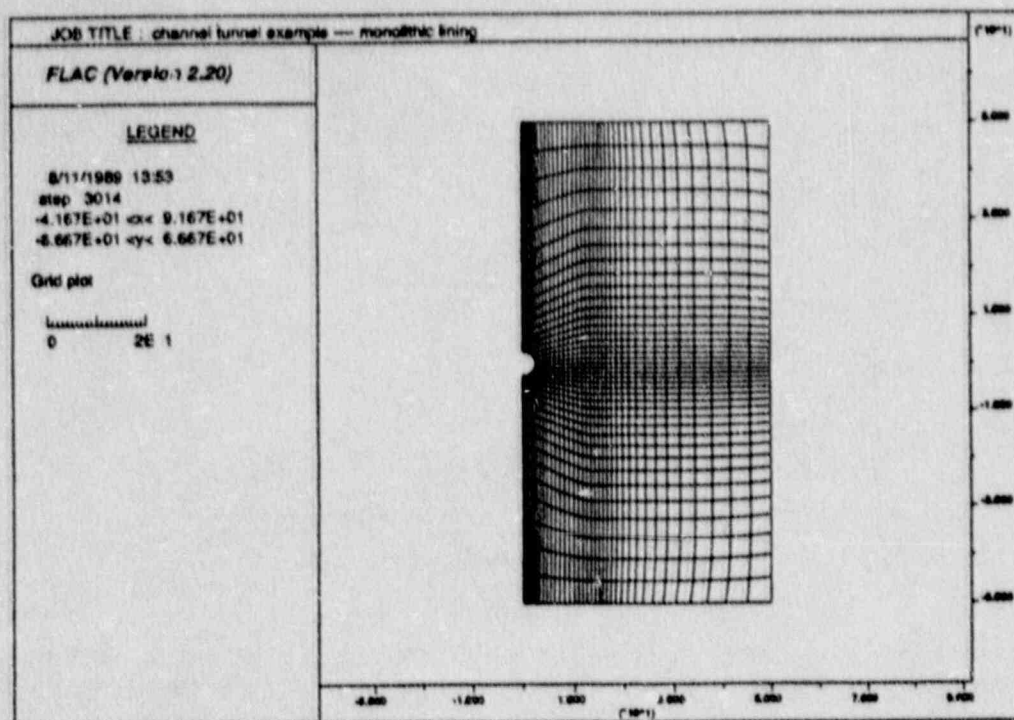
Fig. 3.2.1.4-1   FLAC Grid

Results

The results given in Figs. 3.2.1.4-2 and -3 show a comparison of the FLAC and Einstein analytical solutions for the axial forces (thrust) in the structural elements and the moments at the nodes as functions of the angle counterclockwise from the horizontal axis. The axial forces have a maximum error of roughly 3.5% at the symmetry line. The moments follow the analytically-predicted behavior fairly well, with errors at the symmetry line less than 5%.
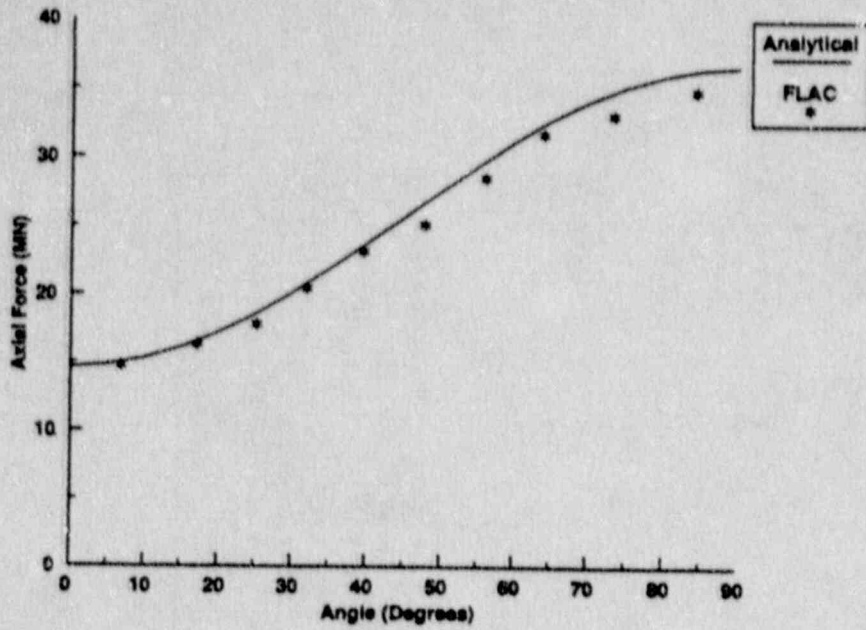
Fig. 3.2.1.4-2   Liner Axial Force Distribution as a Function of Angle Counterclockwise from the Horizontal
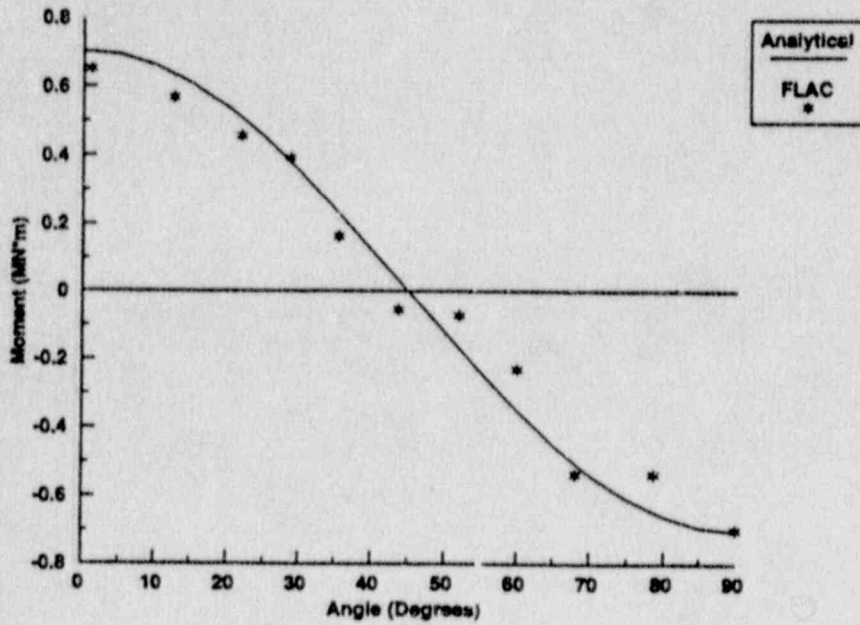
Fig. 3.2.1.4-3   Liner Moment Distribution as a Function of Angle Counterclockwise from the Horizontal

Discussion

The somewhat erratic behavior of the FLAC solution for bending
moments is a result of the irregular nature of the zoning around
the tunnel periphery. Figure 3.2.1.4-4 shows a close-up view of
the tunnel with beam element endpoints marked. The non-uniform
size of the zoning around the periphery results in the erratic
behavior in the bending moments. Better agreement can be ob-
tained if:

  (1) the number of zones around the periphery of the
      tunnel is increased; and

  (2) if the zones along the periphery are of uniform
      size.

For the purposes of this report, it was felt that zoning typical
of standard problems should be used and, therefore, no attempt
was made to provide a geometry which would minimize the error.
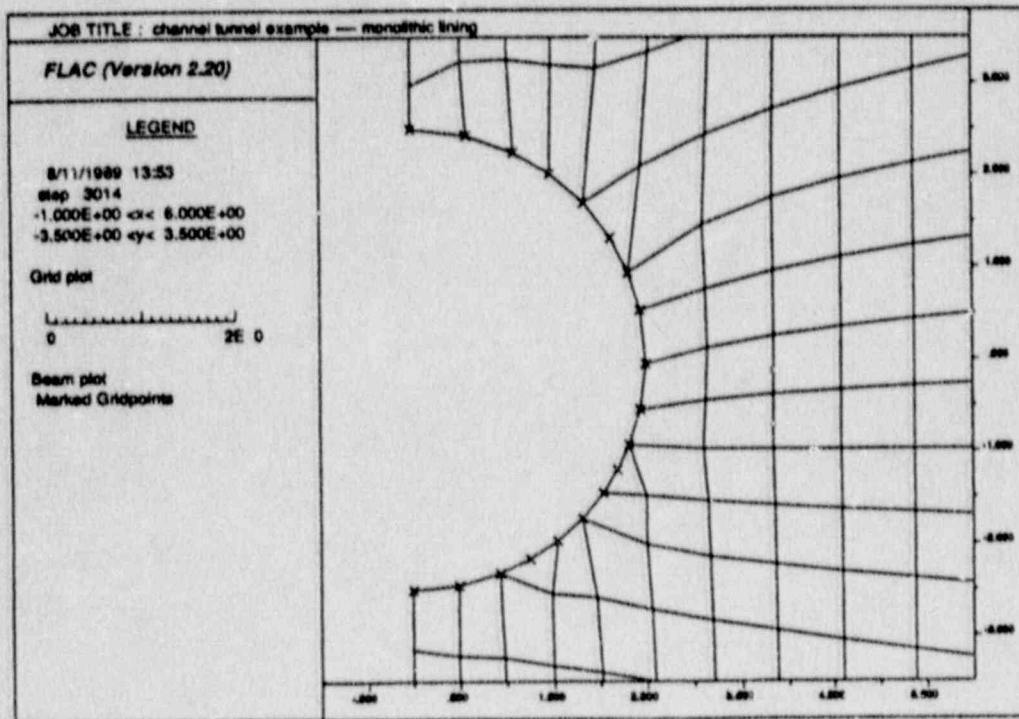
Fig. 3.2.1.4-4 Close-Up View of the Hole, Showing Beam Elements

Reference

Einstein, H. H., and C. W. Schwartz. "Simplified Analysis for Tunnel Supports," J. Geotech. Engr. Div., 499-518 (1979).

Data Input File

```
****************************************************************
* FLAC Verification Problem - Lined, Circular Tunnel in an
* Elastic Media.  Tunnel is Assumed to Be in Intimate Contact
* With the Surrounding  Media.  The Interface Between the
* Liner and Media is Non-Slipping.  Analytic Solution Consists
* Of Liner Axial Force and Bending Moment As Function of
* Angle Around the Tunnel.
****************************************************************
title
channel tunnel example ---- monolithic lining
*
* Form grid
*
grid 36,40
*
* Elastic rock mass
*
m e
*
* Pull grid out to represent infinite boundaries
*
gen -36 0 0 0 0 -30 -36 -30
gen 15 -1 15 50 50 50 50 -1 rat 1.15 1.1 i=21,37 j=21,41
gen 15 -50 15 -1 50 -1 50 -50 rat 1.15 0.909 i=21,37 j=1,21
gen 10 -1 10 50 15 50 15 -1 rat 1 1.1 i=15,21 j=21,41
gen 10 -50 10 -1 15 -1 15 -50  rat 1 0.909 i=15,21 j=1,21
gen 6 -1 6 50 10 50 10 -1 rat 1 1.12 i=11,15 j=21,41
gen 6 -50 6 -1 10 -1 10 -50 rat 1 0.893 i=11,15 j=1,21
gen 3 -1 3 50 6 50 6 -1 rat 1 1.14 i=7,11 j=21,41
gen 3 -50  3 -1 6 -1 6 -50 rat 1 0.877 i=7,11 j=1,21
gen 0 -1 0 50 3 50 3 -1 rat 1 1.16 i=1,7 j=21,41
gen 0 -50 0 -1 3 -1 3 -50 rat 1 0.862 i=1,7 j=1,21
*
* Tunnel represented as 1/2 circle, left hand boundary is
* A symmetry plane
*
gen arc 0,0 0,-5  180
*
* Automatically adjust grid to better conform to circular
* Tunnel
*
gen adjust
*
* Rock properties
*
prop den=1850 bulk=3.333e9 she=2.50e9
```

```
*
* Boundary and initial conditions
*
fix x i=1
apply press=15e6 from 1,41 to 37,41
apply press=30e6 from 37,41 to 37,1
apply press=15e6 from 37,1 to 1,1
ini sxx=-30e6 syy=-15e6
*
* Solve to initial equilibrium state - i.e., stresses in
* Grid, no excavation
*
solve
*
* Now, excavate tunnel and install liner at same time
* In pre-stressed rock mass
*
mod null reg=1,22
*
* concrete liner, e=20 MPa, thick=.5m
* i=(1/12)*1m*(.5m)^3
*
struct prop=1 e=20e9 a=.5 i=1.042e-2
*
* Define beam elements around tunnel to represent
* Liner
*
struct beam beg gr 1 26     end gr 2 26
struct beam beg gr 2 26     end gr 3 26
struct beam beg gr 3 26     end gr 4 26
struct beam beg gr 4 26     end gr 5 26
struct beam beg gr 5 26     end gr 5 25
struct beam beg gr 5 25     end gr 6 25
struct beam beg gr 6 25     end gr 6 24
struct beam beg gr 6 24     end gr 6 23
struct beam beg gr 6 23     end gr 6 22
struct beam beg gr 6 22     end gr 6 21
struct beam beg gr 6 21     end gr 5 21
struct beam beg gr 5 21     end gr 5 20
struct beam beg gr 5 20     end gr 5 19
struct beam beg gr 5 19     end gr 4 19
struct beam beg gr 4 19     end gr 3 19
struct beam beg gr 3 19     end gr 3 18
struct beam beg gr 3 18     end gr 2 18
struct beam beg gr 2 18     end gr 1 18
*
* Structural element boundary condition at
* Symmetry line
```

```
*
struct node=1  fix r
struct node=19 fix r
*
* Histories
*
his nste=20
his unbal
his xdis i=5 j=21
his ydis i=1 j=26
*
* Timestep problem to equilibrium
*
step 3000
*
* Save files
*
save chan.sav
* end of problem
```

3.2.1.5 Slip on a Plane of Weakness Intersecting a Circular Hole

Problem Statement

The cross-section of a circular hole intersected by a flat-lying plane of weakness is illustrated in Fig. 3.2.1.5-1. The host medium is homogeneous, isotropic and linear elastic. The shear strength of the plane of weakness is purely frictional, with an angle of friction, ϕ. As shown by Brady and Brown (1985), when the feature intersects the borehole at an angle θ, such that $\theta > \phi$, slip occurs on the feature near the boundary of the excavation. Substantial modification of the elastic state of stress occurs around the boundary of the hole and in the interior of the medium due to slip on the feature.
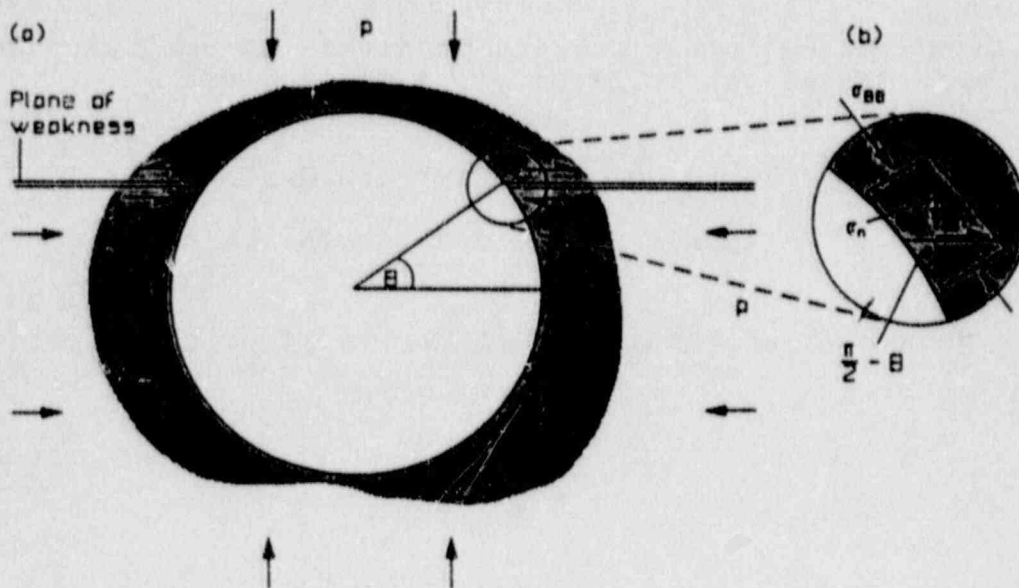
Fig. 3.2.1.5-1   Circular Hole Intersected by a Flat-Lying Plane of Weakness

Purpose

The purpose of this analysis is to demonstrate that FLAC can simulate the changes in stress distribution arising from slip on planes of weakness. The problem involves satisfaction of conditions of limiting friction on a joint, shear deformation at the joint, and redistribution of stress. This simple problem qualifies FLAC for the analysis of stress and displacement in sparsely-jointed media.

Problem Specifications

The possibility of slip on a plane of weakness is determined by the state of stress in the vicinity of the feature and its shear strength. The local state of stress is determined by the field state of stress and the shape of the excavation. For the sake of simplicity, a hydrostatic stress field, defined by

$$P = P_{xx} = P_{yy} = 10 \text{ MPa}$$

has been considered in the current problem. An arbitrary choice of rock mass mechanical properties was made, given by

$$\text{Young's modulus, } E = 10 \text{ GPa}$$

$$\text{Poisson's ratio, } \nu = 0.25$$

The rock mass bulk and shear moduli derived from these parameters are

$$K = 6.667 \text{ GPa}$$

$$G = 4.0 \text{ GPa}$$

The normal and shear stiffnesses of the joint were set high, at

$$k_n = k_s = 1 \text{ GPa m}^{-1}$$

to avoid complications in comparison with independent solutions, arising from joint deformability.

Assumptions

The plane strain condition applied in the analysis exploits the assumption that the long (antiplane) axis of the excavation is parallel to a field principal stress direction. It is also assumed that the plane of weakness strikes parallel to the axis of the excavation.

Independent Solutions

The analytical solution for the stress distribution around a circular hole in a homogeneous, isotropic linear elastic continuum is due to Kirsch (1898). For a hydrostatic stress field, the stress distribution is defined by:

$$\sigma_{rr} = p \left(1 - \frac{a^2}{r^2}\right)$$

$$\sigma_{\theta\theta} = p \left(1 + \frac{a^2}{r^2}\right) \qquad (3.2.1.5-1)$$

$$\sigma_{r\theta} = 0$$

where p = far-field hydrostatic stress,

   a = radius of the tunnel, and

   r = radius to the point of interest.

These expressions indicate that, for this initial state of stress, the stress distribution is independent of the angular coordinate of a point. A point located on the plane of weakness may be defined by a radial coordinate r, or a local coordinate x', as illustrated in Fig. 3.2.1.5-2(a). It is a simple matter to calculate the normal and shear stress components on the plane of weakness at points on the joint from Eqs. (3.2.1.5-1) and the stress transformation equations to rotate the stresses normal and parallel to the plane. The elastic distribution of normal and shear stress along the joint is shown as the solid lines in Fig. 3.2.1.5-3.
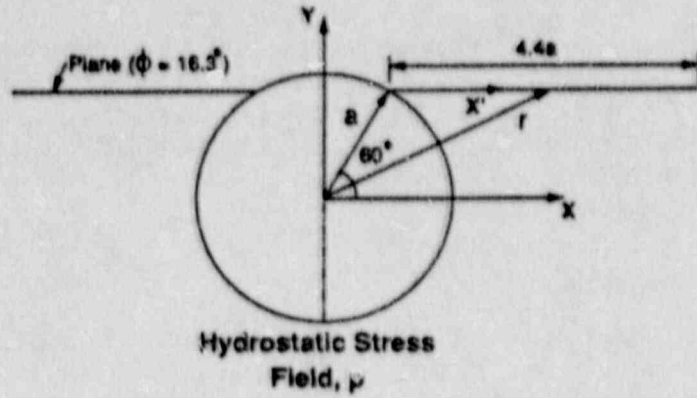
(a)
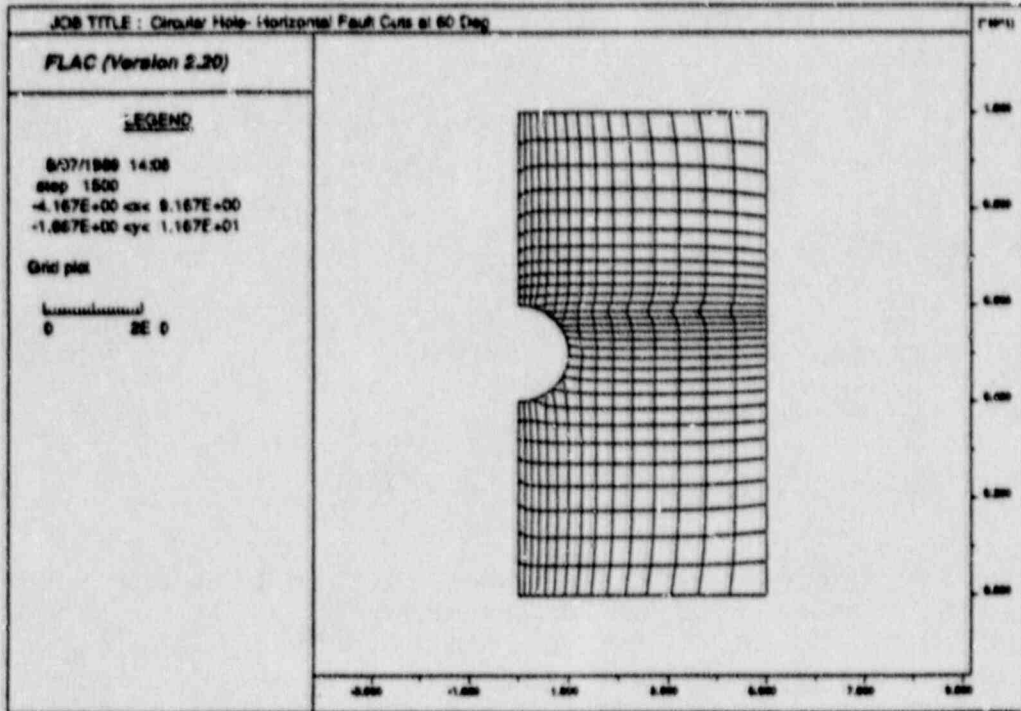
(b)

Fig. 3.2.1.5-2 (a) Problem Geometry for FLAC Analysis;
(b) FLAC Mesh
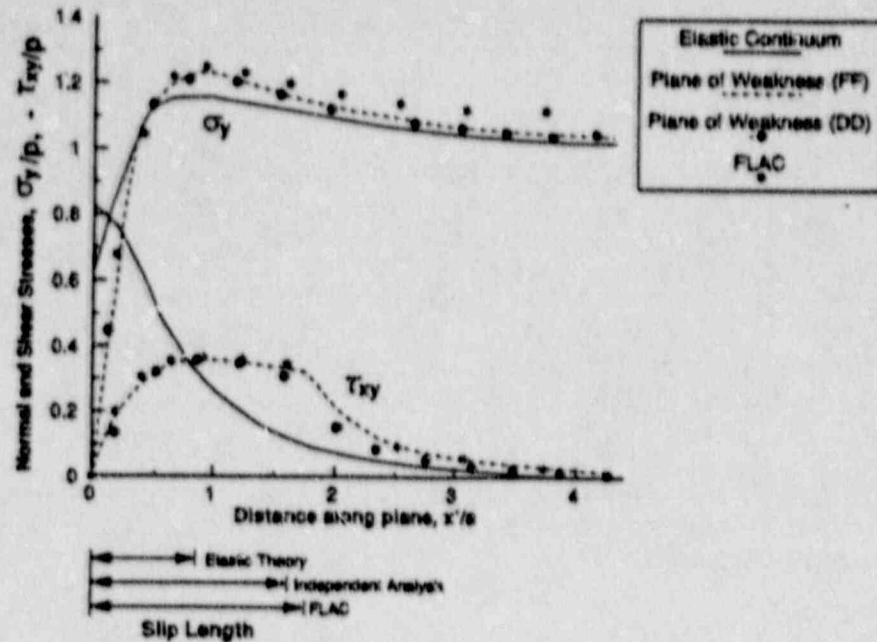
Fig. 3.2.1.5-3 Comparisons of Stress Distributions and Ranges of Slip Along Joint From FLAC and Independent Boundary Element Analysis (FF = fictitious force, DD = displacement discontinuity)

In assessing the state of stress on the joint after slip occurs, it is necessary to examine the conditions near the boundary of the excavation. Considering the small element of the boundary, shown in Fig. 3.2.1.5-1, the normal and shear stress components on the plane of weakness are given by

$$\sigma_n = \sigma_{\theta\theta} \cos^2\theta$$

$$\tau = \sigma_{\theta\theta} \sin\theta \cos\theta$$

$$(3.2.1.5-2)$$

The limiting strength of the joint at normal stress σ_n is

$$\tau = \sigma_n \tan\phi \qquad (3.2.1.5-3)$$

so that, introducing Eqs. (3.2.1.5-2),

$$\sigma_{\theta\theta} \sin\theta \cos\theta = \sigma_{\theta\theta} \cos^2\theta \tan\phi \qquad (3.2.1.5-4)$$

or

$$\tan\theta = \tan\phi$$

Thus, if $\theta = \phi$, the condition for slip on the joint is satisfied. It is observed that the sense of slip, defined by the sense of the shear stress, involves outward displacement of the upper surface of the joint relative to the lower surface.

The equilibrium state of stress at the intersection of the joint and the boundary can be determined from Eq. (3.2.1.5-3), which may be rewritten as

$$\sigma_{\theta\theta} \frac{\sin(\theta-\phi)}{\cos\phi} = 0$$

For $\theta > \phi$, this condition can be satisfied only if $\sigma_{\theta\theta} = 0$. Thus, the regions near the intersection of the opening and the joint are either destressed, or at low confining stress.

Because there is no closed-form solution of the stress and displacement distribution along the joint after slip occurs, it is necessary to compare the results of the FLAC analysis with independent numerical solutions for the problem. The results of two analyses using various boundary element methods, due to Austin et al. (1982) are presented in Fig. 3.2.1.5-3. The boundary element methods employed were a displacement discontinuity method described by Crouch (1978) and an indirect (fictitious force) scheme derived from one described by Brady and Bray (1978).

Computer Model

The model for the plane strain analysis is illustrated in Fig. 3.2.1.5-2(a). It consists of a section which is symmetrical about the vertical centerline through the excavation. The width of the half-section is 5 m, and the height is 10 m. The radius, a, of the circular excavation is 1 m, and the intersection of the joint with the excavation surface is defined by an angle of 60°. The angle of friction of the joint is 16.3°.

The FLAC model for the analysis is shown in Fig. 3.2.1.5-2(b).
The mesh is comparatively coarse, but consistent with the element
density which might be achieved in analysis of a practical prob-
lem.

Results

In the plots of normal and shear stress distribution determined
from the FLAC analysis, shown in Fig. 3.2.1.5-3, it is observed
that the plots converge toward the null state of shear stress
required by the static analysis. Inspection of Fig. 3.2.1.5-3
shows satisfactory correspondence between the stress distribution
on the joint calculated by various methods. In the case of the
shear stress distribution, the plots are virtually indistinguish-
able. For the normal stress distribution, the plots are remark-
ably similar near the excavation. It is possible that the slight
divergence between the FLAC and boundary element plots as the
outer boundary of the FLAC problem domain is approached arises
from imposed boundary conditions in the FLAC analysis. Bearing
in mind the quite substantial changes in the state of stress in
the region close to the boundary where slip occurs, it is clear
that FLAC simulates joint slip and stress redistribution satis-
factorily.

A further comparison between the FLAC and boundary element an-
alyses is provided by the predicted range of joint slip, shown in
Fig. 3.2.1.5-3. It is observed that quite close correspondence
is achieved between the various numerical solutions. In each
case, the range is greater than would be predicted from an elas-
tic analysis, which does not take account of stress redistribu-
tion.

The plots of stress distribution in Fig. 3.2.1.5-4 indicate the
way in which joint slip affects stress redistribution. The con-
tour plots of σ_{yy} and σ_{xy} show that continuity of these stress
components is maintained across the joint, as is required by
simple statics.

The sense and magnitude of displacement associated with joint
slip are illustrated in Fig. 3.2.1.5-5. The vector plots of dis-
placements indicate that the sense of slip is outward on the up-
per side of the joint, and inward on the lower side, consistent
with what was previously. The magnitude of displacement is ob-
served to be small outside the zone of slip, consistent with the
notion of elastic deformation of the joint and rock mass in these
areas.
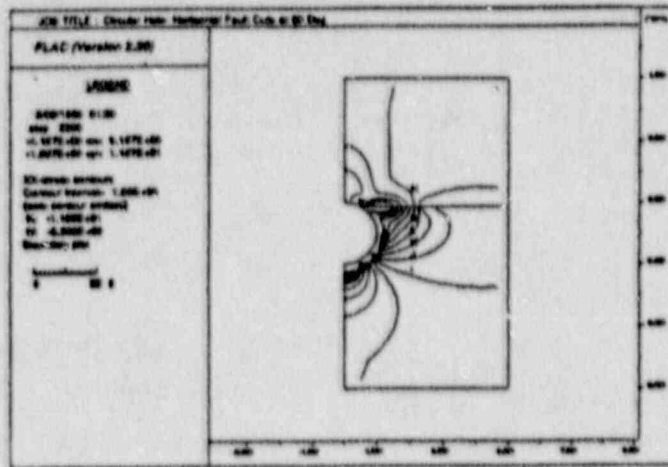
(a)
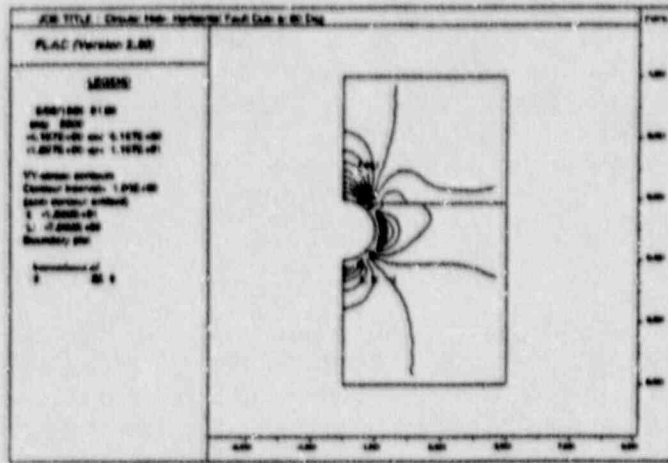
(b)
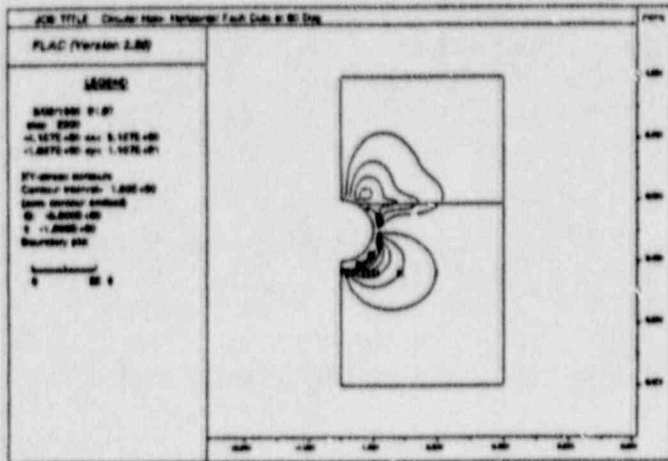
(c)

Fig. 3.2.1.5-4   Contour Plots of Stress Components: (a) σ_{xx};
(b) σ_{yy}; (c) σ_{xy}
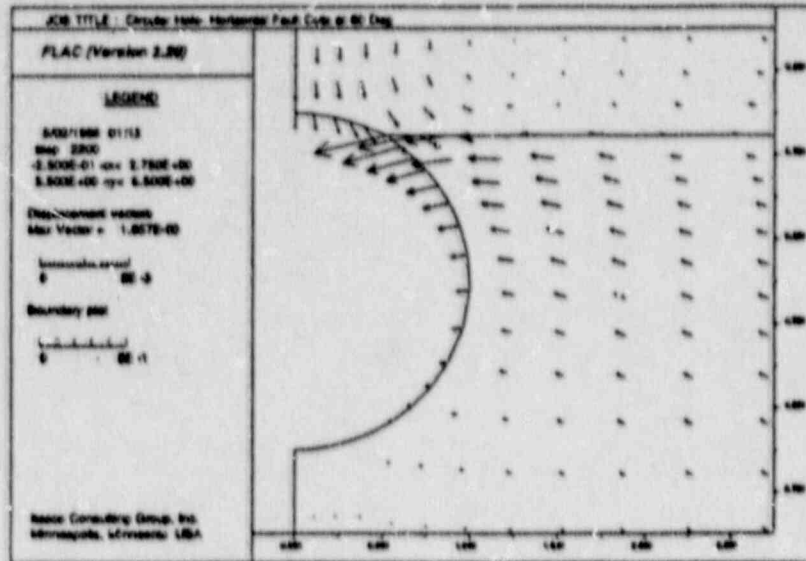
Fig. 3.2.1.5-5   Vector Plot of Slip-Induced Displacements Near
                 Excavation and Joint

Discussion

The FLAC analysis of a circular hole in a sparsely-jointed medium
confirms that the code simulates the key features of joint slip
as follows:

   (1) satisfaction of the destressed condition near the
        joint's intersection with the boundary;

   (2) correspondence with independent solutions for
        normal and shear stress distributions along the
        joint surface;

   (3) continuity of normal and shear stress across the
        joint after slip has occurred; and

   (4) step change in the joint shear displacement in the
        transition from plastic to elastic joint deforma-
        tion.

These features, and the close quantitative agreement with results from independent boundary element analysis of joint slip, indicate the suitability of FLAC for analysis of sparsely-jointed rock.

References

Austin, M. W., J. W. Bray and A. M. Crawford. "A Comparison of Two Indirect Boundary Element Formulations Incorporating Planes of Weakness," Int. J. Rock Mech. Min. Sci. & Geomech. Abstr., 19, 338-344 (1982).

Brady, B.H.G., and J. W. Bray. "The Boundary Element Method for Determining Stresses and Displacement Around Long Openings in a Triaxial Stress Field," Int. J. Rock Mech. Min. Sci. & Geomech. Abstr., 15, 21-28 (1978).

Brady, B.H.G., and E. T. Brown. Rock Mechanics for Underground Mining, 527 pp. London: George Allen and Unwin, 1985.

Crouch, S. L. "Solution of Plane Elasticity Problems By the Displacement Discontinuity Method," Int. J. Num. Meth. Engng., 10, 301-343 (1976).

Kirsch, G. "Die Theorie der Elastizitat und die Bedürfnisse der Festigkeitslehre," Veit. Ver. Deut. Ing., 42, 797-807 (1898).

Data Input File

```
****************************************************************
*FLAC Verification Problem
*Circular Hole Cut By Horizontal Fault
*Comparison To Solutions Generated From Boundary Element
*Models.  This Problem Tests The Interface Logic In FLAC
****************************************************************
title
Circular Hole- Horizontal Fault Cuts at 60 D
*
*Specify Grid
*
gr 15,31
*
*Rock Mass Elastic
*
m e
*
*Properties
*
prop s=4000 b=6667 dens=0.003
*
*Create interface by first nulling a row of zones
*
model null j=19 i=1,15
mark i=5 j=19
mark i=5 j=20
*
*Bring the two halves of the grid together
gen 0,0 0,5.866 5,5.866 5,0 rat 1.15 0.9 j=1,19
gen 0,5.866 0,10 5,10 5,5.866 rat 1.15 1.15 j=20,32
*
*Declare the two interacting faces of the interface
*
int 1 aside from 1,19 to 16,19
int 1 bside from 16,20 to 1,20
*
*Interface properties, initially glued as stresses come to
*initial stress state.  Will later allow slip for check against
*the boundary element solution.
*
int 1 fric=70 coh=1e6 kn=1e6 ks=1e6 tbond=1e6 glued
*
*Form tunnel, 1/2 symmetry
*
gen arc 0,5 0,4 180
*
```

```
*Adjust grid for improved zoning
*
gen adj
mark i=5 j=18
*Horizontal B.C. on left side of model
fix x i=1
*
*Apply a pressure B.C. to 3 sides of model
*
apply press=10 j=32 i=1,16
apply press=10 i=16 j=1,19
apply press=10 i=16 j=20,32
apply press=10 j=1 i=1,16
*
*Initial stresses in grid
*
ini sxx=-10 syy=-10 var 0,0.3 j=1,31
*
*Set up histories
*
his nstep=10
his xdis i=7 j=13
his ydis i=1 j=21
his syy i=7 j=13
his sxx i=1 j=21
his ydis i=8 j=32
his ydis i=8 j=1
his xdis i=5 j=19
his xdis i=10 j=19
his xdis i=10 j=20
*
*Timestep a few times to make certain that interface
*is in equilibrium with initial stresses
*
step 100
ini xdis=0 ydis=0
*
*Save initial state
*
save circut1.sav
*
*Null out (excavate) the region defined by the tunnel
*Two commands necessary since tunnel intersected by interface
*
mod null reg=1,18
mod null reg=1,20
*
* Solve continuum problem
```

```
*
step 700
*
* Save elastic solution
*
save circut2.sav
*
* Now, reset displacements and unglue interface
* Solution indicates slip-induced displacements
*
ini xdis=0 ydis=0
int 1 fric=16.3 coh=0 kn=1e6 ks=1e6 tbond=0 unglued
*
* Timestep problem to final equilibrium state
*
step 1500
*
*Save final state
*
save circut3.sav
*end of problem
```

3.2.1.6 Spherical Hole in an Infinite Elastic Continuum Under Hydrostatic Stress Field

Problem Statement

This problem concerns the determination of stresses and displacements for the case of a spherical cavity in an infinite elastic media subject to hydrostatic in-situ stresses.
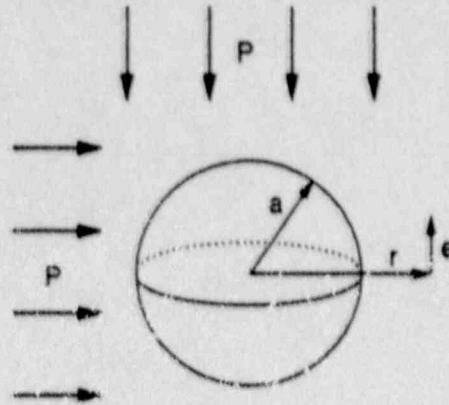
Fig. 3.2.1.6-1 Spherical Cavity in an Infinite Body

Purpose

The purpose of this problem is to determine FLAC's accuracy on a three-dimensional problem using axisymmetry.

Problem Specifications

A spherical cavity is in an infinite elastic body under a uniform in-situ compressive stress of 30 MPa. The material containing the cavity has the following properties:

shear modulus (G)	2.9 GPa
bulk modulus (K)	3.9 GPa
density (ρ)	2500 kg/m^3

Assumptions

The spherical cavity is a homogeneous, isotropic, continuous, infinite media. The material is linearly elastic, and it is assumed that the problem is symmetric about all three Cartesian axes.

Analytic Solution

The radial displacement around a spherical cavity in an infinite elastic media under a hydrostatic stress field is given by Goodman (1980, p. 220):

$$u_r(r) = \frac{p\,a^3}{4r^2\,G}$$

Timenshenko and Goodier (1970, p. 395) provide a solution to the stress field in a hollow sphere subject to internal and external pressure:

$$\sigma_r = \frac{p_o\,b^3\,(r^3 - a^3)}{r^3\,(a^3 - b^3)} + \frac{p_i\,a^3\,(b^3 - r^3)}{r^3\,(a^3 - b^3)}$$

$$\sigma_\theta = \frac{p_o\,b^3\,(2r^3 + a^3)}{2r^3\,(a^3 - b^3)} + \frac{p_i\,a^3\,(2r^3 + b^3)}{2r^3\,(a^3 - b^3)}$$

where p = the external (o) and internal (i) pressure,

b = the outside radius, and

a = the inside radius.

The solution to the problem of a spherical cavity in an infinite media is determined by setting $p_i = 0$ and finding the limit as b approaches infinity. Normalizing by the in-situ stress value, the final solution is:

$$\frac{\sigma_r}{P_o} = \frac{r^3 - a^3}{r^3}$$

$$\frac{\sigma_\theta}{P_o} = \frac{a^3 + 2r^3}{2r^3}$$

Computer Model

Figure 3.2.1.6-2 shows the model used for the FLAC analysis.
Using axisymmetry, one-quarter of the problem was divided into
900 quadrilateral finite difference zones, as shown in Figs.
3.2.1.6-3 and -4. Pressure equal to the in-situ stress was ap-
plied to both free faces and allowed to equilibrate prior to ex-
cavation of the cavity. The problem was timestepped 1000 times
to ensure that equilibrium was achieved.
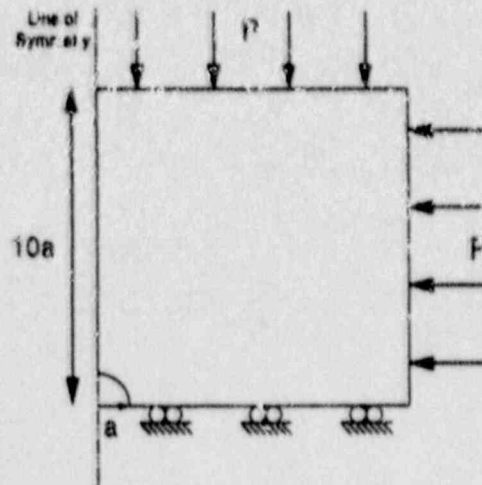
Fig. 3.2.1.6-2 Model for FLAC Analysis
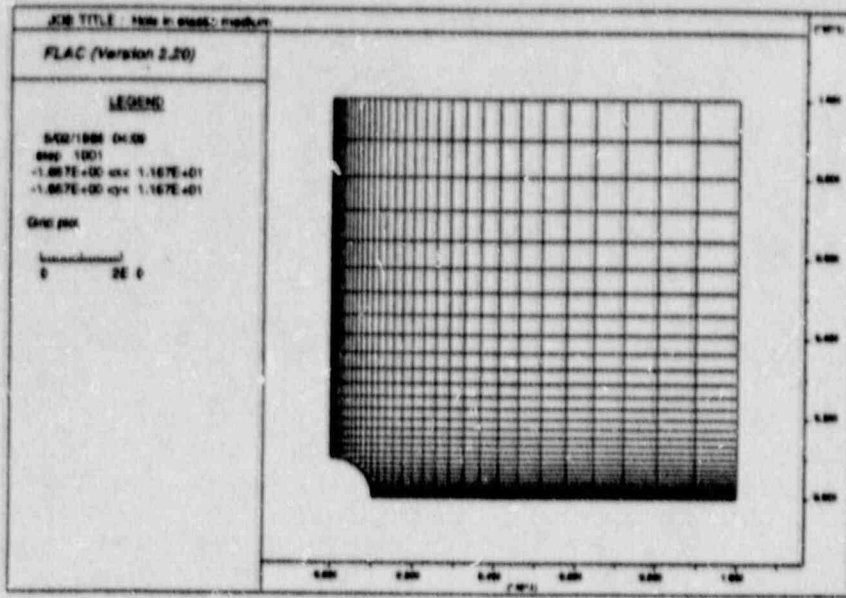
Fig. 3.2.1.6-3   FLAC Zone Geometry
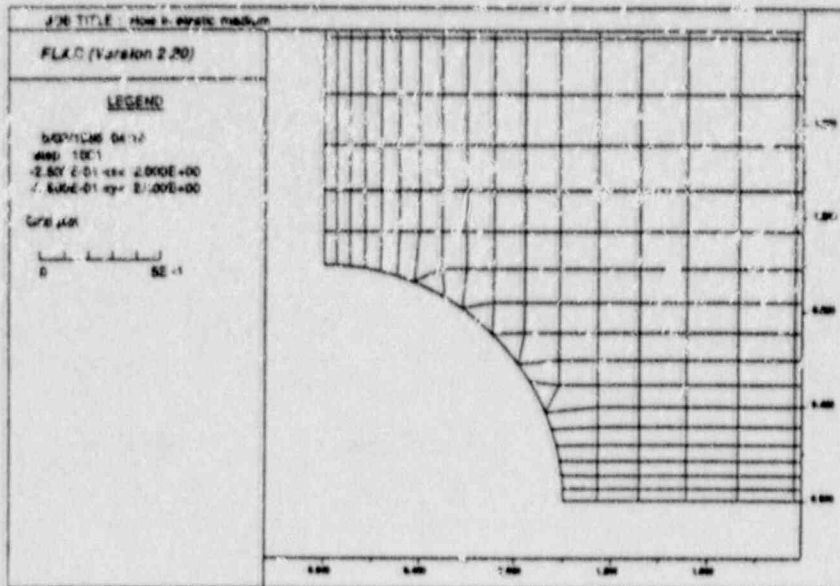
Fig. 3.2.1.6-4   FLAC Zone Geometry in Region Around Hole

Results

Figures 3.2.1.6-5 and -6 show a graphical comparison between the
radial displacement, radial and tangential stresses and the an-
alytical solution.   Table 3.2.1.6-1 shows a more detailed compar-
ison at five points along a radial line from the cavity.
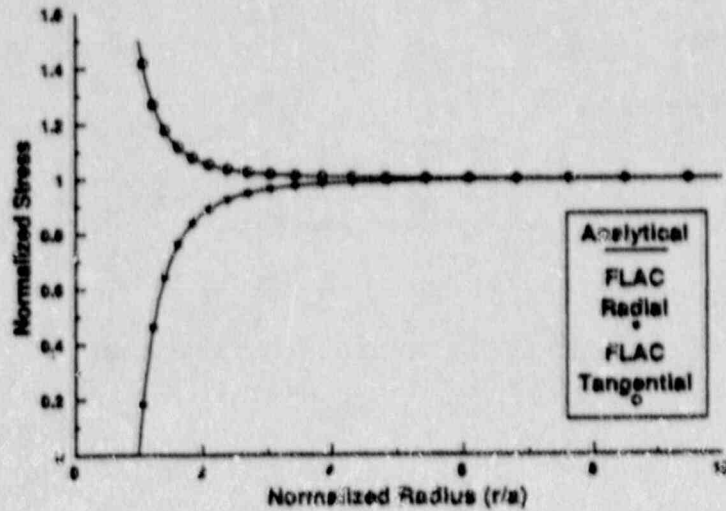
Fig. 3.2.1.6-5   Comparison of Radial (σ_r/p) and Tangential (σ_θ/p)
Stresses for FLAC and Analytic Solutions
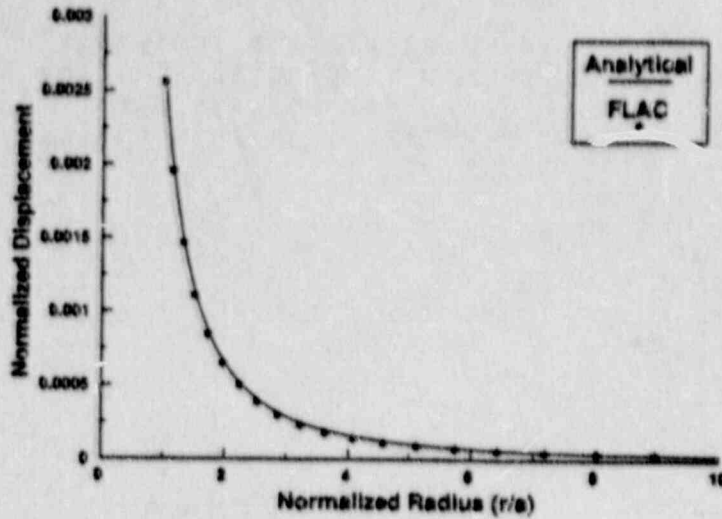
Fig. 3.2.1.6-6 Comparison of Radial Displacements (u_r/a) versus Radial Distance

Table 3.2.1.6-1

COMPARISON OF FLAC RESULTS TO ANALYTIC SOLUTION

r/a	Normalized Radial Stress			Normalized Tangential Stress		
	FLAC	Analytical	% Error	FLAC	Analytical	% Error
1.07	0.183	0.184	-0.54	1.42	1.408	0.85
1.415	0.646	0.647	-0.15	1.179	1.176	0.26
2.105	0.892	0.893	-0.11	1.056	1.054	0.19
4.33	0.989	0.988	0.10	1.007	1.006	0.10
8.09	0.997	0.996	0.10	1.003	1.002	0.10

r/a	Normalized Displacement		
	FLAC	Analytical	% Error
1.0	0.002557	0.002586	-1.12
1.51	0.00111	0.00113	-1.77
1.97	0.000649	0.000666	-2.55
4.08	0.000142	0.000155	-8.39
5.75	0.000072	0.0000782	-7.93

Discussion

The stress results from FLAC are in very close agreement with the analytic solution (4% error). The closeness of the agreement indicates that, for a stress analysis, the far boundaries (now at 10 cavity radii) probably could be closer with little loss of solution accuracy.

The displacement results near the cavity (<2% error) could be improved with a finer grid geometry and/or by increasing the free boundary distance. The increase in deviation as distance from the cavity increases is due to the pressure boundary condition used to simulate an infinite media.

References

Goodman, Richard E. Introduction to Rock Mechanics. New York: John Wiley and Sons, 1980.

Timoshenko, S. P., and J. N. Goodier. Theory of Elasticity. New York: McGraw-Hill, 1970.

Data Input File

```
**********************************************************************
* FLAC Verification Problem - Spherical Hole in an Elastic
* Material
* Under Hydrostatic Stress State
**********************************************************************
tit
 Spherical Hole in elastic medium
*
* Set axisymmetric logic
*
config ax
gr 30,30
*
* Elastic material model
*
m e
* Stretch grid to represent infinite boundaries
*
gen 0,0 0,10 10,10 10,0 rat 1.11 1.11
*
* Generate arc of quarter symmetry
*
gen arc 0,0 1,0 90
*
* Properties
*
prop s=2.9e9 b=3.9e9 dens=2500
*
* Initial stresses
*
ini sxx=-30e6
ini syy -30e6
ini szz -30e6
*
* Boundary conditions
*
fix x    i=1
fix y    j=1
apply press 30e6 i=1,31 j=31
apply press 30e6 i=31 j=1,31
*
```

```
* Histories
*
his nste=1
his syy i=1 j=11
his sxx i=1 j=11
his ydis i=1 j=11
*
* Initial equilibrium under initial stresses before spherical
* Hole excavation
*
solve
*
* Now excavate hole in pre-stressed body
*
mod null region=1,1
*
* Timestep to equilibrium
*
step 1000
*
* Save state
*
save esax2.sav
* end of problem
```

3.2.1.7 <u>Steady-State Creep of a Circular Hole in a Hydrostatic Stress Field</u>

<u>Problem Statement</u>

A flat square plate with a small circular hole in the center is illustrated in Fig. 3.2.1.7-1. The plate is subjected to a constant pressure on all sides, and is under conditions of plane strain. The creep behavior of the plate material is defined by

$$\dot{\varepsilon}_{ij} = (3/2)^{1/2} \; (\sigma_{ij}^{d}/\bar{\sigma}) \; \dot{\varepsilon}_{c} \qquad (3.2.1.7-1)$$

where $\dot{\varepsilon}_{c} = A \; (\bar{\sigma})^{n}$,

$$\bar{\sigma} = (3/2)^{1/2} \; (\sigma_{ij}^{d} \; \sigma_{ij}^{d})^{1/2},$$

σ_{ij}^{d} = ij-components of deviatoric stress, and

A,n = creep law parameters.
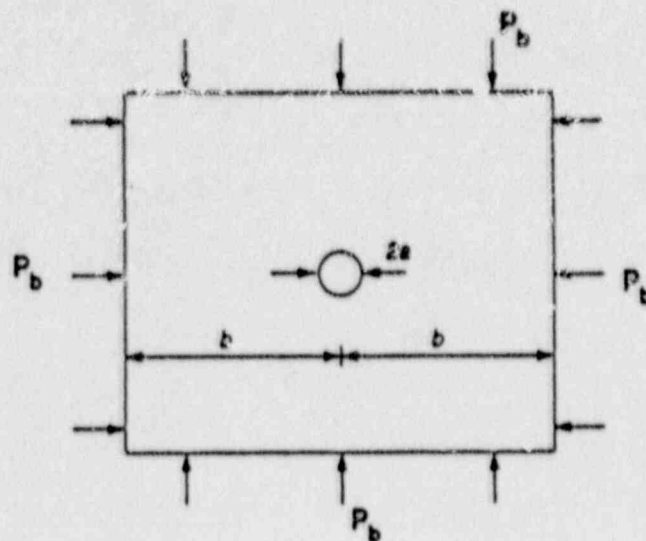
Fig. 3.2.1.7-1 Flat Plate with Circular Hole

Purpose

The purpose of this problem is to verify the ability of FLAC to properly represent the steady-state behavior of a material represented by a standard Norton Power Law (Norton, 1929). The simple single and two-component Norton Law is often used to represent the steady-state creep rate for rock salt or potash.

Problem Specifications

Any modeling of creep behavior is very sensitive to the location of problem boundaries. Here, the plate half-width, b, is set to 400 times the hole boundary in Case I, and 200 times the hole boundary in Case II. The plate is subjected to the following initial conditions:

$$\sigma_{xx} = P_b = 100 \text{ MPa}$$

$$\sigma_{yy} = P_b = 100 \text{ MPa}$$

$$\sigma_{zz} = 72.72 \text{ MPa}$$

The initial out-of-plane stress component, σ_{zz}, is determined from elastic, plane strain conditions. The far-field xx and yy stresses are held constant by applying boundary pressures equal to P_b.

The mechanical and physical properties of the plate are:

Young's Modulus, E	820 MPa
Poisson's Ratio, ν	0.3635
A	1×10^{-7} MPa^{-3} yr^{-1}
n	3

The input to FLAC requires the shear modulus, G, and the bulk modulus, K, rather than E and ν. These are given by

$$G = \frac{E}{2(1 + \nu)} = 300.67 \text{ MPa}$$

and

$$K = \frac{E}{3(1 - 2\upsilon)} = 1001.96 \text{ MPa}$$

The radius, a, of the plate is 1.0.

Assumptions

The plate is assumed to be in a state of plane strain. The plate is assumed to be isotropic with steady-state creep behavior defined by the single component law given previously. Deformations calculated are for creep strains only, and do not include elastic components.

Analytical Solution

The analytic, steady-state solution to this problem is given by van Sambeek (1989)

$$\sigma_R = -P_b \left[\frac{1 - (a/r)^{2/n}}{1 - (a/b)^{2/n}} \right]$$

$$\sigma_\theta = -P_b \left[\frac{1 - [(n-2)/n] (a/r)^{2/n}}{1 - (a/b)^{2/n}} \right] \qquad (3.2.1.7-2)$$

$$\sigma_z = \frac{\sigma_R + \sigma_\theta}{2}$$

$$\dot{u}_R(a) = -A \frac{(3)^{1/2}}{2} \left[\frac{(3)^{1/2}}{n} P_b \frac{1}{1 - (a/b)^{2/n}} \right]^n a$$

where σ_R, σ_θ are radial and tangential stress components,

P_b is the applied boundary stress,

σ_z is the out-of-plane stress component,

$\bar{u}_r$ is the radial displacement rate,

a,b are the radius of hole and half-width of plate, respectively, and

r is the radius to point of calculation.

Computer Model

FLAC was used to solve this problem for two different sets of conditions, namely:

(1) plate half-width (b) = 400 times hole radius (a), coarse grid; and

(2) plate half-width (b) = 200 times hole radius (a), fine grid.

One quarter of the plate in Fig. 3.2.1.7-1 was modeled with FLAC, as shown in Fig. 3.2.1.7-2. A pressure of 100 MPa was applied to the top and right boundaries, the bottom was restrained in the vertical direction, and the left boundary was restrained in the horizontal direction. The last two conditions are required to represent the symmetry correctly. The initial stresses were

$$\sigma_{xx} = P_b = 100 \text{ MPa}$$

$$\sigma_{yy} = P_b = 100 \text{ MPa}$$

$$\sigma_{zz} = 72.72 \text{ MPa}$$

corresponding to an elastic plate in plane strain without a hole.

The plate was allowed to come to elastic equilibrium with the hole in place by setting the creep timestep to zero. Then, creep was initiated and allowed to increase automatically until steady state was reached.
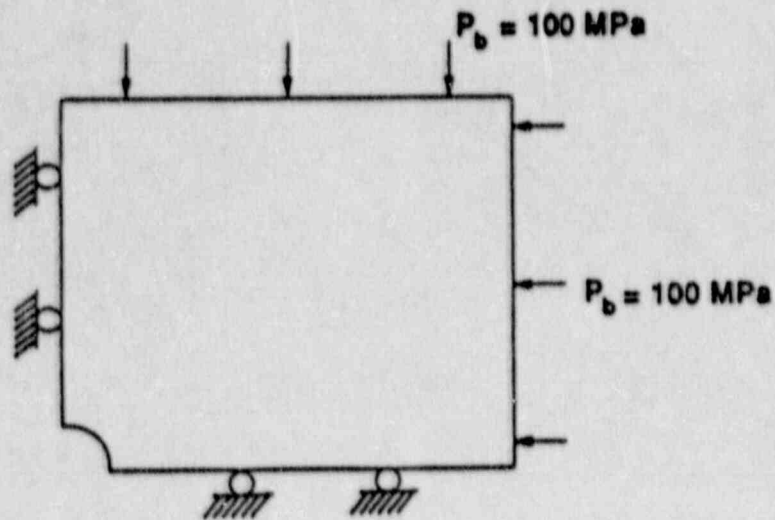
Fig. 3.1.2.7-2   FLAC Representation of a Flat Plate

Results

Case I: Plate Half-Width = 400 Times Hole Radius

A relatively course grid, consisting of only 500 zones, was used for this problem (Fig. 3.1.2.7-3). The results for this case are summarized in Figs. 3.1.2.7-4 to -7. Figure 3.2.1.7-4 shows the radial velocity (i.e., u_R) history of a point on the circumference of the hole. It is apparent from this figure that the velocity starts off significantly higher than the steady-state solution, but drops rapidly to a fairly steady value a little (3%) below the analytical solution. The initial high value is expected because the pre-creep state is far from equilibrium. The stress components obtained from FLAC are compared with the analytical solution in Figs. 3.2.1.7-5 through -7. It is obvious from these figures that the FLAC results are virtually identical to the analytical solution.

(a)   (b)
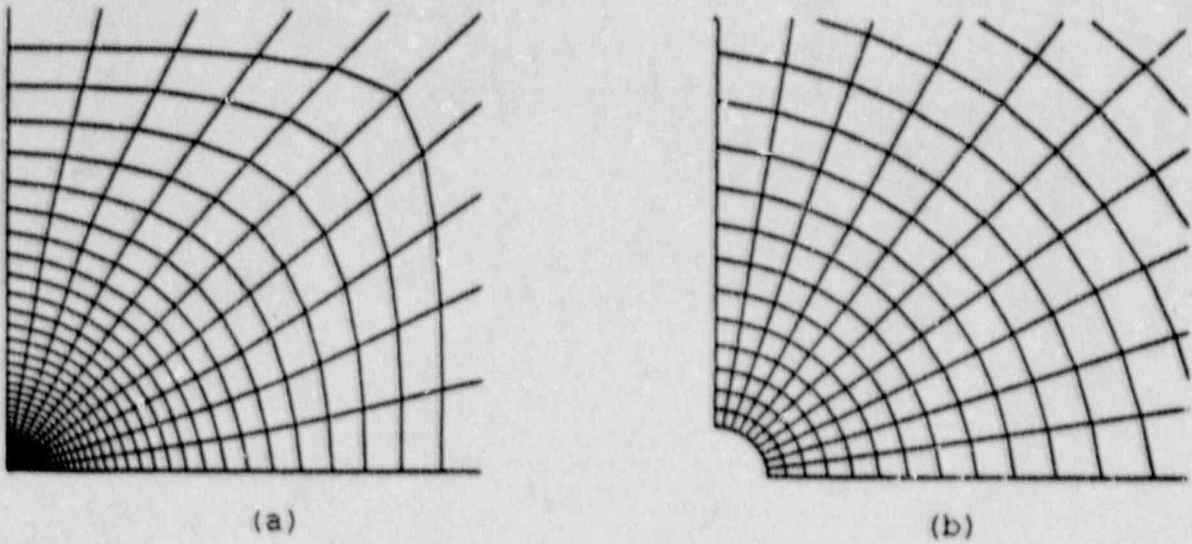
Fig. 3.2.1.7-3   (a) FLAC Grid for Case I; (b) Close-Up View of
                  Grid Around Hole
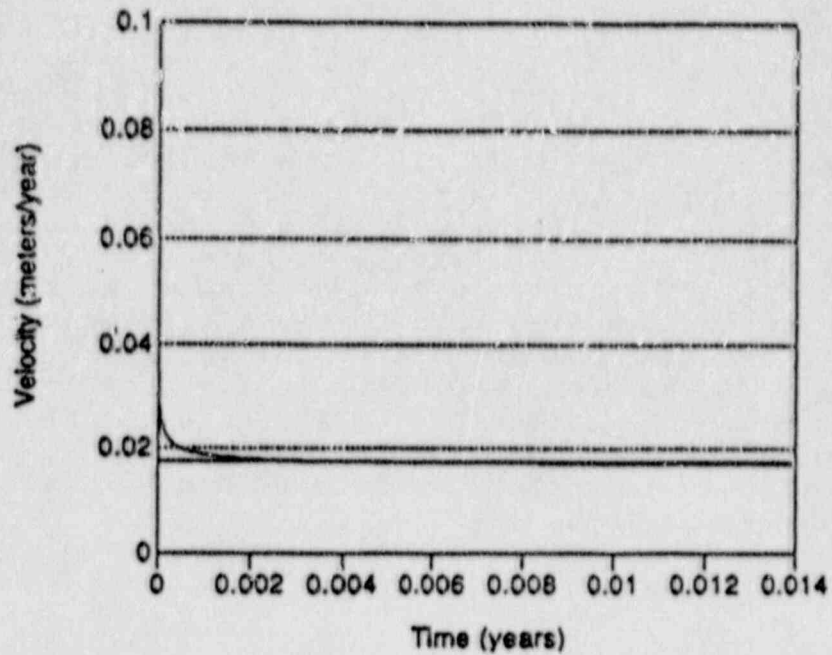
Fig. 3.2.1.7-4   Radial Velocity at Borehole Edge versus Time
                  (Case I)
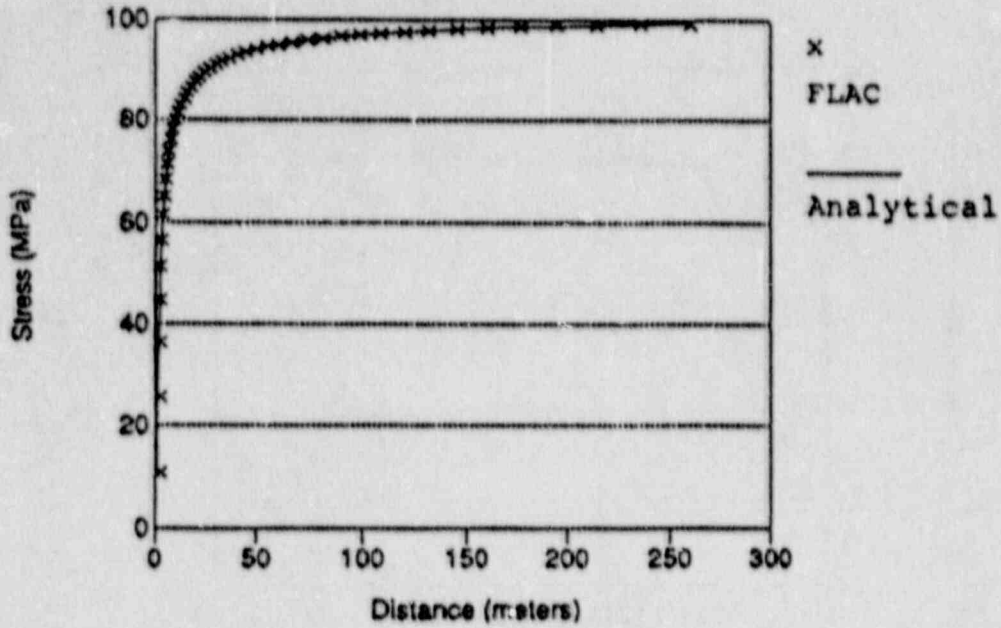
Fig. 3.2.1.7-5   Steady-State Radial Stress (σ_R) versus Distance
from Borehole (Case I)
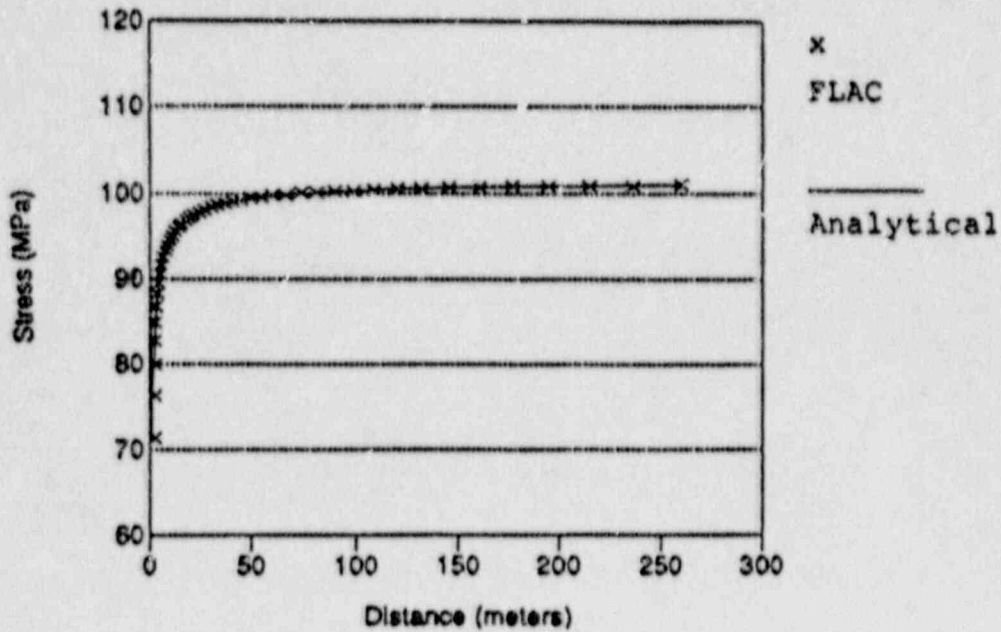
Fig. 3.2.1.7-6   Steady-State Hoop Stress (σ_θ) versus Distance
from Borehole (Case I)
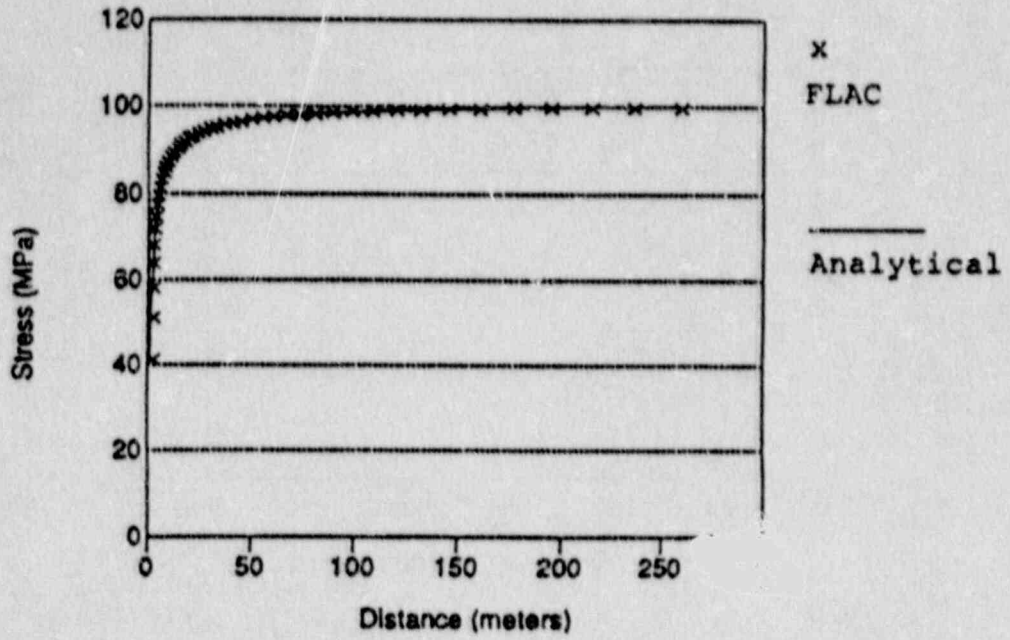
Fig. 3.2.1.7-7   Steady-State Out-of-Plane Stress (σ_{zz}) versus
Distance from Borehole (Case I)

Case II: Plate Half-Width = 200 Times Hole Radius

A finer grid, consisting of 1100 zones, was used for this problem
(Fig. 3.2.1.7-8).   The results for this case are summarized in
Figs. 3.2.1.7-9 through -12.   The radial velocity history (Fig.
3.2.1.7-9) is similar to that of Fig. 3.2.1.7-4, but the steady-
state result is now 2% above the analytical solution. It is pos-
sible that the velocity would drop a little more as time prog-
ressed but, even if this velocity were maintained indefinitely,
it is in excellent agreement with the analytical solution. The
stress components obtained from FLAC are compared with the analy-
tical solutions in Figs. 3.2.1.7-10 through -12. Once again, the
FLAC results are virtually identical to the analytical solution.

(a)   (b)
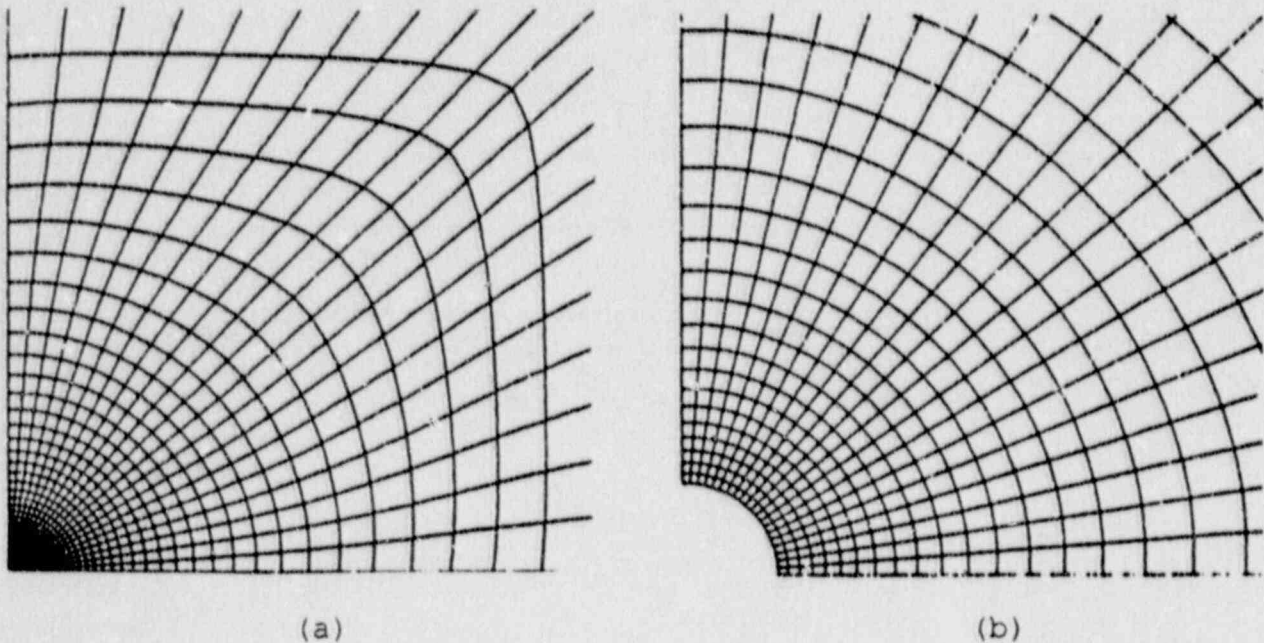
Fig. 3.2.1.7-8   (a) FLAC Grid for Case II; (b) Close-Up View of
                 Grid Around Hole
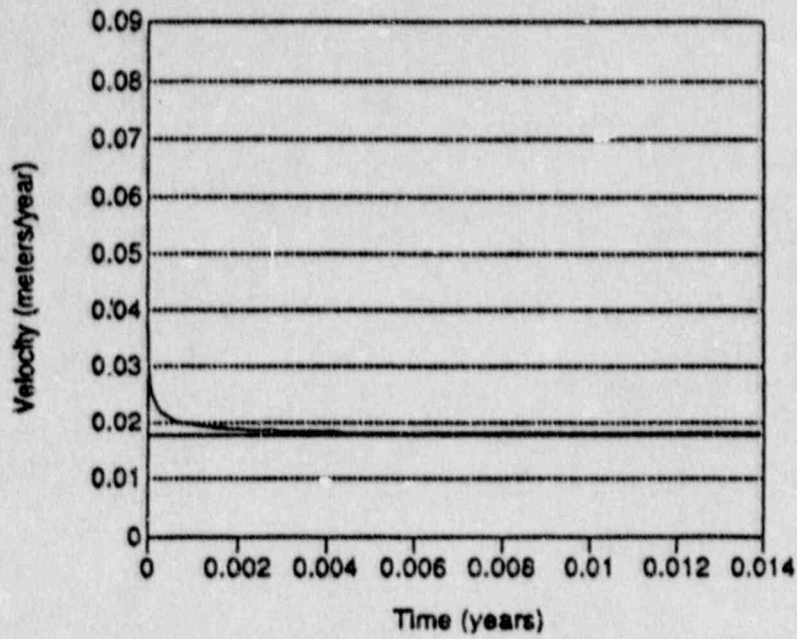
Fig. 3.2.1.7-9   Radial Velocity at Borehole Edge versus Time
(Case II)
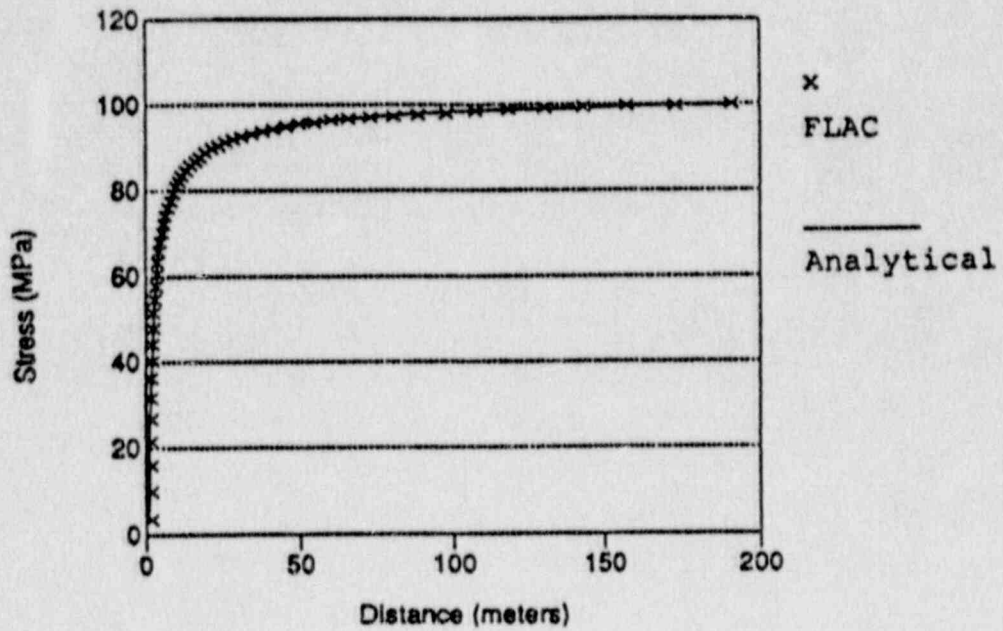
Fig. 3.2.1.7-10   Steady-State Radial Stress (σ_R) versus Distance
from Borehole (Case II)
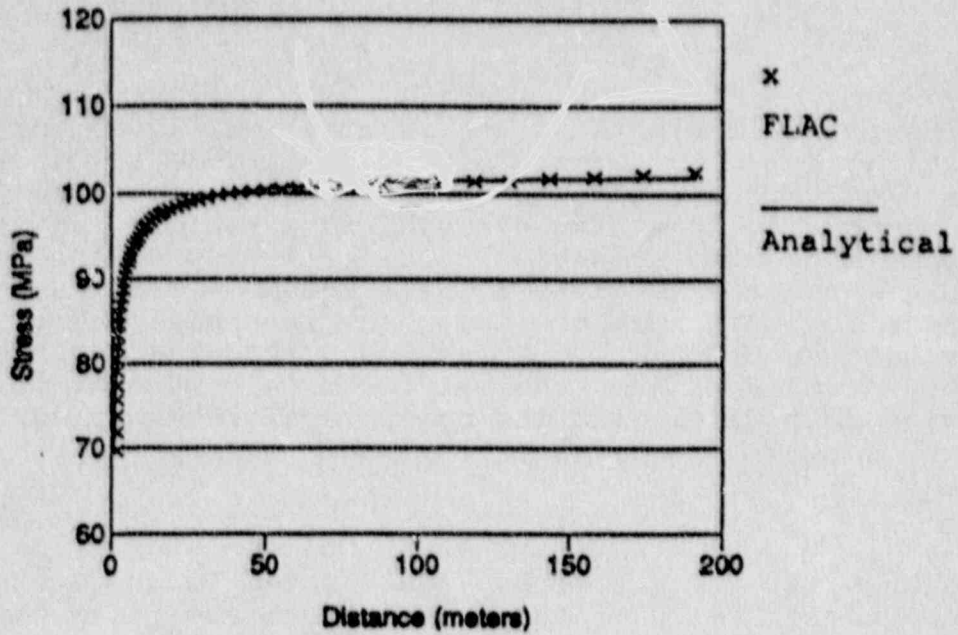
Fig. 3.2.1.7-11   Steady-State Hoop Stress (σ_θ) versus Distance from Borehole (Case II)
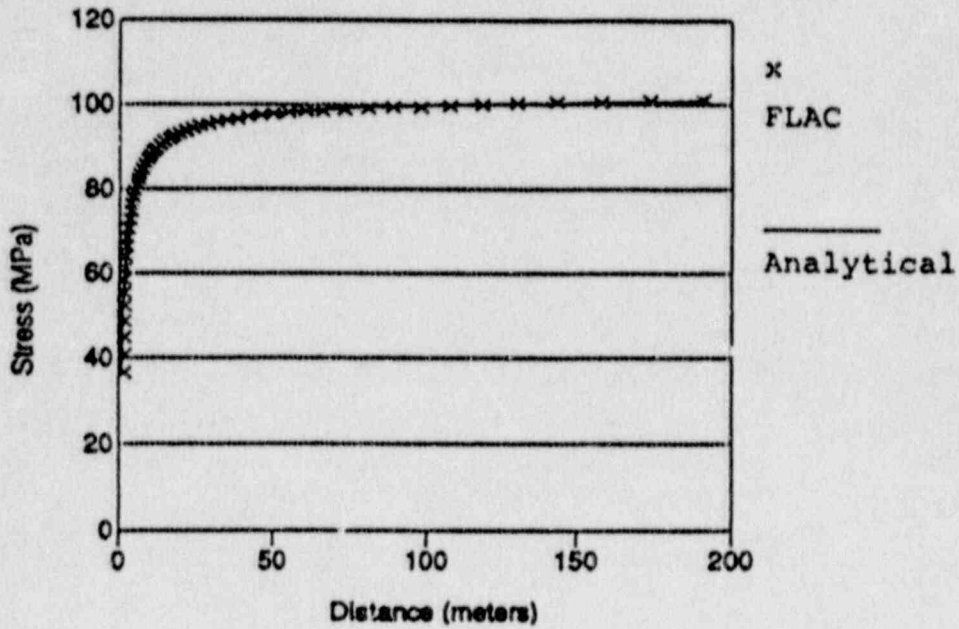
Fig. 3.2.1.7-12   Steady-State Out-of-Plane Stress (σ_{zz}) versus Distance From Borehole (Case II)

Discussion

The results obtained with FLAC are in excellent agreement with the analytical solution for the problem of a hole in a circular plate. Table 3.2.1.7-1 gives a numerical comparison for Case I, where the boundaries are placed at 400 hole radii. The solution to this simple problem complements the complex problems solved in the benchmark tests also given in this volume. The results reported above indicate that the creep law in FLAC operates correctly, while the benchmark problems show that the various features, such as slide-lines, thermal logic, and several different constitutive laws (including the creep laws) interact correctly.

Reference

van Sambeek, L. L. "Creep of Rock Salt Under Inhomogeneous Stress Conditions," Ph.D. Thesis, Colorado School of Mines, Golden, Colorado, 1986.

Norton, F. H. Creep of Steel at High Temperatures. New York: McGraw-Hill Book Company, 1929.

Table 3.2.1.7-1

COMPARISON OF ANALYTICAL AND FLAC RESULTS FOR STEADY-STATE CREEP
OF A HOLE IN A UNIFORM STRESS FIELD

r/a*	FLAC			ANALYTICAL			ERROR (%)		
	σ_r	σ_θ	σ_{22}	σ_r	σ_θ	σ_{22}	σ_r	σ_θ	σ_{22}
381.7	-100	-100.6	-100.2	-99.94	-101.23	-100.59	0.06	-0.62	-0.38
214.4	-99.5	-100.8	-100.1	-99.03	-100.93	-99.98	0.47	-0.13	-0.12
98.7	-97.7	-100.8	-99.4	-97.11	-100.29	-98.70	0.61	0.51	0.71
49.5	-95.0	-99.9	-97.5	-94.32	-99.36	-96.84	0.72	0.55	0.68
40.45	-93.9	-99.5	-96.7	-93.23	-98.99	-96.11	0.72	0.51	0.61
29.8	-91.9	-98.8	-95.4	-91.28	-98.34	-84.81	0.68	0.46	0.62
19.5	-88.6	-97.7	-93.1	-87.84	-97.20	-92.52	0.87	0.52	0.63
10	-80.7	-90.5	-87.9	-79.93	-94.56	-87.24	0.97	0.46	0.75
8.85	-78.9	-94.4	-86.6	-78.07	-93.94	-86.00	1.07	0.49	0.69
7.85	-76.9	-93.7	-85.3	-76.08	-93.94	-84.68	1.07	0.45	0.73
6.95	-74.7	-92.9	-83.8	-73.90	-92.55	-83.23	1.08	0.38	0.69
6.1	-72.1	-92.0	-82.1	-71.36	-91.70	-81.53	1.04	0.32	0.70
5.3	-69.3	-91.0	-80.2	-68.36	-90.71	-79.53	1.37	0.32	0.84
4.6	-66.0	-89.9	-77.9	-65.04	-89.60	-77.32	1.47	0.34	0.75
3.95	-62.1	-88.6	-75.4	-61.11	-89.29	-74.70	1.63	0.36	0.94
3.35	-57.6	-87.0	-72.3	-56.37	-86.71	-71.54	2.18	0.34	1.06
2.85	52.3	-85.2	-68.7	-51.20	-84.98	-68.09	2.16	0.26	0.90
2.35	-45.7	-82.9	-64.3	-44.24	-82.66	-63.45	3.30	0.28	1.34
1.9	-37.5	-80.1	-58.8	-35.47	-79.74	-57.60	5.74	0.45	2.08
1.5	-26.9	-76.6	-51.7	-24.13	-75.96	-50.05	11.48	0.84	3.31

* r taken at the centroid of the zones.

Input Data File

```
******************************************************************
* FLAC Verification Problem
* Steady-state creep of a circular hole in a uniform stress field.
* Comparison to solution by van Sambeek for a
* Single component power law.
******************************************************************
* Configure code to account for z-oriented stress component
conf z_d
*
* Specify grid
*
gr 10,50
*
* Power law
*
m pow
*
* Stretch grid for infinite boundaries
*
gen 0,1 0,400 400,400 1,1 rat 1 1.1 i 1 6
gen same same 400,0 1,0 rat 1 1.1 i 6,11
ini x=1          y=0              i=11 j=1
ini x=0.987688 y=0.156434        i=10 j=1
ini x=0.951057 y=0.309017        i=9 j=1
ini x=0.891007 y=0.45399         i=8 j=1
ini x=0.809017 y=0.587785        i=7 j=1
ini x=0.707107 y=0.707107        i=6 j=1
ini x=0.587785 y=0.809017        i=5 j=1
ini x=0.45399  y=0.891007        i=4 j=1
ini x=0.309017 y=0.951057        i=3 j=1
ini x=0.156434 y=0.987688        i=2 j=1
ini x=0          y=1              i=1 j=1
*
* Adjust grid for better distribution of elements
*
gen adj
gen adj
gen adj
*
* Properties and stresses in Pascal units
*
prop a_1=1e-25 n_1=3 bulk=1e9 shear=3e8 dens=2000
*
* Boundary and initial conditions
*
fix x i=1
```

```
fix y i=11
apply press 100e6 j=51
ini sxx -100e6 syy -100e6 szz -100e6
*
* Keep some histories
*
his unbal
his xvel i=11 j=1
*
* Come to elastic equilibrium first
* By timestepping
*
step 1000
*
* Save elastic state
*
save hol1.sav
*
* Histories, save every 100 timesteps
*
his n=100
his unbal
his xvel i 11 j 1
his sxx syy szz i 10 j 9
his sxx i 10 j 15
his sxx i 10 j 23
his sxx i 10 j 30
*
* Set creep parameters
* Creep parameters based on elastic out-of-balance forces
* Timestep will double when fob less than 5e3, until dt=0.1
*
set dt=1e-4
set fobl=5e3 fobu=1e8 lmul=2 umul=1 maxdt=1e-1 mindt=0
set dt=auto
*
* Time step to steady state, adjusting timestep as problem
* Approaches steady state.  Keep save files in case timestep
* Increase proves to be too large.
*
ste 5000
sav hol2.sav
set maxdt=1
ste 4000
sav hol3.sav
*end of problem
```

3.2.2 <u>Thermal and Thermomechanical Problems</u>

The following verification analyses compare FLAC to analytically-derived solutions for a variety of thermal and thermomechanical problems.

3.2.2.1 Conduction Through a Composite Wall

Problem Statement

An infinite wall consisting of two distinct layers is exposed to
an atmosphere at a high temperature on one side and a low temper-
ature on the other. The wall eventually reaches an equilibrium
where it passes a constant heat flux and the temperature distri-
bution is unchanging.

Purpose

The purpose of this problem is to demonstrate the ability of FLAC
to simulate steady-state temperature effects, including convec-
tive boundary conditions and composite substances.

Problem Specifications

The two layers of the wall have the specifications as presented
in Table 3.2.2.1-1. Figure 3.2.2.1-1 shows the wall geometry and
boundary conditions.

Table 3.2.2.1-1

PROBLEM SPECIFICATIONS

	1	2
temperature of outside ($T_{i,o}$)	3000 °C	25 °C
convection coefficient ($h_{i,0}$)	100 w/m^2 °C	15 w/m^2 °C
thermal conductivity ($k_{1,2}$)	1.6 w/m °C	0.2 w/m °C
thickness ($d_{1,2}$)	25 cm	15 cm

$$k_1 = 1.6 \qquad k_2 = 0.2$$

T_1 T_2 T_3

$h_i = 100$
$T_i = 3000\ C^{\circ}$

$d_1 = 25\ cm$ $d_2 = 15\ cm$

$h_o = 15$
$T_o = 25\ C^{\circ}$
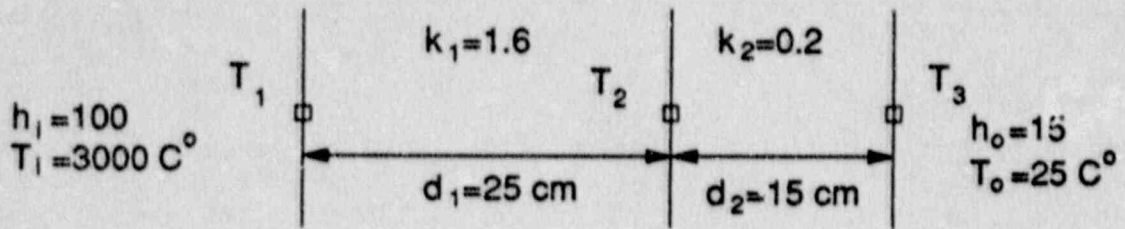
Fig. 3.2.2.1-1 Composite Wall

Assumptions

The wall is of infinite height and width, and the temperatures of the atmosphere on either side are constant. The two layers, individually, are homogeneous and isotropic, and the conductive contact between them is perfect.

Analytical Solutions

The analytical steady-state solution to this problem is quite simple and common. The total equilibrium heat flux is

$$q/A = T_i - T_o / R_T \qquad (3.2.2.1-1)$$

where R_T is the sum of the four thermal resistances:

$$R_1 = 1/h_i,$$
$$R_2 = d_1/k_1,$$
$$R_3 = d_2/k_2, \text{ and} \qquad (3.2.2.1-2)$$
$$R_4 = 1/h_o.$$

This heat flux is constant across the three interfaces, and so after setting this flux equal to the temperature difference divided by the interface resistance and solving for the unknown, we arrive at

$$T_1 = T_i - \frac{q}{A} \cdot \frac{1}{h_i}$$

$$T_2 = T_i - \frac{q}{A} \cdot \frac{d_1}{k_1} \qquad (3.2.2.1-3)$$

$$T_3 = T_2 - \frac{q}{A} \cdot \frac{d_2}{k_2}$$

The temperature will vary linearly between the three.

Computer Model

The wall is idealized by the geometry shown in Fig. 3.2.2.1-2. Since the model is infinitely long in one direction, the model is essentially one-dimensional, and horizontal boundaries may be represented as adiabatic boundaries.
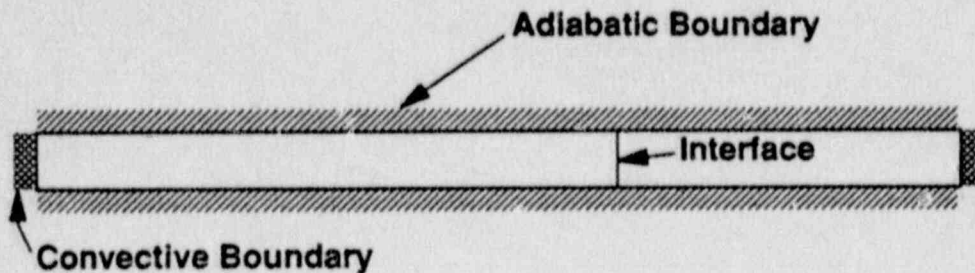
Fig. 3.2.2.1-2 Idealization of the Wall for the FLAC Model

In the FLAC analysis, the wall is discretized into a row of fi-
nite difference zones (Fig. 3.2.2.1-3). An adiabatic boundary
condition (zero heat flux across boundary) is applied to the top
and bottom of this grid to simulate the infinite dimensions of
the wall. The appropriate convective boundary conditions are ap-
plied to the ends of the grid, and two different sets of thermal
properties are applied to model the composite material.
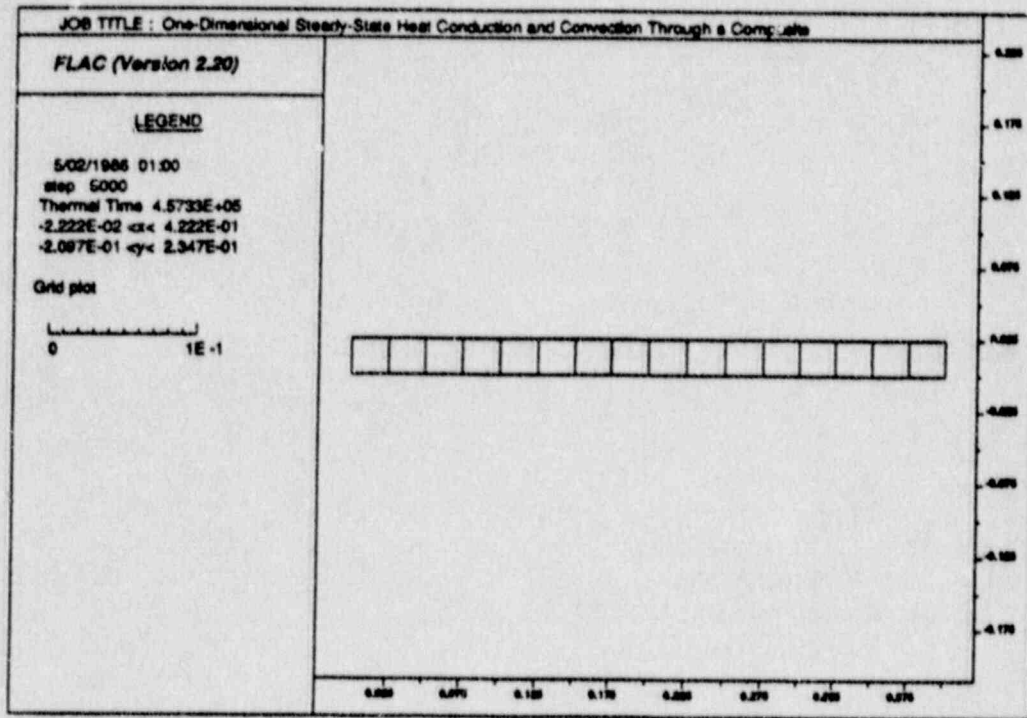
Fig. 3.2.2.1-3 Zone Distribution

Results

Figure 3.2.2.1-4 shows a graphical representation of the steady-state temperature distribution which was normalized with the inside temperature and the distance by the total width of the wall. FLAC results versus the analytical solution are shown. Table 3.2.2.1-2 displays a more precise comparison for five points along the wall, including the three interface points ("Interface" refers to thermal properties, not a mechanical interface.).
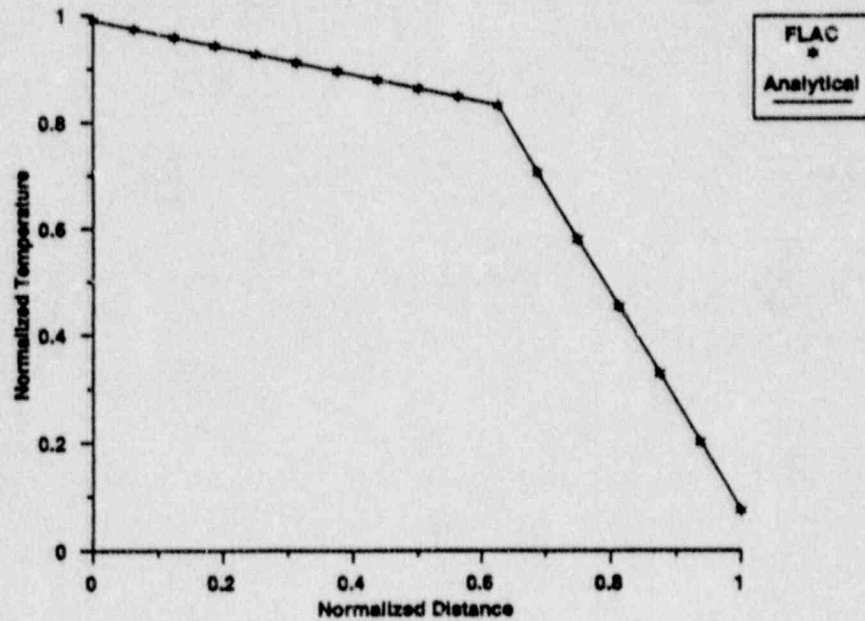
Fig. 3.2.2.1-4   Temperature vs Distance Comparison Between FLAC and Analytical Solution

Table 3.2.2.1-2

COMPARISON of FLAC RESULTS AND THE ANALYTICAL SOLUTION

	Position	Analytical (°C)	FLAC (°C)	% Error
T_1	0	2970	2970	None
	0.125	2733	2733	None
T_2	0.250	2497	2496	-0.04
	0.325	1362	1361	-0.07
T_3	0.400	226.7	226.7	None

Discussion

The comparison between FLAC and the analytical solution shows
that, for this simple one-dimensional problem, FLAC produces ex-
cellent agreement. The errors on both the boundaries and the in-
terface are negligible (< 0.1%).

Input Data File

```
**********************************************************************
* FLAC Verification Problem - One-Dimensional Steady-State Temperature
* Distribution of a Composite Wall Subject to Convective Boundaries
**********************************************************************
* Configure FLAC for thermal calculations
*
conf th
*
* Create grid
*
gri 16 1
*
* Set elastic material and isotropic thermal model
*
m e th_i
*
* Move grid into desired geometry
*
gen 0,0 0,0.025 0.4,0.025 0.4,0
*
*   Material properties
*
prop dens 10000 spec 300
prop cond 1.6 i 1 10 * (material 1)
prop cond .2 i 11 16 * (material 2)
*
* Set Initial Temperature
*
ini tem 2000
*
* Apply Boundary Conditions
*
app conv 3000 100 i 1 * (convection, boundary 1)
app conv 25 15 i 17   * (convection, boundary 2)
*
* No mechanical steps, solve for thermal only
*
set mec of
solv ste 5000 clo 1e10 tem 1e5
*
* Save final state
*
save thcase2.sav
* end of problem
```

3.2.2.2 Steady-State Temperature Distribution Along a Rectangular Fin

Problem Statement

A rectangular fin exchanges heat between a wall of constant temperature and an infinite reservoir of fluid. As equilibrium is reached, the heat flux through the fin and its temperature distribution become constant.
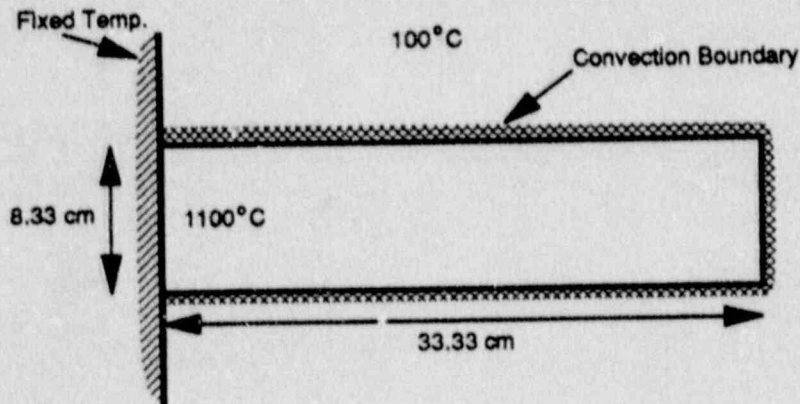
Fig. 3.2.2.2-1 Temperature Distribution of a Rectangular Fin

Purpose

The purpose of this problem is to demonstrate the ability of FLAC to model two-dimensional steady state temperature effects.

Problem Specification

The fin is 8.33 cm high, 33.33 cm wide, and infinitely long. It is attached to a wall maintained at 1100 °C, and is immersed in a fluid maintained at 100 °C. The fin has a thermal conductivity of 15 w/m °C and a convection coefficient of 15 w/m^2 °C.

Assumption

The fin is infinitely long in the plane perpendicular to the ana-
lyzed section, so that the problem may be considered two-
dimensional. The fin is isotropic, homogeneous and continuous,
and its thermal properties are temperature-independent. Both the
wall and the fluid are assumed to be infinite heat reservoirs.

Analytic Model

The solution to the problem of a fin of finite width with a con-
vection condition at the end is given by J. P. Holman (1986).

$$\frac{T - T_\infty}{T_O - T_\infty} = \frac{\cosh\,[m(L-x)] + (h/mk)\,\sinh\,[m(L-x)]}{\cosh\,(mL) + (h/mk)\,\sinh\,(mL)}$$

where T_∞ is the temperature of the fluid (100 °C),

   T_O is the temperature of the wall (1100 °C),

   L is the width of the fin (0.3333 m),

   h is the convection coefficient,

   k is the thermal conductivity (15 w/m^2 °C), and

   m is equal to $(hP/kA)^{1/2}$, where

      P is the perimeter, and

      A the cross-sectional area of the fin.

In the case when the fin is of infinite length, P/A goes to 24;
thus, M has a value of $(24)^{1/2}$, or 4.89898.

Computer Model

In the FLAC model, the fin is divided into a row of finite difference zones (Fig. 3.2.2.2-2). A constant temperature boundary condition is applied to the left side. The problem is then thermally cycled to equilibrium.
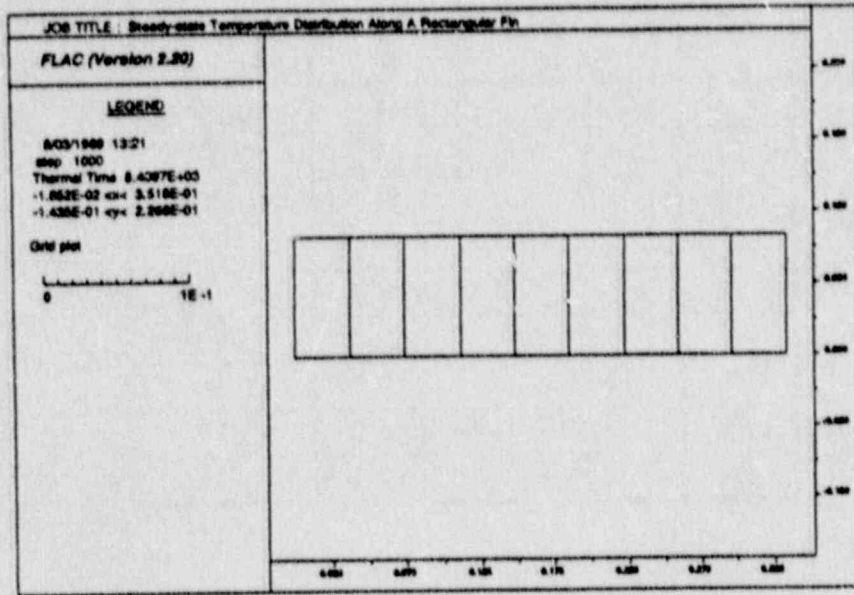
Fig. 3.2.2.2-2   FLAC Zone Distribution

Results

Table 3.2.2.2-1 and Fig. 3.2.2.2-3 show a comparison between FLAC results and the analytical solution. In all cases the error is within ± 0.25%.

Because the FLAC model was only one zone high, the temperature distribution in the y direction was not calculated. This could be done easily by giving the grid a number of zones vertically, although calculation would rise.

Discussion

The agreement provided is excellent, verifying the conductive and convective heat transfer logic in the code.

Reference

Holman, J. P. Heat Transfer, 6th Ed.   New York: McGraw-Hill, 1986.

TABLE 3.2.2.2-1

COMPARISON OF FLAC WITH ANALYTICAL SOLUTION

x/L	T (°C) Analytical	FLAC	% Error
0	1100	1100	None
0.11	943.1	943.3	0.02
0.22	813.9	814.3	0.05
0.33	708.4	708.9	0.07
0.44	623.0	623.5	0.08
0.56	554.7	555.3	0.11
0.67	501.5	502.2	0.14
0.78	463.4	462.3	-0.24
0.89	433.5	434.3	0.18
1.00	416.5	417.3	0.19
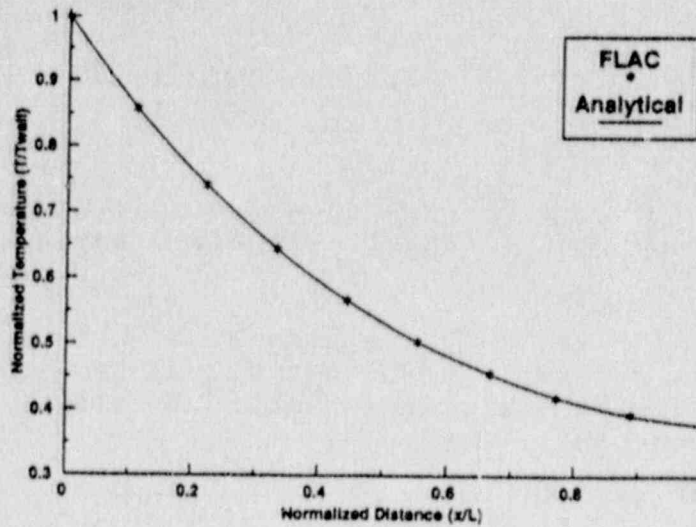
Fig. 3.2.2.2-3   Temperature Distribution of a Rectangular Fin — FLAC Results and Analytical Solution

Data Input File

```
****************************************************************
* FLAC Verification Problem - Steady-State Temperature Distribution
* in a Rectangular Fin With Convection To External Fluid
****************************************************************
tit
Steady-state Temperature Distribution Along A Rectangular Fin
*
*   Configure FLAC for thermal logic
*
conf th
*
*   Create grid
*
gri 9 1
*
*   Set elastic material and isotropic thermal model
*
m e th_i
*
*   Move grid into desired shape
*
gen 0,0 0,0.0833 0.3333,0.0833 0.3333,0 i 1 10
*
*   Material properties
*
prop de 1000 sp 300 con 15
*
*   Apply boundary conditions - convection on three sides, constant
*   Temperature on one side.
*
app conv 100 15 j 1
app conv 100 15 j 2
app conv 100 15 i=10
fix t 1100 i 1
*
*   Set fin's initial temperature
*
ini tem 1100
*
*   Thermal calculation only, step to equilibrium
*
set mech off
*
*   Solve command
*
solv ste 1000 tem 1500 clock 1e10
```

```
*
*   Set up a disk results file
*
set log on
*
*   Write results to disk
*
pr x
pr temp
set log off
*
*   Create save file
*
save thcase1.sav
*   end of problem
```

3.2.2.3 Thermal Response of a Heat-Generating Slab

Problem Statement

An infinite plate of thickness 1 m and constant surface temperature internally generates heat. This problem determines the transient temperature distribution after application of the above initial boundary conditions.

$$q = 40 \text{ kW/m}^3$$

32 C°   1 m   32 C°
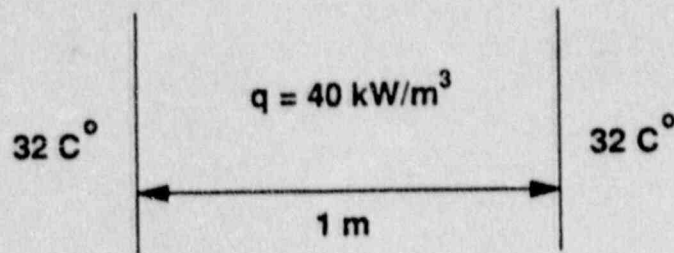
Fig. 3.2.2.3-1   Heat-Generating Slab Showing Initial and Boundary Conditions

Purpose

The purpose of this problem is to demonstrate the ability of FLAC to model transient thermal behavior, including heat generation.

Problem Specification

The physical properties of the plate in question are

density (ρ)	500	kg/m^3
specific heat (C_p)	0.2	kJ/kg °C
thermal conductivity (k)	20	w/m °C

The plate is initially at a uniform temperature of 60 °C, the surface is then fixed at 32 °C, and the plate itself has internal heat generation of 40 kW/m^3.

Assumptions

The plate is infinitely long with a finite width. The material of the plate is homogeneous, isotropic, continuous, and its thermal properties are temperature independent. After the conditions are applied, the surface temperature is constant and the heat generation is uniform. The resulting conditions are assumed to be linear, and symmetric about the midline of the plate.

Analytical Model

The solution to this problem is determined graphically using the Binder-Schmidt construction method. The analytical values in Table 3.2.2.3-1 were derived from Fig. 12-10 of Schneider (1955, p. 309).

Computer Model

The simplification of this problem for analysis is shown in Fig. 3.2.2.3-2 and the corresponding FLAC grid is given in Fig. 3.2.2.3-3. Because the plate is infinitely long, and because the heat generation is uniform, symmetry conditions exist for any plane perpendicular to the long axis of the plate. These are represented by adiabatic boundaries. Since equal temperatures exist one either side of the plate, a symmetry line also exists down the center of the plate.

The thermal timestep is set to 1×10^{-3} seconds, and stepped to a time of 0.2 seconds.

Adiabatic Boundary

Fixed Temp.

32 C°

q = 40 kW/m³

0.5 m
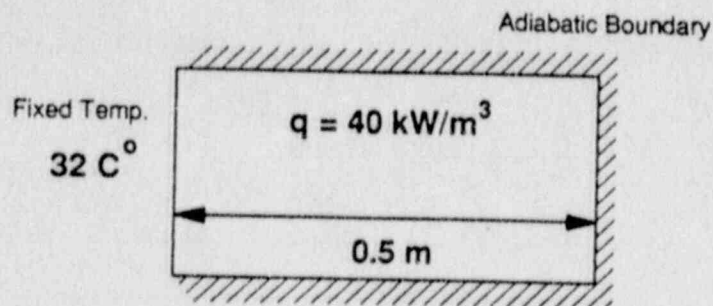
Fig. 3.2.2.3-2   FLAC Model of Slab

JOB TITLE : Thermal Response of a Heat-Generating Slab

FLAC (Version 2.20)

LEGEND

6/03/1989 11:27
step   200
Thermal Time 2.0000E-01
-2.770E-02 <x< 5.270E-01
-2.270E-01 <y< 3.270E-01

Grid plot

0   1E -1
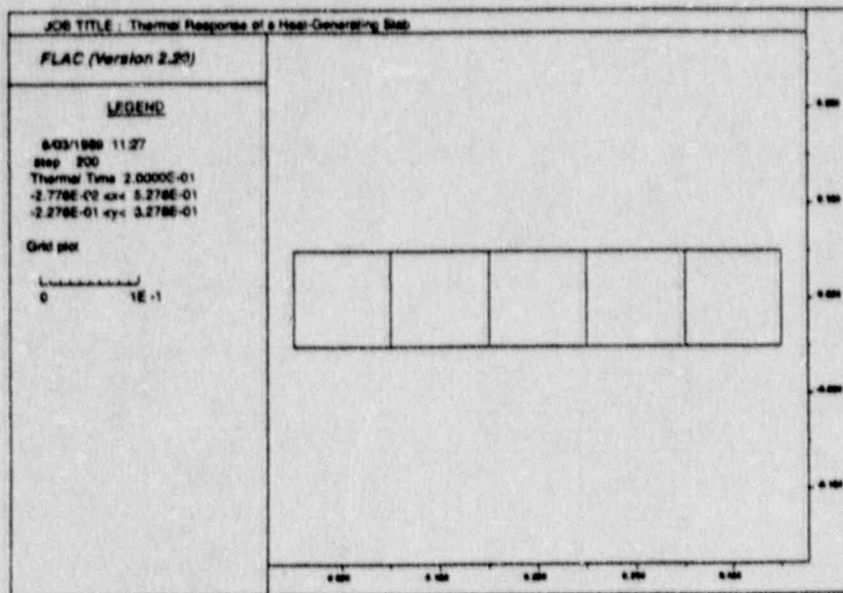
Fig. 3.2.2.3-3   FLAC Zone Distribution

Results

Figure 3.2.2.3-4 shows a graphical representation of the temperature distribution results of both FLAC and the analytical solution. Table 3.2.2.3-1 gives a more exact comparison. It can be seen that the FLAC results are in very good agreement with the analytic solution (1.33% max. error).
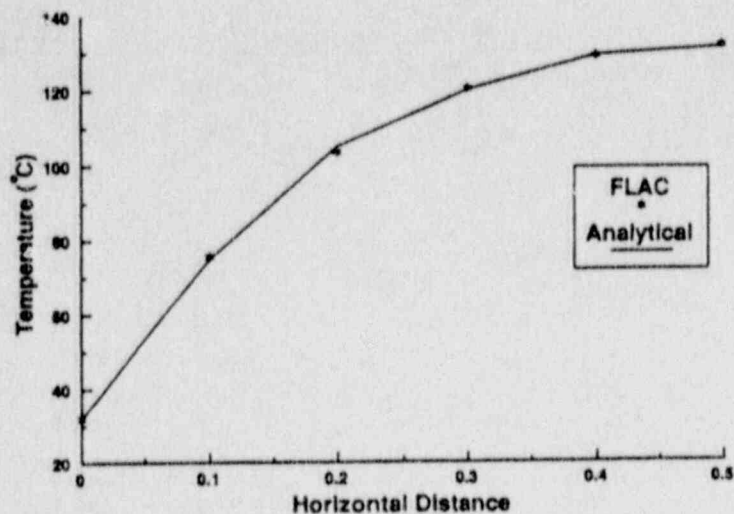
Fig. 3.2.2.3-4   FLAC and Analytical Temperature Distributions Across the Plate at 0.2 Seconds

TABLE 3.2.2.3-1

COMPARISON BETWEEN FLAC RESULTS AND THE ANALYTIC SOLUTION

x (m)	T (°C) Analytical	FLAC	% Error
0.0	32	32	None
0.1	75	75.6	0.80
0.2	105	103.6	-1.33
0.3	120	120.3	0.25
0.4	129	128.9	-0.08
0.5	131	131.5	0.38

Discussion

With only five zones, FLAC produces good agreement with the analytic solution at a particular time, although similar agreement could be obtained for any time. The error could be reduced by increasing the discretization density of the plate.

Reference

Schneider, P. J. Conduction Heat Transfer. Cambridge, Mass.: Addison-Wesley, 1955.

Data Input File

```
******************************************************************
* FLAC Verification Problem - Transient Thermal Response of a Heat
* Generating Slab
******************************************************************
tit
Thermal Response of a Heat-Generating Slab
*
* Set thermal configuration
*
conf th
*
* Grid
*
gr 5 1
*
* Mechanical elastic and thermal isotropic material models
*
m e th_i
*
* Give coordinates to the grid
*
gen 0 0 0 0.1 0.5 0.1 0.5 0
*
* Supply properties
*
prop dens 500 cond 20 spec .2
*
* Initial slab temperature
*
ini tem 60
*
* Apply heat source to slab
*
app source 400 0 0 i 1 5 j 1
*
* Temperature boundary condition at left-hand boundary
*
fix t 32 i 1
*
* Manually set thermal time step
*
set thdt=1e-3
set mec of
*
```

```
* Initiate timestepping
*
sol ste 200 tem 200
*
* Save the results
*
save thcase3.sav
* end of problem
```

3.2.2.4 Transient Temperature Distribution in an Orthotropic Bar

Problem Statement

A long orthotropic rectangular bar at a uniform temperature is exposed to fluid at 100 °C. The temperature at four points are measured after being exposed to the fluid for a known amount of time. The dimensions of the bar is cross-section are given in Fig. 3.2.2.4-1.
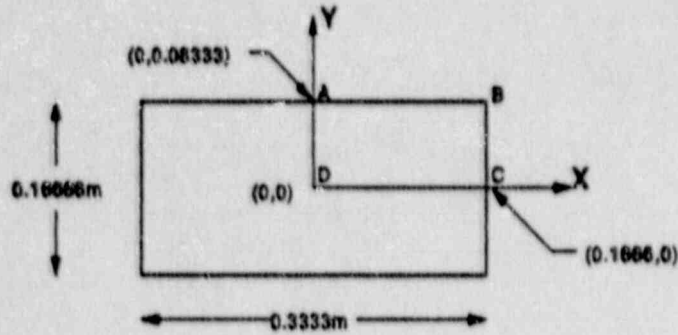
Fig. 3.2.2.4-1 Orthotropic Bar

Purpose

The purpose of this problem is to demonstrate FLAC's ability to model transient thermal response in a two-dimensional orthotropic problem, with convective boundary conditions.

Problem Specification

The bar has dimensions 0.3333 m wide, 0.16666 m high, and is in-finitely long. The material the bar is made of has the following material and thermal properties:

density (p)	40	kg/m^3
x-thermal conductivity (kx)	20	W/m °C
y-thermal conductivity (ky)	3.6036	W/m °C
specific heat (C_p)	9.009×10^{-3}	j/kg °C
convection coefficient	240	W/m^2 °C

The bar is initially at 500 °C, and the surrounding fluid has a
temperature of 100 °C. The temperature distribution is found
after 8.3333×10^{-4} seconds of exposure to the fluid.

Assumptions

The bar is infinitely long, homogeneous, and thermally ortho-
tropic. The thermal properties are temperature independent. It
is assumed that the problem is symmetric about both the x- and y-
axis, the fluid surrounding the bar acts as an infinite heat res-
ervoir.

Analytical Model

The analytical expression for the transient temperatures on the
surface or interior of a semi-infinite rectangular bar subjected
to convective surfaces is computed from products of available
one-dimensional solutions (e.g., Schneider, 1955, p. 247). For a
semi-infinite bar, the product solution is of the form

$$\frac{T(x_1, x_2, x_3, \tau) - T_\infty}{T_0 - T_\infty} = S(x_1, \tau) \, P(x_2, \tau) \, P(x_3, \tau)$$

where $T(x_1, x_2, x_3)$ = temperature at a particular three-
dimensional coordinate,

T_0 = initial temperature of the bar,

T_∞ = temperature of the surrounding fluid,

τ = time,

$S(x_1, \tau)$ = transient solution for a semi-infinite body,
where x is the direction of infinite extent,
and

$P(x_2, \tau), P(x_3, \tau)$ = transient solution for a plane wall.

The values of $S(x_1, \tau)$, $P(x_2, \tau)$ and $P(x_3, \tau)$ are given in table
form as functions of the Fourier and Biot numbers. For this
problem, the $P(x_2, \tau)$ and $P(x_3, \tau)$ functions will be different due
to the directional dependence of the thermal properties. The
calculations for these parameters are given in Schneider (1955,
p. 262).

Computer Model

In the FLAC analysis, an area representing one-quarter of the bar is discretized into infinite difference zones. The zones are concentrated toward the exposed corner of the bar. The inside surfaces are kept at an adiabatic state representative of the symmetry conditions, while the outside are given a convective boundary condition.
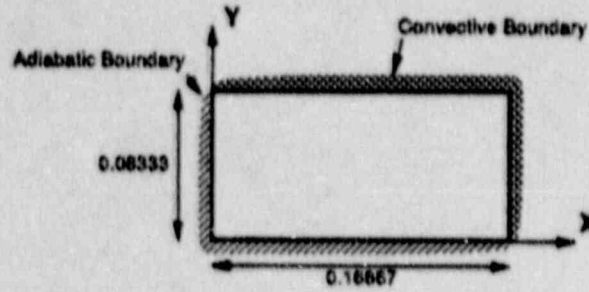
Fig. 3.2.2.4-2   FLAC Model of Orthotropic Bar
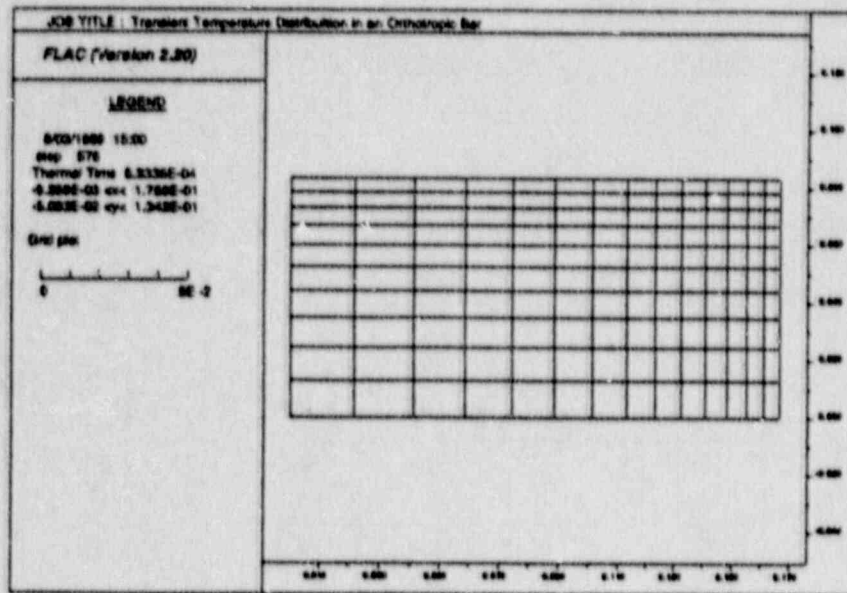
Fig. 3.2.2.4-3   FLAC Zone Distribution

Results

Figure 3.2.2.4-4 shows the temperature contours of the bar after 8.3333×10^{-4} seconds and 576 cycles. Table 3.2.2.4-1 compares the FLAC results with the analytical solution at the four locations shown in Fig. 3.2.2.4-1.
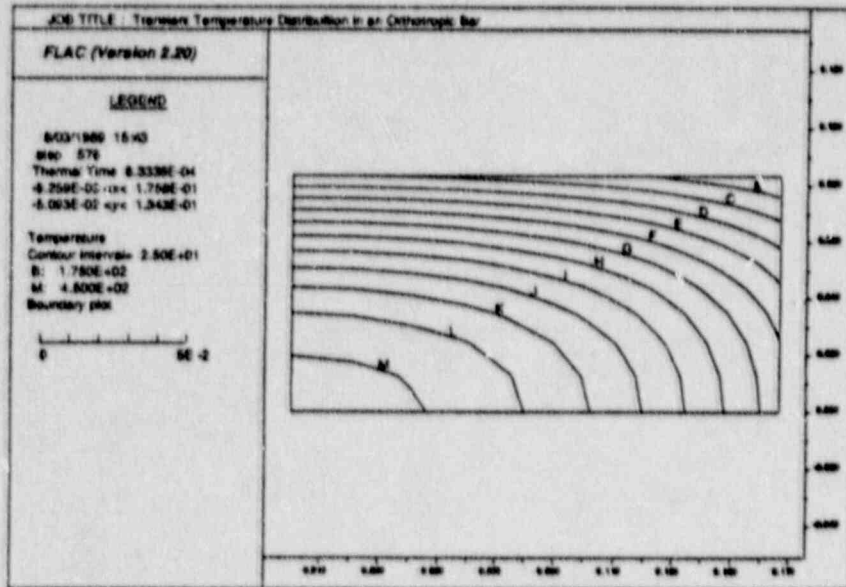
Fig. 3.2.2.4-4   Temperature Contours After 8.3333×10^{-4} Seconds

Table 3.2.2.4-1

COMPARISON OF FLAC RESULTS WITH ANALYTICAL SOLUTION

X	Y	T (°C) Analytical	FLAC	% Error
0	0	458.7	462.1	0.74
0.1666	0	280.5	285.1	1.64
0	0.083333	198.2	199.8	0.81
0.1666	0.083333	149.4	151.0	1.07

Discussion

The results show that the FLAC model agrees very well with the
analytical solution (< ?% error). Reducing the timestep would
have an improving effect, probably more than could be obtained by
increasing the number of zones. This problem verifies the abil-
ity of FLAC to model a transient thermal problem with direction-
dependent thermal properties.

Reference

Schneider, P. J. Conduction Heat Transfer. Cambridge, Mass.:
Addison-Wesley, 1955.

Data Input File

```
****************************************************************
* FLAC Verification Problem - Transient Temperature Distribution
* In A Thermally-Orthotropic Bar.
****************************************************************
tit
Transient Temperature Distribution in an Orthotropic Bar
*
*   Configure FLAC for thermal logic
*
conf th
*
*   Create grid
*
gri 14 10
*
*   Material model elastic, thermal model isotropic
*
m e th_an
*
*   Mechanical and thermal properties
*
prop dens 400 spe 9.009e-3 xcon 20 ycon 3.6036
*
*   Initial temperature condition
*
ini tem 500
*
*   Apply convective boundary conditions
*
app conv 100 240 i 15 j 1 11
app conv 100 240 i 1,15 j 11
*
*   Conform grid to desired geometry
*
gen 0 0 0 8.3333e-2 1.66667e-1,8.3333e-2 1.66667e-1,0 rat .9 .9
*
*   Set thermal timestep and cycle to desired total time
*
set mec of
set thdt=1.4468e-6
*
* Step to specific comparison time
*
ste 576
*
* Save problem state
*
save thcase5.sav
* end of problem
```

3.2.2.5 Semi-Infinite Slab with Applied Heat Flux

Problem Statement

This problem concerns a semi-infinite elastic mass which has a constant heat flux suddenly applied to its surface (Fig. 3.2.2.5-1). Thermal expansion causes a stress change in the slab. Both the transient heat transfer behavior and the stress state can be solved for analytically.
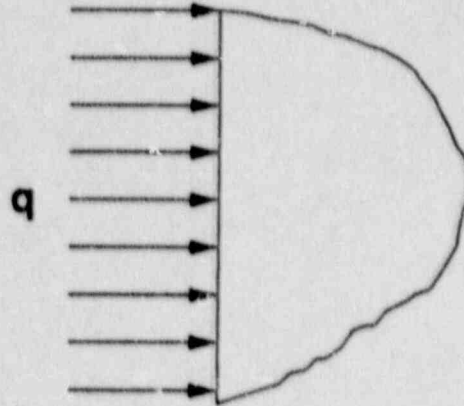
Fig. 3.2.2.5-1   Semi-Infinite Slab with Applied Heat Flux

Purpose

The purpose of this problem is to compare the performance of FLAC on a transient heat transfer problem with corresponding thermally-induced stress for an elastic body.

Problem Specifications

The slab is initially at a uniform temperature of 0 °C. A heat flux of 1 w/m^2 is applied to the surface. The elastic slab was modeled as having the following material properties:

Young's modulus (E)	1 KPa
Poisson's ratio (ν)	0.25
thermal diffusivity (κ)	1 m^2/s

linear thermal expansion $3/^\circ C$
coefficient (α)

thermal conductivity (k) $1\ w/m\ ^\circ C$

Assumptions

The slab is a homogeneous, continuous, and isotropic half-space.
The material is perfectly elastic, and its thermal properties are
temperature independent.

Analytic Solution

The analytical solution for the transient thermal response is
given by Carslaw and Jaeger (1959, p. 75).

$$T(x,t) = \frac{2q}{k} \left[\left[\frac{\kappa t}{\pi} \right]^{1/2} e^{(-x^2/4\kappa t)} - \frac{x}{2} \operatorname{erfc} \left[\frac{x}{2(\kappa t)^{1/2}} \right] \right]$$

where q is the applied heat flux, and

   erfc( ) is the complex error function.

The solution for the thermally-induced stress state is given by
Timoshenko and Goodier (1970, p. 435):

$$\sigma_y = - \frac{\alpha E T}{1-v}$$

The temperature of a zone was calculated by finding the average
temperature of its adjacent gridpoints.

Computer Model

Since the thermal problem is one dimensional (Fig. 3.2.2.5-2), the slab was simulated by a row of zones of one zone width in height (Fig. 3.2.2.5-3). A constant heat flux was applied to the left boundary, while the rest of the boundaries were kept adiabatic to represent thermal symmetry planes. The right boundary was extended far enough to simulate an infinite depth. The upper and lower boundaries were mechanically fixed in the vertical direction to represent shear-free symmetry planes. The problem was then cycled to a time of 0.2 seconds and 1.0 seconds after the application of the heat flux, and the resulting temperature and stress distribution were recorded.
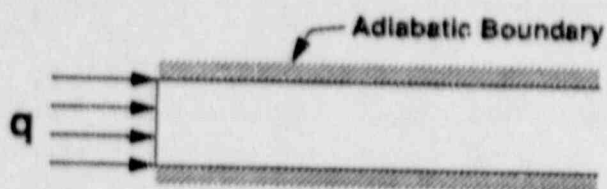
Fig. 3.2.2.5-2 FLAC Conceptual Model
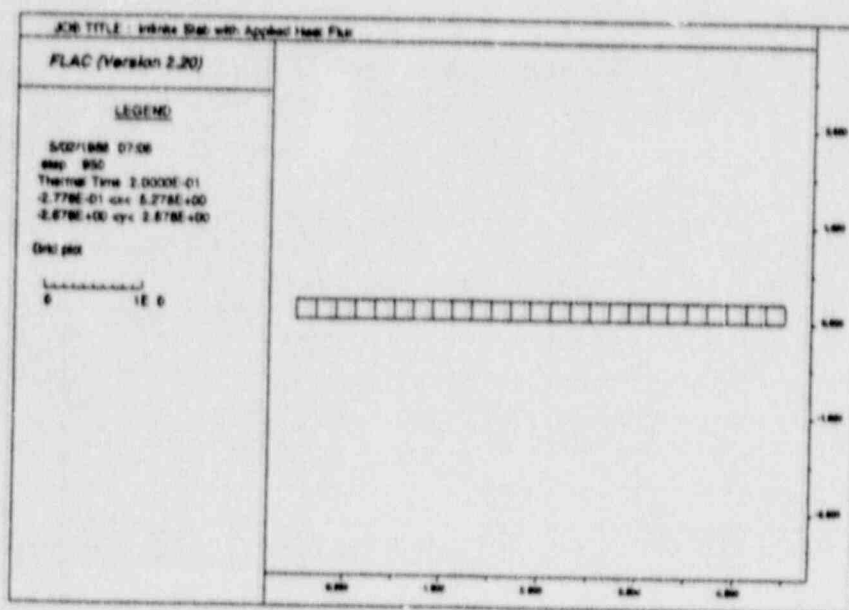
Fig. 3.2.2.5-3 FLAC Zone Distribution

Results

Tables 3.2.2.5-1 and -2 show the agreement between FLAC results for temperature and stress and the analytical solutions. Figures 3.2.2.5-4 and -5 show these results graphically as well.

Table 3.2.2.5-1

COMPARISON OF FLAC WITH ANALYTICAL SOLUTION FOR THERMAL RESULTS

time (sec)	x (m)	Analytical T (°C)	FLAC T (°C)	% Error
0.2	0.0	0.5046	0.4985	-1.21
	0.2	0.3297	0.3240	-1.73
	0.6	0.1161	0.1133	-2.41
	1.0	0.03073	0.03037	-1.17
1.0	0.0	1.128	1.126	-0.18
	0.2	0.9396	0.9370	-0.28
	0.6	0.6284	0.6261	-0.37
	1.0	0.3993	0.3975	-0.45

Table 3.2.2.5-2

COMPARISON OF FLAC WITH ANALYTICAL SOLUTION
FOR STRESS RESULTS

time (sec)	x (m)	Analytical Stress (KPa)	FLAC Stress (KPa)	% Error
0.2	0.1	-1.644	-1.649	0.30
	0.3	-1.041	-1.1047	0.58
	0.5	-0.6184	-0.6259	1.21
	0.7	-0.3426	-0.3514	2.57
	0.9	-0.1763	-0.1859	5.45
1.0	0.1	-4.125	-4.135	0.24
	0.3	-3.415	-3.427	0.35
	0.5	-2.793	-2.804	0.39
	0.7	-2.255	-2.269	0.62
	0.9	-1.798	-1.812	0.78
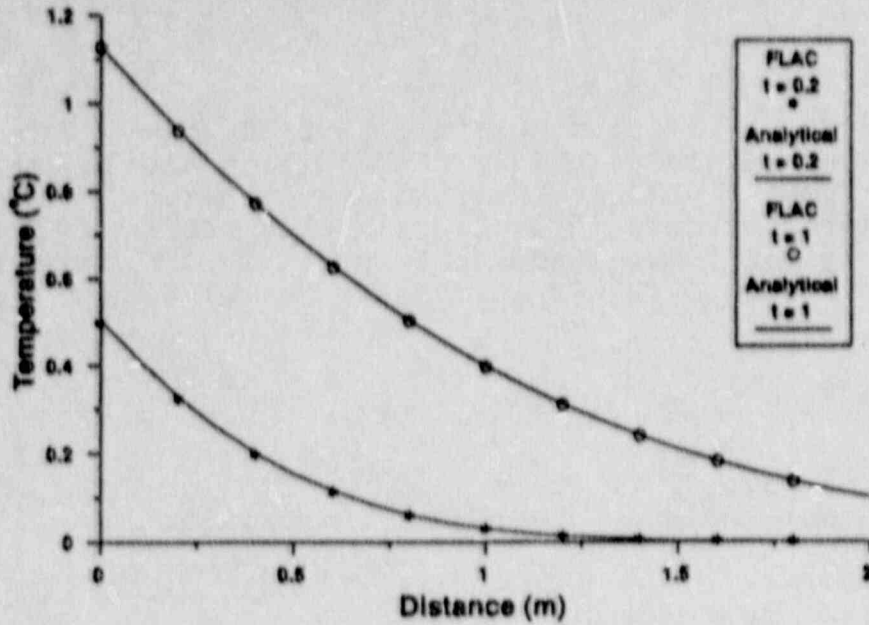
Fig. 3.2.2.5-4   Temperature versus Distance of FLAC Compared to
the Analytic Solution
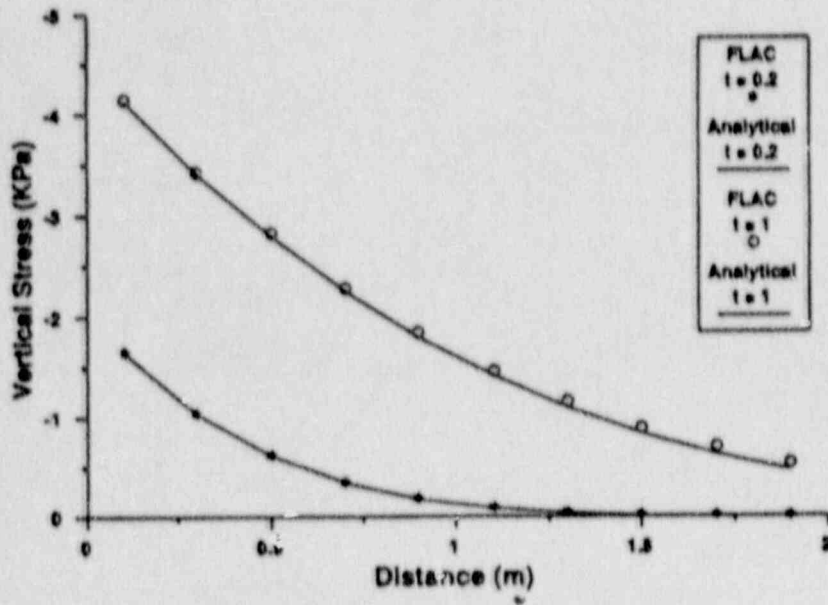
Fig. 3.2.2.5-5   Vertical Stress versus Distance of FLAC Compared
to the Analytic Solution

Discussion

After one second, FLAC produces results that are in excellent agreement with the analytical solution (<1% error in both temperature and stress). While the errors are larger at a time of 0.2 seconds (<3% temperature, <6% stress), this can be attributed to the relatively small magnitude numbers involved. The error could be decreased by using either a smaller thermal timestep, or a finer mesh.

References

Carslaw, H. S., and J. C. Jaeger. Conduction of Heat in Solids, 2nd Ed. London: Oxford University Press, 1959.

Timoshenko, S. P., and J. N. Goodier. Theory of Elasticity, 3rd Ed. New York: McGraw-Hill, 1970.

FLAC Input Data File

```
**************************************************************
* FLAC Verification Problem - Transient Temperature and Stress
* Distributions in a Semi-infinite Slab With Applied
* Surface Heat Flux.  Compare Temperatures and Stresses For
* Times t1 and t2.
**************************************************************
tit
Semi-infinite Slab with Applied Heat Flux

*
* Configure model for thermal analysis
*
conf th
*
* Create grid
*
gri 25 1
*
* Mechanical elastic and isotropic thermal models
*
m e th_i
*
* Properties
*
prop bu .67 s .4 d 1 cond 1 spec 1 thexp 3
*
* Give grid coordinates
*
gen 0 0 0 0.2 5 .2 5 0
*
* Apply flux boundary condition along left-hand side
*
app flux 1 0 i 1
*
* Mechanical boundaries
*
fix y j 1
fix y j 2
fix x y i 26
*
* Manually set thermal time step
*
set thdt=8e-4
*
```

```
* Thermal timesteps only to time t1
*
set mec of th on
*
* Solve
*
solv clo 1e10 tem 1e10 step 250
*
* Now solve mechanical problem
*
set mec on th of
*
* Timestep to mechanical equilibrium
*
ste 700
*
* Save state
*
sav thcase41.sav
*
* Solve thermal only again to time t=t2
*
set mec of th on
*
* Solve thermal problem to t2
*
solv clo 1e10 tem 1e10 step 1000
*
* Again, determine new thermally-induced stresses from
* New temperature distributions
*
set mec on th of
*
* Mechanical timesteps
*
ste 700
*
* Save state 2
*
sav thcase42.sav
* end of problem
```

3.2.3 Fluid Flow and Coupled Hydro-Mechanical Problems

The following verification analyses compare FLAC to analytically-derived solutions for a variety of fluid flow and coupled hydro-mechanical problems.

3.2.3.1 Transient Fluid Flow to a Well in a Confined Aquifer

Problem Statement

Conditions of fluid flow to a well completely penetrating a con-
fined aquifer are illustrated schematically in Fig. 3.2.3.1-1.
Horizontal, radial, axisymmetric flow in the porous medium is re-
sisted by viscous drag forces mobilized in the soil matrix.
Yield of fluid from the pore structure is determined by the com-
pressibility of water, the porosity of the aquifer, and the com-
pressibility of the soil matrix. Production from the aquifer
therefore represents a state of coupled compressible fluid flow
and solid deformation.
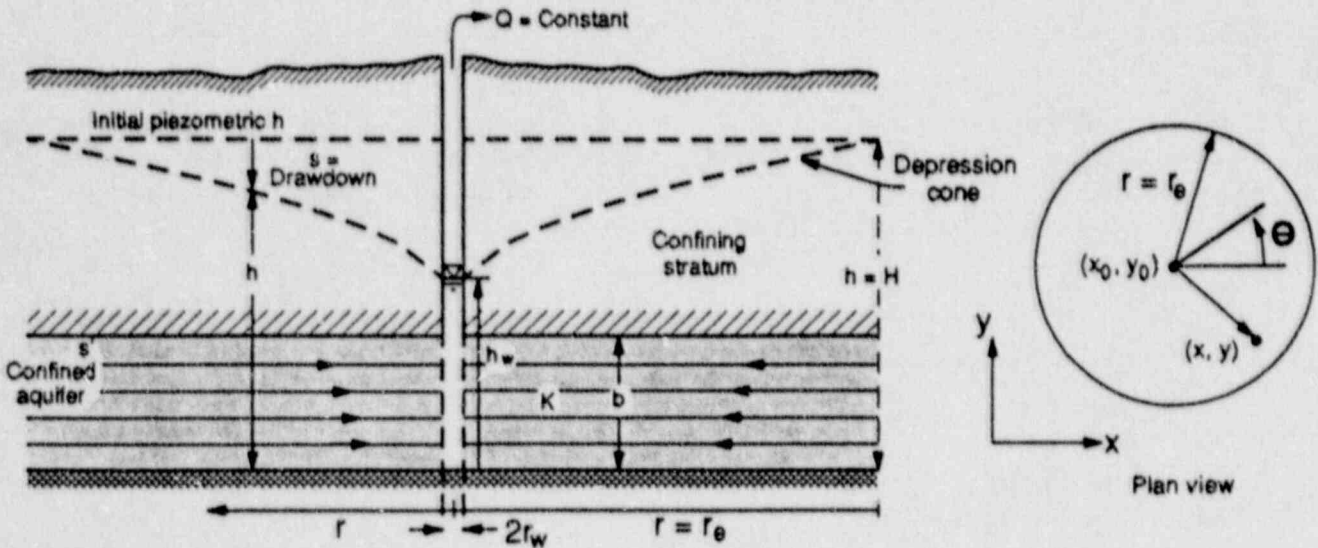
Fig. 3.2.3.1-1   Radial Flow to a Well Completely Penetrating a
                 Confined Aquifer   [de Wiest, 1965]

Purpose

The purpose of this exercise is to demonstrate that FLAC can sim-
ulate porous flow and consolidation in a medium subject to a tri-
axial state of stress. Because analysis of transient flow in a
confined aquifer takes account of both soil matrix consolidation
and fluid motion, the problem examines the performance of the
code in handling coupled porous solid-fluid flow systems.

Analytical Solution

The governing equation for fluid flow to a well penetrating a
confined aquifer is the Poisson equation (de Wiest, 1965)

$$\frac{\partial^2 h}{\partial r^2} + \frac{1}{r} \frac{\partial h}{\partial r} = \frac{S}{T} \frac{\partial h}{\partial t} \qquad (3.2.3.1-1)$$

In this expression, h is the piezometric head, r is the coor-
dinate radius, and S and T are aquifer hydraulic characteristics,
called the storage coefficient and the transmissivity, respec-
tively. The transmissivity is defined by:

$$T = Kb \qquad (3.2.3.1-2)$$

where K is the hydraulic conductivity of the aquifer, and b is
the aquifer thickness. The storage coefficient reflects both the
deformability of the soil matrix and the compressibility of
water. It is given by

$$S = S_s b \qquad (3.2.3.1-3)$$

In Eq. (3.2.3.1-3), S_s is the specific storage, expressed by

$$S_s = \gamma_w (\alpha + n\beta) \qquad (3.2.3.1-4)$$

where γ_w is the unit weight of water,

α is the axial compressibility of the soil matrix,

n is the porosity of the aquifer, and

β is the compressibility of the pore water.

Because the aquifer is subject to uniaxial deformation during consolidation, α is given by the inverse of the elastic modulus for uniaxial strain:

$$\alpha = \frac{1}{E_s} \frac{(1 - 2v)(1 + v)}{(1 - v)} \tag{3.2.3.1-5}$$

where E_s is the Young's modulus for the soil matrix.

The compressibility of the pore water is the inverse of the bulk modulus—i.e.,

$$\beta = \frac{1}{K_w} \tag{3.2.3.1-6}$$

The boundary conditions are, for time $t > 0$, $h \rightarrow h_o$ as $r \rightarrow \infty$ and

$$\lim_{r \rightarrow 0} \left(r \frac{\partial h}{\partial r}\right) = \frac{Q}{2\pi T}$$

The initial condition is, for $t \leq 0$, $h(r,o) = h_o$.

Thies (1935) obtained a solution for Eq. (3.2.3.1-1) in the form

$$h = h_o - \frac{Q}{4\pi T} E_i(-u) \tag{3.2.3.1-7}$$

where $E_1(-u)$ is the exponential integral with argument

$$u = (r^2 S/4Tt).$$

For small values of r, or large values of t, Eq. (3.2.3.1-7) may be expanded in the form

$$s = h_0 - h = \frac{2.30\ Q}{4\pi T} \log(2.25Tt/r^2 S) \qquad (3.2.3.1-8)$$

or

$$s = h_0 - h = \frac{2.30\ Q}{4\pi T} \log(2.25Tt/S) - \frac{2.30\ Q}{2\pi T} \log(r) \qquad (3.2.3.1-9)$$

Because Eq. (3.2.3.1-9) characterizes the performance of the aquifer analytically, it may be used as the solution against which to assess the capability of FLAC to model transient porous flow in a compressible medium.

Computer Model

The FLAC model of the confined aquifer is shown in Fig. 3.2.3.1-2. The aquifer was 10 m thick, and the well was 1 m in diameter. The initial piezometric surface was 15 m above the aquifer upper surface. A uniform aquifer pressure of 147 KPa was assumed. For the axisymmetric problem geometry, the remote boundary of the problem domain was taken as 100 m from the center of the well. The pumping rate from the well was 2.21×10^{-2} m^3/s. Other problem parameters defining the model are as follows.

Mechanical Properties of Soil Matrix

Young's modulus $E = 177$ MPa

Poisson's ratio $v = 0.25$

from which are derived:

shear modulus $G = 71$ MPa

bulk modulus $K = 118$ MPa

<u>Hydraulic Properties</u>

porosity	$n = 0.4$
bulk modulus of water	$K = 2$ GPa
hydraulic conductivity	$K = 2.92 \times 10^{-4}$ ms^{-1}
transmissivity	$T = 2.92 \times 10^{-3}$ m^{2}s^{-1}
storage	$S = 4.81 \times 10^{-4}$

Fig. 3.2.3.1-2   FLAC Mesh for Axisymmetric Analysis of Flow to a Well

The analysis was conducted by modeling discharge from the well for an elapsed time of 100 sec. Because of the relatively high permeability of the aquifer, this elapsed time was sufficient for drawdown to occur over a reasonable radius, and also sufficient to prevent hydraulic interaction between the well and the remote boundary of the model domain.

Results

The performance of FLAC may be assessed by considering the
numerical output from the well analysis in the same manner as a
field pumping test on a well. In this way, via the de Wiest so-
lution to the Theis curve, the aquifer hydraulic conductivity and
storage may be recovered from the simulated drawdown data derived
from the FLAC analysis.

The gridpoint pore pressures determined in FLAC may be converted
directly to piezometric head, for comparison with the distribu-
tion of head defined by Eq. (3.2.3.1-8). A comparison between
the radial distribution of head predicted from the analytical
solution and that derived from the FLAC analysis is presented in
Fig. 3.2.3.1-3. It is observed that there is close cor-
respondence between the independent solutions.
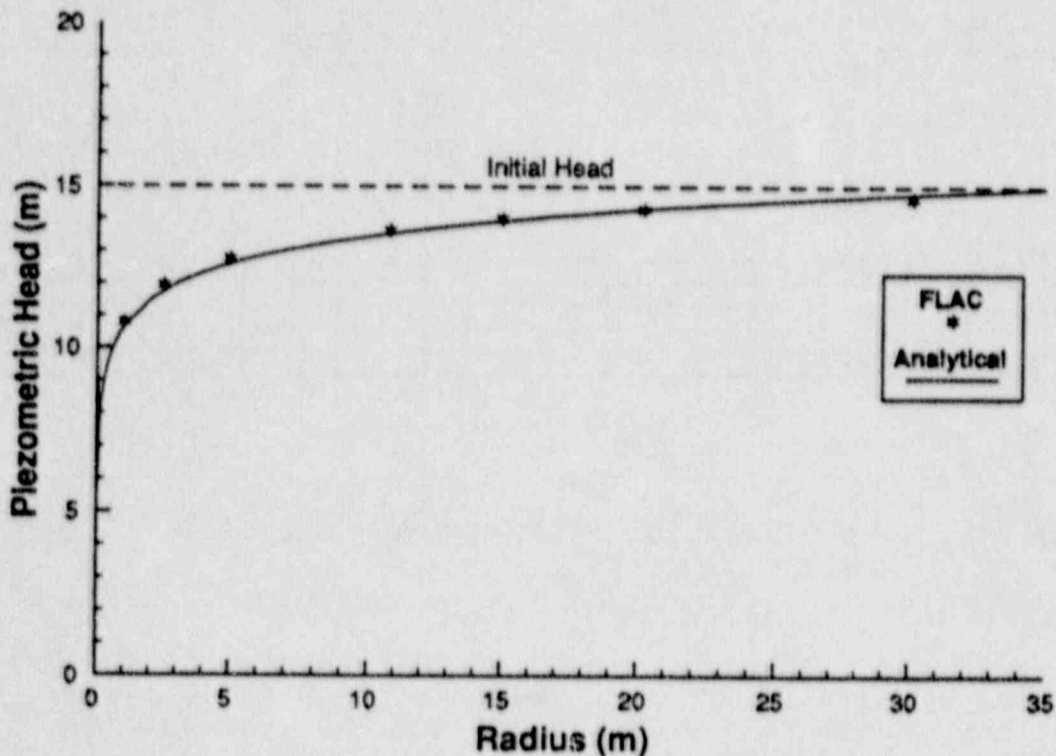
Fig. 3.2.3.1-3 Comparison Between Analytical and FLAC Solutions
for Head Distribution Around a Pumped Well

The FLAC drawdown data is plotted in Fig. 3.2.3.1-4, as a function of the logarithm of the radial coordinate. The linear plot at low values of r yields a slope of -2.76. From Eq. (3.2.3.1-9), this corresponds to a transmissivity of 2.93×10^{-3} $m^2 s^{-1}$, and a hydraulic conductivity of 2.93×10^{-4} ms^{-1}. This compares favorably with the value of K of 2.92×10^{-4} ms^{-1} used in the FLAC analysis.

The storage coefficient may be calculated from the intercept on the log r axis of the linear plot shown in Fig. 3.2.3.1-4. For drawdown s = 0, $\log(r_o)$ = 1.52, and S = $(2.25 Tt/r_o^2)$ = 6.01×10^{-4}.

The mechanical and hydraulic properties of the aquifer used in the FLAC analysis correspond to a storage coefficient of 4.81×10^{-4}, which is about 20% different from the value derived from treatment of the drawdown data. The difference may be accounted for by the logarthmic term involved in the estimation of the storage, and the consequent loss in precision.

Other results of FLAC analysis, including plots of distributions of pore pressure, principal stresses (major, intermediate ($\sigma_{\theta\theta}$) and minor), and y-component of displacement are presented in Figs. 3.2.3.1-5(a-e). The plots are, in all respects, consistent with theoretical predictions of aquifer consolidation during discharge.
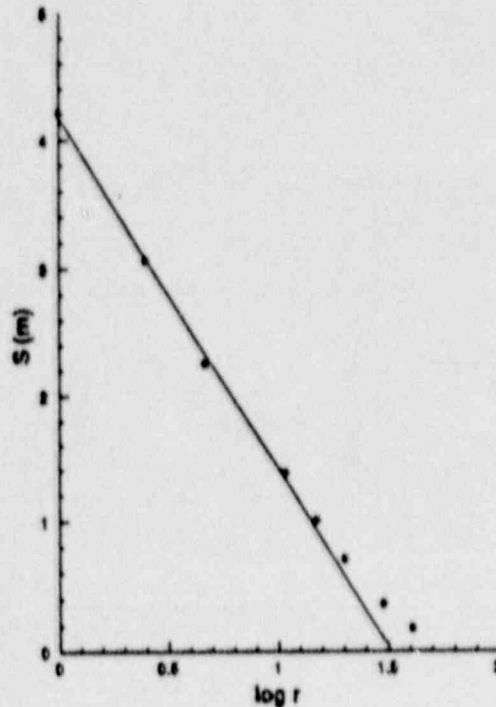
Fig. 3.2.3.1-4   Plot of Drawdown versus Log (Radius Coordinate) [Best fit line to FLAC solution for Estimation of Aquifer Hydraulic Properties]

3.2.3.1-8
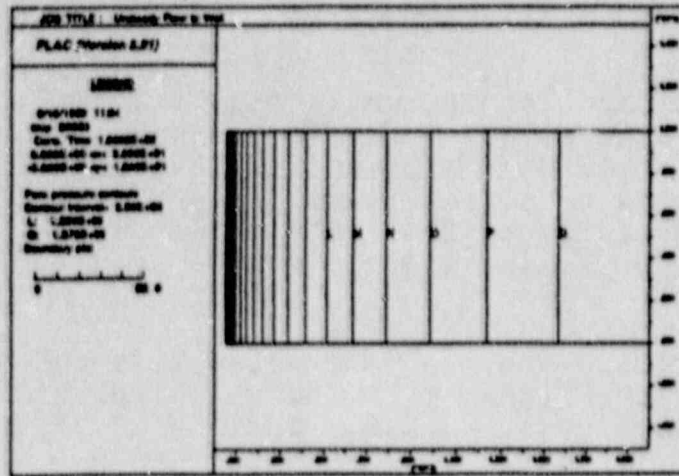
(a)
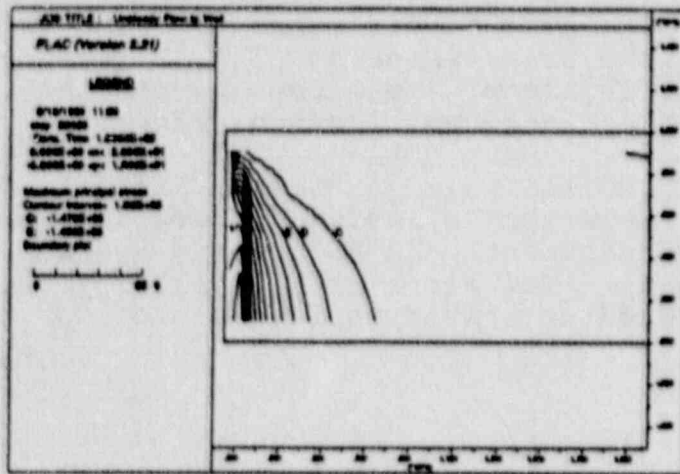
(b)
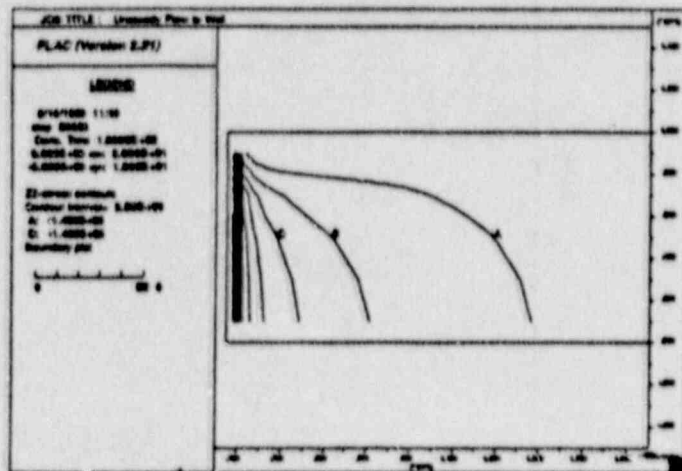
(c)

Fig. 3.2.3.1-5   Plots of Distributions of (a) Pore Pressure,
(b) Major Principal Stress, (c) Intermediate
Principal Stress
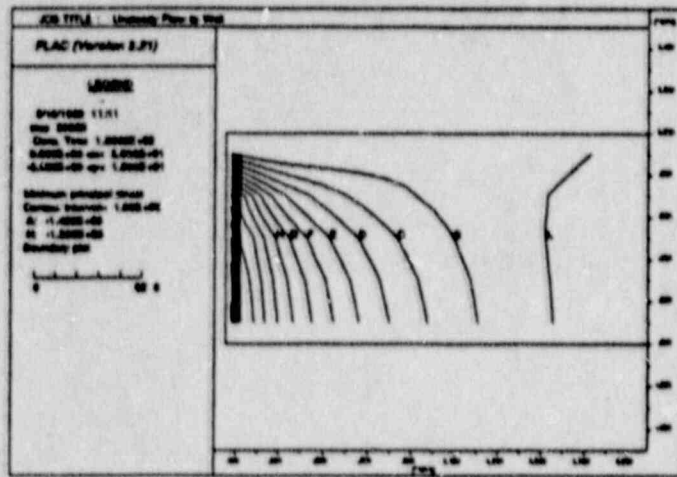
(d)
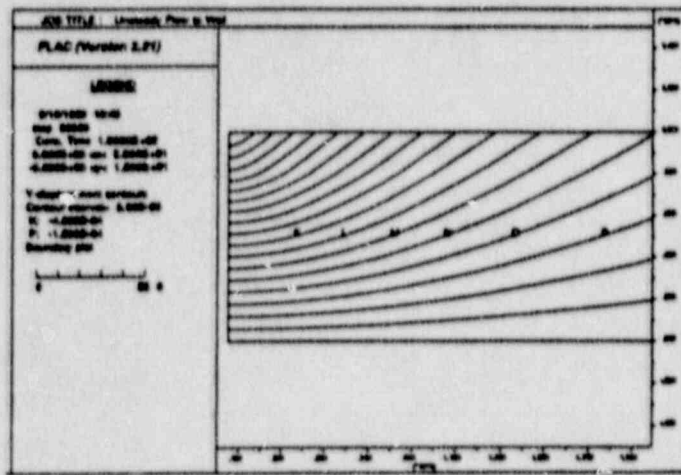
(e)

Fig. 3.2.3.1-5 Plots of Distributions of (d) Minor Principal
Stress, and (e) y-Component of Displacement

Discussion

The FLAC analysis of discharge from a confined aquifer confirms
that the code correctly simulates porous flow and consolidation
in a saturated compressible medium. It suggests the code is use-
ful for many problems in which consolidation or swelling is the
controlling phenomenon.

References

De Wiest, R.J.M. Geohydrology. New York: John Wiley and Sons,
1965.

Thies, C. V. "The Relation Between the Lowering of the
Piezometric Surface and the Rate and Duration of Discharge of a
Well Using Groundwater Storage," Trans. Am. Geophys. Union, 16,
519-524 (1935).

Data Input File

```
**************************************************************************
* FLAC Verification Problem
* Transient Flow to a Well Penetrating a Confined Aquifer
* Comparison with the Theis Solution
* This Problem Tests the Logic for Fluid Flow and Solid Deformation
**************************************************************************
*
title
  Unsteady Flow to Well
*
* Specify axisymmetry and groundwater options
*
config axi gw
*
* Specify grid
*
gr 50,5
*
* Elastic rock mass
*
model elas
*
* Properties
*
prop porosity 0.4 perm 2.98e-8
prop bulk 1.18e8 sh 7.1e7 dens 1560
water dens 1000 bulk 2e9
*
* Create model of problem domain
*
gen 0.5,0 0.5,10 100,10 100,0 rat 1.05 1.0
*
* Set initial and boundary conditions
*
ini pp 1.47e5
ini szz -1.47e5
apply discharge=-7.035e-4 i=1 j=1,6
fix pp i=51 j=1,6
fix y j=1
apply press 1.47e5 j=6
fix x i=1
fix x i=51
*
```

```
* Record histories
*
his nstep 50
his unbal
his ydis i=1 j=6
his ydis i=10 j=6
his pp i=1 j=3
his pp i=10 j=3
his pp i=40 j=3
his sig1 i=1 j=3
his sig2 i=1 j=3
his szz i=1 j=3
his sig1 i=10 j=3
his sig2 i=10 j=3
his szz i=10 j=3
*
* Set parameters for problem execution
*
set flow on
set mech on
set ngw=1
set nmech=1
set clock=4000 step=100000 force 1e-3
*
* Solve
*
step 500
save f11.sav
set ngw 5
step 500
save f12.sav
set ngw 10
solve age=100
save f13.sav
ret
```

3.2.3.2 One-Dimensional Consolidation

Problem Statement

A saturated soil column (Fig. 3.2.3.2-1) with uniform initial excess pore pressure p_o, is free to drain from the top surface. The column is mechanically constrained along its vertical and bottom boundaries. A pressure, σ_v, is suddenly applied to the top surface of the column. The applied pressure is initially carried largely by the fluid but, as time continues, the fluid drains through the upper surface, transferring the load to the soil grain matrix. The theory of consolidation predicts the pore fluid pressure in time and space.

Purpose

This problem provides a check of the ability of FLAC to model the coupled process of fluid flow and mechanical response.

Problem Specifications

A soil column, 20 m in height and 1 m in width has the following initial and boundary conditions (Fig. 3.2.3.2-1):
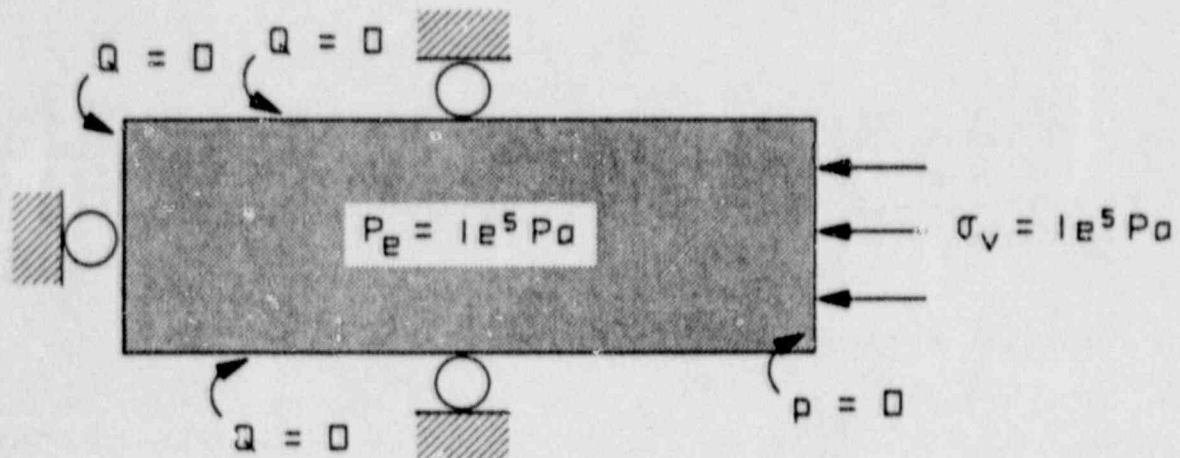
Fig. 3.2.3.2-1   One-Dimensional Consolidation of a Column of
                 Saturated Soil, 20 m in Height

Boundary Condition:

- x-displacement fixed at x = 0 and x = 1

- x- and y-displacement fixed at the base of the column, y = 0

- pore pressure = 0 at top of column (y = 20)

- impermeable boundaries along x = 0 and x = 1 ($\Delta P/\Delta x = 0$) and along y = 0 ($\Delta P/\Delta y = 0$)

- mechanical axial stress, σ_v = 1e5 Pa applied to top surface of column

Initial Condition:

- initial uniform (excess) pore pressure in soil = 1e5 p_a

- initial total stress in soil is equal to the applied stress (i.e., $\sigma_{yy} = \sigma_v = $ 1e5 Pa)

These conditions mean that the soil is free to drain from its top surface, and the pore pressure symmetry condition at the bottom of the column ($\Delta P/\Delta y = 0$) means that column is effectively 2H or 40 m in height from a fluid flow standpoint.

Assumptions

The code assumes isotropic Darcy flow for fluid transport. The soil grain skeleton is assumed to behave elastically. The water is assumed to flow in the vertical direction only, and there is no horizontal strain.

Analytic Solution

The analytic solution for one-dimensional consolidation can be found in many texts on soil mechanics (e.g., Lambe and Whitman, 1969). The basic Terzaghi consolidation equation is given by:

$$C_V \frac{\partial^2 p_e}{\partial y^2} = \frac{\partial p_e}{\partial t} - \frac{\partial \sigma_v}{\partial t} \qquad (3.2.3.2-1)$$

where $C_V = \dfrac{k}{\gamma_w m_v}$, coefficient of consolidation,

    where k = permeability,

        γ_w = unit weight of water, and

        m_v = the coefficient of volume change for the soil, or the inverse of the confined modulus,

$$\frac{1}{K + (4/3)G} \text{ ,}$$

p_e = the excess pore pressure,

σ_v = applied pressure,

y = depth coordinate, and

t = time.

The solution to this equation is found in terms of dimensionless variables:

$$Y = \frac{y}{H}$$

$$T = \frac{C_V t}{H^2} \qquad (3.2.3.2-2)$$

where y and Y are measured from the top of the consolidating column, and

    H is one-half the thickness of the entire column.

Equation (3.2.3.2-1) becomes:

$$\frac{\partial^2 P_e}{\partial y^2} = \frac{\partial P_e}{\partial T}$$

(3.2.3.2-3)

For initial conditions at t = 0:

$$P_e = P_0 \text{ for } 0 \leq Y \leq 2$$

(3.2.3.2-4)

where P_0 = initial uniform pore pressure.

For boundary condition at all t:

$$P_e = 0 \text{ for } Y = 0$$

(3.2.3.2-5)

Due to our no-flow symmetry condition at the base of the column, $P_e = 0$ for Y = 2.

The solution to Eq. (3.2.3.2-3) subject to these constraints is:

$$U_p = \sum_{m=0}^{\infty} \frac{2P_0}{M} (\sin MY)_e M^{-M^2 T}$$

(3.2.3.2-6)

where $M = \frac{\pi}{2} (2m + 1)$.

Computer Model

The computer model consists of a grid one element wide by 20 elements in height (Fig. 3.2.3.2-2). Each element is 1 m wide by 1 m in height. The vertical boundaries (i = 1 and i = 2, and x = 0 and x = 1) have fixed velocities in the x-direction. The base of the column (j = 1; y = 0) has fixed velocities in the x- and y-directions. The top of the grid (y = 20; j = 21) is kinematically free. Conditions of zero fluid flow are given to the vertical boundary and base. The top row of zones (j = 20) have pore pressure fixed at zero to provide for drainage from the top of the column.
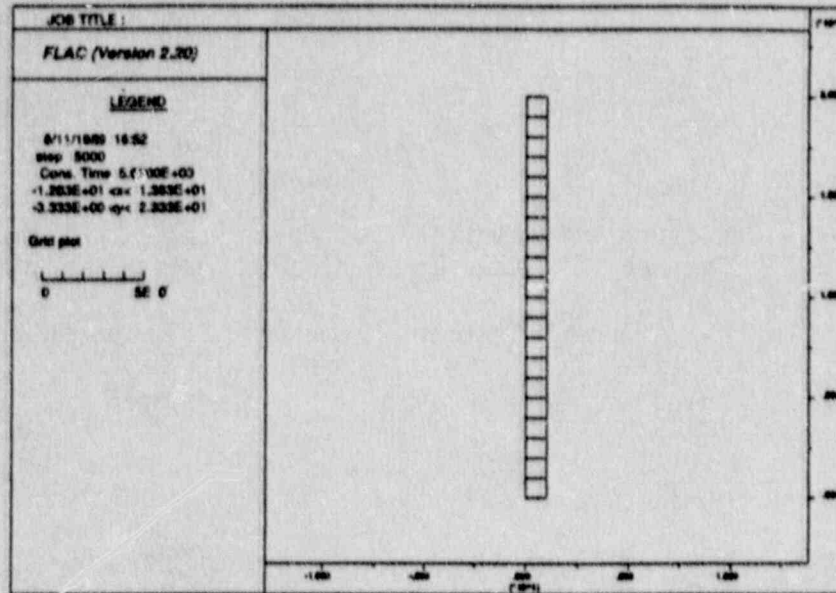
Fig. 3.2.3.2-2 One-Dimensional Geometry (soil elastic, fluid
               flow by Darcy's Law)

A vertical stress, σ_v, is applied to the top of the grid. An in-
itial stress, σ_{yy} equal to σ_v is applied to all zones in the
model to provide initial equilibrium of the stresses. This sup-
presses initial elastic compression of the grain matrix, as we
are only interested in the consolidation due to pore pressure
dissipation.

The properties of the soil and fluid are:

        density, ρ (saturated) 2000 kg/m^3

        bulk modulus, K (dry) $5e^8$Pa

        shear modulus, G (dry) $2e^8$Pa

        Bulk Modulus, fluid, K_w $2e^9$Pa

        Permeability soil, k $1e^{-10}$

The permeability input to FLAC requires units of $[L^3T/M]$ (e.g.,
m^{3}s/kg). These units are derived from the fact that FLAC re-
quires permeability defined as

$$k_{flac} = \frac{k}{gp_w} = \frac{k}{\gamma_w}$$

Greater detail on the input units can be found in Appendix F of the FLAC User's Manual, Volume 2 of this documentation.

The initial conditions and applied loading are given by:

initial excess pore pressure $\qquad$ $P_e = 1e^5 Pa$

applied vertical pressure $\qquad$ $\sigma_v = 1e^5 Pa$

The simulation is conducted by "switching on" fluid flow, and coupling the mechanical model every 25 timesteps. The data file is given at the end of this section.

Results

The history of the pore pressure at the base and mid-height of the soil column are given in Figs. 3.2.3.2-3(a) and -3(b). Time in these plots is given in seconds. As seen here, the pore pressure decay is exponential with time. At the instant of load application (time = 0) and for some time thereafter, the pore water sustains the applied load. As the water flows from the sample, the load is transferred to the grain matrix. Figure 3.2.3.2-4 shows the pore pressure versus depth in the column for various times. The boundary condition, $p_e = 0$ at $y = 20$ m is seen as is the symmetry condition at $y = 0$ m.

Discussion

The analytic solution was given in terms of dimensionless quantities, Y and T. We present the comparison of FLAC results to the analytic solution in terms of pore pressures at the base ($y = H$ or $Y = 1.0$) and the mid-height of the column ($y = H/2$ or $Y = 0.5$) for times of $t = 1000$ sec, 2000 sec, 3000 sec, 4000 sec and 5000 sec. The pore pressures are shown graphically in Fig. 3.2.3.2-5. Table 3.2.3.2-1 lists the analytic and calculated values and the percentage error. As seen, the agreement is excellent.

Reference

Lambe, T. W., and R. V. Whitman. Soil Mechanics. New York: Wiley and Sons, 1969.
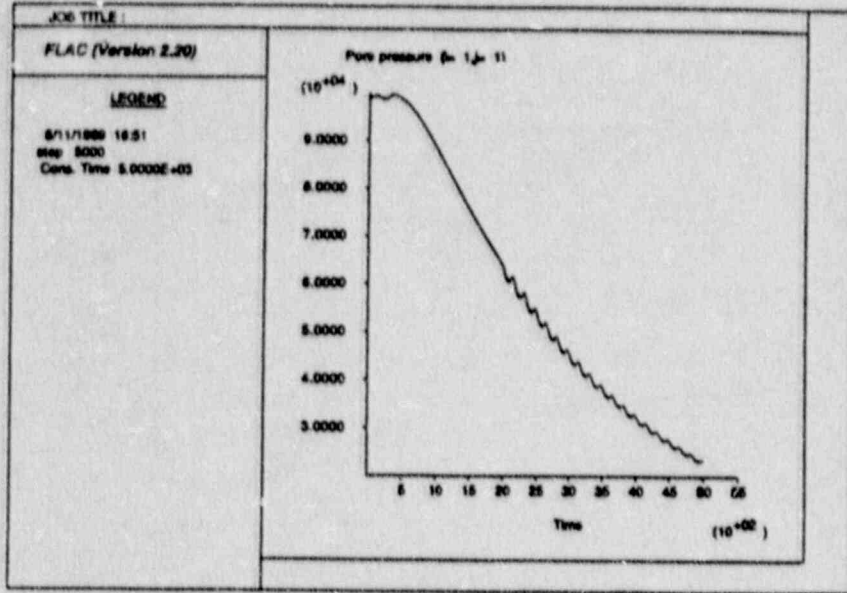
(a)
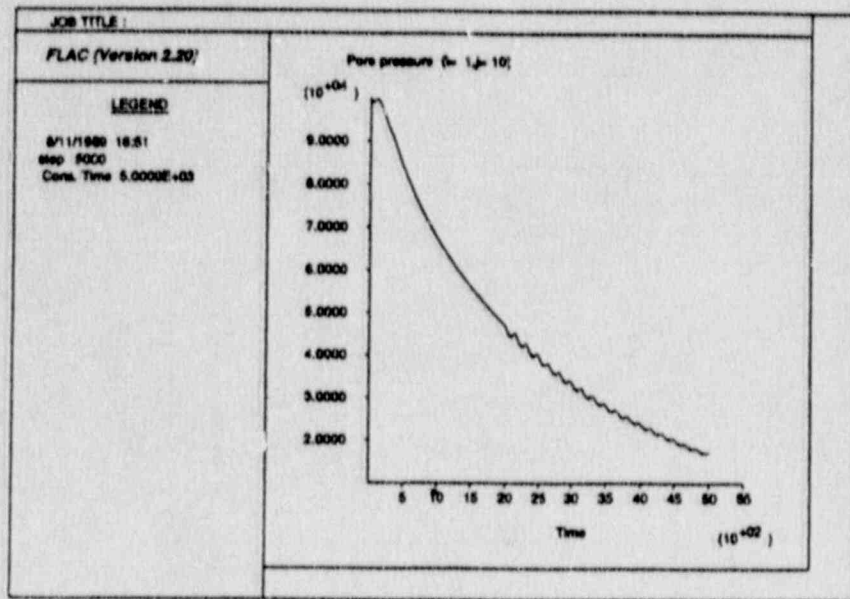
(b)

Fig. 3.2.3.2-3   History of the Pore Pressure at the Base (a) and
Mid-Height (b) of the Soil Column
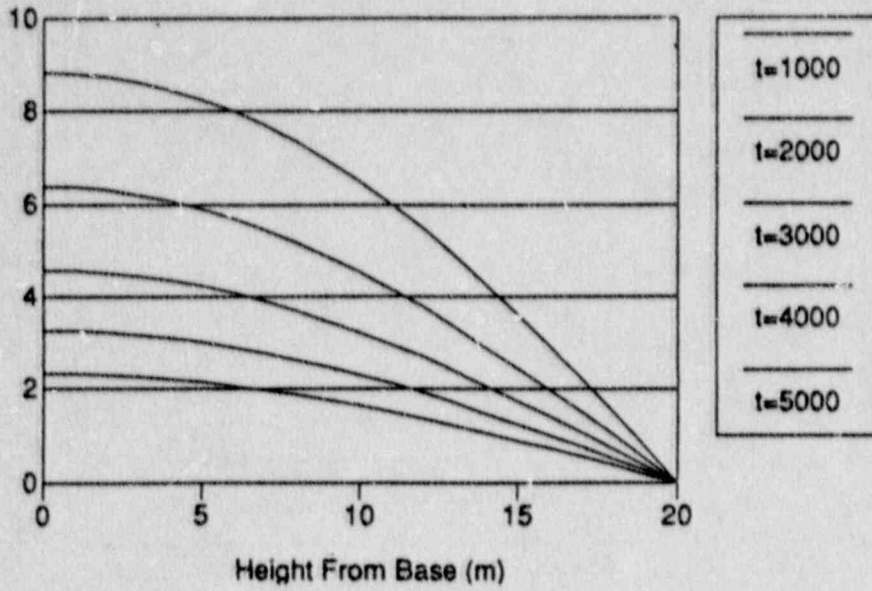
Fig. 3.2.3.2-4   FLAC Pore Pressure Distribution in Soil Column
for Various Times
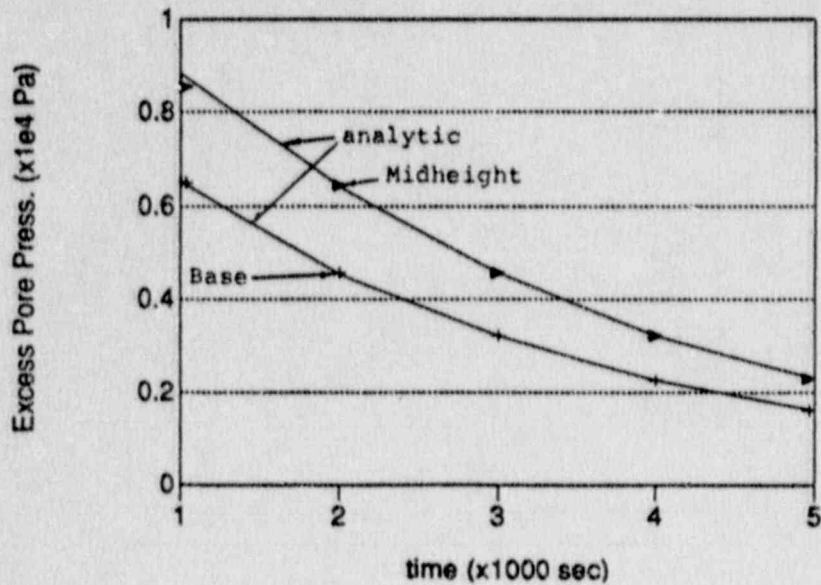
Fig. 3.2.3.2-5   Comparison for One-Dimensional Consolidation FLAC
to Analytic Solution at the Base and Mid-height
of the Column   (FLAC solutions given as symbols)

Table 3.2.3.2-1

COMPARISON OF FLAC TO ANALYTIC RESULTS FOR ONE-DIMENSIONAL CONSOLIDATION

t (sec)	T	y	Y	$P_e(1*10^4 Pa)$ Analytic	$P_e(1*10^4 Pa)$ FLAC	% Error
1000	0.13855	H	1.0	0.885	0.885	< 1%
		H/2	0.5	0.653	0.651	< 1%
2000	0.27711	H	1.0	0.642	0.644	< 1%
		H/2	0.5	0.455	0.457	< 1%
3000	0.41565	H	1.0	0.457	0.457	< 1%
		H/2	0.5	0.323	0.323	< 1%
4000	0.5542	H	1.0	0.324	0.324	< 1%
		H/2	0.5	0.229	0.229	< 1%
5000	0.69275	H	1.0	0.230	0.230	< 1%
		H/2	0.5	0.163	0.163	< 1%

FLAC Input Data File

```
***********************************************************************
*FLAC comparison to 1-D consolidation test.  Assume a twenty meter soil
*column with initial pore pressure of 1e5 is compressed by an axial
*pressure of 1e5.  The top surface of the column is drained, and the
*base is fixed.  Solution may be found in Lambe and Whitman, page 409
***********************************************************************
*
*Use log on feature to dump all screen information to a disk file
*
set log on
*
*set configuration for transient flow analysis
*
config gw
*
*define grid for 1-D consolidation test
*
grid 1 20
*
*grain skeleton behaves elastically
*
model elastic

*
*boundary conditions
*
fix x               * (just allow vertical motion)
fix x y j=1         * (fix the base mechanically)
*
*material mechanical and hydrologic properties
*
prop d 2000 bulk 5e8 shear 2e8
*
*See manual for explanation of permeability units
*
prop perm=1e-10
water bulk=2e9
*
* all zone pore-pressures are equal initially
*
ini pp=1e5
*
```

```
*complete drainage at top surface by fixing 0 pore pressure
*
ini pp=0 j=21
fix pp j=21
*
*set total stresses to equal applied load
*
apply pres=1e5 j=21
*
*stress in the body is set equal to applied pressure to prevent
*initial elastic compression of the skeleton
ini syy=-1e5
*histories
his pp i=1,j=10
his pp i=1 j=1
his ydis i=1 j=21
his unbal
*
*use 25 mechanical steps for every fluid time step.  Note: this will
*be time consuming, but provide a smoothly-varying result
*
set nmech=25
*5000 time steps are taken here, but could continue simulation
*to any desired time. Grid point pore pressures may be printed as
*often as desired (print gpp) for comparison to analytic solution
step 5000
return
*end of problem
```

3.3 EXAMPLE PROBLEMS

The previous verification problems provide assurance that FLAC implements the various individual component models correctly. Verification problems have analytical solutions and are necessarily based on simple boundary conditions and geometries. The following example problems illustrate the more typical use of the FLAC code on complex problems which may exercise many different aspects of the code. Three example problems have been chosen which demonstrate the interactive effects of the thermal, mechanical and support logic.

Room-Scale Simulation of Nuclear Waste in Welded Tuff

This problem illustrates the use of FLAC for analysis of vertical emplacement of spent fuel in welded tuff at the Yucca Mountain site. The rock mass is represented by a ubiquitous joint model with a predominant vertical jointing. Exponentially-decaying heat flux lines are used to represent the waste form. Convective boundaries are used at the excavation to represent ventilation.

Soil-Nailed Wall in Sand

A typical soil mechanics problem involves the reinforcement of the walls of excavations for building foundations. This problem examines the behavior of the vertical walls of a foundation excavation in sand. These walls are supported by a shotcrete surface and soil "nails", which are short, grouted bars. Further support is provided by a single set of cable anchors.

Lined, Circular Tunnels in a Sea Bed

This problem examines the excavation and lining of three circular tunnels in an elastic rock located within the sea bed at a depth of 70 meters below the water level. The thrusts and moments induced in the liner are examined.

3.3.1 Room-Scale Simulation of Nuclear Waste in Welded Tuff

Problem Statement

This problem provides an example of structural stability of disposal rooms in a geologic radioactive waste repository. This subject is important because of requirements to be capable of retrieving the emplaced waste should this become necessary. The problem is taken from Brandshaug (1989), and was completed using Version 2.03 of the FLAC code.

The candidate repository site is at Yucca Mountain, Nevada located in a densely welded tuff. The site is being evaluated as potentially the first radioactive waste repository in the United States. A project position paper on waste retrieval, given by Flores (1986), concludes that the disposal rooms are likely to be stable, but may require a minimal amount of maintenance.

A waste retrieval philosophy and list of design criteria are given in the Site Characterization Plan Conceptual Design Report (SCPCDR) (MacDougall et al., 1987). The "retrievability period" is defined as "the time during which the ability to initiate retrieval will be maintained" and is up to 50 years [U.S. DOE (1986), Appendix D]. The "retrieval period" is defined as "the time period required for removal of the emplaced waste from the underground repository, if a decision to retrieve the waste is made" and is up to 34 years (Flores, 1986).

Assessment of room stability involves the evaluation of inelastic rock behavior such as the creation of new fractures in the intact rock caused by excessive shear stresses, and movement along pre-existing joints such as slip or opening. These movements may result from the excavation of the disposal rooms, the continuous heating of the rock because of the presence of the radioactive waste, and from the effects of forced ventilation for room access.

Purpose

The purpose of this example is to demonstrate the types of numerical analyses that are helpful in evaluating stability of waste disposal rooms during retrieval. Access to and retrieval of the waste are assumed to take place through the disposal rooms.

The focus of the analyses is toward effects that may compromise the structural stability of the rooms. Because two-dimensional models are used, stability of container boreholes is not investigated. The effects of particular interest include the predictions of any inelastic behavior of the rock around the disposal room, such as the creation of new fractures from excessive shear stresses and slip or opening of pre-existing vertical joints.

Problem Specification

Emplacement of waste in vertical boreholes is an alternative considered in the SCPCDR for Yucca Mountain (Fig 3.3.1-1). Because a two-dimensional model is used, the waste containers and emplacement boreholes cannot be modeled explicitly. Therefore, the discrete thermal power of the waste containers is distributed uniformly along the disposal room. The presence of a heat generating vertical plane along the axis of the room at the center of the floor is used. The potential problem of room instability results from the compounded effect of heat transfer from individual waste containers at some distance from the area of interest. Because of the distance, the heat transfer effect of the individual waste containers to the rock around the room will be damped. Therefore, the concept of using a heat generating plane is an adequate idealization for both emplacement concepts.

The analysis includes only the vertical waste emplacement concept, meaning that single waste containers are placed in vertical boreholes along the disposal room floor. The heat transfer associated with the first 50 years of heating is predicted along with the induced thermal stresses, displacements, and inelastic rock behavior. At the beginning of retrieval (year 50), forced convective cooling of the disposal room is initiated to prepare for the retrieval of any emplaced waste and convective cooling is continued for sufficient time to allow retrieve all waste containers from one disposal room. Rock stresses, displacements, and inelastic behavior is also predicted during this period.
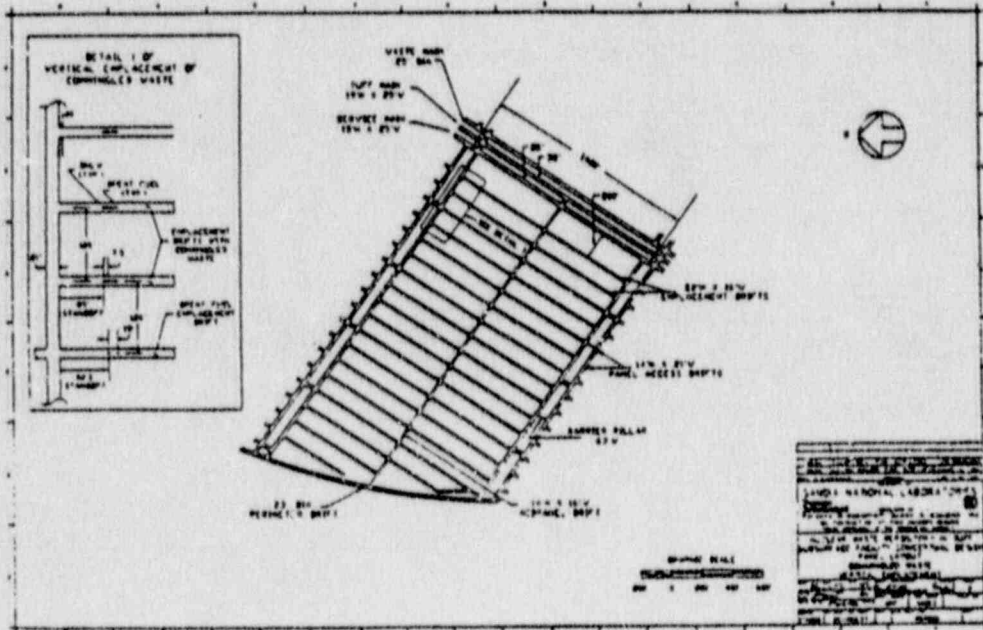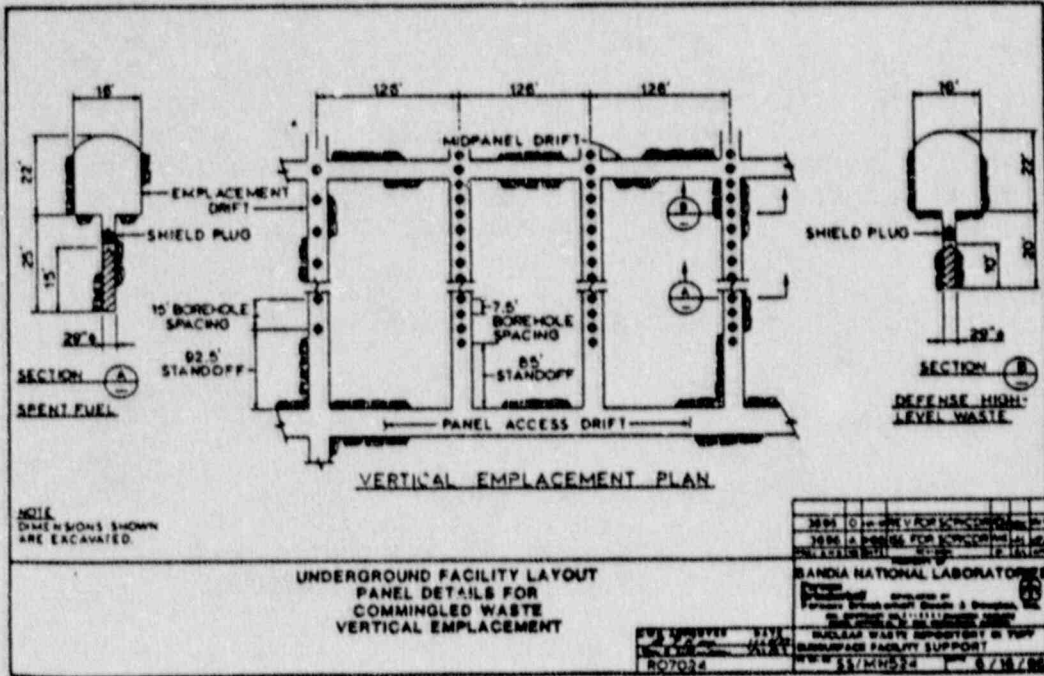
Fig. 3.3.1-1   Plan and Cross-Sectional Views of the Vertical
Commingled SF and DHLW Emplacement Configuration
[MacDougall et al., 1987, Chapter 4]

Assumptions

The assumptions and idealizations used, which affect the outcome
of the model, yield conservative results. With respect to the
heat transfer model, "higher" temperatures are conservative.
With respect to the mechanical model, "higher" deviatoric
stresses are conservative. The assumptions and idealizations
used included:

(a) initial temperature of the rock = 26°C;

(b) retrieval starts 50 years after initial waste em-
placement;

(c) instantaneous waste emplacement;

(d) the disposal room cross-section considered is at
the center of a waste emplacement panel;

(e) no boiling of pore water;

(f) access to and retrieval of the nuclear waste will
take place through the disposal rooms;

(g) the disposal rooms are not backfilled prior to
waste retrieval; and

(h) retrieval starts when the disposal room floor tem-
perature has decreased to less than 50°C.

Being conservative in the predictions of the rock temperatures
results in conservative estimates of rock displacements and devi-
atoric stresses. In addition, when convective cooling of the
disposal rooms begin, the largest possible thermal gradients will
develop, bringing about the largest possible deviatoric stresses
in the rock around the room periphery, and thus, the greatest po-
tential for room instability.

The assumed material properties used are specific to the rock at
the repository horizon (designated as thermal/mechanical unit
TSw2 in the SCPCDR, Chapter 2). The assumed value of the thermal
properties are given in Table 3.3.1-1. Determination of the con-
vective heat transfer coefficient is shown in Appendix C of
Brandshaug (1989). The mechanical properties of the rock mass
are given in Table 3.3.1-2.

Table 3.3.1-1

THERMAL PROPERTIES
[after MacDougall et al., 1987]

PROPERTY	ROCK	DISPOSAL ROOM
Thermal Conductivity (W/m-K)	2.29	50
Specific Heat Capacity (J/kg-K)	931	931
Convective Heat Transfer Coefficient (W/m^2-K)	---	2.61[a]
Coefficient of Thermal Expansion (x 10^{-6} K^{-1})	8.8	---

[a] See Appendix C of Brandshaug (1989) for derivation of this value.

Table 3.3.1-2

MECHANICAL PROPERTIES
[after MacDougall et al., 1987]

PROPERTY	ROCK	JOINTS
Density (kg/m^3)	2320	---
Deformation Modulus (GPa)	15.2	---
Poisson's Ratio	0.22	---
Cohesion (MPa)	17.8	0.1
Angle of Internal Friction (degrees)	23.5	28.4
Uniaxial Compressive Strength (MPa)	166	---

The initial power output of a SF container at the time of emplacement may range from 2.3 kW to 3.4 kW (O'Brien, 1985). The effective Areal Power Density (APD) is based on a conservative initial power of 3.2 kW. The initial power of the DHLW container is chosen as 0.42 kW after Peters (1983). The APD may vary depending on the geometric scale being considered. An APD of 20 W/m^2 representing commingled SF and DHLW (MacDougall et al., 1987, Chapter 4) was used. This APD is higher than in a far-field model because waste emplacement panel stand-off distances have not been included, but lower than the actual waste package heat output. Brandshaug (1989, Appendix B) describes in detail the calculation used to determine the thermal loading.

The thermal decay characteristics of SF and DHLW are given by Peters (1983) for waste ten years out of the reactor:

Spent Fuel $\quad P(t) = 0.54 \exp(\ln(0.5)t/89.3) + 0.44 \exp(\ln(0.5)t/12.8)$

DHLW $\quad\quad\quad P(t) = 0.86 \exp(\ln(0.5)t/34.2) + 0.14 \exp(\ln(0.5)7/15.2)$

where $P(t)$ is a normalized power, and t is time in years. This normalized power function compares well with that given by Mansure (1985) for SF (Brandshaug, (1989). The normalized power is multiplied by the APD to obtain the effective heat output at any given time.

Conceptual Model

Figure 3.3.1-2 illustrates the conceptual models of the vertical waste emplacement mode. Only one-half of the disposal room and pillar needs to be included because of symmetry. The thermal boundary conditions are adiabatic. The two horizontal boundaries have been located sufficiently far from the heat generating waste to remain at the initial temperature of 26°C for the time period simulated.

The kinematic boundary conditions are also shown in Fig. 3.3.1-2, and are such that the two vertical boundaries are restricted from moving in the horizontal direction, while free to move in the vertical direction. The lower horizontal boundary is restricted from moving in the vertical direction, while free to move in the horizontal direction. The upper horizontal boundary is a free-to-move pressure boundary. The initial vertical and horizontal stresses applied to the models are -7 MPa and -3.5 MPa, respectively (MacDougall et al., 1987, Chapter 2). Note, that compressive stresses are negative.
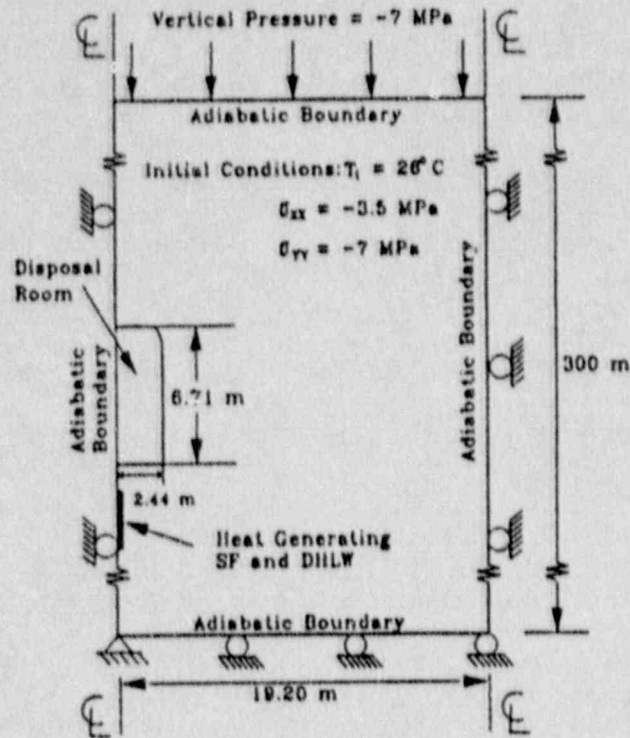
Fig. 3.3.1-2 Conceptual Model of the Disposal Room for Vertical
Waste Emplacement

Computer Model

The FLAC thermal and mechanical portions of the code are used to
simulate the thermal/mechanical response of the rock. A plane
strain model is used, and the rock is characterized as an elas-
tic, perfectly plastic material with ubiquitous vertical joints
(planes of weakness).

A Mohr-Coulomb failure criterion is used to determine if new
fractures are created in the rock matrix (e.g., Brady and Brown,
1985). Slip or opening along the vertical planes of weakness is
determined by a Mohr-Coulomb criterion for joints [e.g., Goodman
(1980)]. The ubiquitous joint model is used to model the behav-
ior of vertical joints. The potential and extent of room in-
stability may be evaluated by allowing inelastic rock behavior to
occur.

The simultaneous mass and heat transfer (coupled convection/dif-
fusion process) which occurs in forced ventilation of a waste
disposal room is not explicitly included in FLAC. However, FLAC
allows the use of effective convective boundaries by applying
Newton's law of cooling (e.g., Pitts and Sissom, 1977) and was
used for this problem.

The following describes the sequence of events which are simulated, and explains some of the specifics related to the heat transfer in the disposal rooms.

- EXCAVATION OF THE DISPOSAL ROOM AT TIME = 0

  Deformations and stresses are determined throughout the rock.

- INITIAL WASTE EMPLACEMENT AT TIME = 0

  Heat transfer calculations start.

- WASTE ISOLATION FROM 0 TO 50 YEARS

  The thermal/mechanical response of the rock is predicted. The disposal room is not ventilated; transfer is by thermal radiation, and some probably by free convection. The effective thermal conductivity of the excavated room is 50 W/m-K.

- WASTE RETRIEVAL FROM 50 YEARS TO THE TIME REQUIRED TO RETRIEVE ALL THE WASTE FROM ONE DISPOSAL ROOM

  The thermal/mechanical response of the rock is predicted during convective room cooling and waste retrieval periods. Forced ventilation starts at year 50 by applying Newton's law of cooling with the room periphery as a convective boundary. If 12 containers/day are removed (Mac-Dougall et al., 1987, Appendix L-2), it takes 14 days to complete retrieval but, conservatively, room cooling is continued for 120 days.

The input files used for FLAC are included at the end of this example. Rock temperatures are predicted at every nodal location throughout the time period simulated. The thermal simulation is followed by mechanical simulation using the elevated temperatures.

Results

The temperatures are illustrated in Fig 3.3.1-3 to 3.3.1-5 as contours (isotherms) at 1, 25 and 50 years after waste emplacement. Because of the short distance between the waste containers and the disposal room, the temperature of the rock around the room starts to increase soon after waste emplacement. When ventilation is initiated at year 50, the room surface temperature significantly drops, (Fig. 3.3.1-6). The results in Fig. 3.3.1-6 are shown for ventilation air temperatures of 10°C and 20°C. Figure 3.3.1-6 also shows that the maximum temperature reached in the floor prior to ventilation is 126°C.

Temperatures along a horizontal straight line from the room wall into the pillar are shown at various times in Fig. 3.3.1-7. Note that high thermal gradients develop adjacent to the room when ventilation starts. The cool rock at the room surface and the high thermal gradients during ventilation may result in a differential thermal contraction and instability of the rock adjacent to the room.
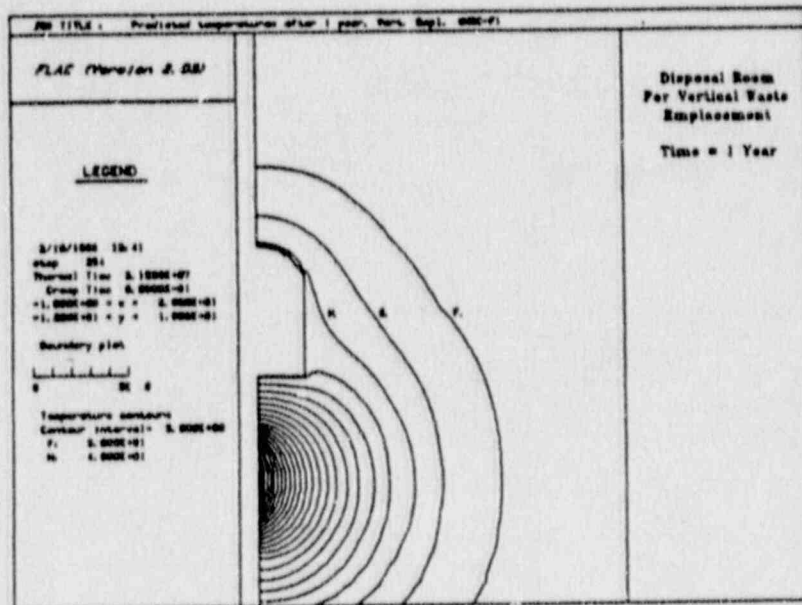
Fig. 3.3.1-3 Predicted Temperature Contours (°C) Around the Waste Disposal Room for Vertical Emplacement 1 Year After Initial Waste Emplacement
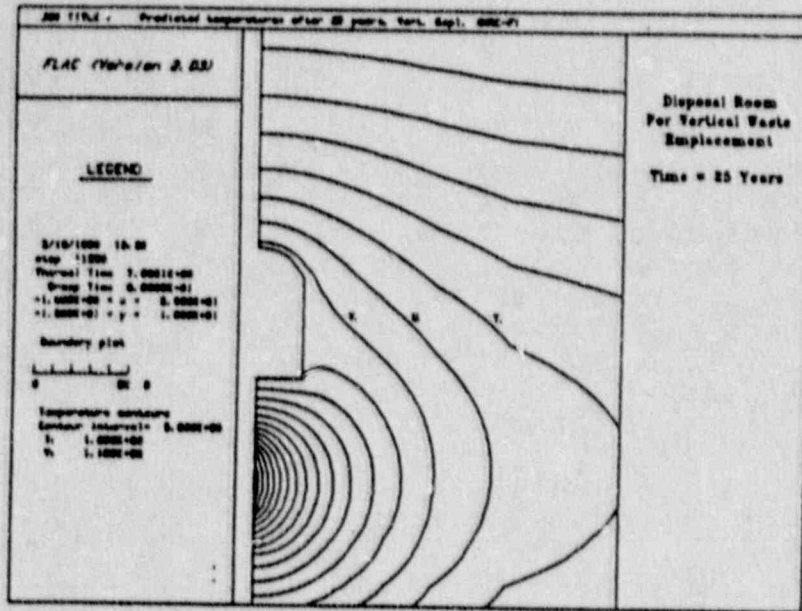
Fig. 3.3.1-4   Predicted Temperature Contours (°C) Around the
                Waste Disposal Room for Vertical Emplacement 25
                Years After Initial Waste Emplacement
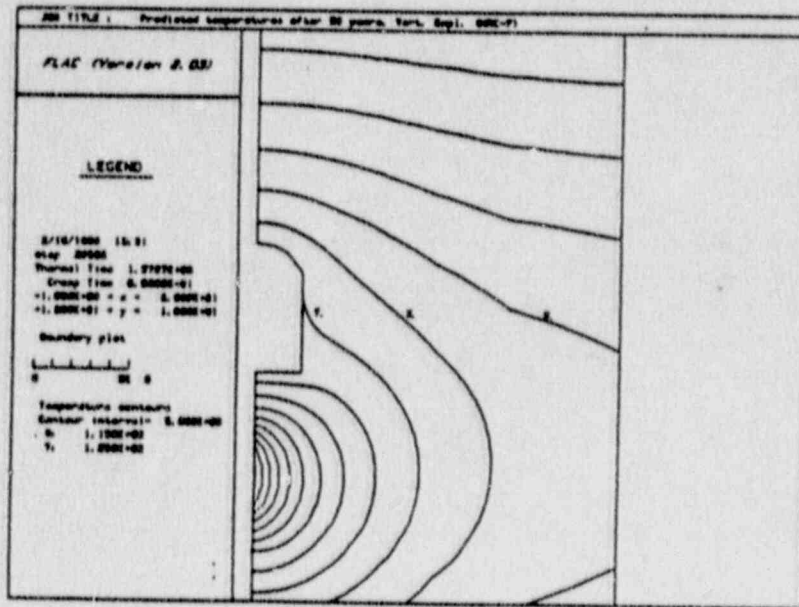
Fig. 3.3.1-5   Predicted Temperature Contours (°C) Around the
                Waste Disposal Room for Vertical Emplacement 50
                Years After Initial Waste Emplacement

50 Year Thermal History
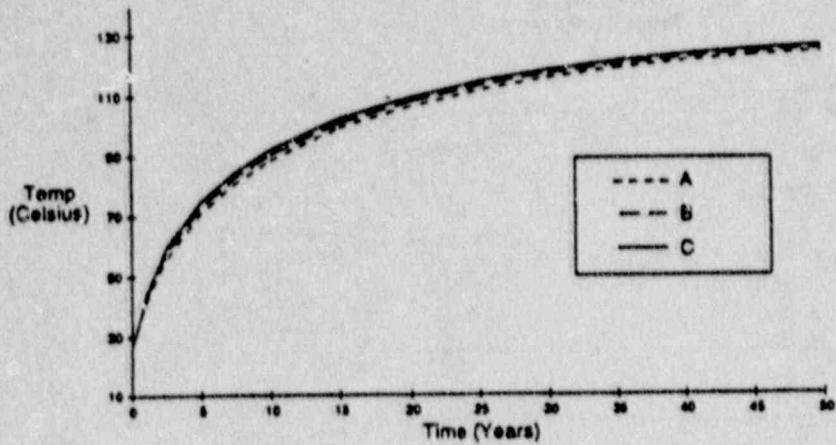
**Ventilation for 120 Days
After 50 Years of Heating
Air Temperature = 10 Deg. C**
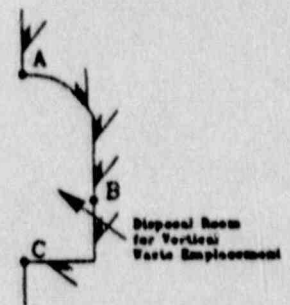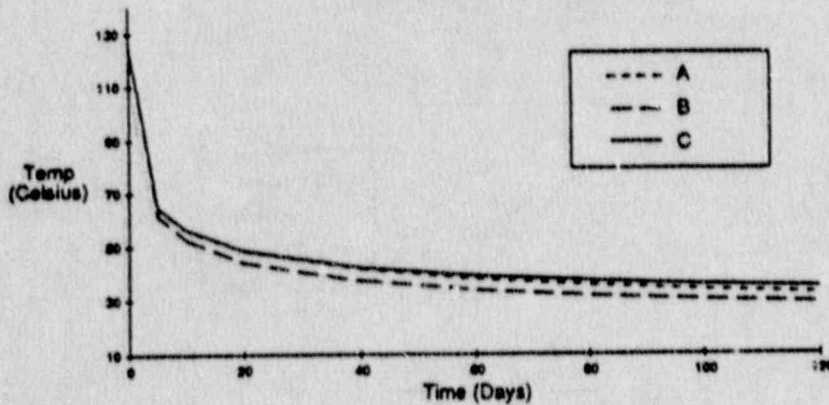
**Ventilation for 120 Days
After 50 Years of Heating
Air Temperature = 20 Deg. C**
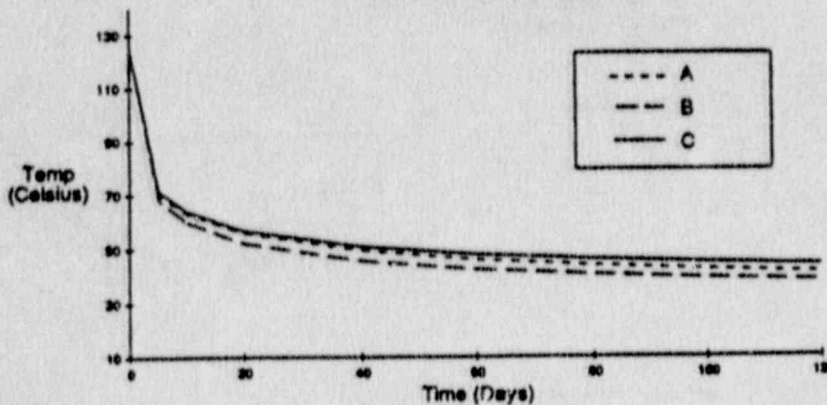
Fig. 3.3.1-6 Predicted Temperature Histories in the Floor, Wall
and Roof of the Waste Disposal Room for Vertical
Emplacement

3.3.1-12
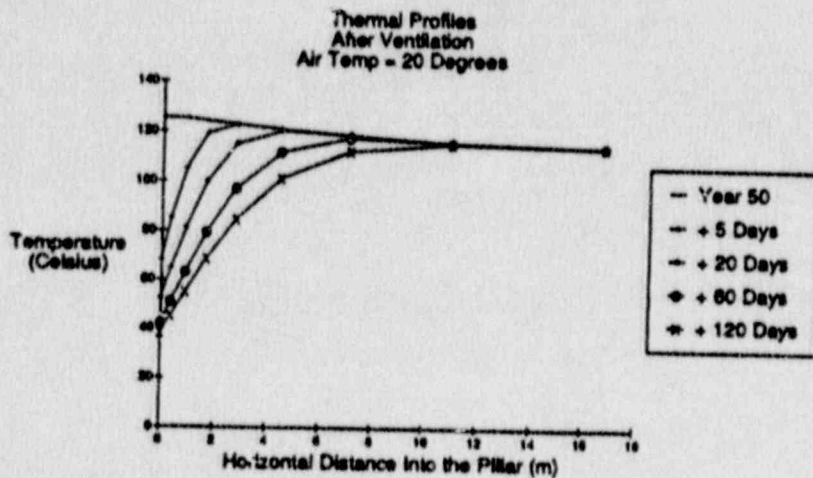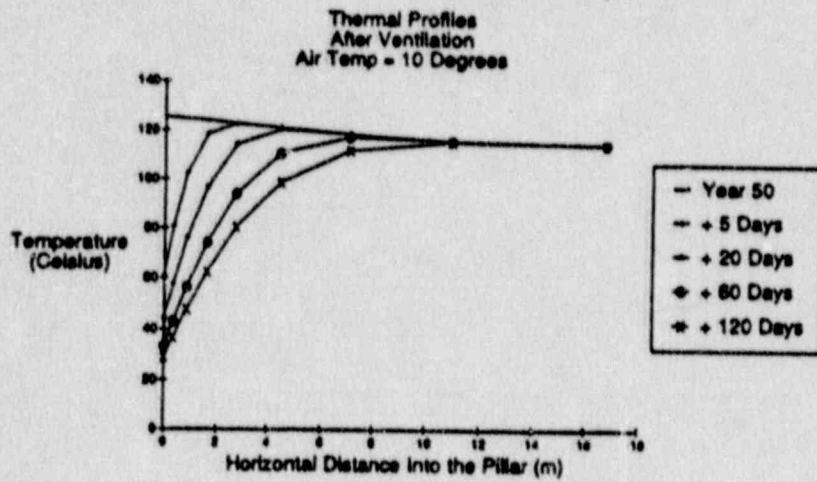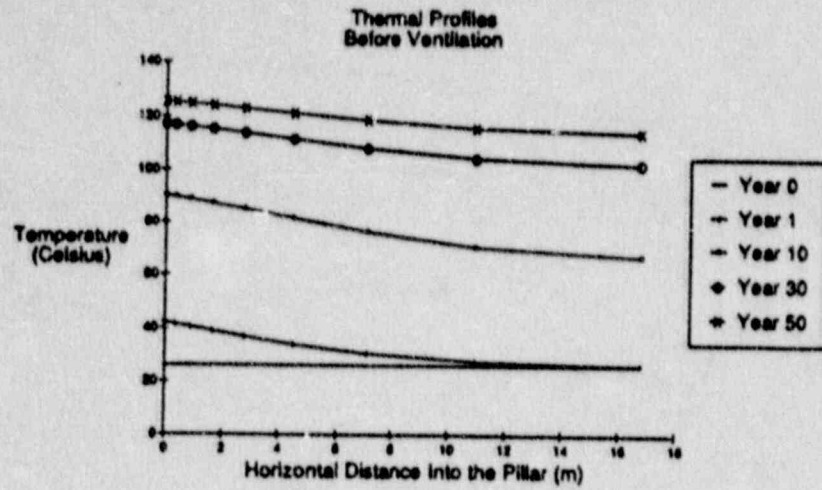
Fig. 3.3.1-7 Predicted Temperature Profiles into the Pillar of the Waste Disposal Room for Vertical Emplacement

Displacements, stresses, and joint slip are predicted in the mechanical model. Results are presented, which show portions of the rock around the room where the vertical joints have slipped (failed in shear). Contours of predicted horizontal and shear stresses are shown, as well as the predicted roof-to-floor closure and wall-to-wall closure.

The mechanical results show that no new fractures are created in the rock as a result of room excavation or thermal expansion of the rock in the period following waste emplacement, but indicate slip along pre-existing vertical joints as a result of room excavation (Figure 3.3.1-8) where the shear stresses exceed the shear strength of the joints. The predicted shear and horizontal stresses (Figure 3.3.1-9) are the same as the shear and normal stresses acting on the joints because the joints are vertical.

The predicted slip along the pre-existing vertical joints is shown in Fig. 3.3.1-10 after 50 years and after 120 additional days of ventilation. There is very little joint slip induced as a result of rock thermal expansion during these periods. Using air of 10°C or 20°C during ventilation has the same effect on the predicted joint slip.

The predicted 50 year history of roof-to-floor closure, and wall-to-wall closure as a result of excavation are shown in Fig. 3.3.1-11. The deformations predicted are very small, and far below the maximum allowable amount of 0.152 m (SCPCDR, Chapter 2).

Joint movement as a result of excavation may not result in room instability, however, it does result in the potential of such an event. Further, decreasing rock temperature resulting from ventilation induces thermal contraction of the rock and, depending on the system of rock fractures around the room, this effect may cause individual blocks of rock to become unstable. The kinematics of individual blocks is not included in the mechanical model and thus this phenomenon is not predicted in this example. A different type of analyses is required to better predict potential block instability.
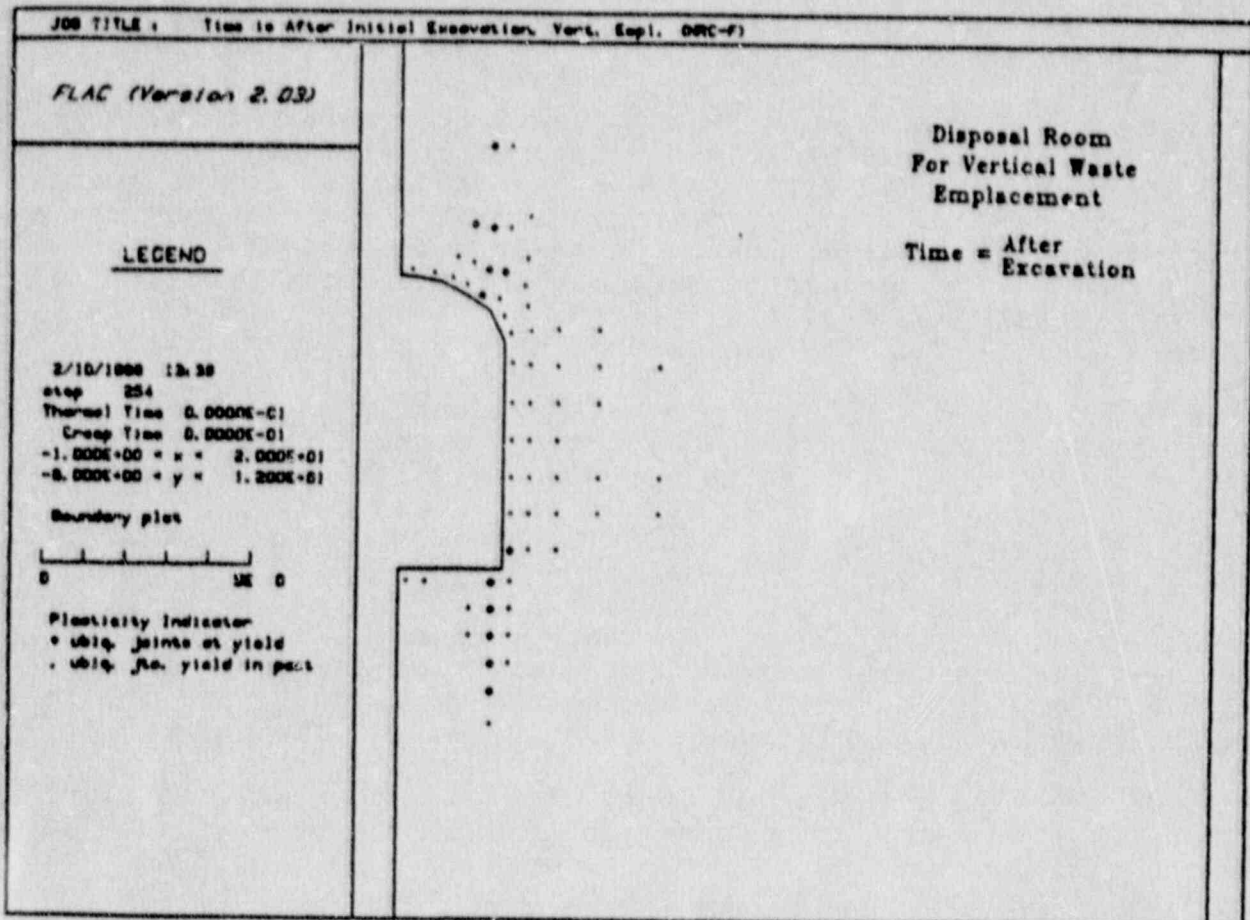
Fig. 3.3.1-8   Predicted Slip Along Vertical Joints as a Result
of Excavation of the Waste Disposal Room for
Vertical Emplacement
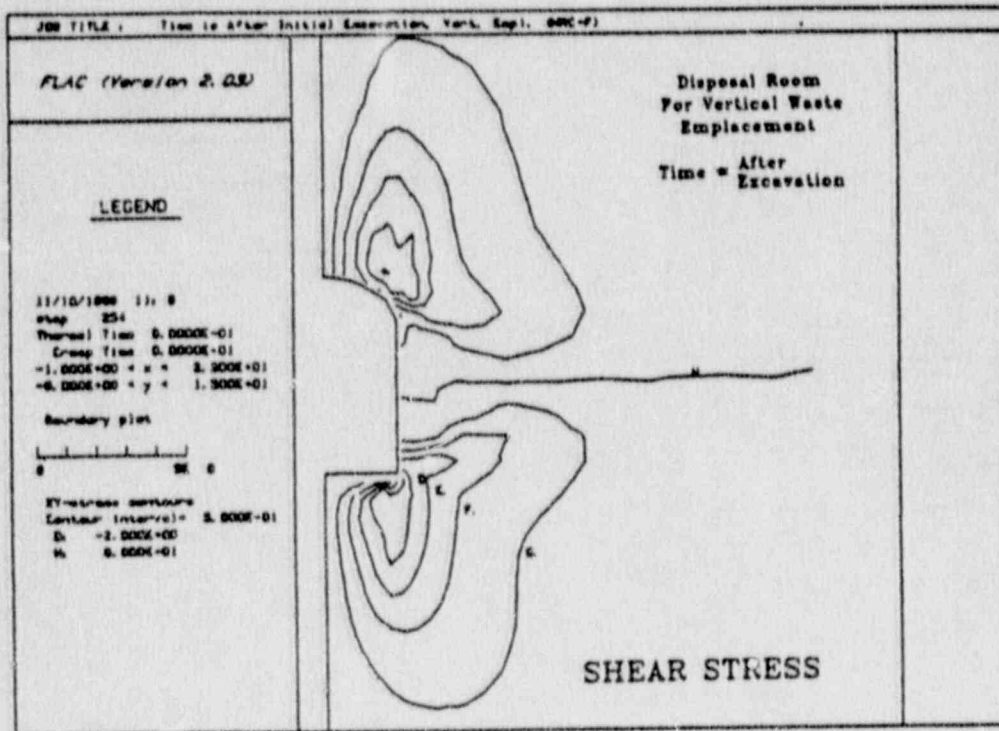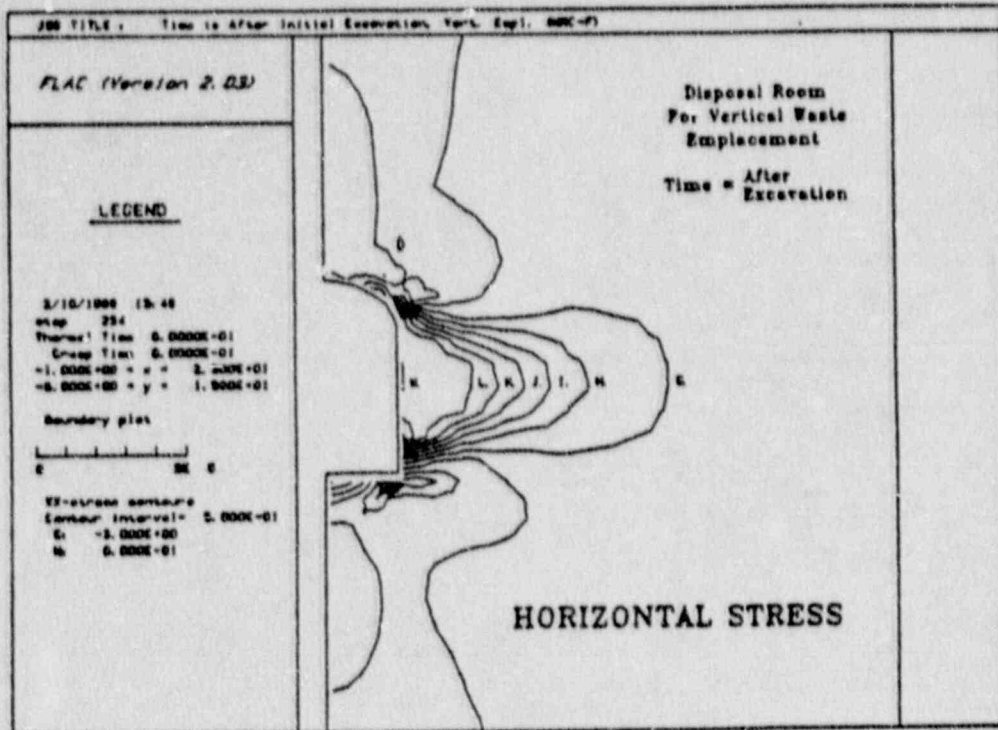
Fig. 3.3.1-9 Predicted Shear and Horizontal Stresses As a Result of Excavation of the Waste Disposal Room for Vertical Emplacement
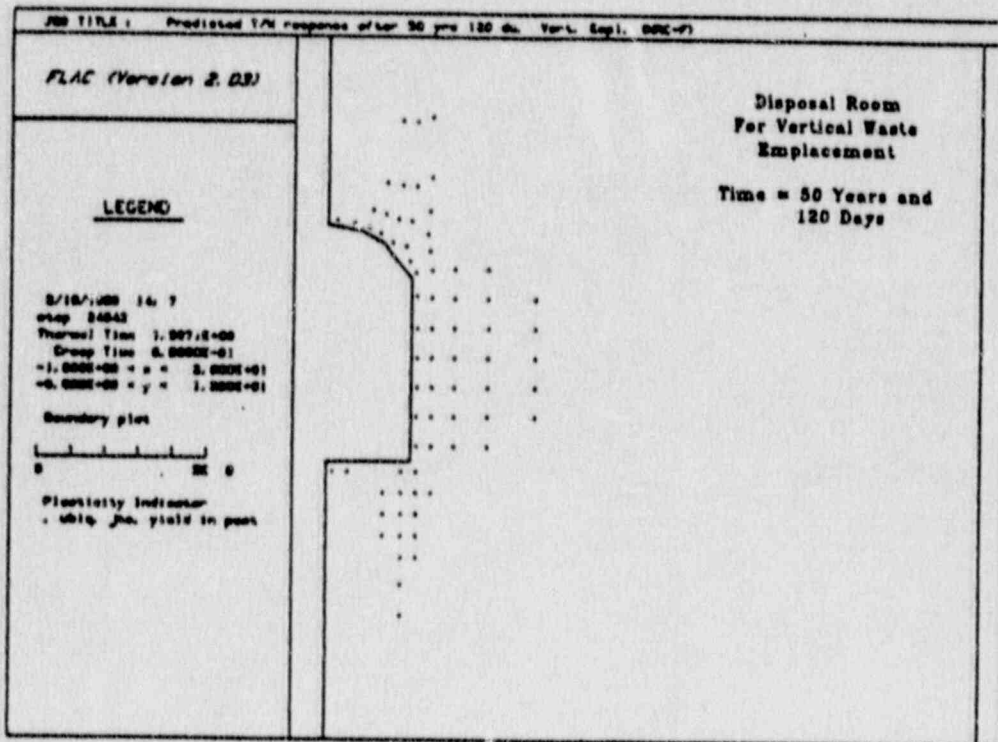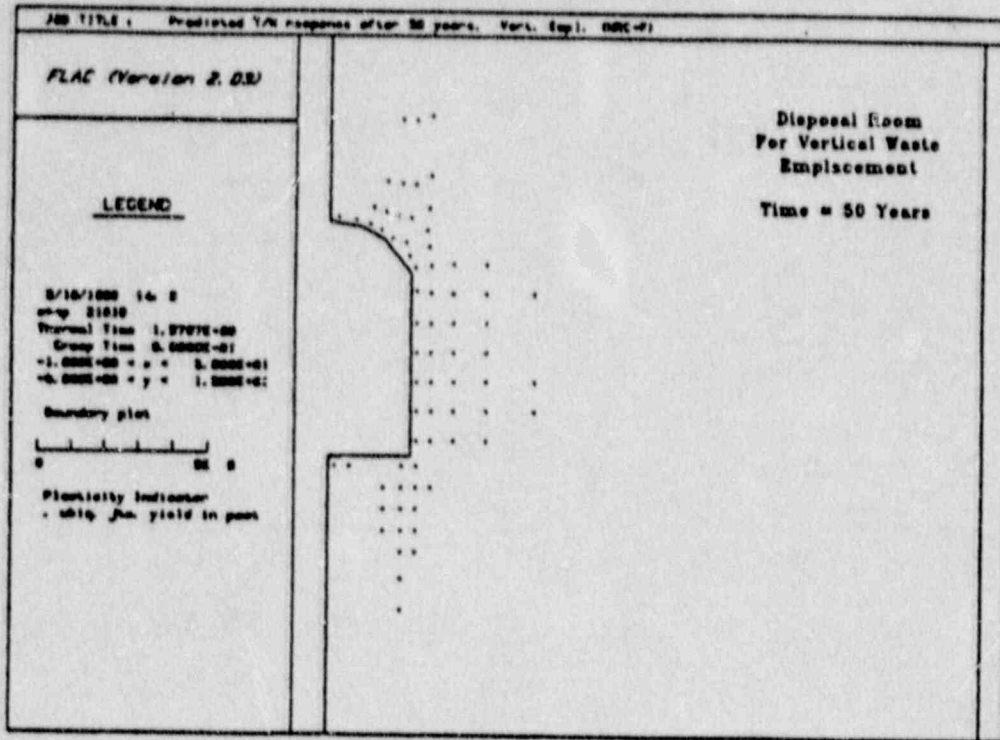
Fig. 3.3.1-10 Predicted Slip Along Vertical Joints Around the
Waste Disposal Room for Vertical Emplacement at
the Time of Waste Retrieval and After Waste
Retrieval

CLOSURE HISTORY
Disposal Room for
Vertical Emplacement
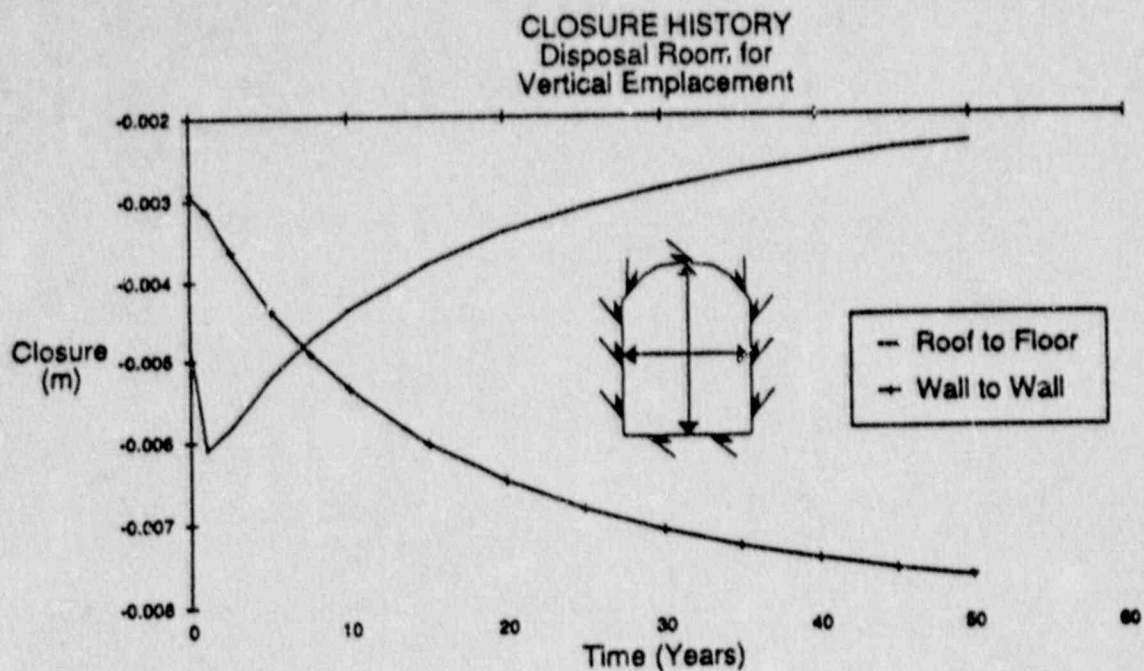
Fig. 3.3.1-11 Predicted History of the Roof to Floor Closure and
Wall to Wall Closure of the Waste Disposal Room
for Vertical Emplacement

Discussion

From the results of the analyses, a set of conclusions can be
made as follows.

1. No new fractures are created as a result of room
excavation, 50 years of thermomechanical rock re-
sponse, or 120 days of convective cooling in prepa-
ration for waste retrieval. Fracturing around the
boreholes was not examined.

2. Slip along pre-existing vertical joints in the rock
is predicted around the disposal room as a result
of room excavation.

3. Fifty (50) years of thermomechanical rock response
has little effect on the development of joint slip
beyond that predicted from room excavation alone.

Note that all of the above conclusions reflect the current under-
standing of the repository site as reported in the SCPCDR. No at-
tempts to determine the effects of uncertainties have been made.

The results contribute to the evaluation of compliance with some of the SCPCDR and CDSCP (U.S. DOE, 1988) design criteria. These most notably include the following.

1. The access and emplacement drifts will remain usable for at least 84 years.

2. The rock displacement in the drifts will be less than 0.152 m (6 in).

References

Brady, B.H.G., and E. T. Brown. Rock Mechanics for Underground Mining. London: George Allen & Unwin, 1985.

Brandshaug, T. "Stability of Disposal Rooms During Waste Retrieval," U.S. Nuclear Regulatory Commission, NUREG/CR-5335, March 1989.

Flores, Richard J. "Retrievability: Strategy for Compliance Demonstration," Sandia National Laboratories, SAND84-2242, January 1986.

Goodman, R. E. Introduction to Rock Mechanics. New York: John Wiley & Sons, 1980.

MacDougall, Hugh R., Leo W. Scully, and Joe R. Tillerson (Compilers). Site Characterization Plan Conceptual Design Report. Sandia National Laboratories, SAND84-2641, September 1987.

Mansure, A. J. "Expected Temperatures for Spent Fuel Borehole Walls and Drifts," Sandia National Laboratories, Sandia Keystone Memo J3 0-85-8, Memo to R. J. Flores, April 15, 1985.

O'Brien, Paul D. "Reference Nuclear Waste Descriptions for a Geologic Repository at Yucca Mountain, Nevada," Sandia National Laboratories, SAND84-1848, September 1985.

Peters, Ralph R. "Thermal Response to Emplacement of Nuclear Waste in Long, Horizontal Boreholes," Sandia National Laboratories, SAND82-2497, April 1983.

Pitts, Donald R., and Leighton E. Sissom. Schaum's Outline of Theory and Problems of Heat Transfer. New York: McGraw-Hill Book Company, 1977,

U.S. Department of Energy (DOE). "Consultation Draft Site
Characterization Plan, Yucca Mountain Site, Nevada Research and
Development Area, Nevada," Nuclear Waste Policy Act, Section 113,
January 1988.

U. S. Department of Energy (DOE). "Generic Requirements for a
Mined Geologic Disposal System, Appendix D, 'Department of Energy
Position on Retrievability and Retrieval for a Geologic Reposi-
tory," OGR/B-2, DOE/RW-0090, Office of Civilian Radioactive Waste
Management, Washington, D.C., September 1986.

FLAC Input Data File

```
*****************************************************************
*                                                               *
*      T H E R M A L / M E C H A N I C A L   A N A L Y S I S    *
*                                                               *
*   Input file to FLAC for determining the effect of ventilation *
*   (Blast Cooling) on disposal room stability during waste retrieval. *
*   Vertical emplacement scheme ...                             *
*   NRC Contract 02-85-002, Task Order No. 006.                 *
*                                                               *
*****************************************************************
*
config thermal
GR 13,40
MOD UBIQUITOUS ; (ubiquitous rock joint model)
MOD TH_iso       ; (isotropic thermal model)
*
*--- CONSTRUCT THE FINITE DIFFERENCE MESH BY VARIOUS
*--- GEOMETRIC ADJUSTMENTS
GEN 0.,-150. 0.,150. 19.2,150. 19.2,-150.
GEN 0.,0. 0.,6.71 2.44,6.71 2.44,0. I=1,6 J=20,28
GEN 2.44,0. 2.44,6.71 19.2,6.71 19.2,0. R 1.5,1. I=6,14 J=20,28
*
*--- The borehole above the waste container ...
GEN 0.,-3.1 0.,0. .37,0. .37,-3.1 I=1,2 J=15,20
*--- To the right of borehole and under floor ...
GEN .37,-3.1 .37,0. 2.44,0. 2.44,-3.1 I=2,6 J=15,20
*--- The container inside the borehole ...
GEN 0.,-7.62 0.,-3.1 .37,-3.1 .37,-7.62 I=1,2 J=10,15
*--- To the right of the container and under floor ......
GEN .37,-7.62 .37,-3.1 2.44,-3.1 2.44,-7.62 I=2,6 J=10,15
*--- To the right of borehole and under pillar ...
GEN 2.44,-3.10 2.44,0. 19.2,0. 19.2,-3.1 R 1.5,1. I=6,14 J=15,20
GEN 2.44,-7.62 2.44,-3.1 19.2,-3.1 19.2,-7.62 R 1.5,1. I=6,14 J=10,15
*--- Below the container and under pillar ...
GEN 0.,-30. 0.,-7.62 2.44,-7.62 2.44,-30. R 1.,.67 I=1,6 J=5,10
GEN 2.44,-30. 2.44,-7.62 19.2,-7.62 19.2,-30. R 1.5,.67 I=6,14 J=5,10
GEN 0.,-150. 0.,-30. 19.2,-30. 19.2,-150. R 1.,.80 I=1,14 J=1,5
*--- Adjusting the lower part of mesh to achieve better
*     element aspect ratios ...
GEN R 1.2,1. I=1,14 J=5
GEN R 1.05,1. I=1,14 J=4
GEN R 1.,1. I=1,8 J=6
*--- Adjusting the mesh above the disposal room ...
GEN 0.,7. 0.,30. 2.44,30. 2.44,7. R 1.,1.7 I=1,6 J=29,35
GEN 2.44,7. 2.44,30. 19.2,30 19.2,7. R 1.5 1.7 I=6,14 J=29,35
```

```
*--- Adjusting the mesh to the top of the model ...
GEN 0.,30. 0.,150. 19.2,150. 19.2,30. R 1.,1.3 I=1,14 J=35,41
GEN R 1.3,1. I=1,14 J=35
GEN R 1.25,1. I=1,14 J=36
GEN R 1.2,1. I=1,14 J=37
GEN R 1.1,1. I=1,14 J=38
*
*--- Constructing the crown of the room by indiv. nodal adjustments ...
INI X=2.44 I=6 J=25
INI Y=5.22 I=6 J=26
INI X=2.30 I=6 J=27
INI Y=5.50 I=6 J=27
INI X=2.10 I=6,J=28
INI Y=5.90 I=6 J=28
INI X=1.65 I=5 J=28
INI Y=6.20 I=5 J=28
INI X=1.30 I=4 J=28
INI Y=6.40 I=4 J=28
INI X=1.00 I=3 J=28
INI Y=6.55 I=3 J=28
INI X=0.50 I=2 J=28
INI Y=6.65 I=2 J=28
INI X=2.50 I=7 J=28
INI Y=6.00 I=7 J=28
INI Y=6.43 I=8 J=28
INI Y=5.60 I=7 J=27
INI Y=5.15 I=7 J=26
*
*--- Second row of nodal points above crown ...
INI X=0.55 I=2 J=29
INI Y=6.95 I=2 J=29
INI X=1.10 I=3 J=29
INI Y=6.85 I=3 J=29
INI X=1.45 I=4 J=29
INI Y=6.70 I=4,J=29
INI X=1.75 I=5 J=29
INI Y=6.55 I=5 J=29
INI X=2.10 I=6 J=29
INI Y=6.35 I=6 J=29
INI X=2.50 I=7 J=29
INI Y=6.35 I=7 J=29
*
```

```
*--- Third row of nodal points above crown ...
INI Y=7.60 I=1 J=30
INI X=0.60 I=2 J=30
INI Y=7.55 I=2,J=30
INI X=1.15 I=3 J=30
INI Y=7.50 I=3,J=30
INI X=1.60 I=4 J=30
INI Y=7.40 I=4 J=30
INI X=2.00 I=5 J=30
INI Y=7.30 I=5 J=30
INI X=2.40 I=6 J=30
INI Y=7.20 I=6 J=30
INI X=2.75 I=7 J=30
INI Y=7.30 I=7 J=30
*
*--- Fourth row of nodal points above crown ...
GEN LINE 0.,8.6  2.78,8.3
*
*--- Some additional mesh adjustments ...
GEN LINE 3.291,6.43 19.2,6.43
*
*--- ASSIGN MATERIAL PROPERTIES (REF: SCPCDR CHAP. 2, SEC. 2.3.1)
*--- USING THE JOINT PROPERTIES AND "ROCK MASS" PROPERTIES.
*--- ALSO USING THE MOST RECENT RESULTS FROM DATA ANALYSIS,
*--- TABLES 2-4, 2-6, AND 2-7.
*--- THE ROCK IS CHARACTERIZED AS AN ELASTIC/PLASTIC MATERIAL
*--- WITH UBIQUITOUS JOINTS.  A MOHR-COULOMB FAILURE CRITERION
*--- IS USED FOR BOTH THE INTACT ROCK AND THE JOINTS ...
*
*--- Rock Mass:
PROP SHEAR=6.23E3 BULK=9.05E3 COH=17.8 ;(MPa)
PROP DENS=2320. ;(kg/m^3)
PROP FRIC=23.5  ;(degrees)
*
*--- Rock Joints:
PROP JCOH=0.1 ;(MPa)
PROP JFRIC=28.4 JANG=90. ;(degrees)
*
*--- THERMAL PROPERTIES OF THE ROCK ...
*    (Ref: SCP-CDR Chap. 2, Sec. 2.3.1.9, Table 2-9)
PROP CON=2.29 ;(W/mK)
PROP SPE=931. ;(J/kgK)
PROP THEX=8.8E-6 ;(1/K)
*
```

```
*--- SET KINEMATIC BOUNDARY CONDITIONS ...
*     (The two vertical boundaries are symmetry planes, thus,
*      they are restricted from moving in the horizontal (x)
*      direction.  The bottom horizontal boundary is restricted
*      from moving in the vertical (y) direction.  The top
*      horizontal boundary is a free-to-move pressure boundary.
*      The pressure is acting downward, and is equal to the
*      initial vertical stress.)
FIX Y I=1,14 J=1
FIX X I=1 J=1,41
FIX X I=14 J=1,41
*
*--- DEFINE THE INITIAL STRESS FIELD (MPa)...
*--- REFERENCE:  SCP-CDR CHAP. 2, SEC. 2.3.1.9
*     (The initial vertical stress is about -7 MPa at
*      the disposal room horizon.  The horizontal stress
*      is determined as 0.5 x SYY.)
INI SXX=-3.5 ;(MPa)
INI SYY=-7.0 ;(MPa)
APPLY PRES=7.0 I=1,14 J=41 ;(MPa)
*
*--- SET THE INITIAL TEMPERATURE TO 26 DEG. CELSIUS ...
INI TEMP=26. ;(Degree Celsius)
*
*--- SET THERMAL BOUNDARY CONDITIONS ...
*--- THE BOUNDARIES ARE BY DEFAULT ADIABATIC (thermally insulated)
*
*--- SET THE CRITERIA FOR AUTOMATIC TERMINATION OF EXECUTION ...
SET F=1E-2 ;Out-of-balance force (Mega Newton)
SET CLOCK=120 ;Maximum execution time (minutes)
SET STEP=5000 ;Maximum number of time steps
set therm off
*
*--- EXCAVATE THE DISPOSAL ROOM (save results) ...
MOD NULL I=1,5 J=20,27
TIT
    Time is After Initial Excavation, Vert. Empl. (NRC-F)
SOLVE
SAVE \NRCV_M0.SAV
*
```

```
*--- THERMAL PROPERTIES OF THE DISPOSAL ROOM FROM 0 TO 50 YEARS.
*      (The maximum thermal time step in FLAC is determined from
*       the element size and associated thermal diffusivity.  Using
*       air in the disposal room with an "equivalent" conductivity
*       results in a maximum time step of insufficient length to
*       complete the analysis within a reasonable time period.
*       Therefore, the room is given thermal properties of TSw2 tuff,
*       but with the thermal conductivity increased about 22 times
*       to 50 W/mK.  The size of the room elements can be increased
*       and interfaces employed, or small timesteps can be used.
*
*--- Restore thermal zones in room ...
MOD th_iso I=1,5 J=20,27
*--- RESET THE INITIAL TEMPERATURE TO 26 DEG. CELSIUS ...
INI TEMP=26. * (Degree Celsius)
*
*
*--- Assign thermal properties to the restored thermal region ...
*
PROP CON=50. I=1,5 J=20,27 * (W/mK)
PROP SPE=931. I=1,5 J=20,27 * (J/kgK)
PROP DENS=2320. I=1,5 J=20,27 * (kg/m^3)
PROP THEX=0. I=1,5 J=20,27 * (1/K)
*
*
*--- ASSIGN DECAYING HEAT SOURCE SIMULATING COMMINGLED SF AND DHLW ...
*      (The thermal decay characteristics are from Peters, 1983,
*       SAND-2497.  The initial heat generating power per meter
*       of room length is 792 W.  Because of symmetry only half
*       of this power is applied.  Note that the decay coefficients
*       have dimension 1/sec and not 1/year, which is commonly
*       used in the literature ...)
APPLY FLUX 41.8 -2.46E-10 I=1 J=10,15 *          (SPENT FUEL FIRST TERM)
APPLY FLUX 34.1 -1.72E-9  I=1 J=10,15 *          (SPENT FUEL SECOND TERM)
APPLY FLUX 8.8 -6.43E-10  I=1 J=10,15 *          (DHLW FIRST TERM)
APPLY FLUX 1.4 -1.45E-9   I=1 J=10,15 *          (DHLW SECOND TERM)
*
*--- DEFINE NODAL POINTS FOR WHICH TEMP. HISTORIES ARE RECORDED ...
*
HIS NSTEP=10 temp ;Record results every 10 time steps ...
HIS TEMP I=1 J=20 ;Location at the floor center ...
HIS TEMP I=6 J=23 ;Location at the rib center ...
HIS TEMP I=1 J=28 ;Location at the crown center ...
HIS TEMP I=1 J=12 ;Location at the waste container center ...
*
```

```
*--- START THE HEAT TRANSFER SOLUTION USING THE EXPLICIT SCHEME ...
SET MECH OFF
SET THERM ON
*
SOLVE CLOCK=6.e3 TEMP=5.E2 STEP=100000 AGE=6.048e5 *              7 days
*
SET THDT=3600.    *                                  Time step of 1 hrs.
SOLVE CLOCK=6.E3 TEMP=5.E2 STEP=100000 AGE=2.592e6 IMPLICIT *   1 month
*
SET THDT=7200. *                                     Time step of 2 hrs.
SOLVE CLOCK=6.E3 TEMP=5.E2 STEP=100000 AGE=5.184e6 IMPLICIT *  2 months
*
SET THDT=10800. *                                    Time step of 3 hrs.
SOLVE CLOCK=6.E3 TEMP=5.E2 STEP=100000 AGE=3.1536e7 IMPLICIT *   1 year
TIT
   Predicted temperatures after 1 year, Vert. Empl. (NRC-F)
SAVE \NRCV_T1.SAV
*
*--- PREDICT THE MECHANICAL RESPONSE OF 1 YEAR OF HEATING ...
SET MECH ON
SET THERM OFF
SOLVE
TIT
   Predicted T/M response after 1 year.  Vert. Empl. (NRC-F)
SAVE \NRCV_M1.SAV
*
*--- CONTINUE HEAT TRANSFER SOLUTION TO 2.5 YEARS ...
SET MECH OFF
SET THERM ON
SET THDT=1620. *                                     Time step of .45 hrs.
SOLVE CLOCK=6.E3 TEMP=5.E2 STEP=100000 AGE=7.884e7 IMPLICIT * 2.5 years
TIT
   Predicted temperatures after 2.5 years, Vert. Empl. (NRC-F)
SAVE \NRCV_T2.SAV
*
*--- PREDICT THE MECHANICAL RESPONSE OF 2.5 YEARS OF HEATING ...
SET MECH ON
SET THERM OFF
SOLVE
TIT
   Predicted T/M response after 2.5 years.  Vert. Empl. (NRC-F)
SAVE \NRCV_M2.SAV
*
```

```
*--- CONTINUE HEAT TRANSFER SOLUTION TO 5 YEARS ...
SET MECH OFF
SET THERM ON
SET THDT=2160. *                                              Time step of .6 hrs.
SOLVE CLOCK=6.E3 TEMP=5.E2 STEP=100000 AGE=1.5768e8 IMPLICIT *  5 years
TIT
    Predicted temperatures after 5 years, Vert. Empl. (NRC-F)
SAVE \NRCV_T5.SAV
*

*--- PREDICT THE MECHANICAL RESPONSE OF 5 YEARS OF HEATING ...
SET MECH ON
SET THERM OFF
SOLVE
TIT
    Predicted T/M response after 5 years.  Vert. Empl. (NRC-F)
SAVE \NRCV_M5.SAV
*

*--- CONTINUE HEAT TRANSFER SOLUTION TO 7.5 YEARS ...
SET MECH OFF
SET THERM ON
SET THDT=2160. *                                              Time step of .6 hrs.
SOLVE CLOCK=6.E3 TEMP=5.E2 STEP=100000 AGE=2.3652e8 IMPLICIT *7.5 years
TIT
    Predicted temperatures after 7.5 years, Vert. Empl. (NRC-F)
SAVE \NRCV_T7.SAV
*

*--- PREDICT THE MECHANICAL RESPONSE OF 7.5 YEARS OF HEATING ...
SET MECH ON
SET THERM OFF
SOLVE
TIT
    Predicted T/M response after 7.5 years.  Vert. Empl. (NRC-F)
SAVE \NRCV_M7.SAV
*

*--- CONTINUE HEAT TRANSFER SOLUTION TO 10 YEARS ...
SET MECH OFF
SET THERM ON
SET THDT=2160. *                                              Time step of .6 hrs.
SOLVE CLOCK=6.E3 TEMP=5.E2 STEP=100000 AGE=3.1536e8 IMPLICIT * 10 years
TIT
    Predicted temperatures after 10 years, Vert. Empl. (NRC-F)
SAVE \NRCV_T10.SAV
*
```

```
*--- PREDICT THE MECHANICAL RESPONSE OF 10 YEARS OF HEATING ...
SET MECH ON
SET THERM OFF
SOLVE
TIT
    Predicted T/M response after 10 years.  Vert. Empl. (NRC-F)
SAVE \NRCV_M10.SAV
*
*--- CONTINUE HEAT TRANSFER SOLUTION TO 15 YEARS ...
SET MECH OFF
SET THERM ON
SET THDT=8640. *                                          Time step of .1 day
SOLVE CLOCK=6.E3 TEMP=5.E2 STEP=100000 AGE=4.7304e8 IMPLICIT * 15 years
TIT
    Predicted temperatures after 15 years, Vert. Empl. (NRC-F)
SAVE \NRCV_T15.SAV
*
*--- PREDICT THE MECHANICAL RESPONSE OF 15 YEARS OF HEATING ...
SET MECH ON
SET THERM OFF
SOLVE
TIT
    Predicted T/M response after 15 years.  Vert. Empl. (NRC-F)
SAVE \NRCV_M15.SAV
*
*--- CONTINUE HEAT TRANSFER SOLUTION TO 20 YEARS ...
SET MECH OFF
SET THERM ON
SET THDT=15120. *                                        Time step of .175 days
SOLVE CLOCK=6.E3 TEMP=5.E2 STEP=100000 AGE=6.3072e8 IMPLICIT * 20 years
TIT
    Predicted temperatures after 20 years, Vert. Empl. (NRC-F)
SAVE \NRCV_T20.SAV
*
*--- PREDICT THE MECHANICAL RESPONSE OF 20 YEARS OF HEATING ...
SET MECH ON
SET THERM OFF
SOLVE
TIT
    Predicted T/M response after 20 years.  Vert. Empl. (NRC-F)
SAVE \NRCV_M20.SAV
*
```

3.3.1-28

```
*--- CONTINUE HEAT TRANSFER SOLUTION TO 25 YEARS ...
SET MECH OFF
SET THERM ON
SET THDT=15120. *                                         Time step of .175 days
SOLVE CLOCK=6.E3 TEMP=5.E2 STEP=100000 AGE=7.884e8 IMPLICIT *  25 years
TIT
    Predicted temperatures after 25 years, Vert. Empl. (NRC-F)
SAVE \NRCV_T25.SAV
*
*--- PREDICT THE MECHANICAL RESPONSE OF 25 YEARS OF HEATING ...
SET MECH ON
SET THERM OFF
SOLVE
TIT
    Predicted T/M response after 25 years. Vert. Empl. (NRC-F)
SAVE \NRCV_M25.SAV
*
*--- CONTINUE HEAT TRANSFER SOLUTION TO 30 YEARS ...
SET MECH OFF
SET THERM ON
SET THDT=15120. *                                         Time step of .175 days
SOLVE CLOCK=6.E3 TEMP=5.E2 STEP=100000 AGE=9.4608e8 IMPLICIT * 30 years
TIT
    Predicted temperatures after 30 years, Vert. Empl. (NRC-F)
SAVE \NRCV_T30.SAV
*
*--- PREDICT THE MECHANICAL RESPONSE OF 30 YEARS OF HEATING ...
SET MECH ON
SET THERM OFF
SOLVE
TIT
    Predicted T/M response after 30 years. Vert. Empl. (NRC-F)
SAVE \NRCV_M30.SAV
*
*--- CONTINUE HEAT TRANSFER SOLUTION TO 35 YEARS ...
SET MECH OFF
SET THERM ON
SET THDT=15120. *                                         Time step of .175 days
SOLVE CLOCK=6.E3 TEMP=5.E2 STEP=100000 AGE=1.10376e9 IMPLICIT *35 years
TIT
    Predicted temperatures after 35 years, Vert. Empl. (NRC-F)
SAVE \NRCV_T35.SAV
*
```

```
*--- PREDICT THE MECHANICAL RESPONSE OF 35 YEARS OF HEATING ...
SET MECH ON
SET THERM OFF
SOLVE
TIT
    Predicted T/M response after 35 years.  Vert. Empl. (NRC-F)
SAVE \NRCV_M35.SAV
*
*--- CONTINUE HEAT TRANSFER SOLUTION TO 40 YEARS ...
SET MECH OFF
SET THERM ON
SET THDT=15120. *                                    Time step of .175 days
SOLVE CLOCK=6.E3 TEMP=5.E2 STEP=100000 AGE=1.26144e9 IMPLICIT *40 years
TIT
    Predicted temperatures after 40 years, Vert. Empl. (NRC-F)
SAVE \NRCV_T40.SAV
*
*--- PREDICT THE MECHANICAL RESPONSE OF 40 YEARS OF HEATING ...
SET MECH ON
SET THERM OFF
SOLVE
TIT
    Predicted T/M response after 40 years.  Vert. Empl. (NRC-F)
SAVE \NRCV_M40.SAV
*
*--- CONTINUE HEAT TRANSFER SOLUTION TO 45 YEARS ...
SET MECH OFF
SET THERM ON
SET THDT=30240. *                                    Time step of .35 days
SOLVE CLOCK=6.E3 TEMP=5.E2 STEP=100000 AGE=1.41912e9 IMPLICIT *45 years
TIT
    Predicted temperatures after 45 years, Vert. Empl. (NRC-F)
SAVE \NRCV_T45.SAV
*
*--- PREDICT THE MECHANICAL RESPONSE OF 45 YEARS OF HEATING ...
SET MECH ON
SET THERM OFF
SOLVE
TIT
    Predicted T/M response after 45 years.  Vert. Empl. (NRC-F)
SAVE \NRCV_M45.SAV
*
```

```
*--- CONTINUE HEAT TRANSFER SOLUTION TO 50 YEARS ...
SET MECH OFF
SET THERM ON
SET THDT=30240. *                                    Time step of .35 days ...
SOLVE CLOCK=6.E3 TEMP=5.E2 STEP=100000 AGE=1.5768e9 IMPLICIT * 50 years
TIT
    Predicted temperatures after 50 years, Vert. Empl. (NRC-F)
SAVE \NRCV_T50.SAV
*
*--- PREDICT THE MECHANICAL RESPONSE OF 50 YEARS OF HEATING ...
SET MECH ON
SET THERM OFF
SOLVE
TIT
    Predicted T/M response after 50 years. Vert. Empl. (NRC-F)
SAVE \NRCV_M50.SAV
*
*****************************************************************************
*                                                                         *
*        S T A R T     C O N V E C T I V E     C O O L I N G     T O       *
*                                                                         *
*        P R E P A R E     F O R     W A S T E     R E T R I E V A L       *
*                                                                         *
*****************************************************************************
*
*--- APPLY THE CONVECTIVE HEAT TRANSFER COEFFICIENT (h=2.61 W/mmK)
*--- TO THE ROOM PERIPHERY, AND ASSIGN THE TEMPERATURE OF THE COOLING
*--- AIR (20 degrees C) AT THE TIME OF WASTE RETRIEVAL (50 YEARS) ...
*
MOD th_null I=1,5 J=20,27
APPLY CONV 2.68 20. I=1,6 J=20
APPLY CONV 2.68 20. I=6 J=20,28
APPLY CONV 2.68 20. I=1,6 J=28
*
SET MECH OFF
SET THERM ON
SOLVE CLOCK=6.E3 TEMP=5.E2 STEP=100000 AGE=1.577232e9
TIT
    Predicted temperatures after 50 yrs & 5 ds. Vert. Empl. (NRC-F)
SAVE \NRCV_T51.SAV
*
```

```
*--- PREDICT THE MECHANICAL RESPONSE OF 50 YRS & 5 DAYS OF HEATING ...
SET MECH ON
SET THERM OFF
SOLVE
TIT
    Predicted T/M response after 50 yrs 5 ds.  Vert. Empl. (NRC-F)
SAVE \NRCV_M51.SAV
*
SET MECH OFF
SET THERM ON
SOLVE CLOCK=6.E3 TEMP=5.E2 STEP=100000 AGE=1.577664e9
TIT
    Predicted temperatures after 50 yrs & 10 ds.  Vert. Empl. (NRC-F)
SAVE \NRCV_T52.SAV
*
*--- PREDICT THE MECHANICAL RESPONSE OF 50 YRS & 10 DAYS OF HEATING ...
SET MECH ON
SET THERM OFF
SOLVE
TIT
    Predicted T/M response after 50 yrs 10 ds.  Vert. Empl. (NRC-F)
SAVE \NRCV_M52.SAV
*
SET MECH OFF
SET THERM ON
SOLVE CLOCK=6.E3 TEMP=5.E2 STEP=100000 AGE=1.578528e9
TIT
    Predicted temperatures after 50 yrs & 20 ds.  Vert. Empl. (NRC-F)
SAVE \NRCV_T53.SAV
*
*--- PREDICT THE MECHANICAL RESPONSE OF 50 YRS & 20 DAYS OF HEATING ...
SET MECH ON
SET THERM OFF
SOLVE
TIT
    Predicted T/M response after 50 yrs 20 ds.  Vert. Empl. (NRC-F)
SAVE \NRCV_M53.SAV
*
SET MECH OFF
SET THERM ON
SOLVE CLOCK=6.E3 TEMP=5.E2 STEP=100000 AGE=1.580256e9
TIT
    Predicted temperatures after 50 yrs & 40 ds.  Vert. Empl. (NRC-F)
SAVE \NRCV_T54.SAV
*
```

```
*--- PREDICT THE MECHANICAL RESPONSE OF 50 YRS & 40 DAYS OF HEATING ..
SET MECH ON
SET THERM OFF
SOLVE
TIT
   Predicted T/M response after 50 yrs 40 ds.  Vert. Empl. (NRC-F)
SAVE \NRCV_M54.SAV
*
SET MECH OFF
SET THERM ON
SOLVE CLOCK=6.E3 TEMP=5.E2 STEP=100000 AGE=1.581984e9
TIT
   Predicted temperatures after 50 yrs & 60 ds.  Vert. Empl. (NRC-F)
SAVE \NRCV_T55.SAV
*
*--- PREDICT THE MECHANICAL RESPONSE OF 50 YRS & 60 DAYS OF HEATING ...
SET MECH ON
SET THERM OFF
SOLVE
TIT
   Predicted T/M response after 50 yrs 60 ds.  Vert. Empl. (NRC-F)
SAVE \NRCV_M55.SAV
*
SET MECH OFF
SET THERM ON
SOLVE CLOCK=6.E3 TEMP=5.E2 STEP=100000 AGE=1.583712e9
TIT
   Predicted temperatures after 50 yrs & 80 ds.  Vert. Empl. (NRC-F)
SAVE \NRCV_T56.SAV
*
*--- PREDICT THE MECHANICAL RESPONSE OF 50 YRS & 80 DAYS OF HEATING ...
SET MECH ON
SET THERM OFF
SOLVE
TIT
   Predicted T/M response after 50 yrs 80 ds.  Vert. Empl. (NRC-F)
SAVE \NRCV_M56.SAV
*
SET MECH OFF
SET THERM ON
SOLVE CLOCK=6.E3 TEMP=5.E2 STEP=100000 AGE=1.58544e9
TIT
   Predicted temperatures after 50 yrs & 100 ds.  Vert. Empl. (NRC-F)
SAVE \NRCV_T57.SAV
*
```

```
*--- PREDICT THE MECHANICAL RESPONSE OF 50 YRS & 100 DAYS OF HEATING
...
SET MECH ON
SET THERM OFF
SOLVE
TIT
    Predicted T/M response after 50 yrs 100 ds.  Vert. Empl. (NRC-F)
SAVE \NRCV_M57.SAV
*
SET MECH OFF
SET THERM ON
SOLVE CLOCK=6.E3 TEMP=5.E2 STEP=100000 AGE=1.587168e9
TIT
    Predicted temperatures after 50 yrs & 120 ds.  Vert. Empl. (NRC-F)
SAVE \NRCV_T58.SAV
*
*--- PREDICT THE MECHANICAL RESPONSE OF 50 YRS & 120 DAYS OF HEATING
...
SET MECH ON
SET THERM OFF
SOLVE
TIT
    Predicted T/M response after 50 yrs 120 ds.  Vert. Empl. (NRC-F)
SAVE \NRCV_M58.SAV
```

3.3.2 Soil-Nailed Wall in Sand

Problem Statement

This problem concerns the stress equilibrium loading of a soil nailed retaining wall subjected to gravitational loading. A test wall was constructed in well-graded sand and supported by shotcrete, tiebacks, and "nails" (ASCE, 1988). The "nails" consisted of No. 10 grade 60 steel bars grouted into the soil mass, as shown in Figs. 3.3.2-1 and -2. The analysis includes:

(1) explicit modeling of eight excavation stages;

(2) explicit modeling of all emplaced support components at each excavation stage; and

(3) development of forces in support components as a result of soil deformation.

The analyses here were conducted using FLAC Version 2.02.
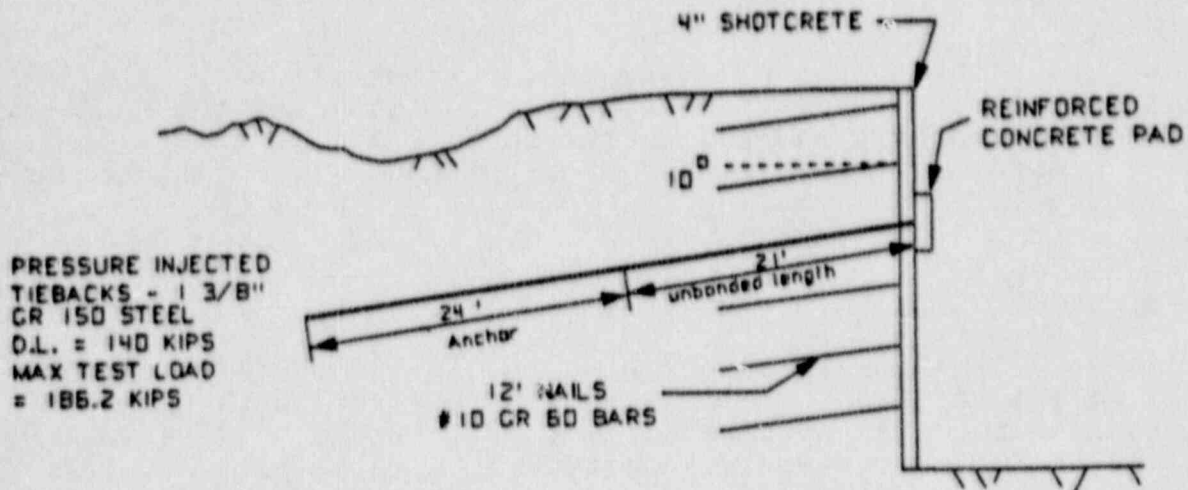
Fig. 3.3.2-1 Cross-Section Through Test Wall
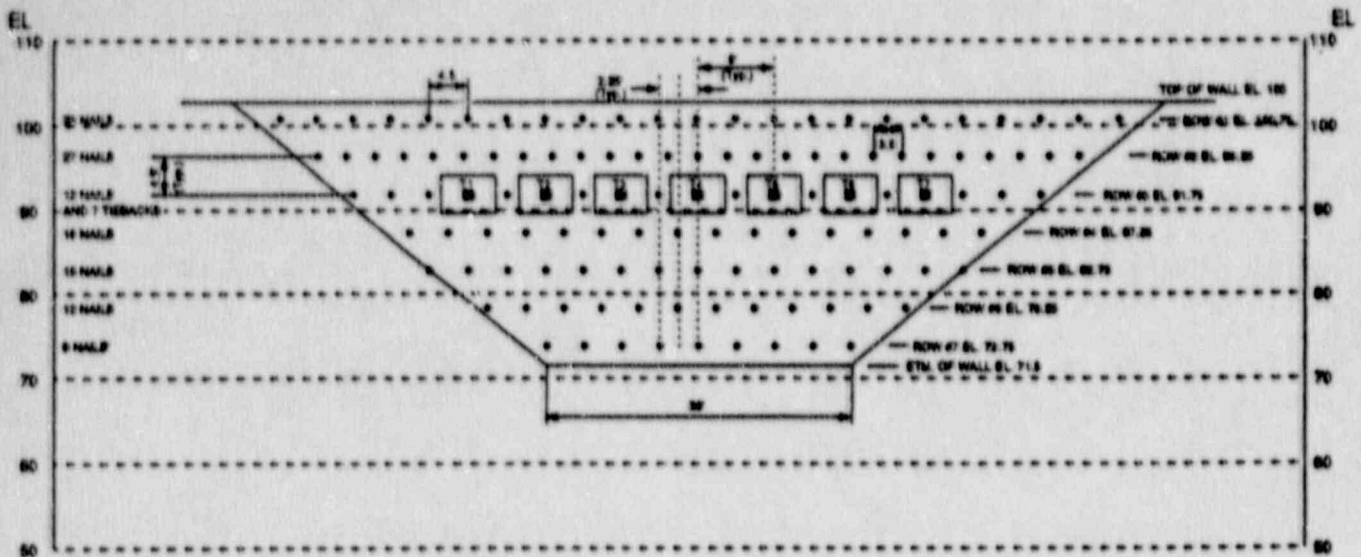
Elevation A-A

Fig. 3.3.2-2   Test Wall Elevation

Purpose

The purpose of this problem is to demonstrate satisfactory simulation of the soil excavation sequences and to model the response of structural anchors and nails coupled to the soil zones. This problem provides an example of typical problems involving sequential excavations.

Problem Specification

The geometry of the wall as depicted in Fig. 3.3.2-1 is based on a wall height of 31.5 ft. The wall was constructed of 4 inch thick shotcrete. The shotcrete was tied into the soil by 12 foot long #10 GR 60 rebar nails with a typical spacing pattern of 4.5 ft. by 4.5 ft (see Fig. 3.2.2-2 for exact spacing). The nails were inclined 10° below horizontal. One row of #11 GR 140 inclined tieback anchors were located 11.25 feet below the top of the wall and extended 45 feet back into the soil.

The wall was constructed in 9 stages. Each stage consisted of excavating 5 feet of soil (typically), applying the shotcrete, and installing the soil nails.

As the soil deforms under its own gravitational weight, load is transferred to the shotcrete wall face which is tied to the soil nails. The nails make use of the weight of the soil to develop shear resistance in preventing the face of the wall from undergoing large displacements. The tieback anchors perform the same role as the nails but they carry more load and transfer the shear resistance deep into the soil beyond the active soil displacement wedge.

Assumptions

The soil was assumed to be homogeneous and behave as a Mohr-Coulomb material with the following properties:

density	3.63 slugs/ft^3
friction	36°
cohesion	0
dilation	7.5°
bulk modulus	1.33e6 psf
shear modulus	0.836 psf

The shotcrete was assumed to be a homogeneous isotropic linearly elastic material with the following properties:

Young's modulus	5.00e8 psf
moment of inertia	3.00e-3 ft^3
area	0.333 ft^2

The nails and tiebacks were assumed to be a homogeneous isotropic linearly elastic material with the following properties:

Property	Row 1 Nails	Row 2 Nails	Row 3 Nails	Grouted Tieback	Ungrouted Portion	Row 4-7 Nails
Young's Modulus (psf)	9.3e8	1.2e9	4.65e8	4.65e8	4.65e8	9.3e8
Area (ft^2)	8.5e-3	8.5e-3	8.5e-3	.0103	.0103	8.5e-3
Bond Stiffness (psf)	1.4e7	1.8e7	7.0e6	7.0e6	1	1.4e7
Bond Strength (psf)	220	1430	667	1000	1	1333
Yield Strength (psf)	16360	21040	8180	24750	24750	16360

Conceptual Model

Several investigators have proposed simple conceptual models of nailed retaining walls. The analyses are greatly simplified if the model can be represented in two-dimensions. A schematic of the conceptual model is shown in Fig. 3.2.2-3.
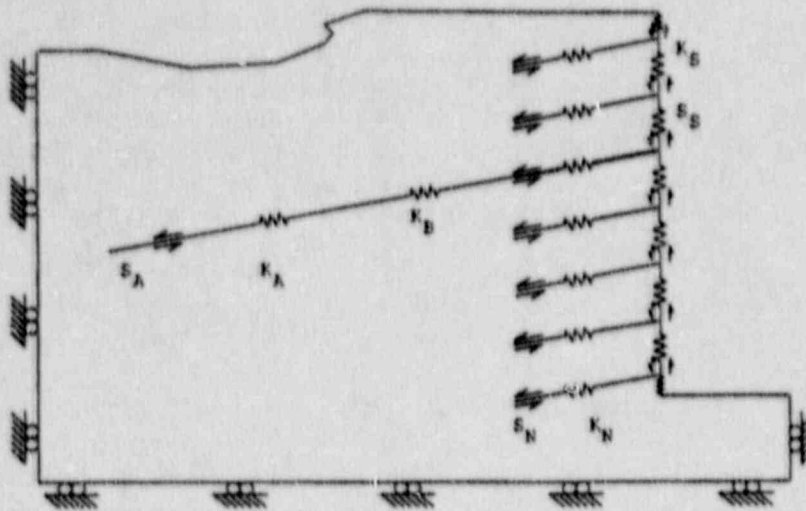
Fig. 3.3.2-3 Conceptual Model of Mohr-Coulomb Material Contain-
ing Elastic Beam and Cable Structures

Reducing three-dimensional problems with regularly spaced rein-
forcement to two-dimensional problems involves averaging the re-
inforcement effect in three dimensions over the distance between
the reinforcement. Donovan et al. (1984) suggest that linear
scaling of material properties is a simple and convenient way of
distributing the discrete effect of reinforcement over the dis-
tance between reinforcement in a regularly spaced pattern.

This approach was followed in this analysis, using a one-foot
problem width. The scaling factors for each row of reinforcement
consisted of:

Row	Scaling Factor
1	4.5
2	3.5
3	9.0
4	4.5
5	4.5
6	4.5
7	4.5

Note that the scaling factors correspond to the reinforcement
horizontal spacing (in feet).

Computer Model

The numerical analysis was performed by first compressing the un-
excavated soil mass under gravity to establish equilibrium in-
situ conditions and then sequentially excavating to various lev-
els and introducing support elements. The complete input data
file for the analysis is contained in at the end of this section.
Various stages in the modeling sequence are discussed below.

Compression Stage — The problem was discretized into approxi-
mately 1225 zones, as shown in Fig. 3.3.2-4. Elements repre-
senting soil immediately behind the wall were one foot square.
Elements further from the wall were slightly larger. Bottom and
side boundaries were fixed (i.e., no x- or y-displacement al-
lowed). The ground surface was free (i.e., no applied stress).
An initial stress state given by a coefficient of earth pressure
at rest of 0.45 was assumed. The problem was then timestepped to
equilibrium.
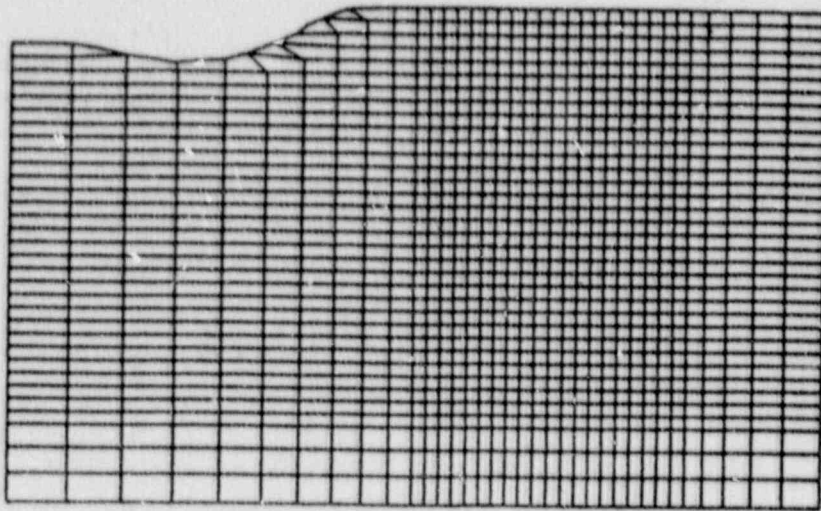
Fig. 3.3.2-4   Plot of Grid Used in Test Wall Analysis

<u>Excavation Stage I</u> — The first increment of excavation was modeled by deleting elements to a depth of 5 feet. At the same time, beam elements representing the shotcrete face support and one "cable" representing row no. 1 of nails were introduced. The nail was divided into six (6) segments, or elements. The problem was timestepped 500 cycles.

<u>Excavation Stage II</u> — The next increment was modeled by deleting elements equivalent to 2 feet of excavation. Again, support elements were introduced and the problem timestepped 500 cycles.

<u>Excavation Stage III</u> — The next increment was modeled by deleting elements equivalent to 5 feet of excavation. Shotcrete and "nail" were introduced, as before. The tieback at this level was modeled as a grouted unstressed portion (24 feet) and a pretensioned ungrouted portion (21 feet). The pretension force was equivalent to 186.2 kips. The end of the tieback at the excavation face was connected directly to a nodal point which was common to the shotcrete and soil mass in order to simulate the effect of the reinforced concrete pads. The problem was timestepped 1000 cycles.

<u>Excavation Stages IV - VII</u> — The next stages consisted of deleting elements to simulate soil excavation, simultaneous introduction of support elements, and timestepping to allow passive forces to develop in reinforcement. The simulated excavation lifts were 4, 5, 5, and 4 feet respectively.

<u>Excavation Stage VIII</u> — The final stage consisted of deleting elements equivalent to one foot of excavation for a total excavated face of 31.5 feet. Simultaneously, a beam element was introduced equivalent to one foot of shotcrete. The problem was then allowed to timestep to equilibrium (approximately 9000 cycles beyond the end of Stage VII). The problem geometry at the completion of all excavation stages is shown in Fig. 3.3.2-5. Figure 3.3.2-6 shows the location of nails and tieback.
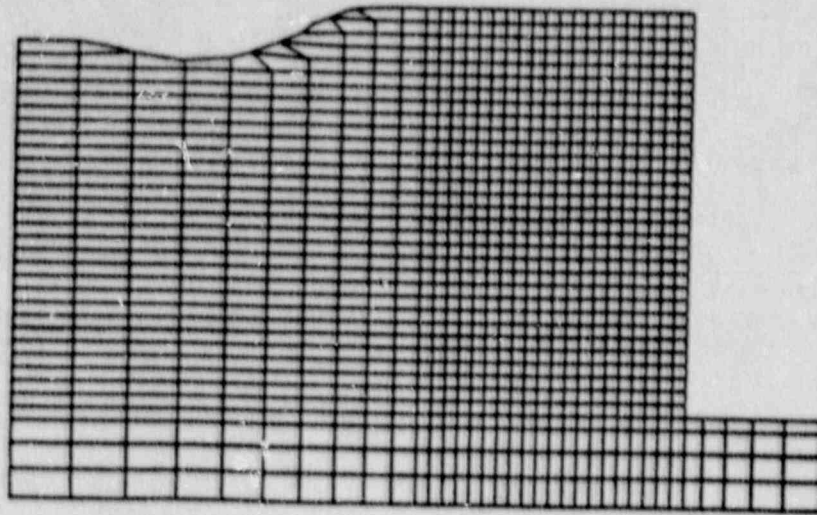
Fig. 3.3.2-5 Plot of Grid Following Removal of Elements
Representing Soil in Front of Wall
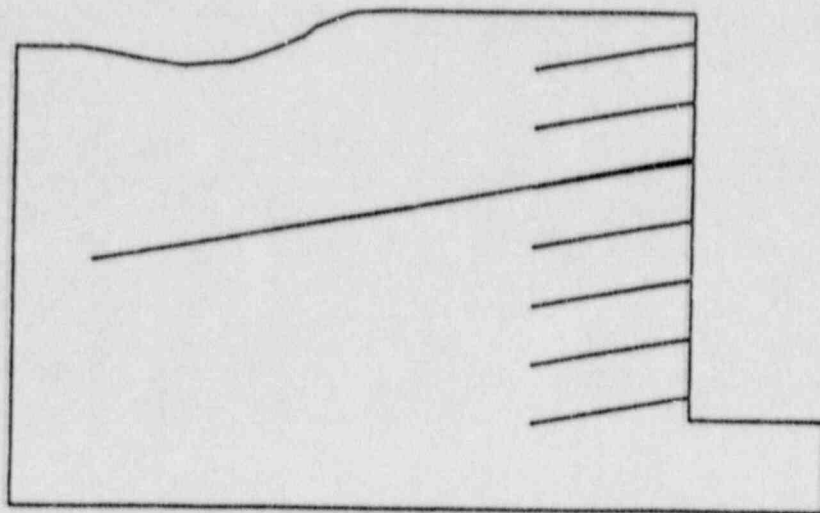
Fig. 3.3.2-6 Location of Nails and Tieback Used in Analysis

Results

The results presented in Figs. 3.3.2-7 through -9 represent the
state of the analysis following all excavation and support in-
troduction (i.e., the end of the analysis). Figure 3.3.2-7
shows the axial tensile forces in the nails and tieback. Figure
3.3.2-8 indicates the distribution of tensile forces in the nails
along their length. Figure 3.3.2-9 is a vector plot of gridpoint
displacements.

Intermediate results at the end of each stage, as well as dis-
placement loads in the shotcrete, are also available but are not
presented here.
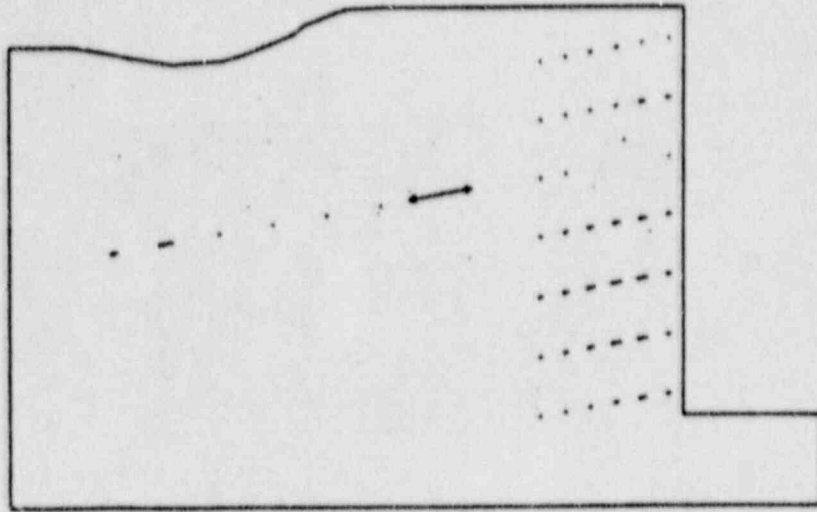
Fig. 3.3.2-7 Distribution of Axial Tensile Forces in Nails and
              Tieback
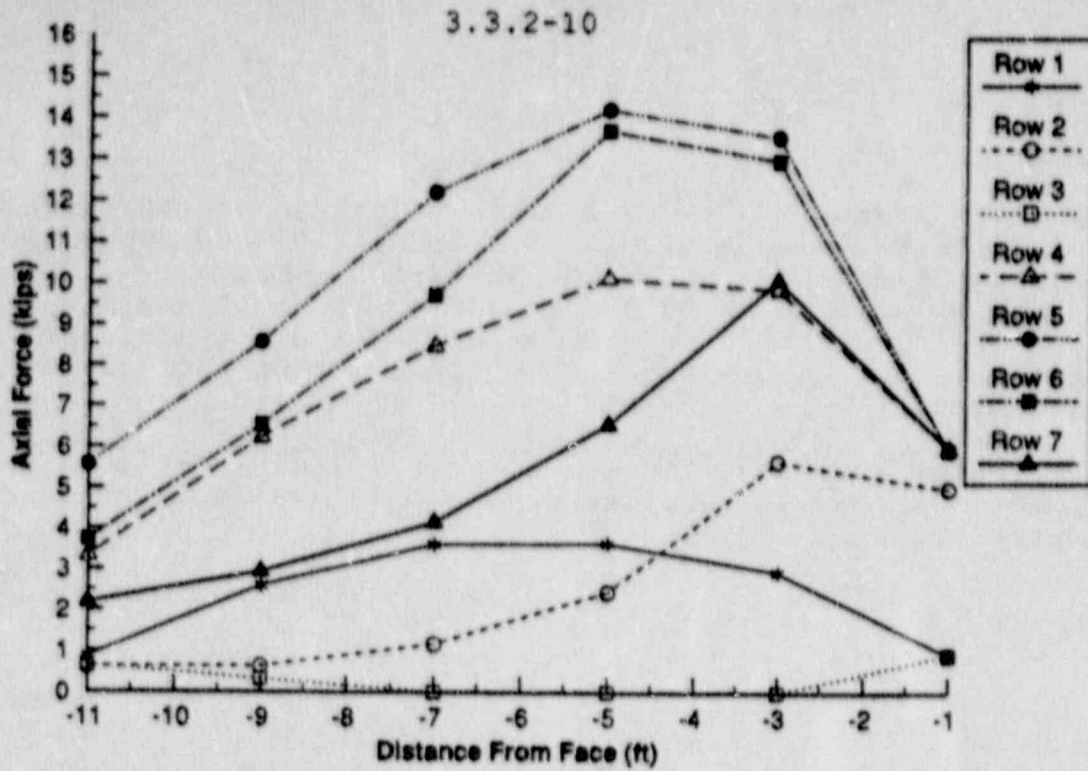
Fig. 3.3.2-8 Detailed Distribution of Axial Tensile Forces in Nails
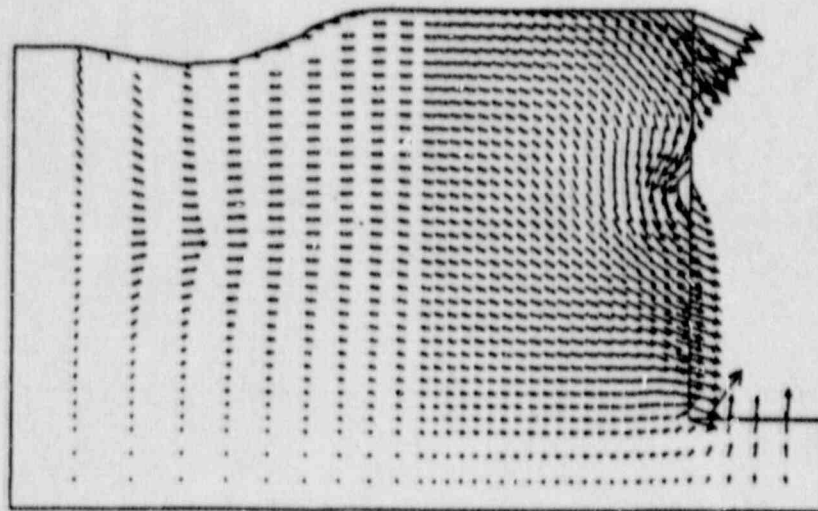
Fig. 3.3.2-9 Plot of Displacement Vectors for Test Wall Analysis

Discussion

The reference article from which this problem was taken did not
contain measured loads in the nails or tiebacks, nor measured
wall displacements. Had those data been available the results of
this analysis could be validated or checked against actual mea-
surements. Also, the accuracy of the scaling factors used to re-
duce the problem to two-dimensions could be checked.

The tensile forces in the nails shown in Fig. 3.3.2-7 indicated
the expected response of nearly uniform distribution along the
length with the highest value at the third point, as indicated in
Fig. 3.3.2-8. However, the tieback has an expected high tensile
stress indicated where the grouted portion of the anchor transi-
tions to the ungrouted segment as the anchor is long enough to
develop good shear resistance.

The displacement diagram in Fig. 3.3.2-9 shows the expected pin-
ning effect of the tieback. The wall above the tieback cantilev-
ers in a expected linear manner while the lower portion of the
wall buldges like a simply supported beam pinned at the tieback
end and a passive reaction force applied at the base of the exca-
vation. In front of the wall at the base of the excavation the
floor has begun to heave as expected.

References

ASCE (American Society of Civil Engineers). "Full Scale Wall
Tests Soil Nailing in Sand," Civil Engineering, 58(5), 12 (May
1988).

Donovan, K., W. G. Pariseau and M. Cepak. "Finite Element Ap-
proach to Cable Bolting in Steeply Dipping VCR Stopes," in Geome-
chanics Applications in Underground Hardrock Mining, pp. 65-90.
New York: AIME, 1984.

Data Input File

```
************************************************************
* Test Wall Problem in Sand Illustrating the Use of Support  *
* Logic in FLAC.                                             *
************************************************************

title
TEST WALL --
* establish problem geometry
grid 35,35
model mohr
gen -30 68 -30 103 5 103 5 68
gen -50 71 -50 103 -20 103 -20 71 ratio .9 1 i=1,11 j=4,36
gen -50 65 -50 71 -20 71 -20 65 ratio .9 .9 i=1,11 j=1,4
gen -20 65 -20 71 0 71 0 65 ratio 1 .9 i=11,31 j=1,4
gen 0 65 0 71 10 71 10 65 ratio 1.2 .9 i=31,36 j=1,4
gen 0 71 0 103 10 103 10 71 ratio 1.2 1 i=31,36 j=4,36
table 1 -60,100 -44.8,100 -40.3,99 -36.6,98.5
table 1 -33.6,99 -30.6,100.2 -27.3,102.1 -25.2,102.8 -24,103
gen table 1
mark j=35 i=8
mod null reg i=2 j=35
ini x -29 y 100.9 i 7 j 34
ini x -27 y 102.1 i 8 j 35
* boundary conditions for consolidation
fix x i 1
fix x i 36
fix y j 1
* initial stresses assume coefficient of earth pressure at rest = 0.45
ini syy -4446 var 0 4446
ini sxx -2000 var 0 2000
* conditions during execution
set large
prop tens 0
set grav 32.2
* properties for medium dense well graded sand
prop dens 3.63 fric 36 coh 0 dil 7.5 bulk 1.33e6 shear 0.8e6
```

```
* displacement monitoring points
hist n 100
hist unbal
hist xdisp i 31 j 36
hist ydisp i 31 j 36
hist xdisp i 31 j 30
hist ydisp i 31 j 30
hist xdisp i 31 j 24
hist ydisp i 31 j 24
hist xdisp i 31 j 18
hist ydisp i 31 j 18
hist xdisp i 31 j 12
hist ydisp i 31 j 12
hist xdisp i 31 j 6
hist ydisp i 31 j 6
* consolidate for initial gravity stress state prior to excavation
step 700
* save consolidated state
save n0.sav
* re-initialize some parameters prior to starting problem
ini xdisp =0
ini ydisp =0
ini xvel 0 i 1 36 j 1 36
ini yvel 0 i 1 36 j 1 36
fix x y i 1
fix x y j 1
fix x y i 36
*
* STAGE I
*
mod null i 31 35 j 31 35
title
EXCAVATION -- STAGE I
* shotcrete properties
struct prop 1 e=5e8 i=3e-3 a=.333
struct beam beg grid 31 36 end grid 31 35 seg 1 prop 1
struct beam beg grid 31 35 end grid 31 34 seg 1 prop 1
struct beam beg grid 31 34 end grid 31 33 seg 1 prop 1
struct beam beg grid 31 33 end grid 31 32 seg 1 prop 1
struct beam beg grid 31 32 end grid 31 31 seg 1 prop 1
* nail properties top row
struct prop 2 a 8.5e-3 e 9.3e8 y=16360 kbond=1.4e7 sbond 220
struc cable begin -11.9,98.65 end -0.1,100.75 seg 6 prop 2
step 500
save nI.sav
*
```

```
* STAGE II
*
title
EXCAVATION -- STAGE II
mod nul i 31 35 j 29 30
struct beam beg grid 31 31 end grid 31 30 seg 1 prop 1
struct beam beg grid 31 30 end grid 31 29 seg 1 prop 1
* nail properties -- row 2
struct prop 3 a 8.5e-3 e 1.2e9 y 21040 kbond=1.8e7 sbond 1430
struc cable begin -11.9,94.15 end -0.1,96.25 seg 6 prop 3
step 500
save nII.sav
*
* STAGE III
*
title
EXCAVATION -- STAGE III
model null i 31 35 j 24 28
struct beam beg grid 31 29 end grid 31 28 seg 1 prop 1
struct beam beg grid 31 28 end grid 31 27 seg 1 prop 1
struct beam beg grid 31 27 end grid 31 26 seg 1 prop 1
struct beam beg grid 31 26 end grid 31 25 seg 1 prop 1
struct beam beg grid 31 25 end grid 31 24 seg 1 prop 1
* nails -- row 3
struc cable begin -11.9,89.65 end -0.1,91.75 seg 6 prop 4
stru prop 4 a 3.5e-3 e 4.65e8 kbond 7e6 sbond 667 y 8180
* tieback - anchor
struc cable begin -44.3,83.9 end -20.7 88.1 seg 6 prop 5
stru prop 5 a .0103 e 4.65e8 y 24750 kbond 7e6 sbond 1000
* tieback - ungrouted portion
struc cable beg node 41 end grid 31 25 seg 1 prop 6 ten 20689
stru prop 6 a .0103 e 4.65e8 y 24750 kbond 1 sbond 1
step 1000
save niii.sav
*
```

```
* STAGE IV
*
title
EXCAVATION -- STAGE IV
model null i 31 35 j 20 23
struct beam beg grid 31 24 end grid 31 23 seg 1 prop 1
struct beam beg grid 31 23 end grid 31 22 seg 1 prop 1
struct beam beg grid 31 22 end grid 31 21 seg 1 prop 1
struct beam beg grid 31 21 end grid 31 20 seg 1 prop 1
* nail properties - row 4 to 7
struct prop 7 a 8.5e-3 e 9.3e8 sbond 1333 yi 16360 kbond 1.4e7
struct cable beg -11.9 85.17 end -0.1 87.25 seg 6 prop 7
step 500
save niv.sav
*
* STAGE V
*
title
EXCAVATION -- STAGE V
mod null i 31 35 j 15 19
struct beam beg grid 31 20 end grid 31 19 seg 1 prop 1
struct beam beg grid 31 19 end grid 31 18 seg 1 prop 1
struct beam beg grid 31 18 end grid 31 17 seg 1 prop 1
struct beam beg grid 31 17 end grid 31 16 seg 1 prop 1
struct beam beg grid 31 16 end grid 31 15 seg 1 prop 1
struct cable beg -11.9 80.67 end -0.1 82.75 seg 6 prop 7
step 500
save nv.sav
*
* STAGE VI
*
title
EXCAVATION -- STAGE VI
mod null i 31 35 j 11 14
struct beam beg grid 31 15 end grid 31 14 seg 1 prop 1
struct beam beg grid 31 14 end grid 31 13 seg 1 prop 1
struct beam beg grid 31 13 end grid 31 12 seg 1 prop 1
struct beam beg grid 31 12 end grid 31 11 seg 1 prop 1
struct cable beg -11.9 76.17 end -0.1 78.25 seg 6 prop 7
step 500
save nvi.sav
*
```

```
* STAGE VII
*
title
EXCAVATION -- STAGE VII
mod null i 31 35 j 6 10
struct beam beg grid 31 11 end grid 31 10 seg 1 prop 1
struct beam beg grid 31 10 end grid 31 9 seg 1 prop 1
struct beam beg grid 31 9 end grid 31 8 seg 1 prop 1
struct beam beg grid 31 8 end grid 31 7 seg 1 prop 1
struct beam beg grid 31 7 end grid 31 6 seg 1 prop 1
struct cable beg -11.9 71.67 end -0.1 73.75 seg 6 prop 7
step 500
save nvii.sav
*
* STAGE VIII
*
title
EXCAVATION -- STAGE VIII
mod null i 31 35 j 5
struct beam beg grid 31 6 end grid 31 5 seg 1 prop 1
step 2500
save nviii.sav
step 2500
save nviii.sav
step 2500
save nviii.sav
step 1500
save nviii.sav
ret
```

3.3.3 Lined Circular Tunnels in Sea Bed

Problem Statement

This problem deals with the stress equilibrium loading of a set of three tunnels sequentially excavated and subjected to gravitational loading. This problem is adapted from Douat (1988), and was completed using FLAC Version 2.12.

The Channel Tunnel currently is being built in chalk beneath the English Channel and, when completed, will connect Dover, England, and Calais, France. The Channel Tunnel actually consists of three separate tunnels: two main tunnels and a service tunnel, as shown in Fig. 3.3.3-1. The service tunnel is excavated ahead of the main tunnels and serves as a pilot tunnel to probe ground conditions ahead. The service tunnel is connected to the main tunnels at 500 m intervals. All tunnels are lined with precast concrete segments. The analyses presented here consider both monolithic and segmented linings.
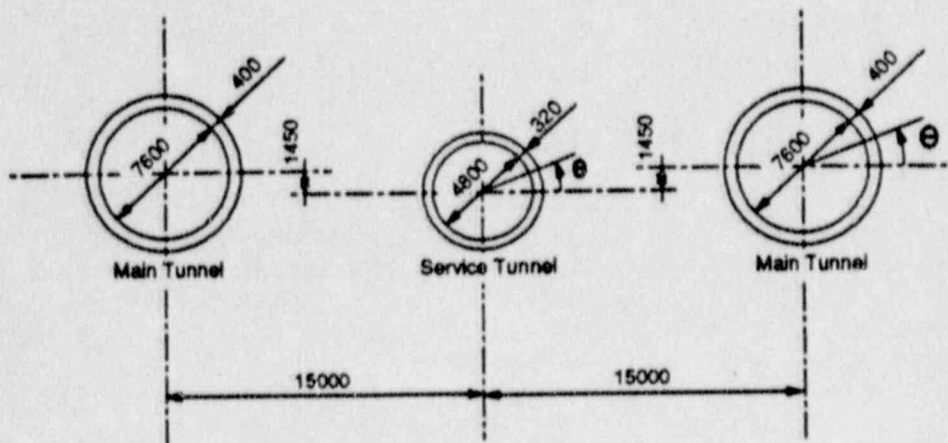
Fig. 3.3.3-1   Channel Tunnel Cross-Section   (dimensions in mm)
             [Douat, 1988]

Purpose

The purpose of this problem is to demonstrate FLAC's ability to satisfactorily simulate stress relaxation after excavation and prior to liner installation, and to model liner loads after subsequent excavations are made. This problem provides a typical example of problems involving multiple lined excavations.

Problem Statement

The cross-section to be studied here is for the tunnels shown in Fig. 3.3.3-1, where it is assumed that the depth from the channel floor to the mid-height of the main tunnels is 57.1 m, and the depth of water above the channel bottom is 42.8 m.

The circular service tunnel has an excavated diameter of 4.8 m and the precast liner is 32 cm thick. The center line location is 1.45 m below the centerlines of the two main tunnels. The tunnels are separated by 15 m. The larger circular main tunnels have an excavated diameter of 8.0 m and their liners are 40 cm thick.

The construction sequence employed consisted of:

(1) excavating the service tunnel;

(2) installing the service tunnel liner;

(3) excavating the main tunnels; and

(4) installing the main tunnel liners.

The stress field around the service tunnel begins to relax as the excavation face approaches and continues to relax for some time after the face is advanced. The lining is installed for each tunnel at some distance behind the tunnel face. After the liner is installed, stresses are redistributed again, and some load is shifted to the liner segments. The perturbed stress field redistributes again when the main tunnel is excavated in response to excavation of the main tunnels, and again when the main tunnel liners are installed.

Assumptions

The chalk exhibits time-dependent behavior associated with con-
solidation and creep in response to differential stresses. The
analysis presented here is limited to study of the short-term
elastic behavior of the tunnel lining. In the real problem, the
time delay of liner installation may produce larger or smaller
displacements depending on the length of delay. The analyses pre-
sented here assume that 60% of total peripheral displacement (for
an unlined excavation) occurs before the lining is installed.

The chalk was assumed to be a homogeneous isotropic linearly
elastic material with the following properties:

density	2350 kg/m^3
bulk modulus (short-term)	0.6e9 Pa
shear modulus (short-term)	0.36e9 Pa

The vertical in-situ stresses were assumed to hydrostatically in-
crease with depth as the sum of the water weight and rock weight.
The horizontal stress was assumed to have an effective stress
ratio of 0.5. In-situ stresses were determined as follows:

$$\sigma_v = g \, (\gamma_w \, h_w + \gamma_{chalk} \, h)$$

$$= 9.81 \, (1030 \times 42.6 + 2350 \times 57.1)$$

$$= 1.75 \text{ MPa}$$

$$\sigma_h = g \, [\gamma_w \, (h_w + h) + K_o \, (\gamma_{chalk} - \gamma_w) h]$$

$$= 9.81 \, [1030 \, (99.9) + 0.5 \, (1320) \, 57.1]$$

$$= 1.38 \text{ MPa}$$

Depth stress gradients were not considered, and gravity was not
specified in the analysis.

The concrete liner segments were assumed to be a homogeneous isotropic linearly elastic material with the following elastic properties:

$$E_{concrete} \text{ (short-term)} \quad 43.1 \text{ GPa}$$

$$\nu_{concrete} \text{ (short-term)} \quad 0.2$$

The density of the liner was not used as gravitational forces were not specified and the liner interacted with the rock as a structural element only. In order to account for plane strain conditions assumed for the tunnel lining, the input value for E was divided by $(1 - \nu^2)$. A value of 44.9 GPa was input.

The second moment of area, I, for each lining was determined from $I = t^3/12$, as follows:

service tunnel $\quad I = (0.32)^3/12 = 2.73e^{-3} \text{ m}^3$

main tunnel $\quad I = (0.40)^3/12 = 5.33e^{-3} \text{ m}^3$

To model the segmented linings, structural nodes corresponding to segment joints were pinned to free moments at the specified segment locations.

Other basic assumptions that were applied include the following.

1. The geometry of the tunnels are the same along the tunnel length permitting the three-dimensional problem to be modeled in two-dimensions using plane strain analysis.

2. The location and geometry of the main tunnels are symmetric about the center of the service tunnel permitting only half of the problem to be simulated along the line of symmetry.

3. The excavation face is advanced gradually permitting the use of constant inward velocity boundary condition at the edge of the excavation until 60% of the displacement occurs.

Conceptual Model

The boundary conditions and geometry of the model are shown by the conceptual model in Fig. 3.3.3-2. A zero x-displacement boundary was used to model zero displacement along the line of symmetry. A constant vertical pressure boundary was applied along the top and bottom sides of the model, and a constant horizontal pressure boundary applied along the right side of the model was used to simulate in-situ stresses.

The liners are conceptually represented by structural beam elements behaving like springs connected from node to node around the excavation. The liner segments are not bonded in shear resistance to the rock.

Computer Model

Figure 3.3.3-2 also shows the mesh that was used for the analysis. A close-up of the mesh in the region around the excavations is shown in Fig. 3.3.3-3. Figure 3.3.3-4 shows the discretization of the liner segments. Each structural element had nodal end points which coincided with node points describing the excavation periphery.
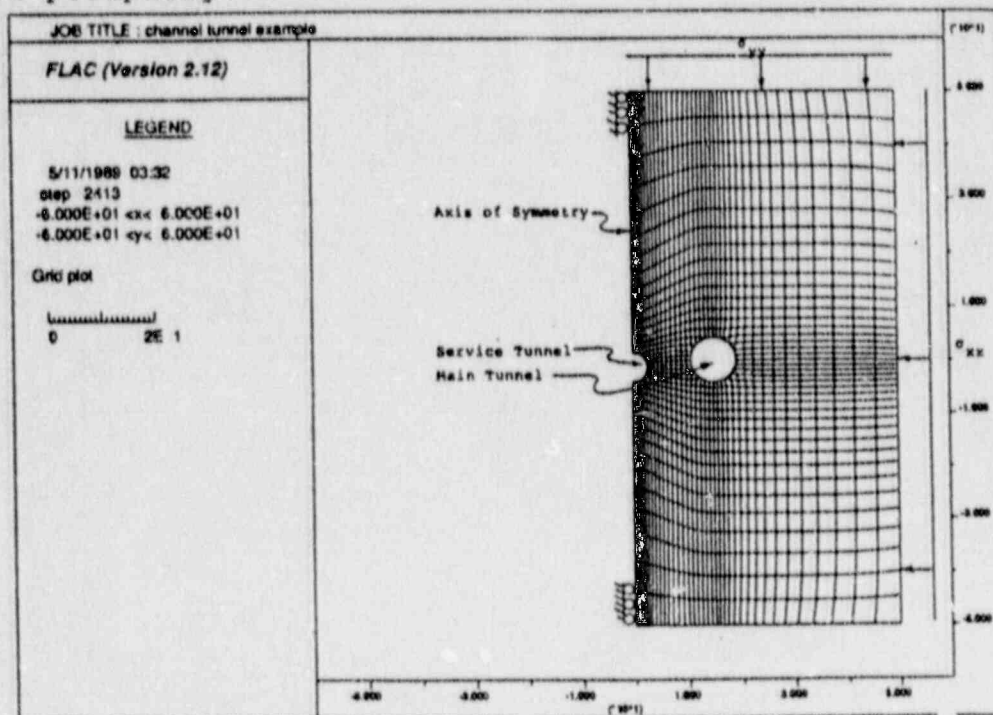

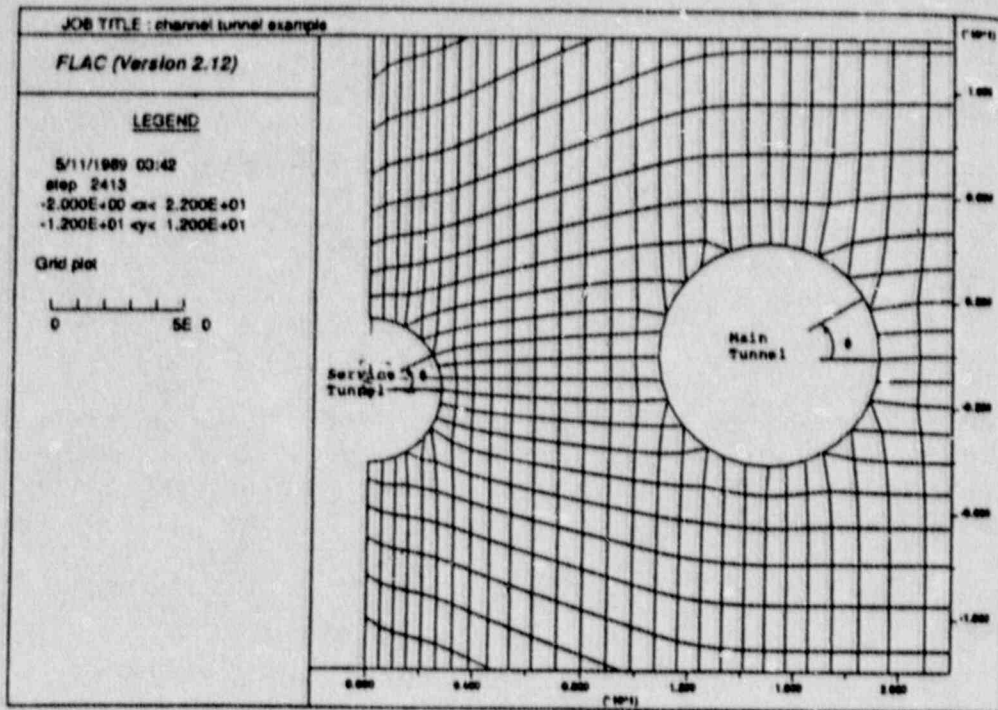Fig. 3.3.3-2 Boundary Conditions and Mesh Used for Analyses
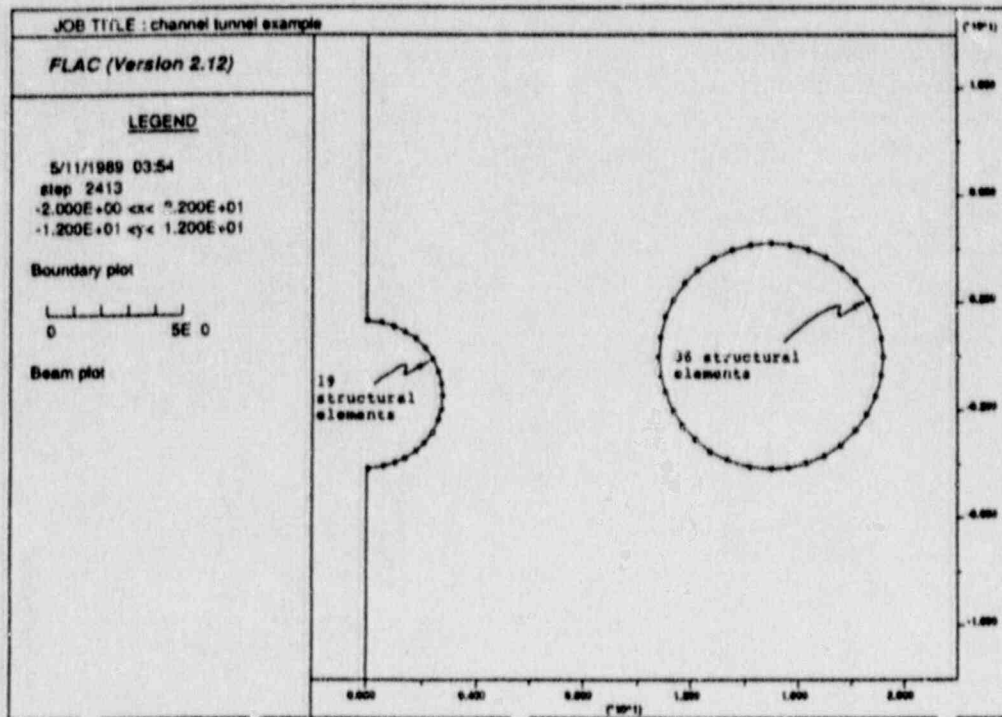
Fig. 3.3.3-3 Close-Up of Mesh Around Tunnel

Fig. 3.3.3-4 Liner Segments in Tunnels

Determination of peripheral displacements for an unlined excavation was performed first. The modeling approach to determine the lining stresses consisted of the following stages.

Stage I   Establish equilibrium conditions to initialize stresses.

Stage II   Excavate service tunnel and allow peripheral displacements equivalent to 60% of the displacements without tunnel lining.

Stage III   Install tunnel lining and timestep to equilibrium.

Stage IV   Excavate main tunnel and allow peripheral displacements equivalent to 60% of the displacements without tunnel lining.

Stage V   Install tunnel lining and timestep to equilibrium.

The analyses were first performed using simple beam elements to represent the liners then repeated with the beam elements restrained in rotation at the ends. The second analysis models the response of a monolithic liner. The input data file is listed at the end of this example.

Results

Figures 3.3.3-5 through -8 shows the distribution of axial forces and moments in the tunnel linings assuming the lining is monolithic. Figures 3.3.3-9 through -12 show the distribution of axial forces and moments in the tunnel linings, assuming the lining is segmented. The forces and moments are plotted as a function of radial angle from the x-axis in a counter-clockwise direction. The location of liner joints are shown in the plots as dots.

Discussion

The results shown in Figs. 3.3.3-5 and -6 indicate that the forces and moments for the service tunnel alone are within 2% of the analytical solution given by Panet (see verification problem in Section 3.2.1.4 for comparison). Loads in the lining of the service tunnel increase with excavation of the main tunnel.

The results shown in Figs. 3.3.3-7 and -8 indicate that the results for the main tunnel also agree well with the analytical solution when accounting for the larger diameter tunnel. This indicates that the service tunnel excavation and lining installation does not significantly effect the loads on the main tunnel liner.

Comparing the results for the segmented liner (Figs. 3.3.3-9 through -12) to the monolithic liner (Figs. 3.3.3-5 through -8) shows that the forces in the service and main tunnel liners are identical. However, the moments in the segmented liners are much less due to rotation at the joints between segments.

References

Douat, Christophe. "Calcul de Revetement de Tunnel sur Micro-Ordinateur a l'Aide d'un Programme de Differences Finies. Application au Tunnel Sous La Manche," Spie-Batignolles/University of Minnesota, March 1988.

Panet, M. "Calcul du Soutenement des Tunnels a Section Circulaire par la Methode Convergence-Confinement avec un Champs de Contraintes Initiales Anisotrope."

Fig. 3.3.3-5   Distribution of Axial Forces in Service Tunnel
Lining Before (ETAP2) and After (ETAP4) Excavation
of Main Tunnel   (Results shown assume lining is
monolithic.)

Fig. 3.3.3-6   Distribution of Bending Moments in Service Tunnel
Lining Before (ETAP2) and After (ETAP4) Excavation
of Main Tunnel   (Results shown assume lining is
monolithic.)

Fig. 3.3.3-7   Distribution of Axial Forces in the Main Tunnel
Lining Assuming Lining is Monolithic

Fig. 3.3.3-8   Distribution of Bending Moments in Main Tunnel
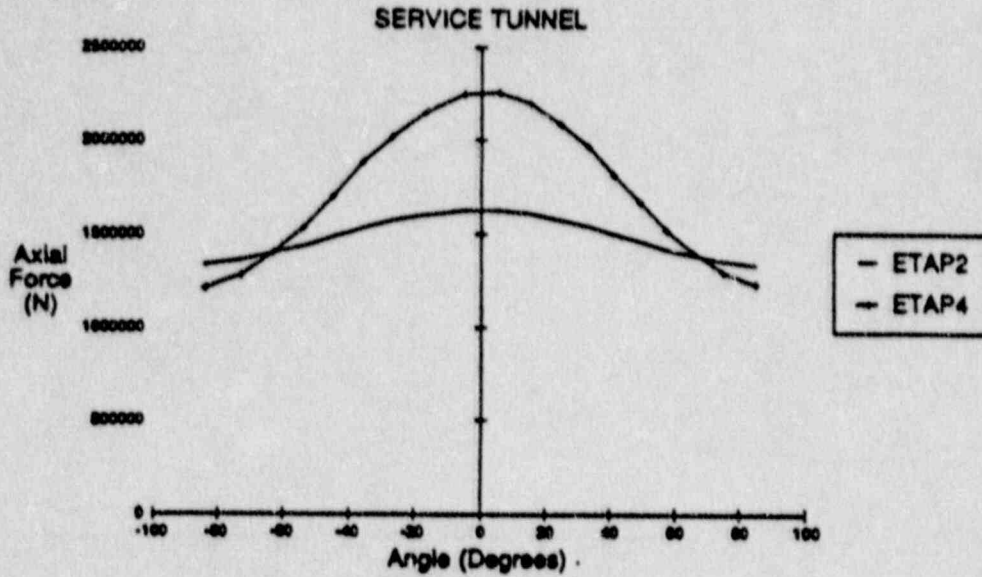Assuming Lining is Monolithic

Fig. 3.3.3-9   Distribution of Axial Forces in Service Tunnel
Lining Before (ETAP2) and After (ETAP4) Excavation
of Main Tunnel   (Results shown assume lining is
segmented.)

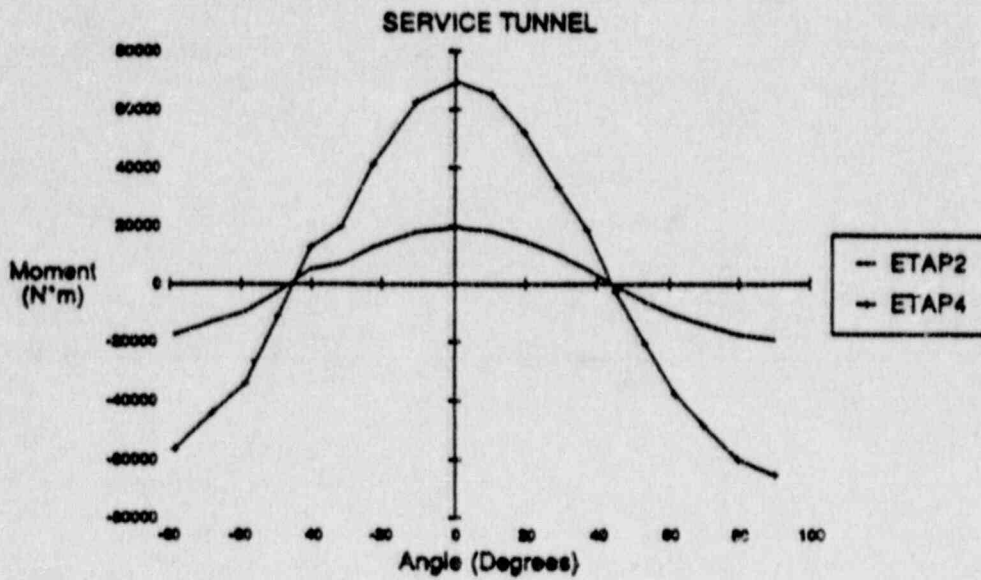Fig. 3.3.3-10   Distribution of Bending Moments in Service Tunnel
Lining Before (ETAP2) and After (ETAP4) Excavation
of Main Tunnel   (Results shown assume lining is
segmented.)
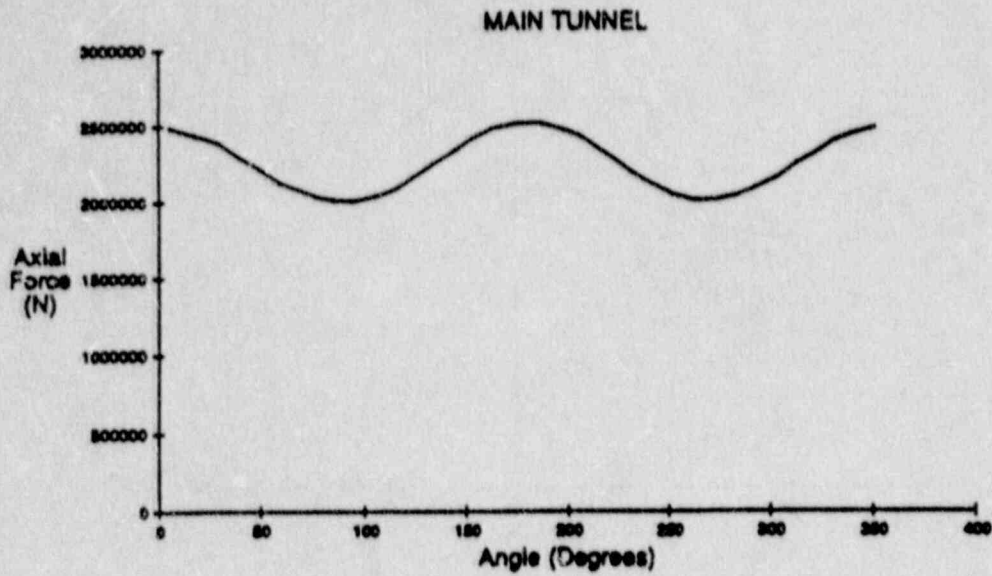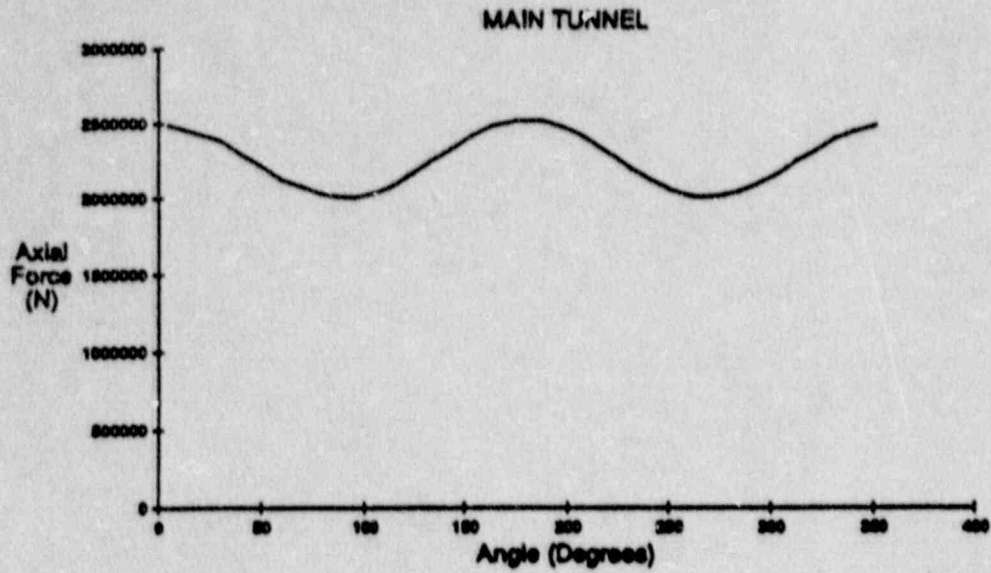
MAIN TUNNEL

Fig. 3.3.3-11 Distribution of Axial Forces in the Main Tunnel
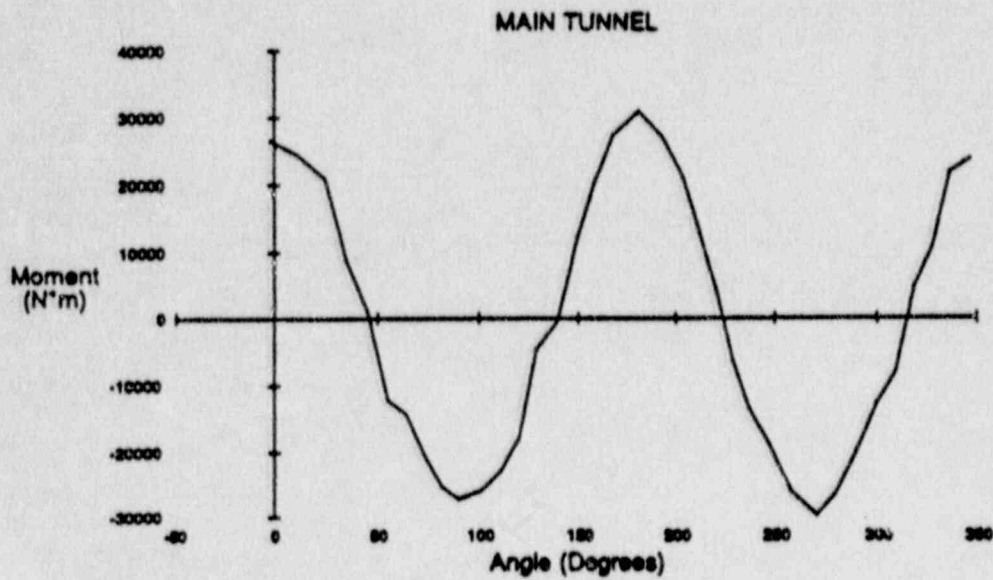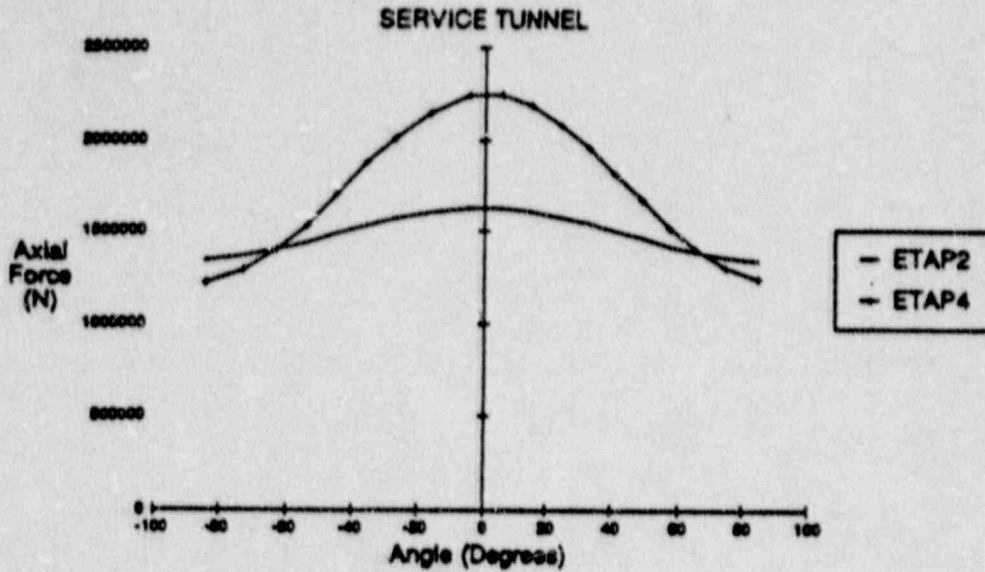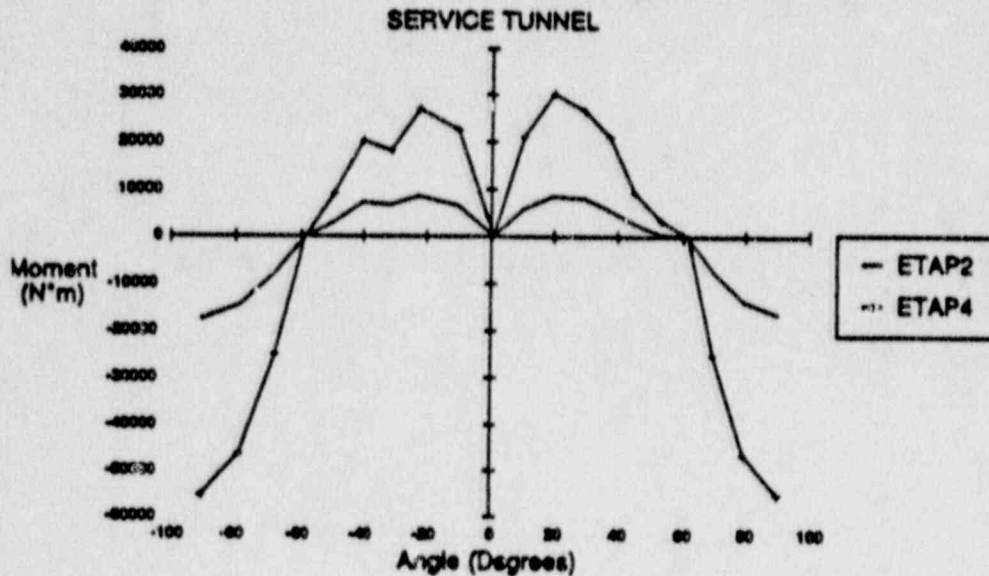Lining Assuming Lining is Segmented
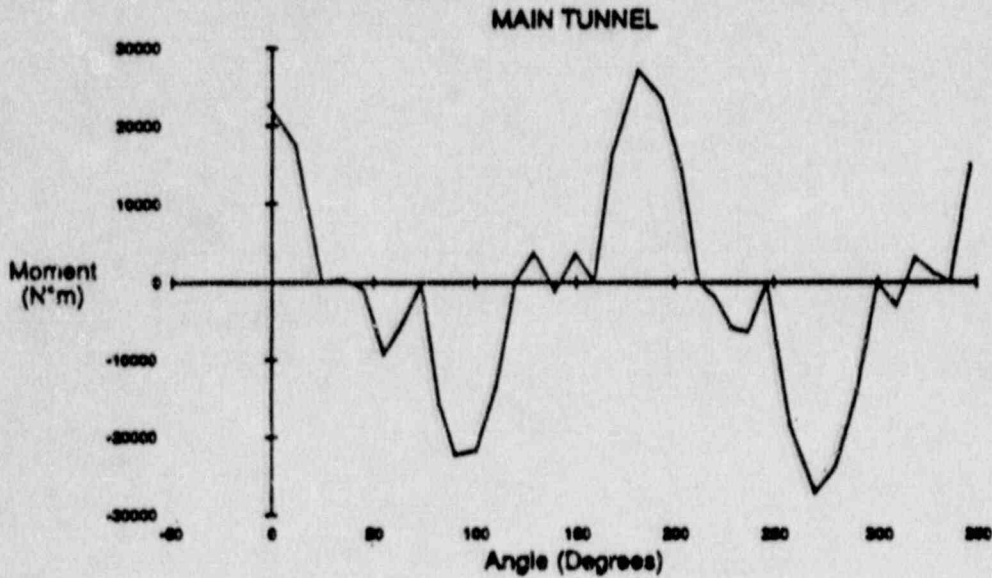
MAIN TUNNEL

Fig. 3.3.3-12 Distribution of Bending Moments in Main Tunnel
Assuming Lining is Segmented

Data Input File

```
*************************************************************
* This example illustrates the use of FLAC for solution of a   *
* problem of multiple excavation and interior concrete lining.  *
*************************************************************

title
channel tunnel example ---- monolithic lining

grid 36,40
window 0 20 -10 10
m e
gen -36 0 0 0 0 -30 -36 -30
gen 15 -1 15 50 50 50 50 -1 rat 1.15 1.1 i=21,37 j=21,41
gen 15 -50 15 -1 50 -1 50 -50 rat 1.15 0.909 i=21,37 j=1,21
gen 10 -1 10 50 15 50 15 -1 rat 1 1.1 i=15,21 j=21,41
gen 10 -50 10 -1 15 -1 15 -50  rat 1 0.909 i=15,21 j=1,21
gen 6 -1 6 50 10 50 10 -1 rat 1 1.12 i=11,15 j=21,41
gen 6 -50 6 -1 10 -1 10 -50 rat 1 0.893 i=11,15 j=1,21
gen 3 -1 3 50 6 50 6 -1 rat 1 1.14 i=7,11 j=21,41
gen 3 -50  3 -1 6 -1 6 -50 rat 1 0.877 i=7,11 j=1,21
gen 0 -1 0 50 3 50 3 -1 rat 1 1.16 i=1,7 j=21,41
gen 0 -50 0 -1 3 -1 3 -50 rat 1 0.862 i=1,7 j=1,21

gen arc 0 -1.45 0 -4.17 180
gen circle 15 0 4.2

gen adjust

        **** Stage I   Elastic Equilibrium ********************
prop s=0.36e9 b=0.6e9 dens=2350

fix x i=1

apply pressure 1.38e6  i=37    j=41,1
apply pressure 1.75e6 i=37,1 j=1
apply pressure 1.75e6 i=1,37 j=41
ini sxx=-1.38e6 syy=-1.75e6
solve
        **** Stage II  Excavate Service Tunnel ***************
model null reg 1 21
ini xdis 0 ydis 0
fix x y i=1 j=16
fix x y i=2 j=16
fix x y i=3 j=16
fix x y i=4 j=16
fix x y i=4 j=17
```

```
fix x y i=5 j=17
fix x y i=6 j=17
fix x y i=6 j=18
fix x y i=6 j=19
fix x y i=6 j=20
fix x y i=6 j=21
fix x y i=6 j=22
fix x y i=6 j=23
fix x y i=5 j=23
fix x y i=5 j=24
fix x y i=4 j=24
fix x y i=4 j=25
fix x y i=3 j=25
fix x y i=2 j=25
fix x y i=1 j=25
ini xvel=0            yvel=7.209e-4 i=1 j=16
ini xvel=-0.919e-4   yvel=7.051e-4 i=2 j=16
ini xvel=-1.711e-4   yvel=6.642e-4 i=3 j=16
ini xvel=-2.337e-4   yvel=6.106e-4 i=4 j=16
ini xvel=-2.971e-4   yvel=5.520e-4 i=4 j=17
ini xvel=-3.410e-4   yvel=4.617e-4 i=5 j=17
ini xvel=-3.748e-4   yvel=3.822e-4 i=6 j=17
ini xvel=-4.095e-4   yvel=2.822e-4 i=6 j=18
ini xvel=-4.379e-4   yvel=1.401e-4 i=6 j=19
ini xvel=-4.446e-4 yvel=-0.003e-4 i=6 j=20
ini xvel=-4.368e-4 yvel=-1.233e-4 i=6 j=21
ini xvel=-4.172e-4 yvel=-2.394e-4 i=6 j=22
ini xvel=-3.831e-4 yvel=-3.476e-4 i=6 j=23
ini xvel=-3.591e-4 yvel=-4.337e-4 i=5 j=23
ini xvel=-3.142e-4 yvel=-5.031e-4 i=5 j=24
ini xvel=-2.718e-4 yvel=-5.763e-4 i=4 j=24
ini xvel=-2.153e-4 yvel=-6.211e-4 i=4 j=25
ini xvel=-1.579e-4 yvel=-6.665e-4 i=3 j=25
ini xvel=-0.837e-4 yvel=-7.023e-4 i=2 j=25
ini xvel=0            yvel=-7.158e-4 i=1 j=25


        **** 60% Displacement Relaxation *******************
step 6

ini xvel=0 yvel=0
free x y
fix x i=1
        **** Stage III Install Service Lining ***************
struct prop=1 e=44.896e9 i=2.73067e-3 a=.32
```

```
*service tunnel
struct beam beg gr 1 25      end   gr 2 25
struct beam beg gr 2 25      end   gr 3 25
struct beam beg gr 3 25      end   gr 4 25
struct beam beg gr 4 25      end   gr 4 24
struct beam beg gr 4 24      end   gr 5 24
struct beam beg gr 5 24      end   gr 5 23
struct beam beg gr 5 23      end   gr 6 23
struct beam beg gr 6 23      end   gr 6 22
struct beam beg gr 6 22      end   gr 6 21
struct beam beg gr 6 21      end   gr 6 20
struct beam beg gr 6 20      end   gr 6 19
struct beam beg gr 6 19      end   gr 6 18
struct beam beg gr 6 18      end   gr 6 17
struct beam beg gr 6 17      end   gr 5 17
struct beam beg gr 5 17      end   gr 4 17
struct beam beg gr 4 17      end   gr 4 16
struct beam beg gr 4 16      end   gr 3 16
struct beam beg gr 3 16      end   gr 2 16
struct beam beg gr 2 16      end   gr 1 16
*
struct node=1  fix r
struct node=20 fix r
step 1000
save mtap2.sav
            **** Stage IV  Excavate Main Tunnel *****************
model null reg 21 21
fix x y i=16 j=24
fix x y i=17 j=24
fix x y i=17 j=25
fix x y i=18 j=25
fix x y i=19 j=25
fix x y i=19 j=26
fix x y i=20 j=26
fix x y i=21 j=26
fix x y i=22 j=26
fix x y i=23 j=26
fix x y i=24 j=26
fix x y i=24 j=25
fix x y i=25 j=25
fix x y i=25 j=24
fix x y i=26 j=24
fix x y i=26 j=23
fix x y i=26 j=22
fix x y i=26 j=21
fix x y i=26 j=20
fix x y i=25 j=20
fix x y i=25 j=19
```

```
fix x y i=24 j=19
fix x y i=24 j=18
fix x y i=23 j=18
fix x y i=22 j=18
fix x y i=21 j=18
fix x y i=20 j=18
fix x y i=19 j=18
fix x y i=18 j=18
fix x y i=18 j=19
fix x y i=17 j=19
fix x y i=17 j=20
fix x y i=16 j=20
fix x y i=16 j=21
fix x y i=16 j=22
fix x y i=16 j=23

ini xve  5.336e-4 yve -0.457e-3 i=16 j=24
ini xve  5.038e-4 yve -0.635e-3 i=17 j=24
ini xve  4.222e-4 yve -0.812e-3 i=17 j=25
ini xve  3.417e-4 yve -0.957e-3 i=18 j=25
ini xve  2.555e-4 yve -1.080e-3 i=19 j=25
ini xve  1.633e-4 yve -1.140e-3 i=19 j=26
ini xve  0.553e-4 yve -1.196e-3 i=20 j=26
ini xve -0.662e-4 yve -1.212e-3 i=21 j=26
ini xve -1.624e-4 yve -1.194e-3 i=22 j=26
ini xve -2.652e-4 yve -1.146e-3 i=23 j=26
ini xve -3.628e-4 yve -1.069e-3 i=24 j=26
ini xve -4.510e-4 yve -0.997e-3 i=24 j=25
ini xve -5.378e-4 yve -0.837e-3 i=25 j=25
ini xve -6.230e-4 yve -0.695e-3 i=25 j=24
ini xve -6.600e-4 yve -0.492e-3 i=26 j=24
ini xve -7.193e-4 yve -0.252e-3 i=26 j=23
ini xve -7.343e-4 yve  0.007e-3 i=26 j=22
ini xve -7.118e-4 yve  0.242e-3 i=26 j=21
ini xve -6.637e-4 yve  0.434e-3 i=26 j=20
ini xve -6.342e-4 yve  0.624e-3 i=25 j=20
ini xve -5.633e-4 yve  0.755e-3 i=25 j=19
ini xve -4.856e-4 yve  0.916e-3 i=24 j=19
ini xve -3.997e-4 yve  1.009e-3 i=24 j=18
ini xve -2.905e-4 yve  1.108e-3 i=23 j=18
ini xve -1.743e-4 yve  1.168e-3 i=22 j=18
ini xve -0.634e-4 yve  1.190e-3 i=21 j=18
ini xve  0.759e-4 yve  1.168e-3 i=20 j=18
ini xve  1.980e-4 yve  1.095e-3 i=19 j=18
ini xve  2.934e-4 yve  0.997e-3 i=18 j=18
ini xve  3.705e-4 yve  0.904e-3 i=18 j=19
ini xve  4.330e-4 yve  0.761e-3 i=17 j=19
ini xve  4.949e-4 yve  0.633e-3 i=17 j=20
```

```
ini xve   5.258e-4 yve   0.469e-3 i=16 j=20
ini xve   5.713e-4 yve   0.263e-3 i=16 j=21
ini xve   5.910e-4 yve   0.011e-3 i=16 j=22
ini xve   5.718e-4 yve  -0.265e-3 i=16 j=23
            **** 60% Displacement Relaxation    *******************
step 6
*
ini xvel=0 yvel=0
free x y
fix x i=1
*
            **** Stage V  Install Main Liner    *******************
struc  prop=2 e=44.896e9 i=5.3333e-3 a=.40
*
struct beam beg gr 16 24 end   gr 17 24 pro 2
struct beam beg gr 17 24 end   gr 17 25 pro 2
struct beam beg gr 17 25 end   gr 18 25 pro 2
struct beam beg gr 18 25 end   gr 19 25 pro 2
struct beam beg gr 19 25 end   gr 19 26 pro 2
struct beam beg gr 19 26 end   gr 20 26 pro 2
struct beam beg gr 20 26 end   gr 21 26 pro 2
struct beam beg gr 21 26 end   gr 22 26 pro 2
struct beam beg gr 22 26 end   gr 23 26 pro 2
struct beam beg gr 23 26 end   gr 24 26 pro 2
struct beam beg gr 24 26 end   gr 24 25 pro 2
struct beam beg gr 24 25 end   gr 25 25 pro 2
struct beam beg gr 25 25 end   gr 25 24 pro 2
struct beam beg gr 25 24 end   gr 26 24 pro 2
struct beam beg gr 26 24 end   gr 26 23 pro 2
struct beam beg gr 26 23 end   gr 26 22 pro 2
struct beam beg gr 26 22 end   gr 26 21 pro 2
struct beam beg gr 26 21 end   gr 26 20 pro 2
struct beam beg gr 26 20 end   gr 25 20 pro 2
struct beam beg gr 25 20 end   gr 25 19 pro 2
struct beam beg gr 25 19 end   gr 24 19 pro 2
struct beam beg gr 24 19 end   gr 24 18 pro 2
struct beam beg gr 24 18 end   gr 23 18 pro 2
struct beam beg gr 23 18 end   gr 22 18 pro 2
struct beam beg gr 22 18 end   gr 21 18 pro 2
struct beam beg gr 21 18 end   gr 20 18 pro 2
struct beam beg gr 20 18 end   gr 19 18 pro 2
struct beam beg gr 19 18 end   gr 18 18 pro 2
struct beam beg gr 18 18 end   gr 18 19 pro 2
struct beam beg gr 18 19 end   gr 17 19 pro 2
struct beam beg gr 17 19 end   gr 17 20 pro 2
struct beam beg gr 17 20 end   gr 16 20 pro 2
struct beam beg gr 16 20 end   gr 16 21 pro 2
struct beam beg gr 16 21 end   gr 16 22 pro 2
```

```
struct beam beg gr 16 22 end   gr 16 23 pro 2
struct beam beg gr 16 23 end   gr 16 24 pro 2
step 1000
save mtap4.sav
step 400
save mtap4.sav
```

3.4 BENCHMARK PROBLEM

The problems in Section 3.2 were performed to verify the proper
operation of the FLAC code against analytically-derived solu-
tions. By nature, analytical solutions can be obtained only for
simple geometries and uncomplicated boundary conditions. Realis-
tic problems often involve unknown interactive effects of geom-
etric and material complexities which cannot be explored through
comparison to simple analytic solutions. In these cases, various
codes are sometimes run for a common problem which attempts to
exercise many of the capabilities of the code. These are most
often termed "benchmark" tests. One well-documented benchmark
problem was the analysis of the thermomechanical response of the
rock mass at the Waste Isolation Pilot Plant (WIPP) site to em-
placement of high-level nuclear waste (Morgan, et al., 1981).

In this exercise, nine codes capable of performing steady-state
thermal and isothermal creep analysis of salt were used to exam-
ine the identical problem. The following is adapted from a re-
port by Mack (1987) in which FLAC Version 2.0 is benchmarked
against these nine codes.

Reference

Mack, M. "Thermal-Mechanical Benchmark Testing of FLAC," Itasca
Consulting Group Report to the U.S. Nuclear Regulatory Commis-
sion, June 1987.

3.4.1 Thermal-Mechanical Benchmark Testing of FLAC for the Second WIPP Benchmark Problem

Introduction

This example presents the results of a benchmark test study performed with FLAC. A benchmark test is a comparative analysis of a specific problem using several codes which are based on different numerical algorithms but which contain the same constitutive behavior. The approach is identified as a viable method to indicate the accuracy of the algorithms used to represent mathematically the specific material behavior. This approach is necessary for codes containing non-linear material models because closed-form, classical solutions incorporating non-linear behavior are normally not available for comparison to the numerical solution.

The exercise described as the "Second WIPP Benchmark Problem" (Morgan et al., 1981) was used to benchmark FLAC. This problem is identified as the most thorough benchmark exercise to date for thermomechanical codes performing analyses related to nuclear waste isolation studies (Hart et al., 1987). This exercise was performed specifically for the WIPP Salt Testing Program and emphasized the verification of codes containing a salt creep constitutive model. However, the exercise also covered other material behaviors not specific to salt, such as the behavior of interbedded materials, slip along discontinuities, and temperature-dependent conductivity. Thus, the WIPP exercise provides a means to verify the accuracy of several thermal-mechanical features in FLAC.

The primary material behavior model studied in the benchmark exercise was the WIPP Baseline Creep Law. This law has frequently been used to model nuclear waste isolation in salt and is implemented in FLAC. The law is a non-linear, empirical relation that cannot be verified in a code by comparison to closed-form solutions.

Interface, or slideline, logic was also verified in this exercise. Interface logic in FLAC models the presence of discontinuous features such as clay seams, joints, or bedding planes. Additionally, the FLAC representation of the behavior of interbedded materials was evaluated by prescribing different material behaviors for different regions in the test model.

The behavior of temperature-dependent thermal conductivity can be simulated in FLAC by defining conductivity as a non-linear function of the following form:

$$k(T) = k_0 + k_1 T^{n_1} + k_2 T^{n_2} \qquad (3.4.1-1)$$

where T is the temperature in Kelvin, and k_0, k_1, k_2, n_1 and n_2 are fitting parameters. This algorithm in the code was verified in this test.

The Benchmark Exercise

Morgan et al. (1981) describe a benchmarking exercise in which nine (9) codes were used to model two different problems involving hypothetical drifts for nuclear waste isolation. The nine codes (ANSALT, DAPROK, JAC, REM, SANCHO, SPECTROM, STEALTH, and two different version of MARC) did not produce identical results, but showed the differences that can arise between codes even when all input parameters and model dimensions are identical.

The first problem represented an isothermal waste emplacement drift; the second was heated. The two drift configurations are shown in Figs. 3.4.1-1 and -2. The figures also show the various materials modeled, the dimensions of the drifts, and the location of the slidelines. For the FLAC simulation, the boundary conditions were changed slightly: the "fixed line" boundary shown in the upper right-hand corner of the models in Figs. 3.4.1-1 and -2 was changed to a slideline, and the lower pressure boundary was replaced by a fixed y-displacement boundary.

In the second (heated) problem, the heat source was taken as a long source beneath the floor. Its output was

$$s(t) = 169.5 \exp(-t/1.365e9) \ W/m \qquad (3.4.1-2)$$

where t is time in seconds. Radiation was modeled indirectly, as a high-conductivity material in the drift.

The material properties for the various layers are summarized in Tables 3.4.1-1 and -2.
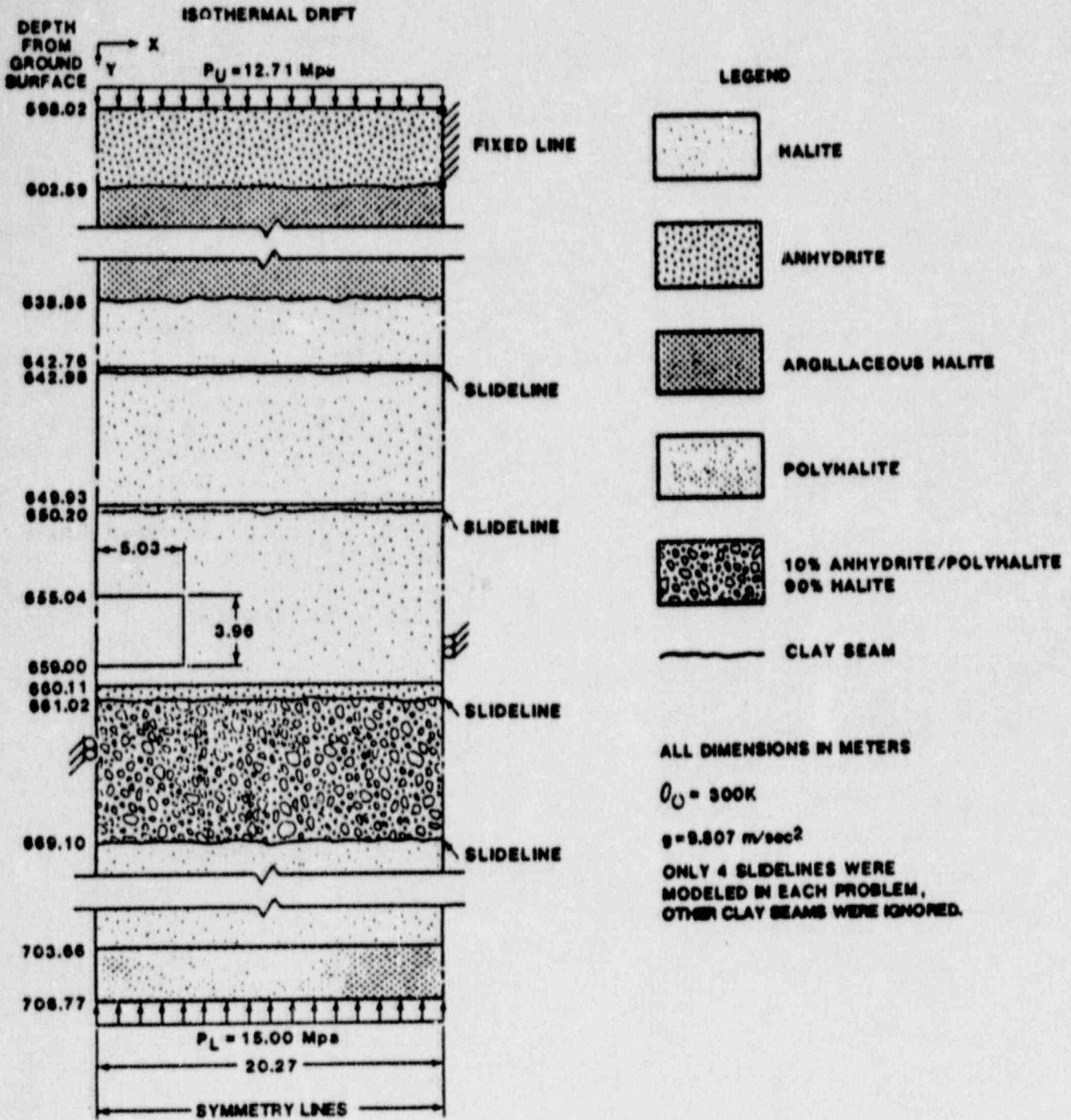
Fig. 3.4.1-1 Isothermal Drift Configuration
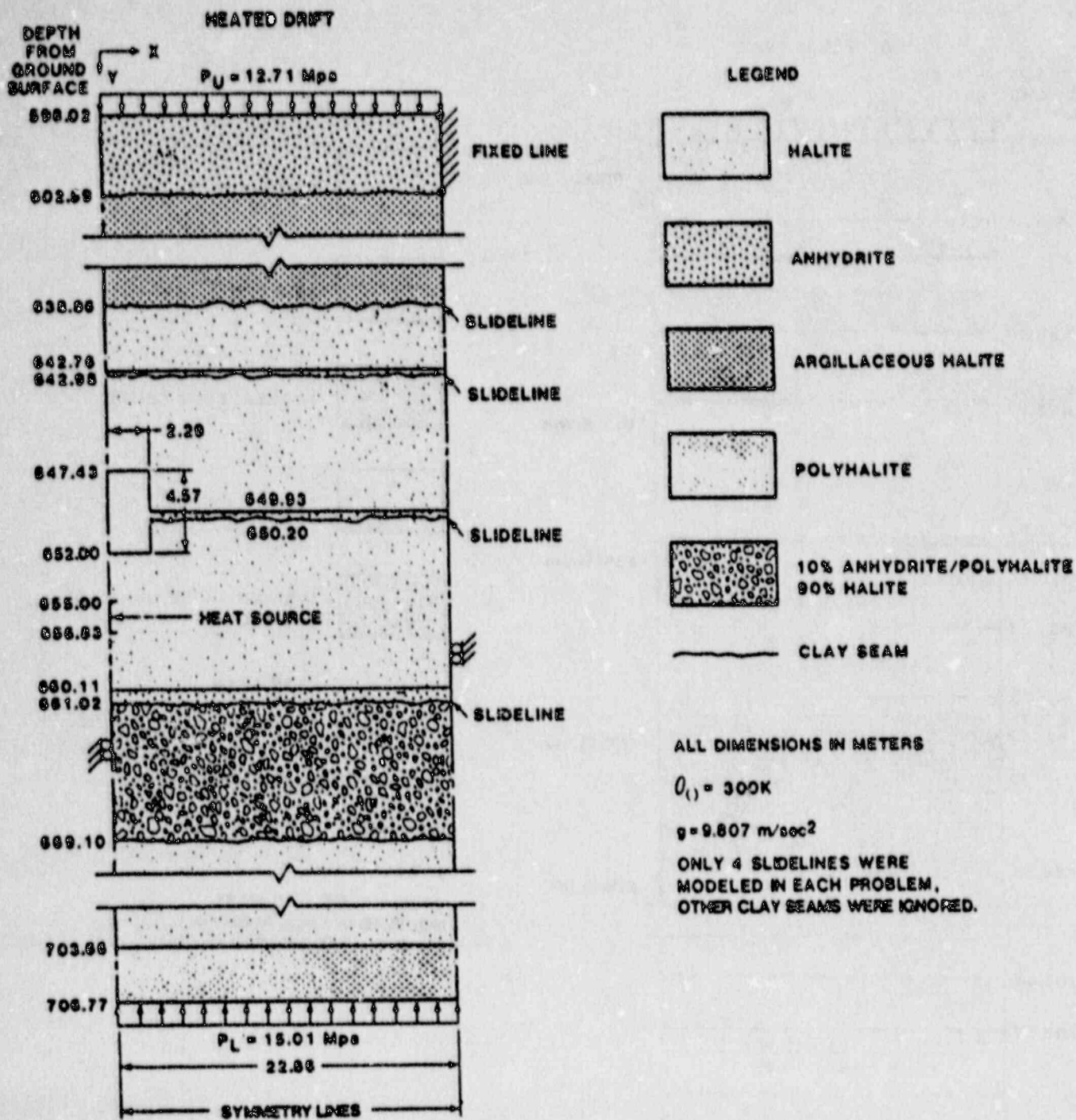[Morgan et al., 1981]

Fig. 3.4.1-2 Heated Drift Configuration [Morgan et al., 1981]

Table 3.4.1-1

MECHANICAL PROPERTIES FOR THE SECOND BENCHMARK PROBLEM

[after Morgan et al., 1981]

| Material | Elastic Constants | | Creep Constants | | |
	v	E (Pa)	D ($Pa^{-4.9} \cdot s^{-1}$)	n	Q (kcal/mole)
halite	0.25	2.48E+10	5.79E-36	4.9	12.0
argillace-ous salt	0.25	2.48E+10	1.74E-35	4.9	12.0
10% A-P, 90% H	0.25	2.65E+10	5.21E-36	4.9	12.0
anhydrite	0.33	7.24E+10	0.0	---	----
polyhalite	0.33	7.24E+10	0.0	---	----
clay seam	friction slip line: $\mu_{static} = \mu_{dynamic} = 0.0$				

Table 3.4.1-2

THERMAL PROPERTIES FOR THE SECOND BENCHMARK PROBLEM

[after Morgan et al., 1981]

Material	Density (ρ) Mg/m^3	Specific Heat (C_p) J/(kg·K)	Coefficient of Linear Thermal Expansion (α) K^{-1}	Thermal Conductivity* Parameters λ_o W/(m·K)	γ
halite	2.167	860.0	45.0E-6	5.0	1.14
argillace-ous salt	2.167	860.0	40.0E-6	4.0	1.14
10% A-P, 90% H	2.167	860.0	42.7E-6	5.0	1.14
anhydrite	2.167	860.0	20.0E-6	4.5	1.14
polyhalite	2.167	860.0	24.0E-6	2.0	1.00
"Equivalent Thermal Material"	1	1000.0	-------	50.0	0.0

* $k = \lambda_o(300/\theta)^\gamma$, where θ is temperature in Kelvin

According to Morgan et al. (1981, p. 20), the "conductivity k was originally . . . incorrectly prescribed as $k = \lambda_o (\theta/300)^\gamma$.

All participants in Benchmark II were instructed to use the incorrect expression because most of the calculations were near completion when the error was discovered . . . . The Benchmark II comparisons were not affected by this error, because all participants used the same expression. However, if the properties in this table are used for calculations other than the Benchmark II calculations, the correct conductivity expression should be used." For comparison purposes, the incorrect expression was used in the FLAC simulations.

The creep law used is described below in terms of the total strain rate:

$$\dot{\varepsilon}_{ij} = - \frac{v}{E} \dot{\sigma}_{kk} \delta_{ij} + \frac{1 + v}{E} \dot{\sigma}_{ij} + \dot{\varepsilon}_{ij}^c \qquad (3)$$

where $\dot{\sigma}_{ij}$ = derivative with time of stress i,j ,

δ_{ij} = Kronecker's delta,

v = Poisson's ratio,

E = Young's modulus, and

$\dot{\varepsilon}_{ij}^c$ = creep strain rate,

where $\dot{\varepsilon}_{ij}^c = (1.5)^{1/2} \dot{\bar{\varepsilon}} \dfrac{\sigma_{ij}'}{(\sigma_{mn}' \sigma_{mn}')^{1/2}}$

where $\dot{\bar{\varepsilon}} = D \bar{\sigma}^n \exp(-Q/R\theta)$,

σ_{ij}' = deviatoric stress i,j ,

D, Q, n = creep model parameters,

R = universal gas constant, and

θ = temperature (in K).

FLAC Results

The results from FLAC were compared to the results reported by Morgan et al. (1981) for the two benchmark problems. Additionally, certain key features of the problems were varied to evaluate their effect on the results.

Isothermal Problem

Figures 3.4.1-3 to -11 show the results from FLAC, compared to the other codes. All the results agree extremely well. The closure histories in Figs. 3.4.1-3 and -4 show FLAC almost exactly centered between the results for the most closely clustered codes. The stress profiles in Figs. 3.4.1-5, -6 and -7 also show FLAC agreeing well with the other codes. In addition, the results from FLAC seem to vary more smoothly than some of the others, which is probably more realistic. The relative slip profiles shown in Figs. 3.4.1-8 to -11 are also in good agreement. In these figures, FLAC does not show the average behavior of the other codes, but this is not indicative of any error or problem. No one set of results should be considered as the "correct" solution. Only if the results vary distinctly from the average behavior should the assumptions of the code be checked.

For example, if the slidelines and the thin anhydrite interbeds are ignored in the FLAC analysis, the results are on the lower extreme of those reported in the benchmark study (see Figs. 3.4.1-3 and -44). Also, the stress profile in this instance does not exhibit the sharp spike seen from the other models (Fig. 3.4.1-5). However, if only the clay seams are modeled (i.e., slidelines are used but the anhydrite interbeds are ignored), the comparison of results worsens. In this case, the vertical room closure, for example, is approximately three times greater than the maximum values shown in Fig. 3.4.1-3. The poor agreement is attributed to the omission of the thin, stiff anhydrite layers, especially the layer immediately beneath the floor.

These simulations indicate both the importance of modeling inhomogeneous behavior correctly in the numerical analysis and, also, the apparent significance of inhomogeneities on rock mass behavior.
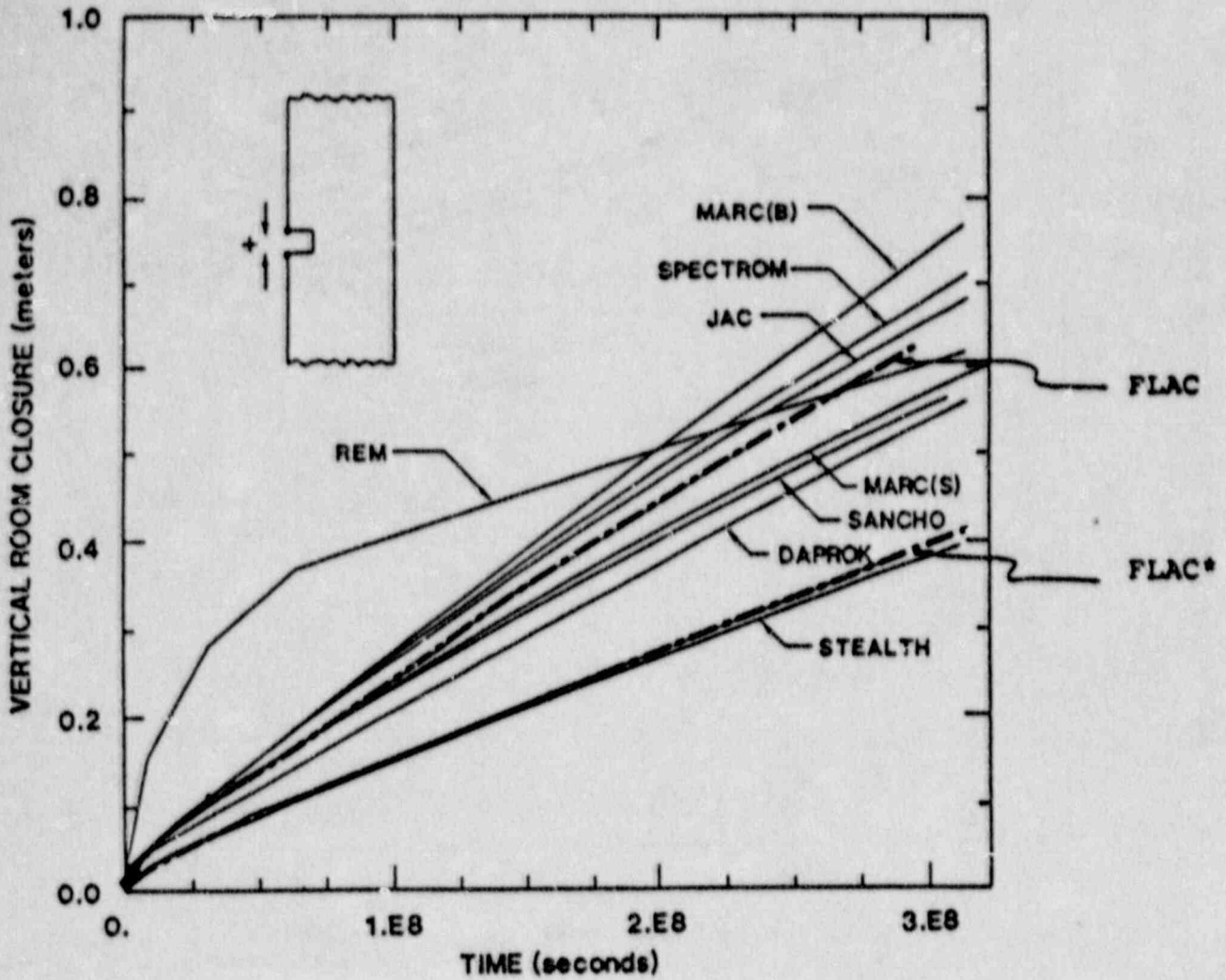
*model without interface elements and anhydrite layers

Fig. 3.4.1-3 Vertical Closure Histories for the Isothermal Room
[adapted from Morgan et al., 1981]
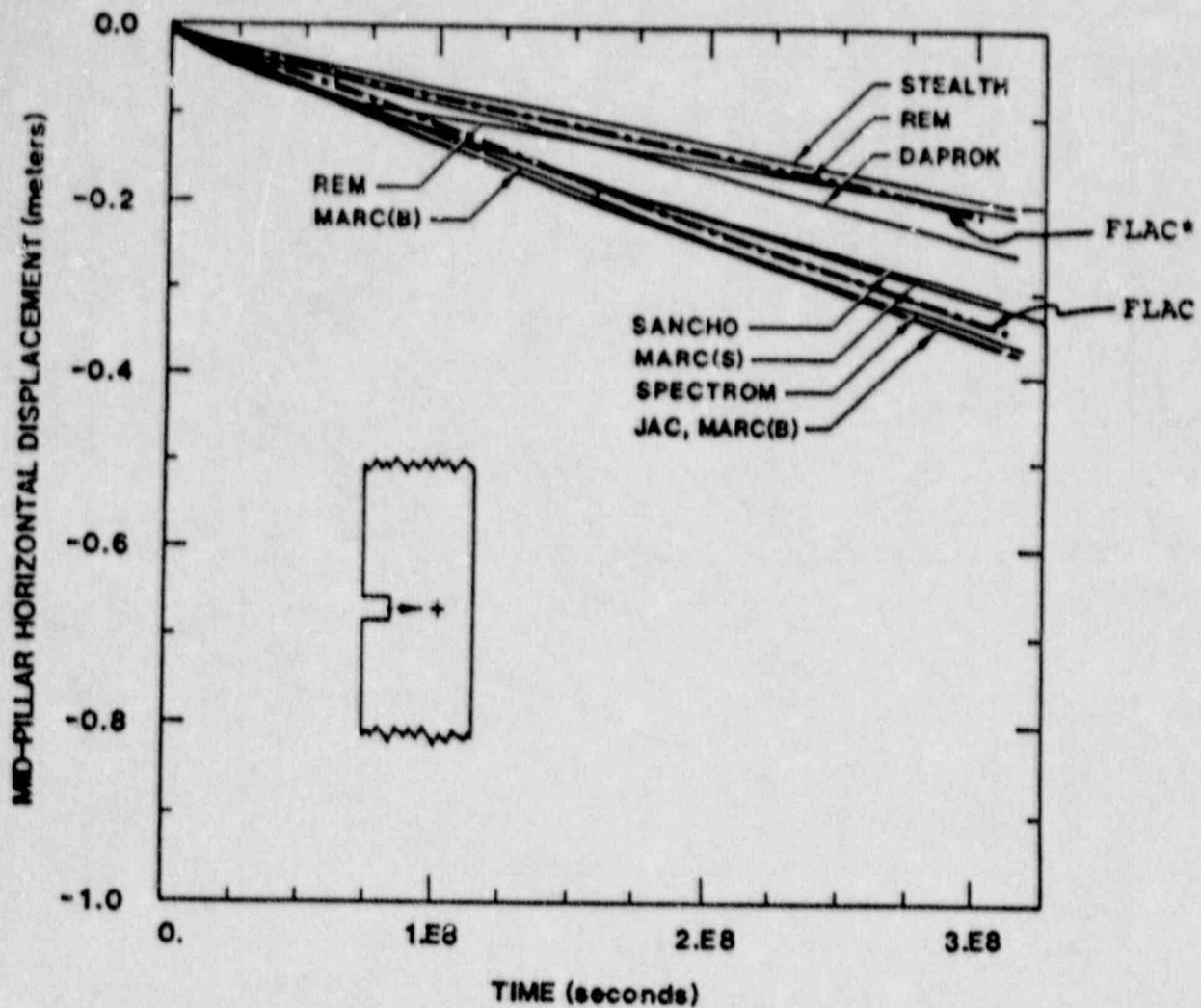
*model without interface elements and anhydrite layers

Fig. 3.4.1-4   Mid-Pillar Horizontal Displacement Histories for
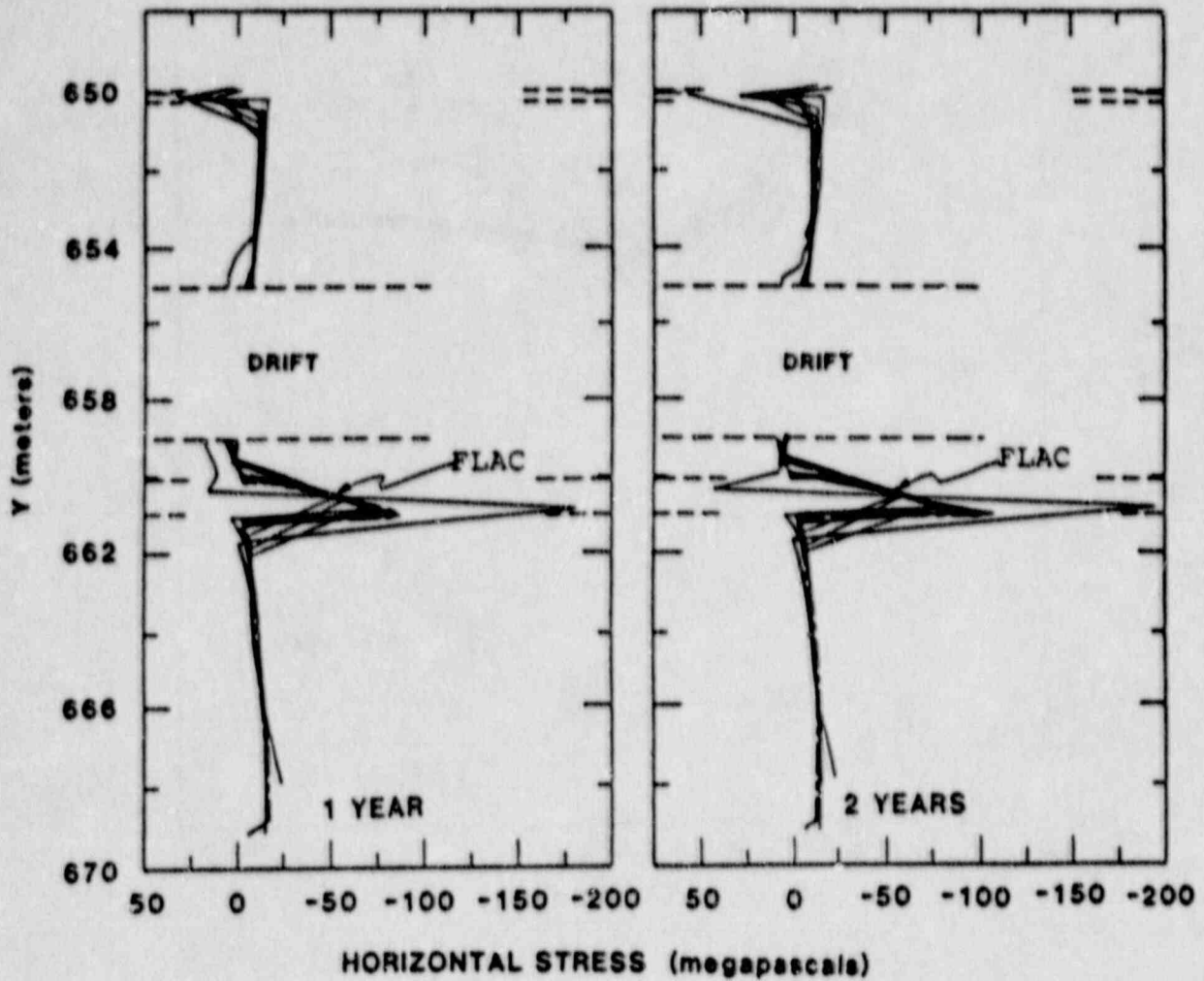the Isothermal Room   [adapted from Morgan et al.,
1981]

Fig. 3.4.1-5 Horizontal Stress Profiles Along the Vertical
Centerline of the Isothermal Room at 1 and 2 Years
[adapted Morgan et al., 1981]

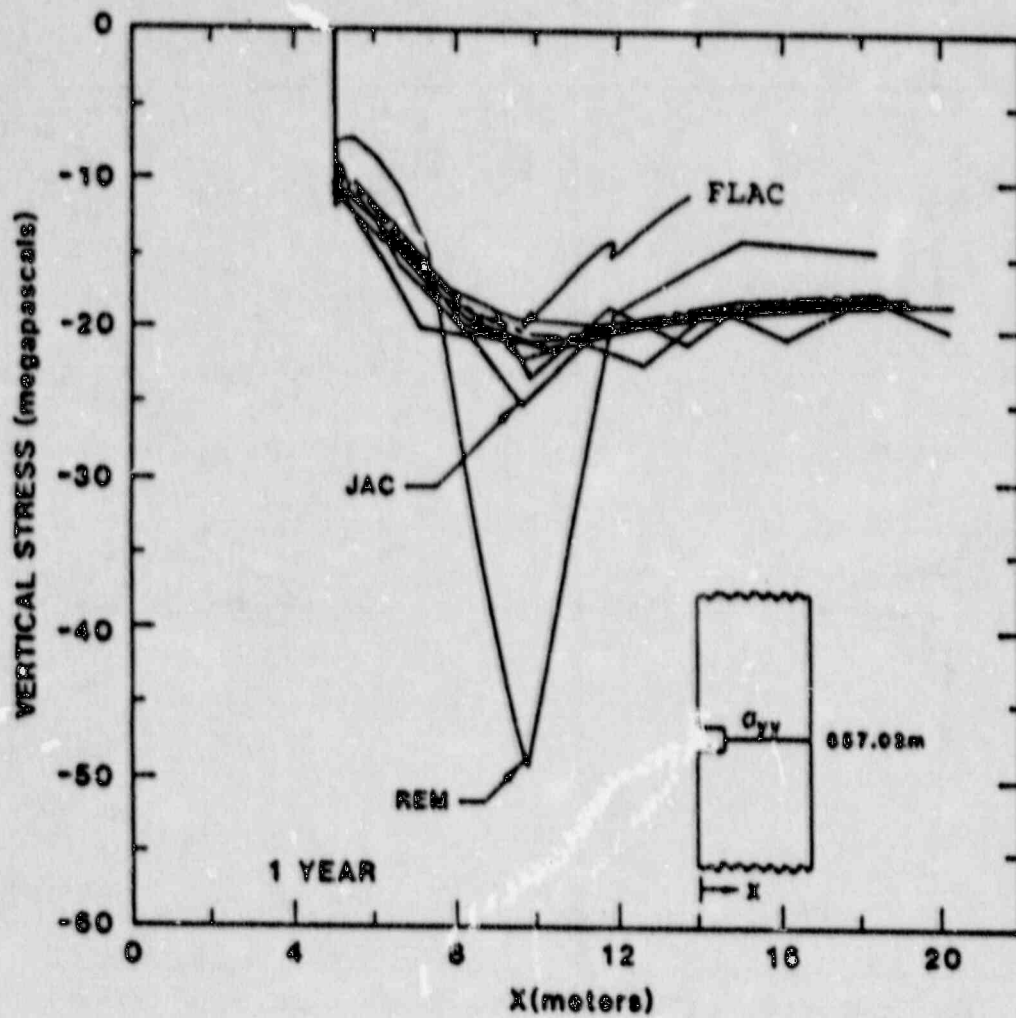Fig. 3.4.1-6   Vertical Stress Profiles Through the Pillar of the
               Isothermal Room at 1 Year   [adapted Morgan et al.,
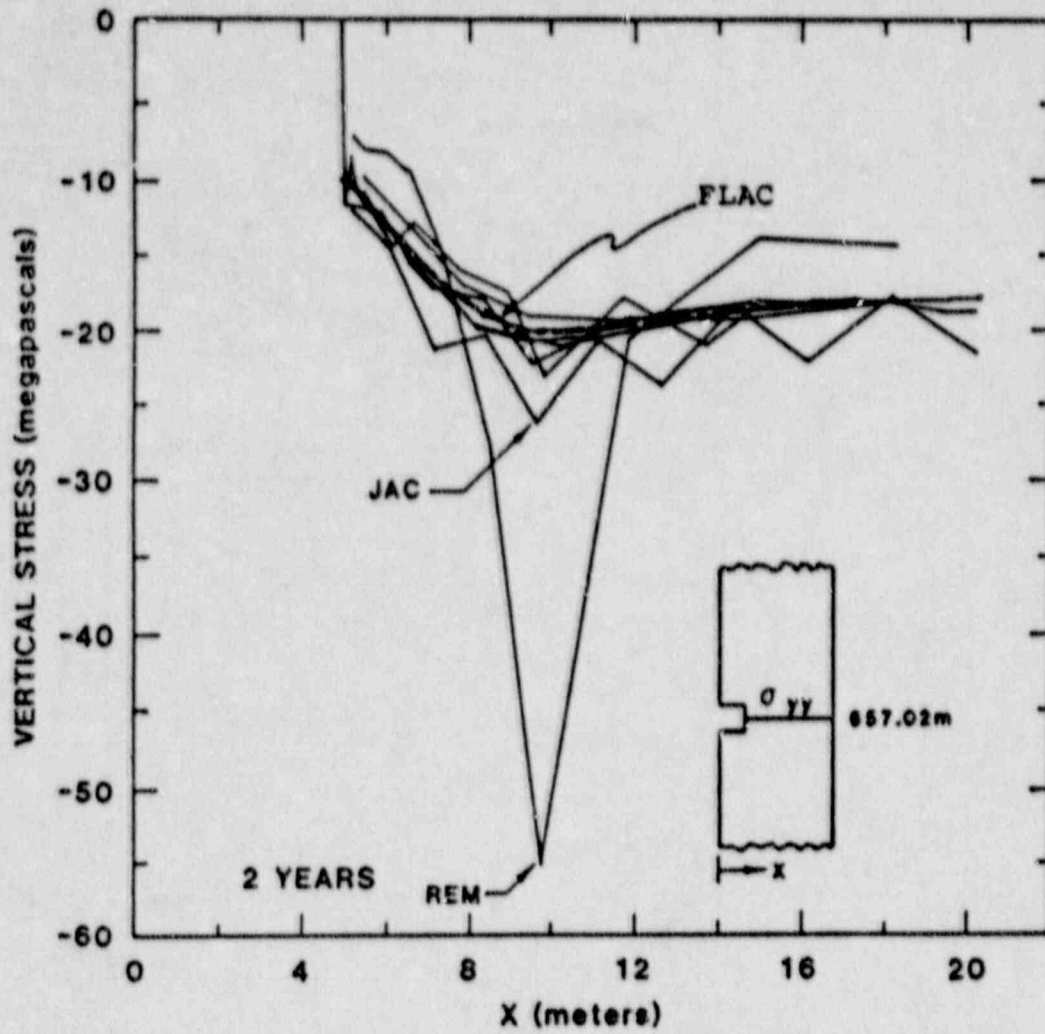   1981]

Fig. 3.4.1-7   Vertical Stress Profiles Through the Pillar of the
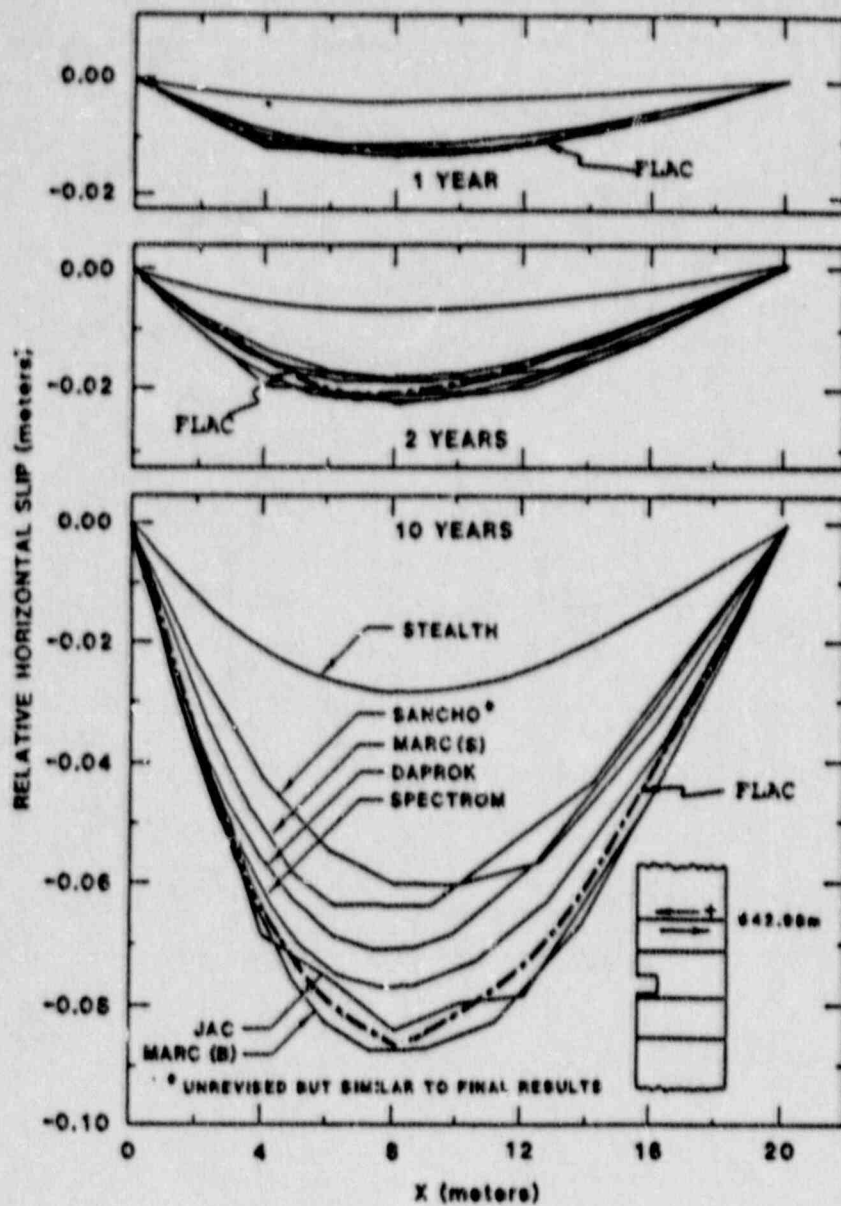Isothermal Room at 2 Years   [adapted from Morgan et
al., 1981]

Fig. 3.4.1-8 Relative Slip Across the 642.98 m Slide Line for the Isothermal Room at 1, 2 and 10 Years [adapted from Morgan et al., 1981]
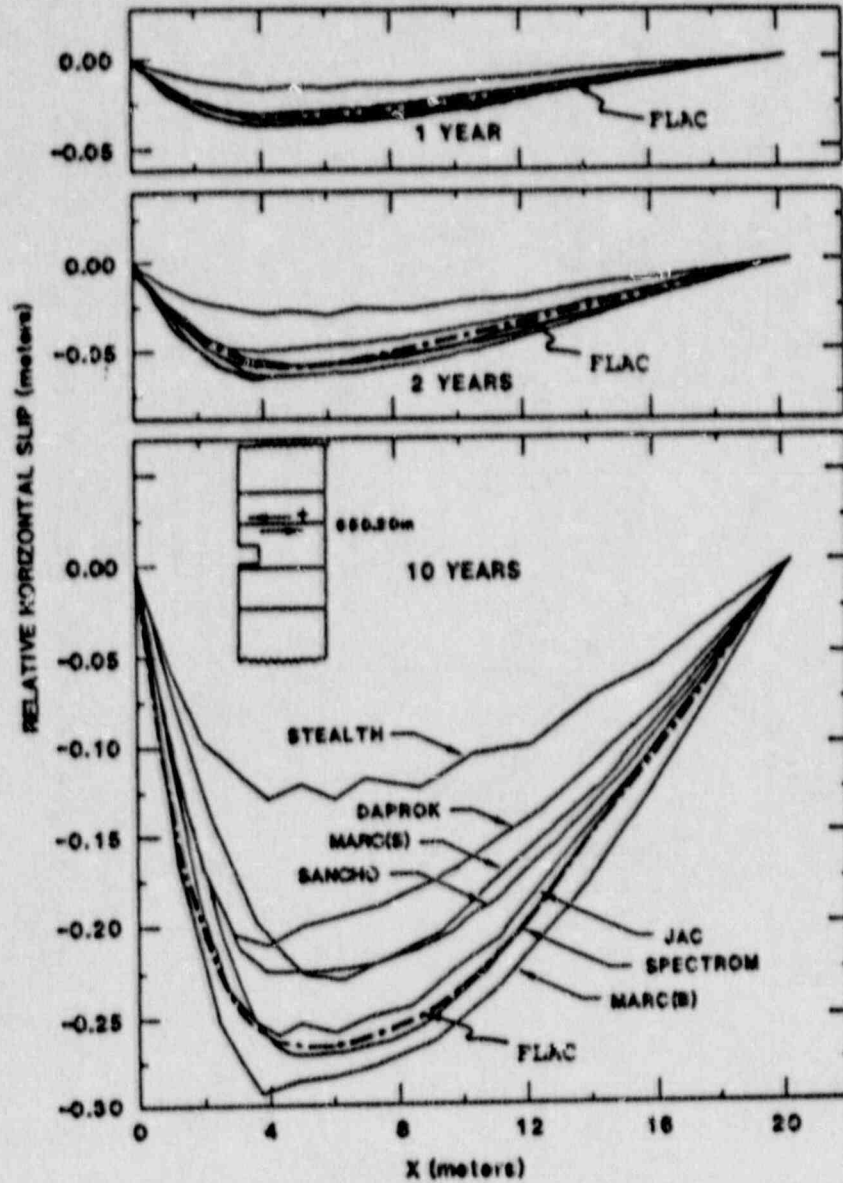
Fig. 3.4.1-9 Relative Slip Across the 650.20 m Slide Line for the Isothermal Room at 1, 2 and 10 Years [adapted from Morgan et al., 1981]
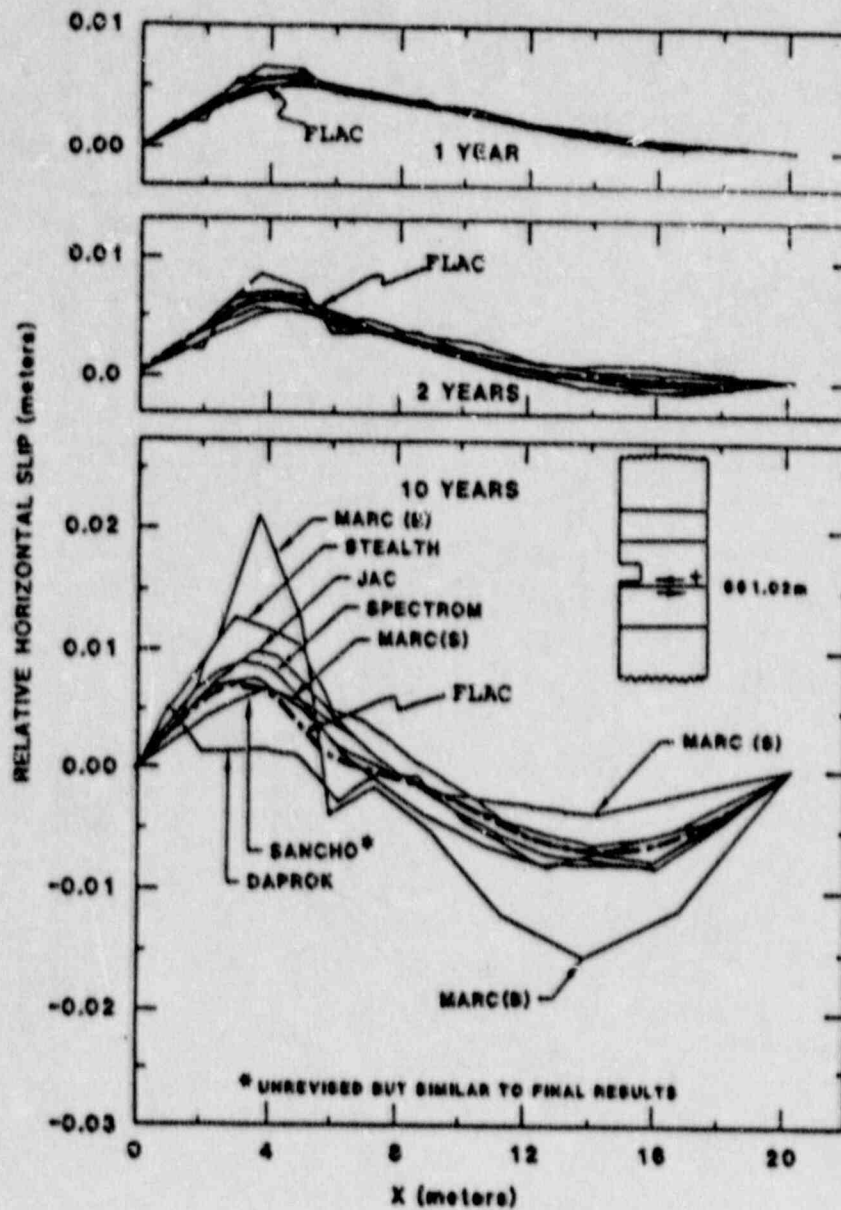
Fig. 3.4.1-10 Relative Slip Across the 661.02 m Slide Line for
the Isothermal Room at 1, 2 and 10 Years [adapted
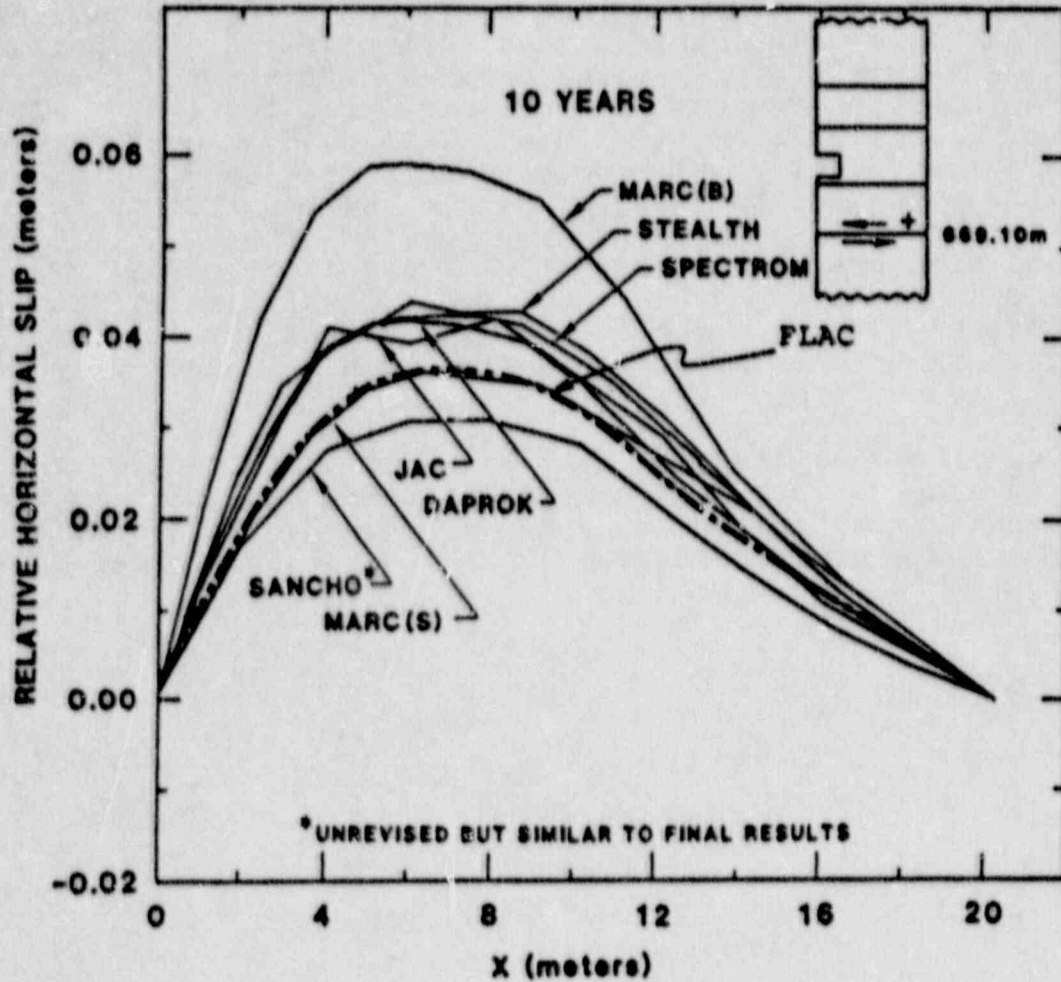from Morgan et al., 1981]

Fig. 3.4.1-11   Relative Slip Across the 669.10m Slide Line for
the Isothermal Room at 10 Years   [adapted from
Morgan et al., 1981]

Heated Room

The comparison of FLAC results for the heated room problem to the other benchmark codes is presented in Figs. 3.4.1-12 through -19. Calculations of heat transfer were performed using the implicit logic in the code. The explicit heat transfer logic is not well suited to this example. The high thermal diffusivity used to represent the room (see "equivalent" material, Table 3.4.1-2) required very small explicit time steps. Truncation errors tend to accumulate for the personal computers used resulting in inaccurate results. The implicit logic does not suffer from this problem. The vertical closure predicted by FLAC (Fig. 3.4.1-13) and horizontal displacement agree well with the other codes. The relative slip profiles on the interfaces (Figs. 3.4.1-15 to -17) agree extremely well after one year, and are slightly lower after two years. The stress profiles in Figs. 3.4.1-1J and -19 agree well with the other codes.

The heated room analysis with FLAC was also performed for the case of constant thermal conductivity rather than the temperature-dependent relation given in Table 3.4.1-2. This simulation produced temperatures 10% greater than the values plotted in Fig. 3.4.1-12.
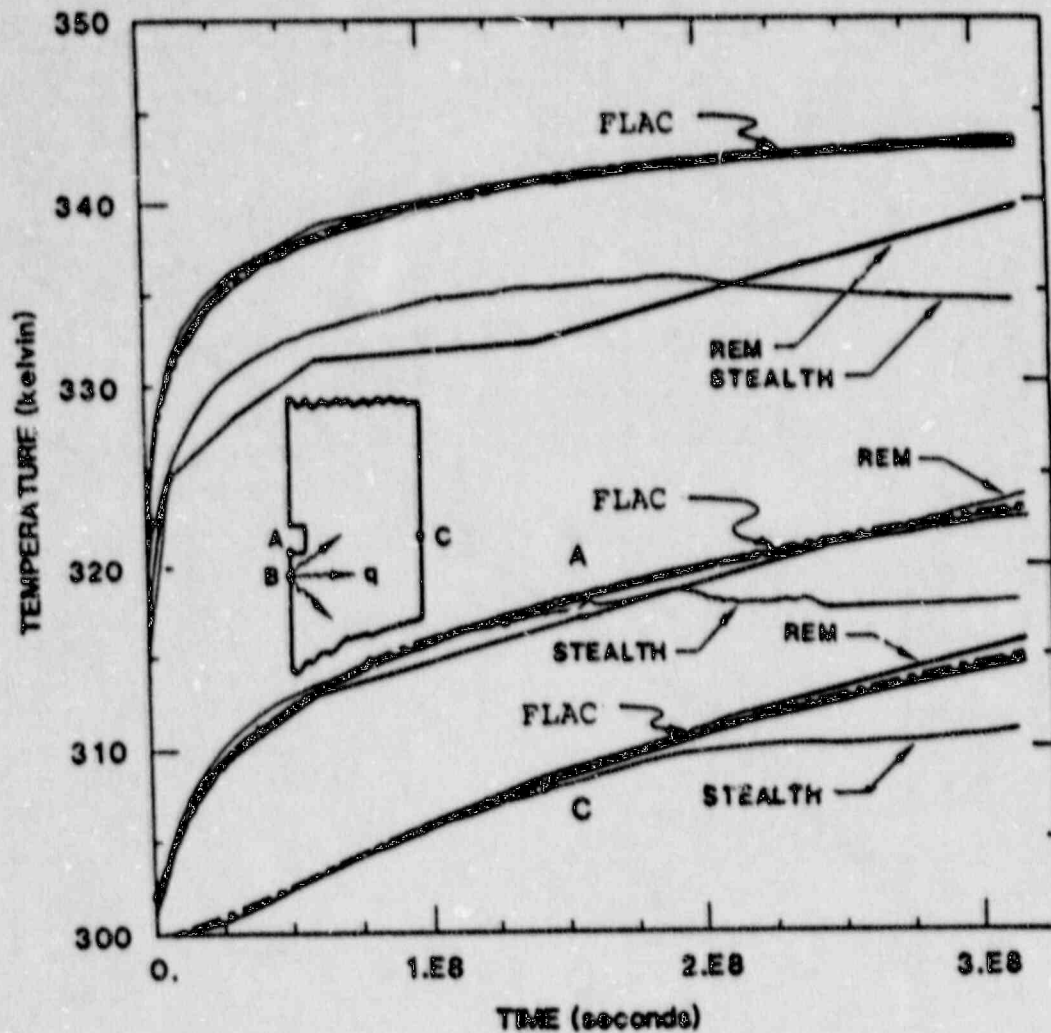
Fig. 3.4.1-12   Temperature Histories for the Heated Room at (A)
the Center of the Room Floor, (B) the Heat Source
and (C) the Intersection of the Pillar Centerline
with the Horizontal Centerline of the Room
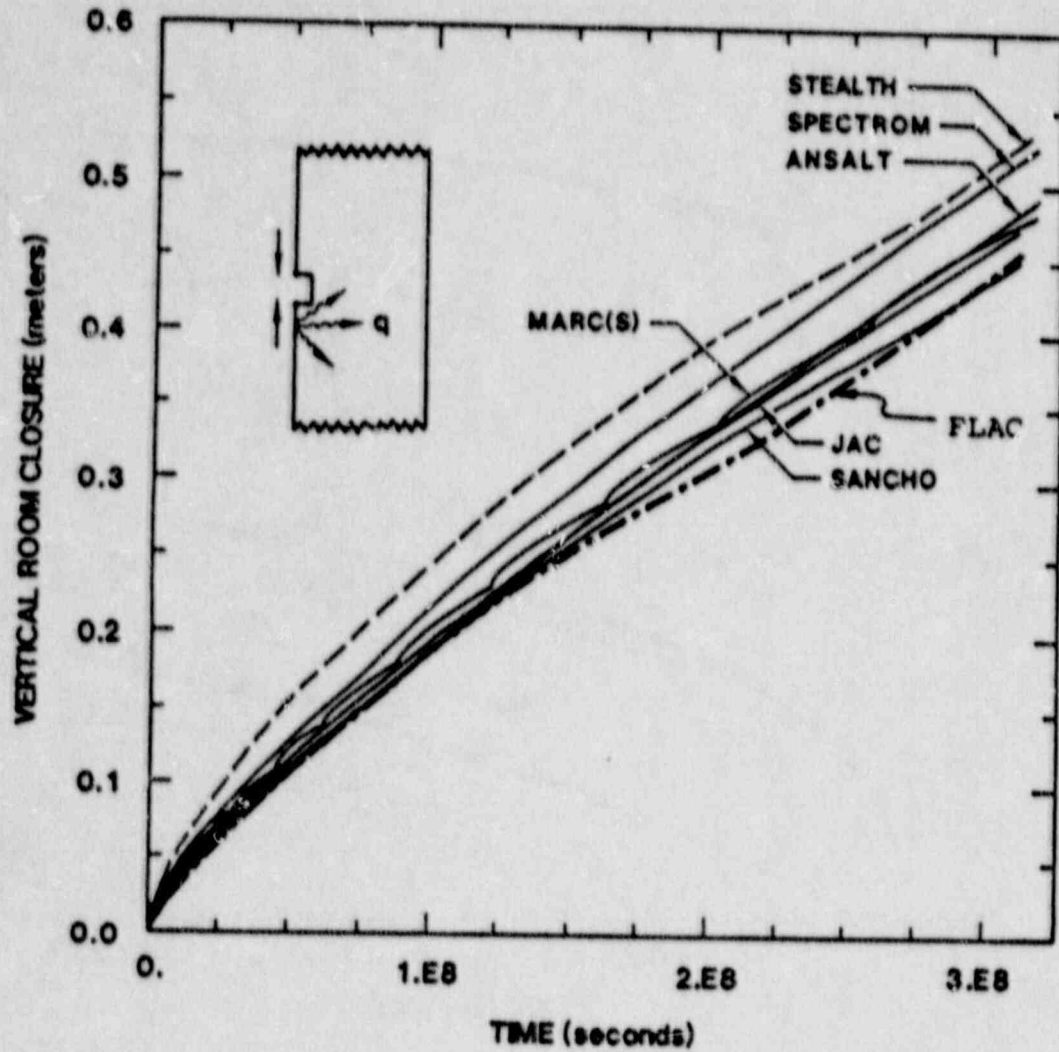[adapted from Morgan et al., 1981]

Fig. 3.4.1-13   Vertical Closure Histories for the Heated Room
[adapted from Morgan et al., 1981]
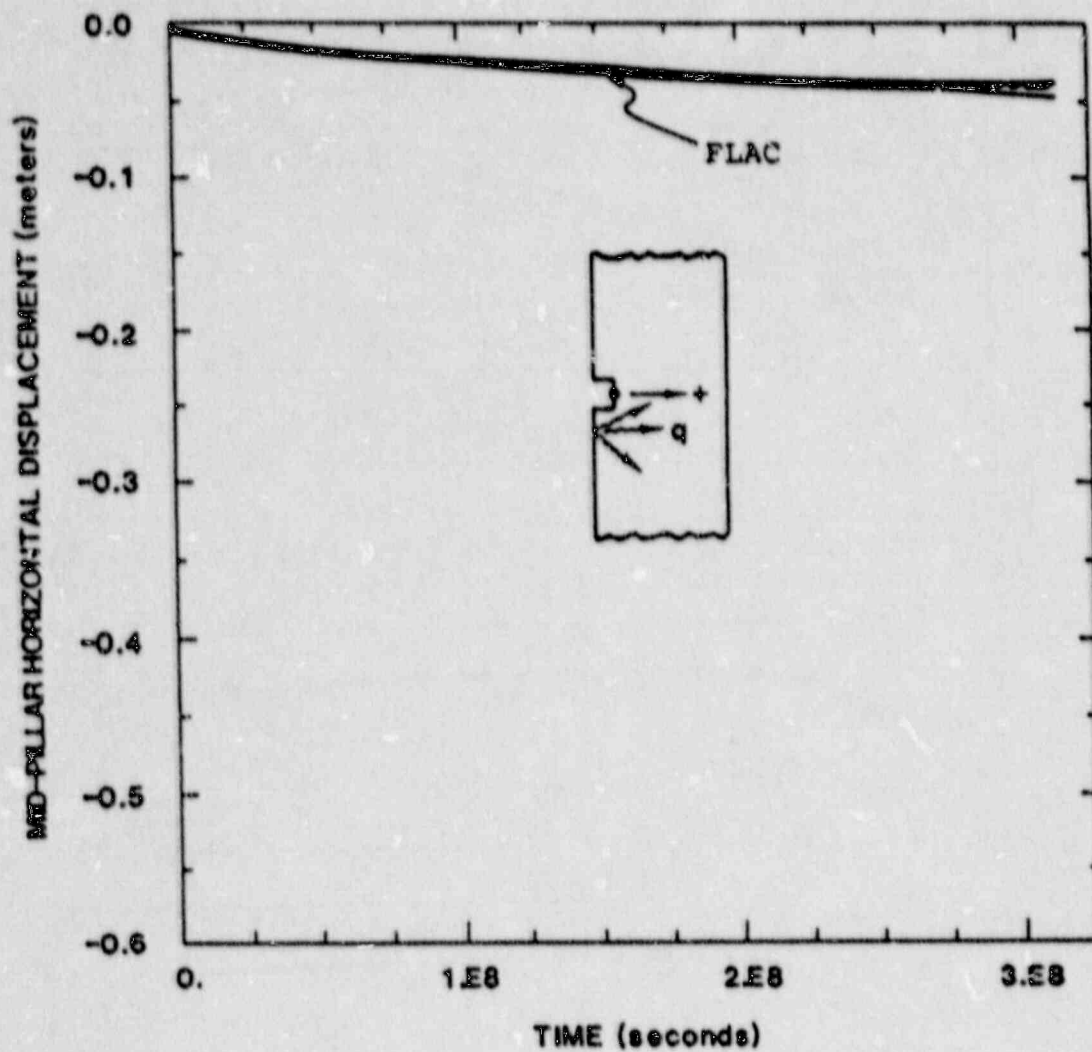
Fig. 3.4.1-14 Mid-Pillar Horizontal Displacement Histories for the Heated Room [adapted from Morgan et al., 1981]

Fig. 3.4.1-15 Relative Slip Across the 642.98 m Slideline for the Heated Room at 1 and 2 Years [adapted from Morgan et al., 1981]

Fig. 3.4.1-16 Relative Slip Across the 650.20 m Slideline for the Heated Room at 1 and 2 Years [adapted from Morgan et al., 1981]

Fig. 3.4.1-17   Relative Slip Across the 661.02 m Slide Line for
the Heated Room at 1 and 2 Years   [adapted from
Morgan et al., 1981]

Fig. 3.4.1-18   Horizontal Stress Profiles Along the Vertical
Centerline of the Heated Room at 2 Years
[adapted from Morgan et al., 1981]

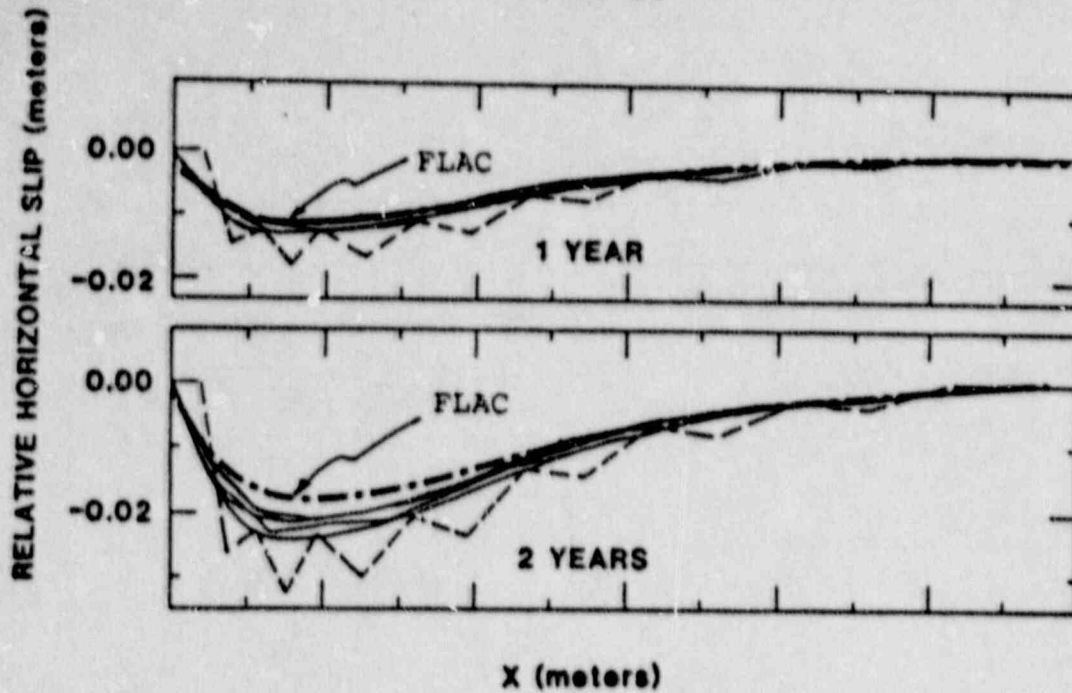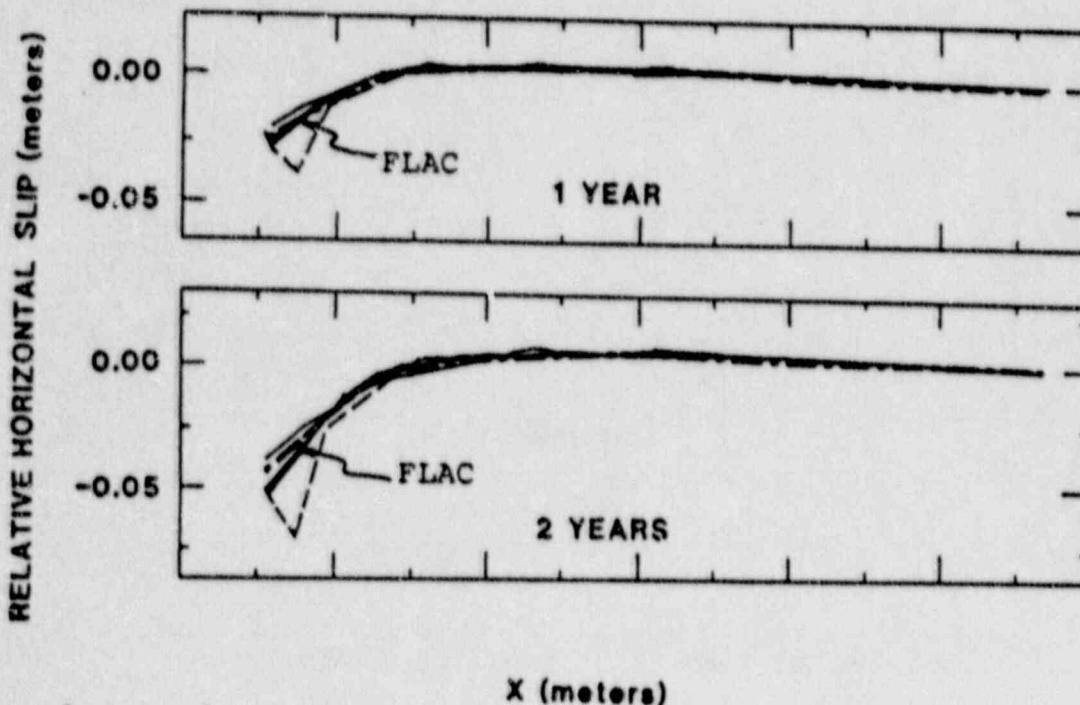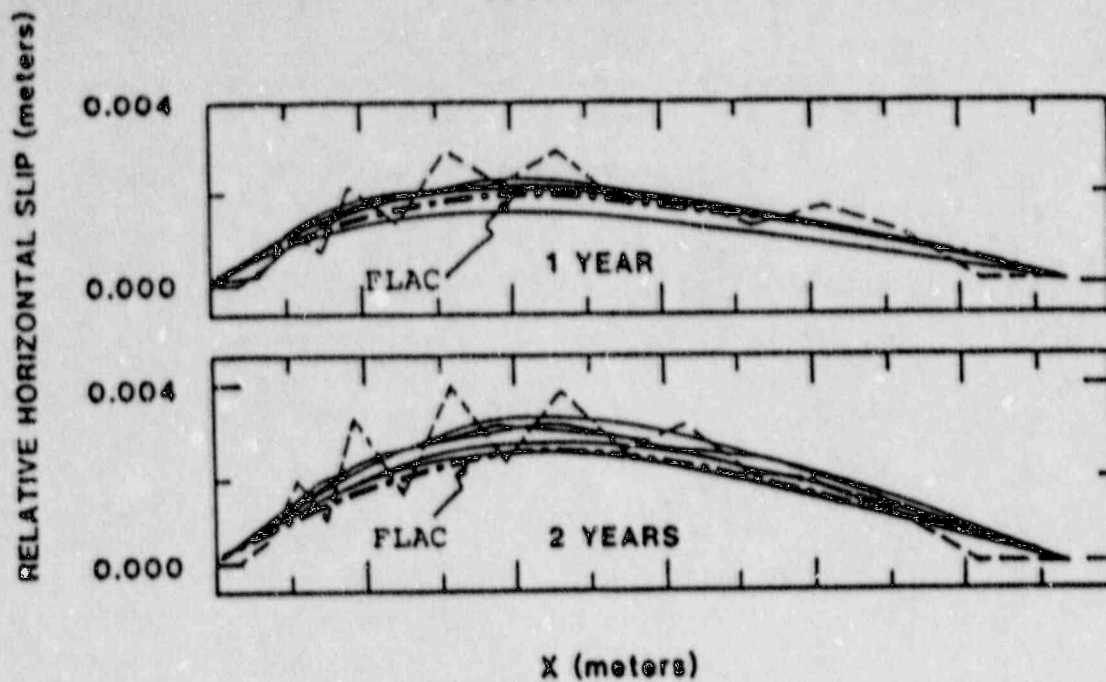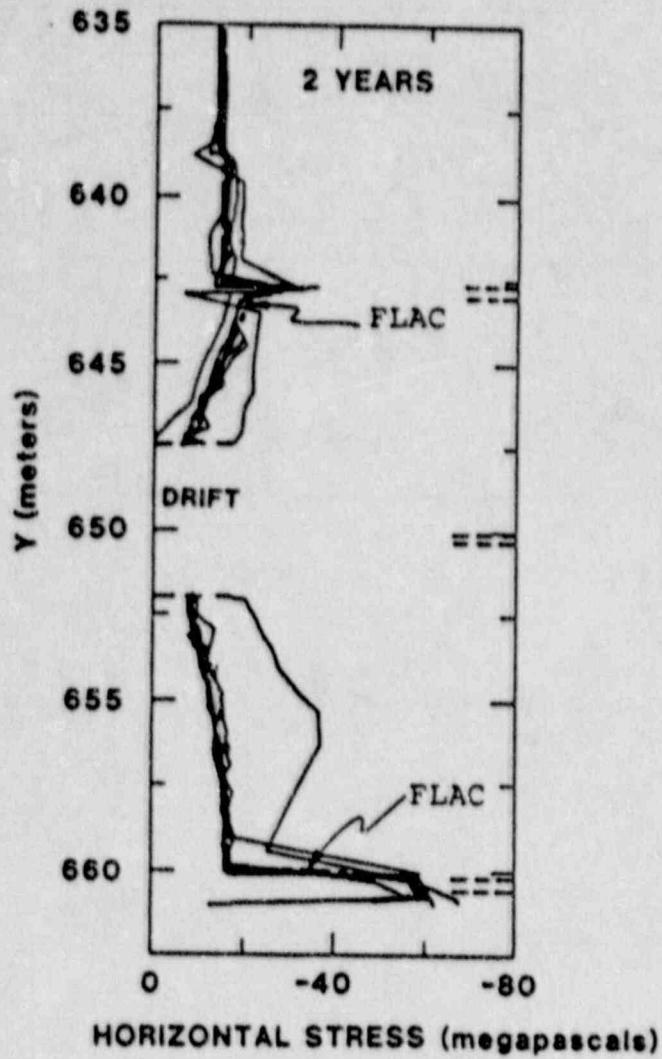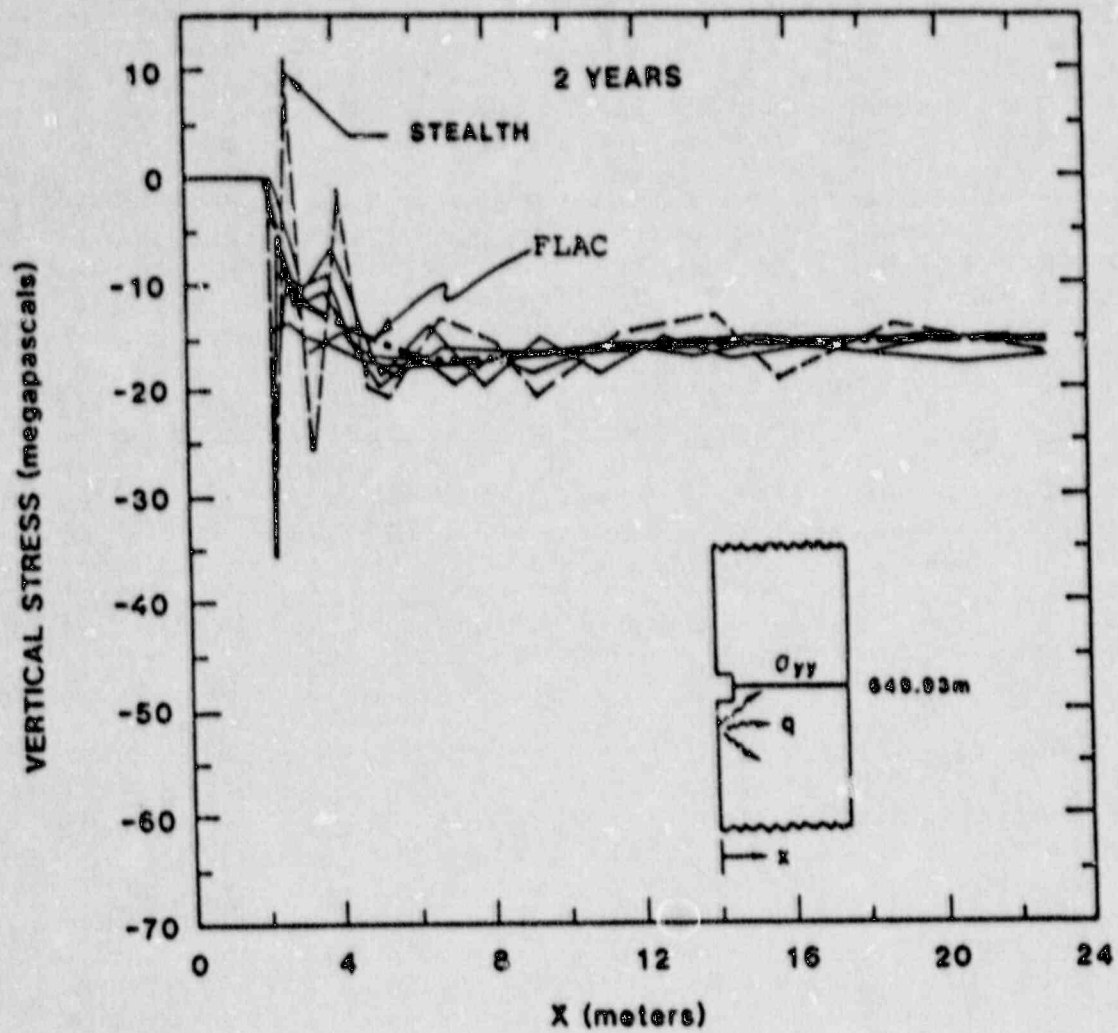Fig. 3.4.1-19   Vertical Stress Profiles Through the Pillar of the Heated Room at 2 Years   [adapted from Morgan et al., 1981]

Discussion and Conclusions

The results of this benchmark example indicate that FLAC compares well with other codes for performing thermal-mechanical analysis in nuclear waste isolation studies. The isothermal analysis showed good agreement for the FLAC model incorporating the WIPP creep model, interface logic, and interbedded materials.

In initial thermomechanical simulations, FLAC showed good agreement to other codes for early time heating where temperature changes were great. However, at late-time heating, a discrepancy in results was observed. This was traced to the large difference between the thermal diffusivity of the "equivalent material" used to model the room radiation and that of the other materials in this model. This effect is analogous to the difficulties sometimes observed in mechanical modeling of materials with large stiffness differences. The explicit solution procedure in this case resulted in very small thermal timesteps. The use of single precision arithmetic (on the PC) resulted in truncation of the significant temperature change digits for these small timesteps. The result was that error increased as time increased. The incorporation of an implicit thermal solution scheme in FLAC was found to resolve this problem since small timesteps are not required.

This example illustrates an important benefit of benchmarking. While the explicit thermal logic in FLAC has been verified against analytical solutions, inaccuracy arose in the application of the code to this problem for late times as a result of truncation errors for the computer used. A solution to the accuracy problem was found through the use of the implicit logic where truncation errors do not accumulate. It was only through benchmarking against other codes that this problem was detected. It also appears (Fig. 3.4.1-12) that other well-established codes had deficiencies which were detected in the original study.

References

Hart, Roger D., Loren J. Lorig, Mark Board, Mark G. Mack and
Krishan Wahi. "A Review of Thermomechanical Analysis Methodolo-
gies for NNWSI, BWIP and SRP", Itasca Consulting Group, U.S.
Nuclear Regulatory Commission, Contract No. NRC-02-85-002, March
1987.

Itasca Consulting Group, Inc. FLAC: Fast Lagrangian Analysis of
Continua (Version 2.0), User Manual. Minneapolis: Itasca Con-
sulting Group, Inc., 1987.

Mack, M. G. "Code Verification of FLAC for Thermomechanical An-
alysis," Itasca Consulting Group, U.S. Nuclear Regulatory Com-
mission, Contract No. NRC-02-85-002, April 1987.

Mack, Mark G. "Implicit Thermal Logic in FLAC," Itasca Consult-
ing Group, U.S. Nuclear Regulatory Commission, Contract No. NRC-
02-85-002, March 1988.

Morgan, Harold S., Raymond D. Krieg and Rudolph V. Matalucci.
"Comparative Analysis of Nine Structural Codes Used in the Second
WIPP Benchmark Problem," Sandia National Laboratories, SAND81-
1389, November 1981.

3.5 CODE MAINTENANCE AND SUPPORT

Itasca Consulting Group maintains a formal system for performing maintenance and updating of the FLAC code, as well as for providing procedural controls for ensuring quality assurance. The quality assurance program* provides a formalized system for:

(1) testing of the code against relevant analytic solutions or test problems;

(2) reporting and documenting errors in code logic, and fixing these errors;

(3) maintaining a system of unique identifiers for all code changes;

(4) documenting all code modifications; and

(5) peer code reviews.

Figure 3.5-1 gives an organizational chart showing the management of the FLAC code within Itasca Consulting Group.

```
        CODE CUSTODIAN
           M. Mack
              |
   +----------+----------+
   |          |          |
P.A. Cundall  M. Board   M. Christianson
Engineer      Engineer   Engineer
```
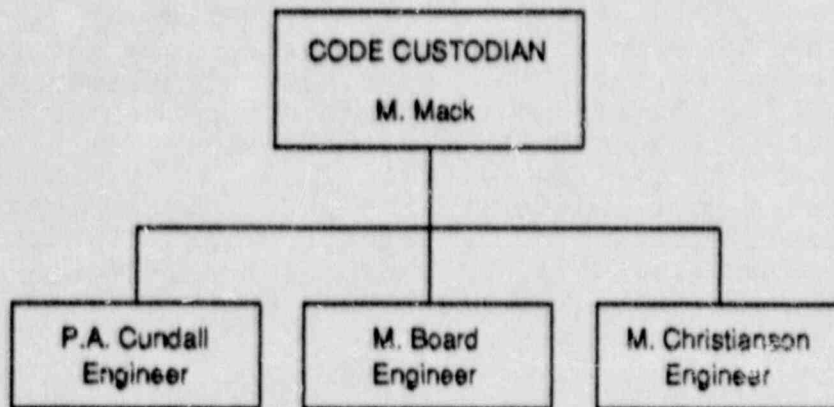
Fig. 3.5-1 Organizational Chart Illustrating Management of FLAC Maintenance and Support

---

*A Quality Assurance Plan has not been submitted for formal NRC approval.

The code custodian is Mark Mack, who maintains code documentation, defines the required work effort in upgrades and maintenance, and arranges internal, and peer review as necessary. Because FLAC is marketed to the general engineering community, modifications and additions are made on a continuing basis. Depending upon the modification, individuals with varying expertise may be required for the specific developments. It is the responsibility of the code custodian to assign the work effort to the development engineers listed in Fig. 3.5-1.

3.5.1 Code Modifications

Code modifications may result from two sources: (1) errors discovered in the code logic; or (2) planned additions to the code logic. A development plan for code updates is defined by Itasca, with updates issued approximately every year. These updates may include items such as the addition of heat transfer logic, fluid flow, etc., and thus may be considered major additions. Code modifications resulting from errors or minor code changes or additions are handled by the code custodian or any Itasca engineer on an as-required basis at the code custodian's discretion.

Two records are kept of code modifications: (1) a paper hardcopy; and (2) a disk "mod" file. The code custodian (with or without consultation with other staff) defines the necessary scope of work to be performed and completes a code modification form (Fig. 3.5-2). This form is kept in the permanent FLAC files. An additional record, called the FLAC.MOD file, is kept on floppy disk in the disk archives at Itasca. As the code developer performs a modification to the code, he updates this file with a complete description of the changes made. The FLAC.MOD file, therefore, provides a history of code modifications. A hard-copy is kept in the permanent FLAC files.

CODE MODIFICATION

CODE _____   VERSION_____

PROPOSED MODIFICATION

PURPOSE

NEW COMMAND/KEYWORD _____
MODIFICATION PLAN (INCLUDE LIST OF ROUTINES TO BE CHANGED, ADDED OR DELETED)

PERSON RESPONSIBLE_____
EST. TIME REQUIRED_____
REVIEWED BY_____
- -
FILL-IN AFTER MODIFICATION COMPLETED

COMPLETION DATE_____
COMMENTS

REVIEWER _____ DATE _____
ATTACH LISTING OF MODIFIED CODE

Fig. 3.5-2 Code Modification Form

A simple numbering system is followed for setting a unique code identification number. Any code modification which does not result in a need to change the save files created by the code is considered a minor modification. Major modifications require additional offsets to be added to the main array in the program. Therefore, previous versions of the code will not be compatible with the new array structure, and it is impossible to restart the old save files. The basic version numbering scheme is

Version A.XY

where A is an integer starting with 1, which is incremented for every released update of the code,

> X is an integer which is incremented whenever a major modification is made (This number is reset to zero whenever a new code update is released.), and

> Y is a one- or two-digit number which is incremented whenever minor modifications are made. (The Y-value is reset to zero each time a major modification is made, with the previous minor modifications are considered to be part of the ensuing major modification.)

The example below illustrates a series of minor and major FLAC modifications.

Version 2.000	**update issued, Version 2.00**
2.100	**1 major modification (change in save file)**
2.11	
2.12	
2.13	**6 minor modifications**
2.14	
2.15	
2.16	
2.20	**save file change constituting a major modification; Version 2.20 includes all previous modifications.**

The history of each minor and major modification can be traced via the FLAC.MOD file.

5.3.2 Code Verification

Code verification involves performing a set series of problems
with analytical solutions which exercise all critical functions
of the code operation. The problem set used for verification is
given in Section 7 of Volume 2 of this report, User's Manual.
New code logic may require additional problems to be added to
this set.

5.3.3 Technical Review

Technical peer review of the FLAC code is conducted at the dis-
cretion of the code custodian. Dr. Peter Cundall, author of the
FLAC code, is used in this capacity. It is noted that FLAC is
actively used for research and design by over 300 organizations
worldwide. In effect, this group constitutes a peer review in
that FLAC users submit the code to wide variety of problems on a
continuous basis. The comments and error reports of this user
group form a portion of the basis for code modifications and ad-
ditions. An example of the format used to report errors is given
in Fig. 3.5-3.

5.3.4 Restrictions

The FLAC code is proprietary, and was developed entirely by
Itasca Consulting Group, Inc. and Peter Cundall. Access to the
source code is not generally available, and an executable version
only is distributed. The FLAC source code may be examined
through special arrangement with the FLAC code custodian, who can
be reached at:

> Itasca Consulting Group, Inc.
> Suite 210
> 1313 5th Street SE
> Minneapolis, Minnesota 55414
> (612) 623-9599

CODE SUPPORT

CODE _____   VERSION _____

SERIAL NO. _____

NAME _____

COMPANY _____

COMMENT/PROBLEM

RESOLUTION

RECORDED BY _____   DATE _____

Fig. 3.5.3 Code Support Document Form

2. TITLE AND SUBTITLE

FLAC (Fast Lagrangian Analysis of Continua)
Version 2.20

Verification, Example and Benchmark Problems

5. AUTHOR(S)

Mark Board

6. TYPE OF REPORT

Formal

7. PERIOD COVERED *(Inclusive Dates)*

8. PERFORMING ORGANIZATION – NAME AND ADDRESS *(If NRC, provide Division, Office or Region, U.S. Nuclear Regulatory Commission, and mailing address; if contractor, provide name and mailing address.)*

Itasca Consulting Group, Inc.
1313 5th Street, SE, Suite 210
Minneapolis, MN 55414

9. SPONSORING ORGANIZATION – NAME AND ADDRESS *(If NRC, type "Same as above"; if contractor, provide NRC Division, Office or Region, U.S. Nuclear Regulatory Commission, and mailing address.)*

Division of High-Level Waste Management
Office of Nuclear Material Safety and Safeguards
U.S. Nuclear Regulatory Commission
Washington, DC 20555

10. SUPPLEMENTARY NOTES

11. ABSTRACT *(200 words or less)*

FLAC, Version 2.20, is a two-dimensional, large-strain, explicit
finite difference program for analysis of problems in geotechni-
cal engineering. Principal features of the code include various
mechanical constitutive models, heat transfer analysis, fluid
flow analysis, structural element coupling and frictional and
cohesive interfaces. The thermal and fluid flow analyses may be
coupled to the mechanical portion of the code. The following re-
port presents the documentation of FLAC in compliance with NUREG-
0856, Documentation of Computer Codes for High Level Waste Man-
agement. The report is in three volumes: the first presents the
mathematical formulation of the various portions of the code; the
second, a user's manual; and the third, assessment of the code
and support.

12. KEY WORDS/DESCRIPTORS *(List words or phrases that will assist researchers in locating the report.)*

FLAC, Version 2.20	coupled
large-strain	interfaces
finite difference	structural elements
computer program	NUREG-0856
geotechnical	documentation
mechanical	code assessment
thermal	
fluid flow	

13. AVAILABILITY STATEMENT

Unlimited

14. SECURITY CLASSIFICATION

(This Page)
Unclassified

(This Report)
Unclassified

15. NUMBER OF PAGES

16. PRICE